

# **An investigation into the anionic thia-Fries rearrangement in metal $\pi$ -complexes**

**Von der Naturwissenschaftlichen Fakultät der  
Gottfried Wilhelm Leibniz Universität Hannover  
zur Erlangung des Grades**

**Doktorin der Naturwissenschaften  
(Dr. rer. nat.)**

genehmigte Dissertation

von

Geanne Marize Romêro Boston, Master of Science (Schweiz)

**2022**

Referent: Prof. Dr. rer. nat. Holger Butenschön

Korreferentin: Prof. Dr. rer. nat. Irmgard Frank

Korreferentin: Prof. Dr. rer. nat. Evamarie Hey-Hawkins

Tag der Promotion: 14.02.2022

*A minha família*

*To my family*

# Acknowledgments

The completion of this dissertation involved the contributions of many people to whom I would like to express my genuine appreciation and gratitude. To start with, my sincere thanks go to Wing-Yin Tsang, Adeline Tchouankem, Robert Gathy, Lauren Heinisch, Sinem Schmiel, Julian Georgi and Burkhon Elmuradov for their theoretical and practical support in the laboratory and exchange of ideas in our weekly group meetings. I would also like to thank my bachelor and master students Jessica Niers, Hendrik Philipp, Denise Ohlendorf, Kim Hess and Henry Struwe for their cooperation.

I am especially indebted to Prof. Dr. Holger Butenschön for the supervision of my dissertation. His ideas, feedback and analytical contributions have been immensely valuable. I am particularly grateful to Prof. Dr. Irmgard Frank for her assistance and contributions to this work. I also thank Prof. Andreas Kirschning for agreeing to be the third examiner of this work.

I wish to show my appreciation to Dr. Jörg Fohrer, Linn Müggenburg, Dagmar Körtje and Monika Rettstadt from the NMR department for their support, to Sabine Ohlrogge for her assistance with the measurement of IR samples and to Roswitha Reichel and Anne Schulz from the MS department.

I would like to thank Dr. Michael Wiebcke, Dr. Gerald Dräger and Dr. Andreas Schaate for many X-ray measurements, which enriched this thesis.

Many thanks go to both former and current member of the Institute of Organic Chemistry, Leibniz Universität Hannover for their friendship.

Finally, my unlimited gratitude goes to my husband Charles and my two beloved children Lizzie and Nicky for their love and encouragement, and to my family, for their support during my studies.

## Kurzfassung

### Untersuchungen zur Anionischen Thia-Fries-Umlagerung in Metall- $\pi$ -Komplexen

Ferrocenyltriflat und 1,1'-Ferrocenylditriflat sind dafür bekannt, dass sie bei niedriger Temperatur eine anionische Thia-Fries-Umlagerung in hoher Ausbeute durchlaufen. Die doppelte Umlagerung von 1,1'-Ferrocenylditriflat führt auf faszinierende Weise ausschließlich zu *meso*-Diastereomeren.

Durch experimentelle und theoretische Untersuchungen unter Anwendung von DFT-Berechnungen wurde das Verständnis des Mechanismus der anionischen Thia-Fries-Umlagerung vertieft und die Anwendungsbreite dieser Reaktion und ihres Produkts erweitert. Das Umlagerungsprodukt vor der Hydrolyse wurde isoliert und kristallisiert, und die Kristallstrukturanalyse wurde als Benchmark für die Auswahl von Funktionalen, Basissätzen und Pseudopotenzialen verwendet. In dieser Arbeit werden die Mechanismen der anionischen Thia-Fries-Umlagerung für Ferrocenyltriflat und 1,1'-Ferrocenylditriflat analysiert und die Ursache für die beispiellose *meso*-Diastereoselektivität der doppelten anionischen Thia-Fries-Umlagerung des letzteren geklärt.

Der Anwendungsbereich der Reaktion wurde auf Ferrocenylfluorsulfonat und zum ersten Mal auf einen Kobaltkomplex erweitert. Das anionische Thia-Fries-Umlagerungsprodukt der Cobaltoceniumsalze erwies sich als stabiler als das entsprechende Ferrocen-Derivat. Die Untersuchung der Reaktivität neuer Ferrocenylsulfonate führte auch zur Synthese eines seltenen anellierten Oxathiin-Derivats von Ferrocen.

Das monoanionische Thia-Fries-Umlagerungsprodukt wurde als neuer elektrophiler Partner für die Suzuki-Miyaura-Kreuzkupplung untersucht, und die Untersuchungen dazu führten neben (Trifluormethylsulfonyl)ferrocen auch zu Fluorsulfonylferrocen. Diese beiden neuen Ferrocen-Derivate wurden als *ortho*-dirigierende Gruppen für Ferrocen untersucht und schnitten als solche sehr gut ab.

Schlüsselwörter: Anionische Thia-Fries-Umlagerung; Ferrocen; Cobaltocenium; *ortho*-Lithiierung; DFT Berechnungen.

## Abstract

### An investigation into the anionic thia-Fries rearrangement in metal $\pi$ -complexes

Ferrocenyl triflate and 1,1'-ferrocenediyl ditriflate are known to undergo anionic thia-Fries rearrangements in high yields at low temperature. The double rearrangement of 1,1'-ferrocenediyl ditriflate leads in an intriguing manner exclusively to the *meso* diastereomer.

Through experimental and theoretical research using DFT calculations, the understanding of the mechanism of the anionic thia-Fries rearrangement was expanded, and the use of this reaction and its product was broadened. The rearrangement product before hydrolysis was isolated and crystallized, and the crystal structure analysis was used as a benchmark for the selection of functionals, basis sets, and pseudopotentials. This thesis demonstrates the mechanism of the anionic thia-Fries rearrangement for ferrocenyl triflate and 1,1'-ferrocenediyl ditriflate and explains the reason for the unprecedented *meso* diastereoselectivity of the double anionic thia-Fries rearrangement of the latter.

The scope of the reaction was expanded to ferrocenyl fluorosulfonate, and for the first time, to a cobalt complex. The anionic thia-Fries rearrangement product of the cobaltocenium salts proved more stable than the corresponding ferrocene derivative. The investigation of the reactivity of new ferrocenyl sulfonates also led to the synthesis of a rare ferrocene annellated oxathiine derivative.

The mono anionic thia-Fries rearrangement product was explored as a new electrophilic partner for Suzuki-Miyaura cross-coupling, and the investigation around it gave rise to the syntheses of fluorosulfonylferrocene in addition to (trifluoromethylsulfonyl)ferrocene. These two new ferrocene derivatives were investigated as *ortho* metalating groups at ferrocene, and they performed very well as such.

Keywords: Anionic thia-Fries rearrangement; ferrocene; cobaltocenium; *ortho* lithiation; DFT calculations.

*The most exciting phrase to hear in science, the one that heralds new discoveries, is not 'Eureka! ' but 'That's funny...'*

**Isaac Asimov**

## Abbreviations

Å	Angstrom(s)
Ac	Acetyl
acac	Acetylacetonate
aq.	Aqueous
Ar	Aryl
a.u.	Atomic unit(s)
br	Broad (spectral)
BrettPhos	2-(Dicyclohexylphosphino)3,6-dimethoxy-2',4',6'-triisopropyl-1,1'-biphenyl
Bu	Butyl
<i>t</i> -Bu	<i>tert</i> -Butyl
°C	Degrees Celsius
calcd.	Calculated
cat.	Catalyst
cm <sup>-1</sup>	Wavenumber(s)
<sup>13</sup> C NMR	<sup>13</sup> C Nuclear Magnetic Resonance
Cp	Substituted cyclopentadienyl ring
Cp'	Unsubstituted cyclopentadienyl ring
CPMD	Car-Parrinello Molecular Dynamics (either method or software)
<i>d</i>	Chemical Shift (in parts per million)
d	Doublet (spectral)
DBU	1,8-Diazabicyclo [5.4.0] undec-7-ene



dd	Doublet of Doublet (spectral)
DCM	Dichloromethane
DFT	Density functional theory
DIPA	<i>N,N</i> -Diisopropylamine
DMF	Dimethylformamide
DMSO	Dimethyl sulfoxide
DPIBF	1,3-Diphenylisobenzofuran
dppf	1,1'-Bis(diphenylphosphino)ferrocene
dtbpf	1,1'-Bis(di-tert-butylphosphino)ferrocene]dichloropalladium(II)
E	Electrophile
ee	Enantiomeric Excess
EI	Electron ionization
equiv.	Equivalent
Et	Ethyl
eV	Electron Volt ( $1.602 \times 10^{-19}$ J)
<sup>19</sup> F NMR	<sup>19</sup> F Nuclear Magnetic Resonance
fs	Femtosecond(s)
g	Gram
h	Hour(s)
<sup>1</sup> H NMR	<sup>1</sup> H Nuclear Magnetic Resonance
HOMO	Highest Unoccupied Molecular Orbital
HPLC	High-performance Liquid Chromatography
HRMS	High-resolution Mass Spectrometry
HMQC	Heteronuclear Multiple Quantum Coherence

HSQC	Heteronuclear Single Quantum Coherence
HMBC	Heteronuclear Multiple Bond Correlation
Hz	Hertz
iPr	Isopropyl
IR	Infrared
<i>J</i>	Coupling Constant in NMR Spectroscopy
K	Kelvin
$k_H/k_D$	Ratio constant for a reaction involving a hydrogen substituted and deuterium substituted reactants
kcal	Kilocalorie(s)
KJ	Kilojoule(s)
LDA	Lithium Diisopropylamide
LiTMP	Lithium 2,2,5,5-tetramethylpiperidine
m	Multiplet (spectral)
m	Medium (IR spectra)
M	Molar (moles per liter)
M <sup>+</sup>	Parent Molecular Cation (mass spectrometry)
Me	Methyl
MD	Molecular dynamics
mL	Millilitre(s)
MLWF	Maximally localized Wannier Functions
min	Minutes
mmol	Millimol
m. p.	Melting point

Ms	Mesyl
MS	Mass spectrometry
$m/z$	Mass-to-charge Ratio (in mass spectrometry)
NHC Ipr	<i>N,N</i> -(2,6-Diisopropylphenyl)dihydroimidazolium chloride
NMR	Nuclear Magnetic Resonance
ODG	<i>ortho</i> Directing group(s)
PE	Petroleum Ether
Ph	Phenyl
ppm	Part(s) per Million
q	Quartet (spectral)
<i>rac</i>	Racemic
RuPhos	2-Dicyclohexylphosphino-2',6'-diisopropoxybiphenyl
s	Singlet (spectral)
s	Sharp (IR spectral)
SMC	Suzuki-Miyaura-Coupling
SPhos	2-Dicyclohexylphosphino-2',6'-dimethoxybiphenyl
SuFEx	Sulfur(VI) Fluoride Exchange
t	Triplet (spectral)
TASF	Tris(dimethylamino)sulfonium difluorotrimethylsilicate
TBAF	Tetra- <i>n</i> -butylammonium fluoride
TBAT	Tetrabutylammonium difluorotriphenylsilicate
Tf	Trifluoromethanesulfonyl
THF	Tetrahydrofuran
TLC	Thin Layer Chromatography

TMEDA	<i>N,N,N',N'</i> -Tetramethylethane-1,2-diamine
Ts	Tosyl
UV	Ultraviolet
$\tilde{\nu}$	Wave number
VT NMR	Variable temperature Nuclear Magnetic Resonance
w	weak (IR spectral)
XPhos	2-Dicyclohexylphosphino-2',4',6'-triisopropylbiphenyl

# Contents

<b>Dedication .....</b>	<b>iii</b>
<b>Acknowledgments .....</b>	<b>iv</b>
<b>Kurzfassung .....</b>	<b>v</b>
<b>Abstract .....</b>	<b>vi</b>
<b>Quote .....</b>	<b>vii</b>
<b>Abbreviations .....</b>	<b>viii</b>
<b>CHAPTER 1.....</b>	<b>1</b>
<b>1. Introduction .....</b>	<b>1</b>
1.1 An overview of the Fries rearrangement .....	1
2.1 Objectives of this thesis.....	5
<b>CHAPTER 2.....</b>	<b>6</b>
<b>2. Anionic thia-Fries rearrangement at Ferrocene.....</b>	<b>6</b>
2.1. Introduction.....	6
2.2. Results and discussion.....	17
2.2.1. Extension of the scope of the anionic thia-Fries rearrangement to other functional groups... ..	17
2.2.2. Investigation of the potential use of the anionic thia-Fries rearrangement product for Suzuki cross-coupling reaction.....	34
2.2.3. <i>ortho</i> Lithiation of fluorosulfonylferrocene ( <b>142</b> ) and (trifluoromethylsulfonyl)ferrocene ( <b>134</b> ) .....	44
2.2.4. Asymmetric anionic thia-Fries rearrangement .....	47
2.3. Conclusion.....	57
<b>CHAPTER 3.....</b>	<b>58</b>
<b>3. Anionic thia-Fries rearrangement at Cobaltocenium .....</b>	<b>58</b>
3.1 Introduction.....	58
3.2 Results and discussion.....	63
3.3 Conclusion.....	78

<b>CHAPTER 4.....</b>	<b>79</b>
<b>4. Computational studies .....</b>	<b>79</b>
4.1. Introduction.....	79
4.2. Results and discussion.....	81
4.3. Conclusion.....	103
<b>CHAPTER 5.....</b>	<b>104</b>
<b>5. Summary and future work.....</b>	<b>104</b>
<b>CHAPTER 6.....</b>	<b>111</b>
<b>6. Experimental and theoretical method section .....</b>	<b>111</b>
6.1. Theoretical Method Section .....	111
6.2. Experimental section .....	112
6.2.1 General Considerations.....	112
6.2.2 Synthesised compounds .....	115
6.2.2.1. Ferrocenyl triflate ( <b>79</b> ) <sup>[17]</sup> .....	115
6.2.2.2. Ferrocenyl methanesulfonate ( <b>94</b> ) .....	116
6.2.2.3. Ferrocenyl (4-methylphenyl)sulfonate ( <b>95</b> ) <sup>[31]</sup> .....	116
6.2.2.4. (Methylsulfonyl)ferrocenium tetrafluoroborate ( <b>102</b> ) .....	117
6.2.2.5. [(4-Methylphenyl)sulfonyl]ferrocenium tetrafluoroborate ( <b>103</b> ) .....	118
6.2.2.6. [(Trifluoromethyl)sulfonyl]ferrocenium tetrafluoroborate ( <b>104</b> ).....	118
6.2.2.7. <i>rac</i> -2-[(Trifluoromethyl)sulfonyl]ferrocenyl methanesulfonate ( <i>rac</i> - <b>105</b> ).....	119
6.2.2.8. Ferrocenyl benzenesulfonate ( <b>111</b> ) <sup>[29]</sup> .....	120
6.2.2.9. Ferrocenyl (2,4,6-triisopropylbenzene)sulfonate ( <b>112</b> ) .....	121
6.2.2.10. Ferrocenyl (2,6-difluorobenzene)sulfonate ( <b>113</b> ) .....	122
6.2.2.11. Ferrocenyl (2,6-dichlorobenzene)sulfonate ( <b>114</b> ) .....	123
6.2.2.12. Ferrocenyl (2,3,4,5,6-pentafluorobenzene)sulfonate ( <b>110</b> ).....	124
6.2.2.13. Ferrocene annelated 6,7,8,9-tetrafluorobenzo[c,e]-[1,2]oxathiine 5,5-dioxide ( <i>rac</i> - <b>116</b> ).....	125
6.2.2.14. Ferrocenyl fluorosulfonate ( <b>118</b> ) .....	126
6.2.2.15. 2-Hydroxyferrocenesulfonyl fluoride ( <i>rac</i> - <b>119</b> ) .....	127
6.2.2.16. Chloroferrocene ( <b>135</b> ) .....	128
6.2.2.17. 1,1'-Dichloroferrocene ( <b>138</b> ) <sup>[59]</sup> and 1,1'-dichlorobiferrocenyl ( <b>139</b> ) <sup>[60]</sup> .....	129
6.2.2.18. Fluorosulfonylferrocene ( <b>142</b> ) .....	130
6.2.2.19. (Trifluoromethyl)sulfonylferrocene ( <b>134</b> ) .....	130

6.2.2.20.	<i>rac</i> -2-(2,6-Dimethoxybenzoyl)ferrocenesulfonyl fluoride ( <i>rac</i> - <b>150</b> ).....	132
6.2.2.21.	<i>rac</i> -2-Methylferrocenesulfonyl fluoride ( <i>rac</i> - <b>151</b> ) and 2,5-dimethylferrocenesulfonyl fluoride ( <b>152</b> ) .....	133
6.2.2.22.	<i>rac</i> -2-Methyl-1-(trifluoromethylsulfonyl)ferrocene ( <i>rac</i> - <b>153</b> ) and 2,5-dimethyl-1-(trifluoromethylsulfonyl)ferrocene ( <b>154</b> ).....	134
6.2.2.23.	2,2,6,6-Tetramethyl-1-(ferrocenylsulfonyl)piperidine ( <b>155</b> ) and <b>156a</b> .....	135
6.2.2.24.	[4-(Trifluoromethyl)phenyl]ferrocene ( <b>145</b> ) <sup>[151]</sup> .....	136
6.2.2.25.	<i>rac</i> -2-Methoxy-1-[4-(trifluoromethyl)phenyl]ferrocene ( <i>rac</i> - <b>132</b> ) .....	137
6.2.2.26.	4-(Methoxybenzenesulfonate) ferrocene ( <b>148</b> ) .....	139
6.2.2.27.	1-Trifluoromethanesulfonyl-2-pyridinium-cyclopentadienylide ( <b>171</b> ).....	140
6.2.2.28.	1-Trifluoromethanesulfonate-1'-acetoxoferrocene ( <b>181</b> ) .....	140
6.2.2.29.	(Cyclopentadienyl)(cyclopentadienone)cobalt(I) ( <b>203</b> ) <sup>[107]</sup> .....	141
6.2.2.30.	[(trifluoromethylsulfonyl)oxy]cobaltocenium trifluoromethanesulfonate ( <b>204</b> ) .....	142
6.2.2.31.	[2-(Trifluoromethylsulfonyl)cyclopentadienone]cyclopentadienylcobalt(I) ( <b>205</b> ) .....	143
6.2.2.32.	1-[(trifluoromethylsulfonyl)oxy]-2,5-bis(trimethylsilyl)cobaltocenium trifluoromethane-sulfonate ( <b>206</b> ) .....	144
6.2.2.33.	(Cyclopentadienyl)[2-(trifluoromethylsulfonyl)-5(trimethylsilyl)cyclopentadienone]-cobalt(I) ( <b>207</b> ) .....	145
6.2.2.34.	1-[(methanesulfonyl)oxy]-2,5-bis(trimethylsilyl)cobaltocenium methanesulfonate ( <b>224</b> ) .....	146
6.2.2.35.	1-[( <i>p</i> -toluenesulfonyl)oxy]-2,5-bis(trimethylsilyl)cobaltocenium <i>p</i> -toluenesulfonate ( <b>225</b> ) .....	147
6.2.2.36.	Lithium 2-(trifluoromethylsulfonyl)ferrocenolate ( <b>237</b> ) .....	148

**7. REFERENCES.....149**

**ATTACHMENTS.....158**

**CURRICULUM VITAE .....174**

## Chapter 1

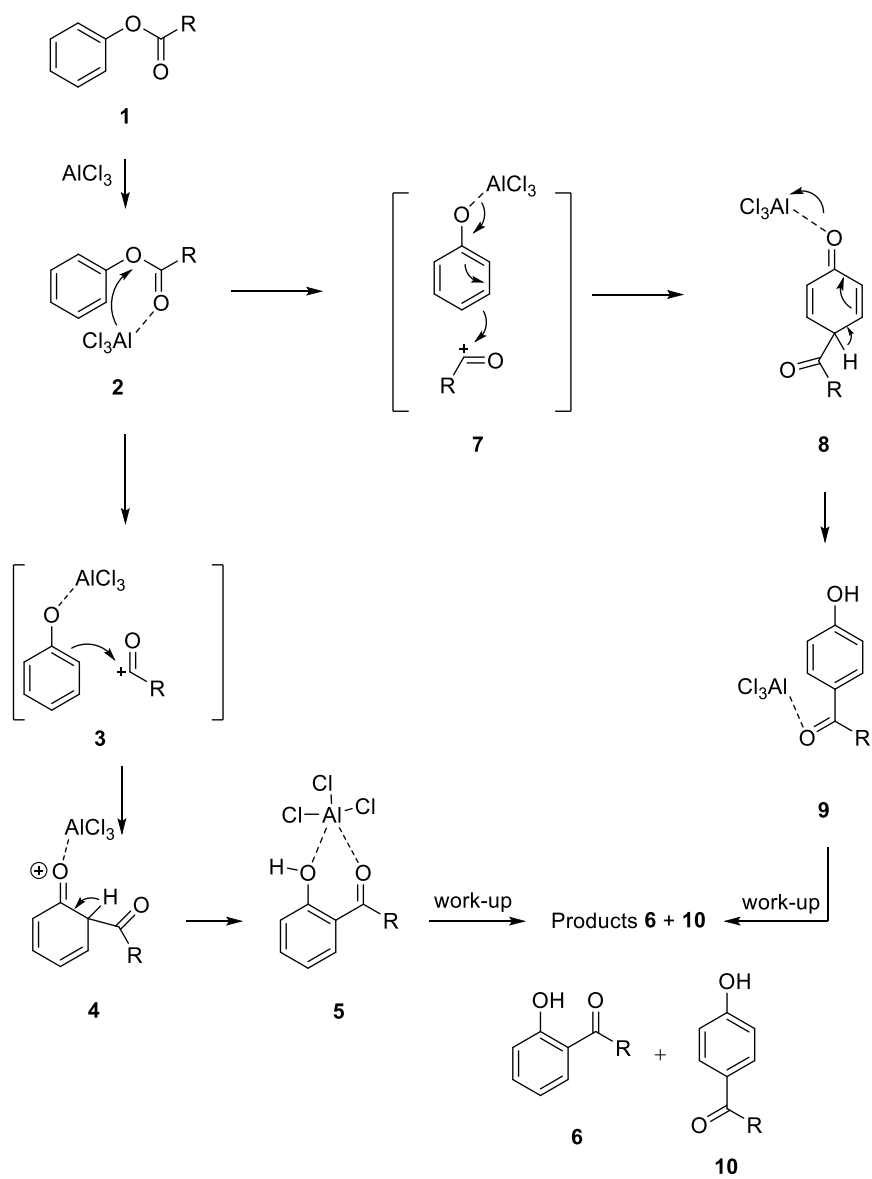
### 1. Introduction

#### 1.1 An overview of the Fries rearrangement

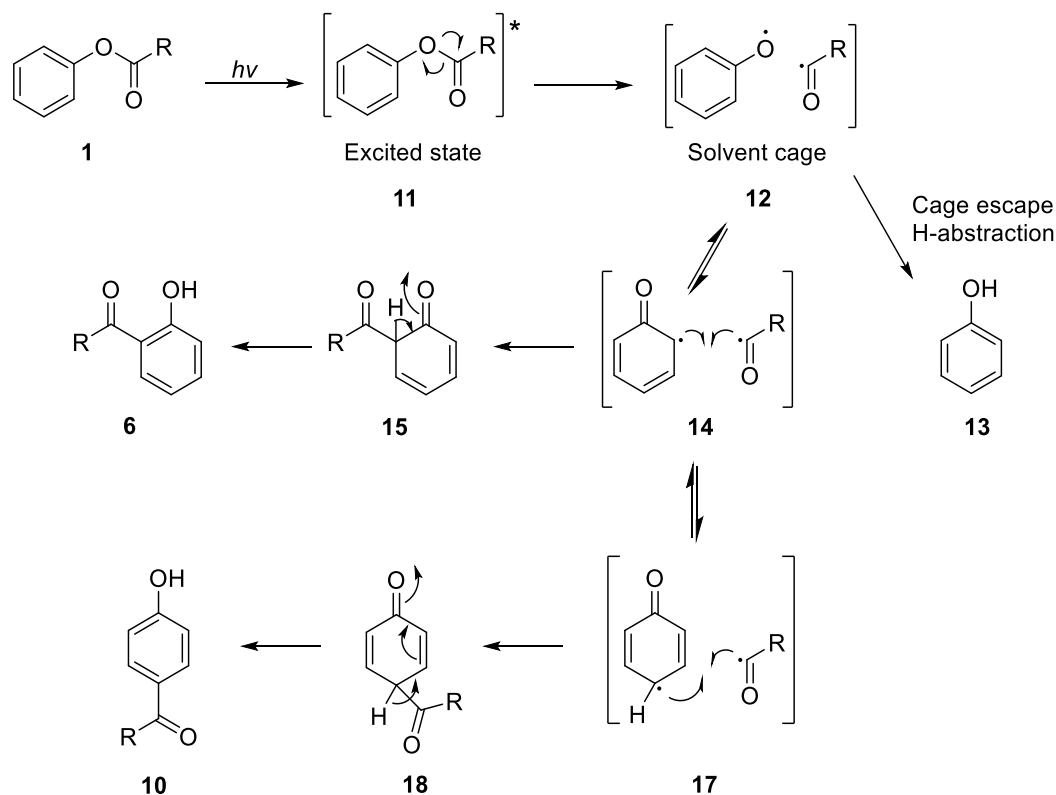
The Fries rearrangement is named after Karl Theophil Fries based on his work published in 1908: *Über Homologe des Cummanons und ihre Abkömmlinge*.<sup>[1]</sup> The rearrangement is a transformation of aryl esters (**1**) into *ortho* and/or *para* hydroxylaryl ketones (**6** and **10**) catalysed by acid, being either a Lewis or Brønsted acid as shown in Scheme 1.1. Over the years, several modifications of the original procedure and analogous reactions were developed. In 1960, Anderson and Reese,<sup>[2]</sup> presented the first photo-induced Fries rearrangement. They reported that the normal acid-catalysed Fries rearrangement yielded predominately the product of the 1,5-O→C migration, whilst the photochemical Fries rearrangement favoured the product of the 1,3-O→C migration. The reaction requires the homolytic cleavage of the C-O bond as shown in Scheme 1.2.<sup>[3]</sup> The selectivity and ratio of the products depend on the structure of the starting material and reaction conditions such as temperature, solvent etc.<sup>[4]</sup>

A comparable rearrangement of *N*-acetylcarbazole (**19**) to 3-acetylcarbazole (**20**) was achieved in 1934 by Plant and Williams<sup>[5]</sup> and improved on later by Meitzner,<sup>[6]</sup> known as the Fries-Rosenmund Rearrangement as shown in Scheme 1.3.<sup>[3]</sup> The selectivity and ratio of the products depend on the structure of the starting material and reaction conditions such as temperature, solvent etc.<sup>[4]</sup>

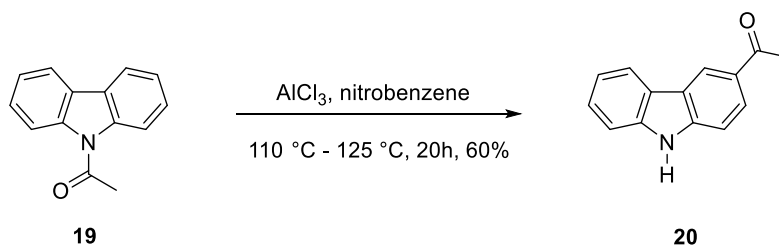




**Scheme 1.1.** Proposed mechanism for an acid-catalysed Fries rearrangement.<sup>[4,7]</sup>

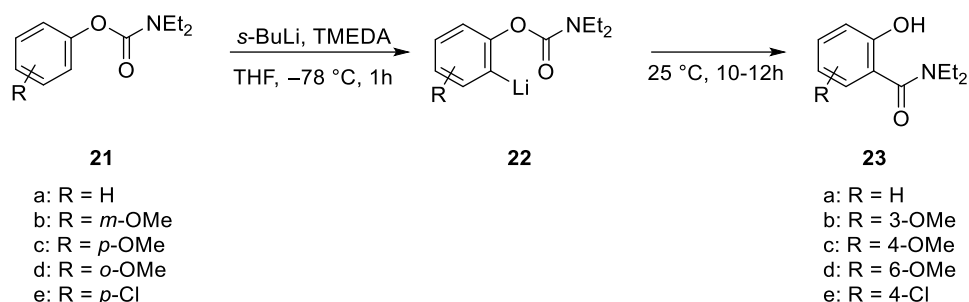


**Scheme 1.2.** Proposed mechanism for a photo-Fries rearrangement.<sup>[3,4]</sup>



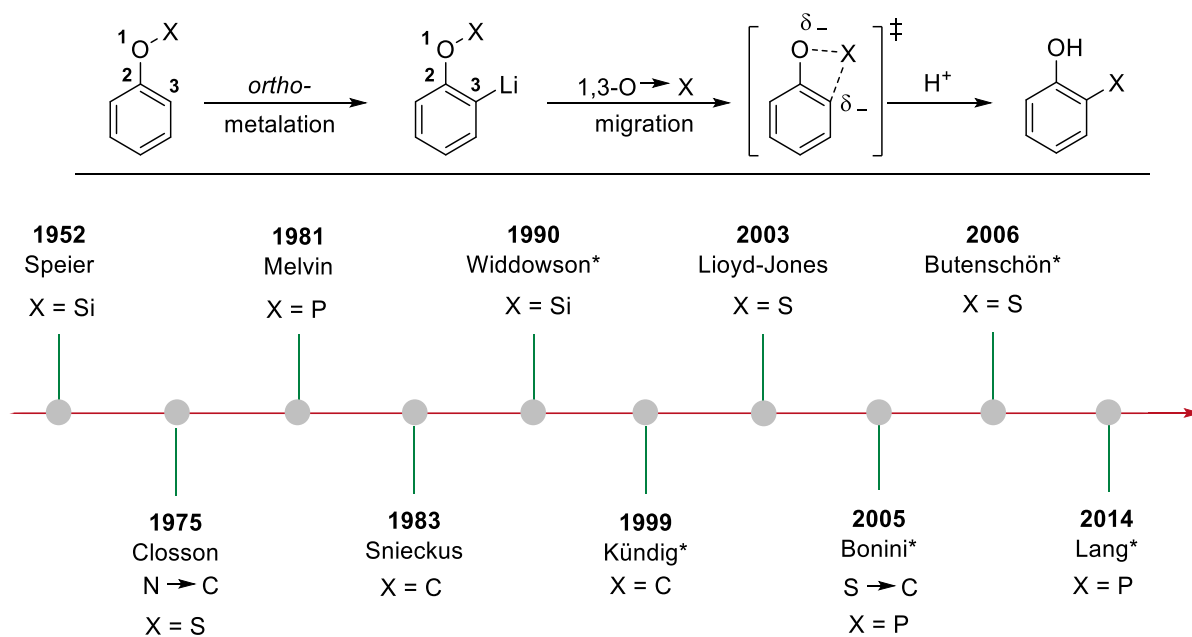
**Scheme 1.3.** Fries-Rosenmund rearrangement.<sup>[6]</sup>

In 1983 Snieckus expanded the scope describing the first anionic-Fries rearrangement.<sup>[8]</sup> An organolithium base was used to directly *ortho* lithiate an *O*-aryl carbamate (**21a - e**) which was followed by a 1,3 carbamoyl migration as shown in Scheme 1.4 . This transformation not only provided a new way to generate a C-C bond, but also promoted further metalation chemistry through the formed product, since the 'carried' group is a tertiary amide, one of the most powerful *ortho* metalation directing group.<sup>[8]</sup>



**Scheme 1.4.** *ortho* Lithiation of O-aryl carbamates. An anionic equivalent of the Fries rearrangement.

The scope of the anionic Fries rearrangement is not restricted to the migration of esters' carbonyl groups. Over the years, several heteroanionic Fries rearrangements, e.g., 1,3-O→X migration, were reported in the literature. These include sila-, thia- and phospho-Fries rearrangements which are the *ortho* migrations respectively, of silicon, sulfur and phosphorus as shown in Figure. 1.1.



\*On organometallic compounds (ferrocene,  $\eta^6$ -Cr(CO)<sub>3</sub> compounds, etc)

**Figure 1.1.** Brief timeline of transformations analogous to the Fries rearrangement.<sup>[4,9–16]</sup>

## 2.1 Objectives of this thesis

The objectives of this thesis are to broaden the anionic thia-Fries rearrangement at ferrocene reported by Butenschön et al.<sup>[17]</sup> to different functional groups besides the triflate group, expanding it to other metal  $\pi$  complexes, and to explore the potential to use the anionic thia-Fries rearrangement product, e.g., as ligands in catalysis and as starting material for Suzuki cross-coupling.

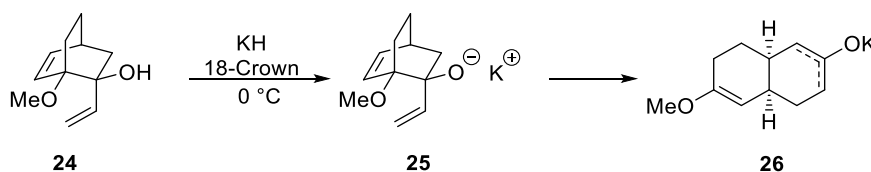
A further objective is to understand the mechanism of the anionic thia-Fries rearrangement at ferrocenyl triflate and 1,1'-ferrocenediyl ditriflate, and especially the unprecedented interannular stereinduction of the latter.

## Chapter 2

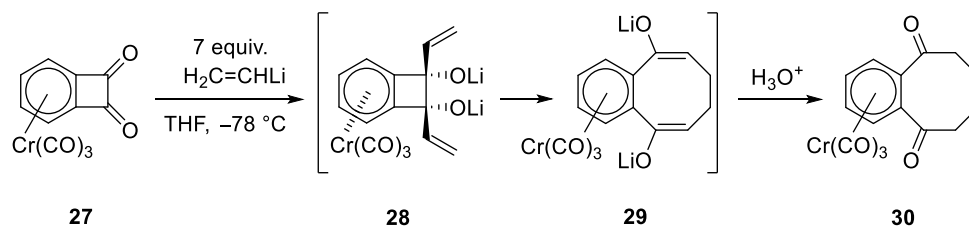
# 2. Anionic thia-Fries rearrangement at Ferrocene

## 2.1. Introduction

The anionic thia-Fries rearrangement can be counted as part of a larger group of oxyanion accelerated reactions which display a dramatic rate acceleration compared to their electron neutral or cationic counterparts.<sup>[18]</sup> In 1975, Evans et al. reported the classical and first anionic oxy-Cope rearrangement, Scheme 2.1. The use of a base allowed for lower temperatures, increased yields and a dramatically enhanced reaction rate compared to their neutral equivalents.<sup>[19]</sup> Yang et al. showed other examples comprising of oxyanion ring openings of benzocyclobutenols<sup>[20]</sup> and Butenschön et al. reported a double anionic oxy-Cope rearrangement of arene tricarbonyl-chromium complexes under mild conditions, Scheme 2.2.<sup>[21]</sup>

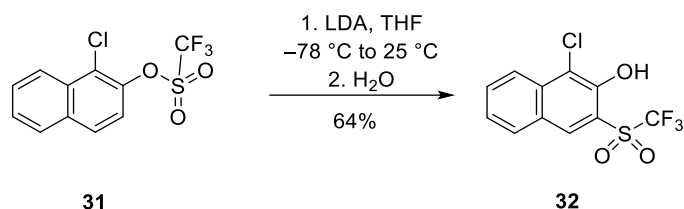


**Scheme 2.1.** Anionic Oxy-cope rearrangement.<sup>[19]</sup>



**Scheme 2.2.** Double anionic oxy-Cope rearrangement of (benzocyclobutenedione) tricarbonyl-chromium(0) (**27**).<sup>[21]</sup>

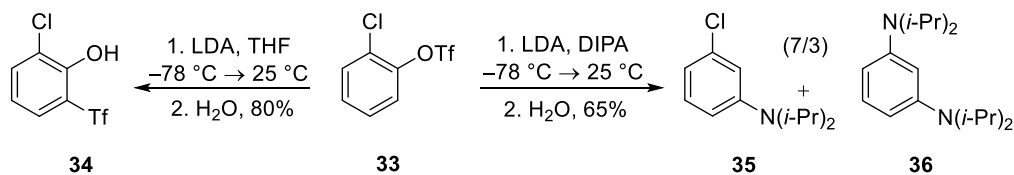
The first anionic thia-Fries rearrangement was reported in 2003 by Lloyd-Jones et al.<sup>[10]</sup> In an attempt to perform a Pd-catalysed cross-coupling of 1-chloro-2-naphthalene triflate (**31**) with a pyridyl zinc halide, generated in situ using LDA/ZnCl<sub>2</sub>, the side product **32** was observed. The reaction was optimized using 1.0 equiv. of LDA in THF at -78 °C giving 64% yield after warming up to 25 °C and quenching with water, as shown in Scheme 2.3.



**Scheme 2.3.** Anionic thia-Fries rearrangement of the aryl triflate **31**.<sup>[10]</sup>

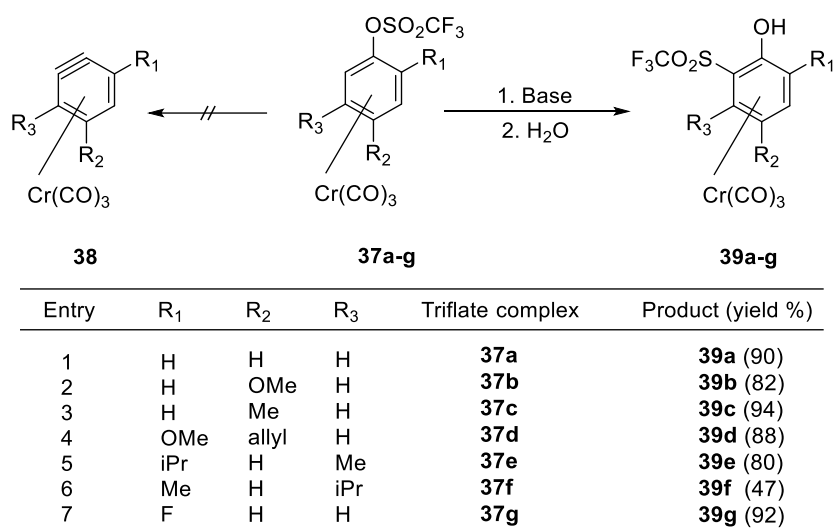
Other aryl triflates were tested under analogous conditions where it was observed that substrates bearing an electron withdrawing group *ortho* to the triflate group exclusively undergo anionic thia-Fries rearrangement. Furthermore those with an electron donating group exclusively undergo elimination generating benzyne as a reactive intermediate.<sup>[10]</sup>

Another interesting result of the study was the tenuous balance between rearrangement and elimination, depending on the presence and concentration of THF and diisopropylamine (DIPA) for substrates bearing an electron withdrawing group. *ortho* Chlorophenyl triflate (**33**), for example, undergoes the thia-Fries rearrangement exclusively when reacted with LDA in the presence of THF. However, if DIPA is used as a solvent, no trace of the rearranged product is observed, whereby only the mono- and bis- anilines **35** and **36** are observed as shown in Scheme 2.4. Interestingly, if DIPA is the main solvent and as little as 4% of THF is added, the rearrangement product **34** is also generated (40% yield).<sup>[10]</sup>



**Scheme 2.4.** Balance between anionic thia-Fries rearrangement and elimination at **34** according to used solvent.<sup>[10]</sup>

Arynes are very versatile reactive neutral compounds, and strong support for their existence was presented only in the 1940/50s by Wittig et al.<sup>[22]</sup> and Vaughan et al.<sup>[23]</sup> Over the years, several methodologies were developed to prepare them *in situ*, e.g. dehydrohalogenation of aryl halides, fluoride displacement of trimethylsilyl group on trimethyl-silylaryl triflates, hexadehydro Diels-Alder reaction among several others.<sup>[24,25]</sup> In 2006, in an attempt to prepare (aryne)tricarbonylchromium complexes via triflate elimination using either butyllithium or lithium diisopropylamide (LDA), Butenschön et al. described the first anionic thia-Fries rearrangement on an organometallic compound (Scheme 2.5). Several *ortho* (trifluoromethylsulfonyl)phenol tricarbonylchromium complexes were obtained in up to 94% yield, and no evidence of aryne complex formation was obtained.<sup>[15]</sup> This finding corroborates the theory of Lloyd-Jones since the tricarbonylchromium fragment is very electron withdrawing.<sup>[26]</sup>



**Scheme 2.5.** Thia-Fries rearrangement of (aryltriflate)tricarbonylchromium complexes.<sup>[15]</sup>

After reporting that the anionic thia-Fries rearrangement can compete with aryne generation,<sup>[10]</sup> later in 2008, Lloyd-Jones et al. described mechanistic studies using isotopically labelled aryl triflates and DFT calculations in order to unveil the remaining puzzling behaviour exemplified by regioisomers obtained from chlorobenzene triflates (**33**, **40**, **41**) with LDA (Figure 2.1).<sup>[26]</sup> It is possible to see that the *ortho* substituted **33** undergoes rearrangement, while the *meta* substituted **40** undergoes solely elimination, but the *para* substituted **41** undergoes elimination and rearrangement in a ratio of 9:5, respectively.<sup>[26]</sup>

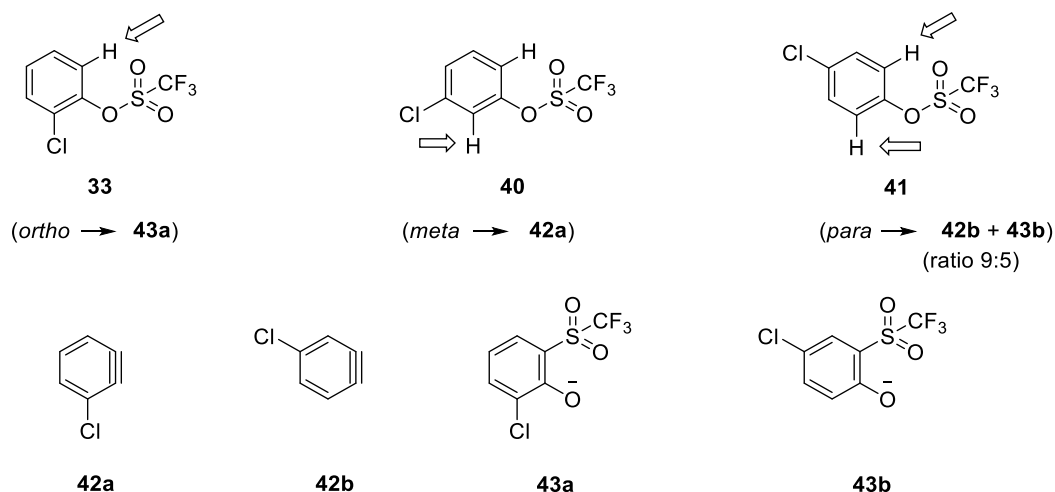
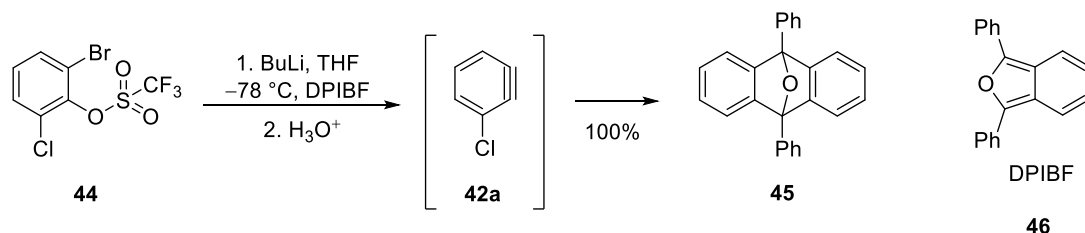


**Figure 2.1.** Sites of reaction (arrows) for *ortho*, *meta*, and *para* isomers **33**, **40** and **41** to give **42** and **43**. Conditions: LDA (1.05 equiv.) in THF at  $-78\text{ }^{\circ}\text{C}$ .<sup>[26]</sup>

The hydrogen at **40** pointed to with an arrow in Figure 2.1, was exchanged by deuterium demonstrating that the C-H bond cleavage is irreversible and allows for the calculation of the net isotopic effect by reaction of **40** with LDA at  $-40\text{ }^{\circ}\text{C}$ . The values obtained for the rearrangement ( $k_{\text{H}}/k_{\text{D}} = 2.5 \pm 0.2$ ) versus elimination ( $k_{\text{H}}/k_{\text{D}} = 2.6 \pm 0.6$ ) are the same within the standard deviation, and a common intermediate was suggested.<sup>[26]</sup>

The reaction of the bromo-bearing aryl triflate **44** (Scheme 2.6) with butyllithium at  $-78\text{ }^{\circ}\text{C}$  afforded exclusively **45**, via benzyne generation, as expected for *ortho* metalated aryltriflates. The results obtained up to that point alluded to the generation of intermediates that do not involve Ar-Li binding, for example aryl anions.<sup>[26]</sup>



**Scheme 2.6.** Benzyne generation via triflate elimination after lithium halide exchange at **44**.<sup>[26]</sup>



Following this idea, DFT calculations were carried out to detangle the pathways leading to the rearrangement and elimination intermediates. According to Figure 2.2, the energy of the transition states leading either to elimination or to rearrangement are comparable. However, the resulting 1,3-O→C migration process is much more exothermic than the elimination one. The hypothetical 1,2-oxethietane intermediate **52** was not located during the migration process. One should keep in mind though that the used model is very simple and the starting intermediate has higher potential energy than the elimination transition state, which should be a saddle point and is therefore not in agreement with the transition state theory, which clearly states that a transition state of a reaction has the maximum potential energy.<sup>[27]</sup>

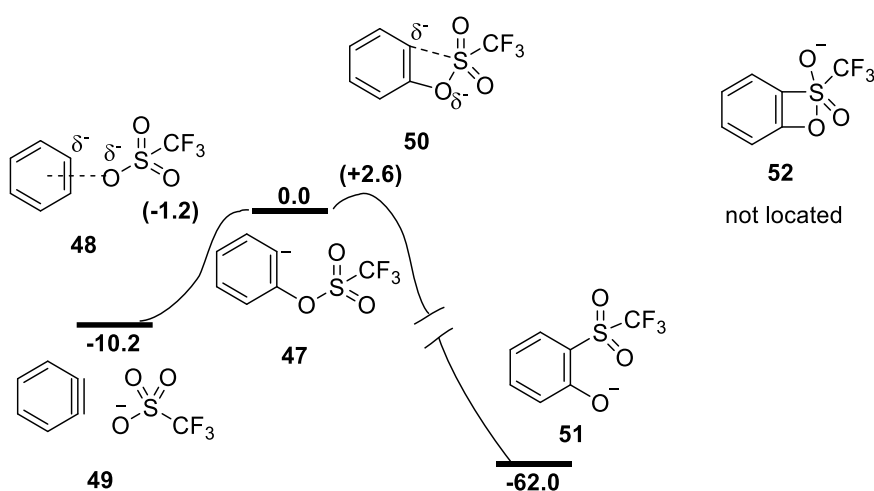
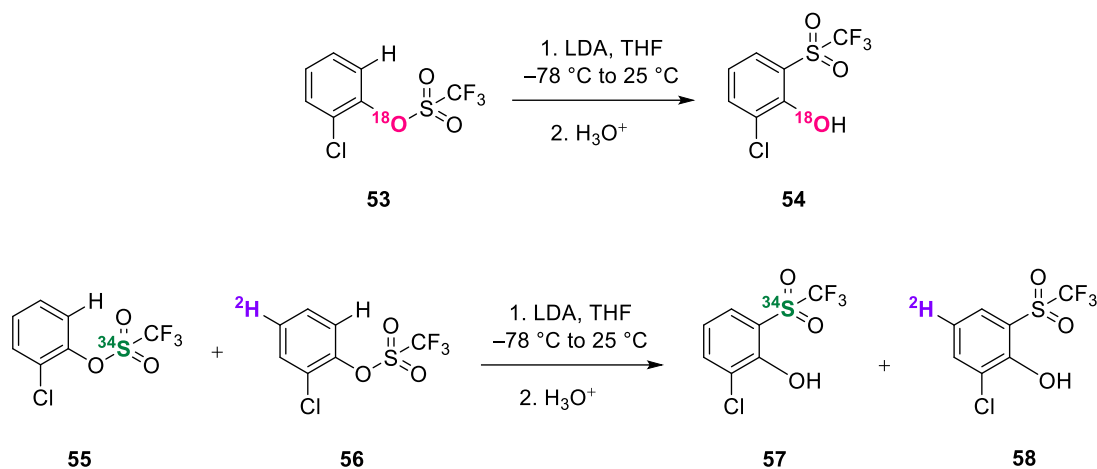


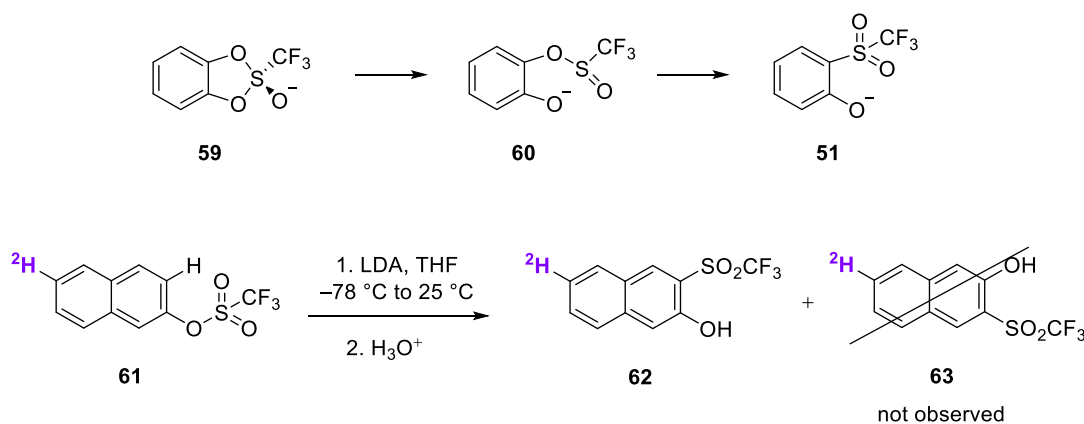
**Figure 2.2.** Gas phase B3LYP/6-31G(d) calculations and single point B3LYP/6-311G(d,p) calculations in continuum THF solvent. Relative energies ( $\text{kcal}\cdot\text{mol}^{-1}$ ) for the elimination or rearrangement of aryl triflate anion.<sup>[26]</sup>

Very interesting isotopic labelling scrambling and crossover experiments were published in the same article by Lloyd-Jones et al.<sup>[26]</sup> to further comprehend the mechanisms behind those transformations. Firstly, there was no  $^{18}\text{O}/^{16}\text{O}$  scrambling in product **54** after the anionic thia-Fries rearrangement of **53**, evidencing no reversible formation of a benzyne/triflate ion-molecule complex. Secondly no crossover was observed when **55** and **56** were reacted with LDA in the same vessel, indicating only intramolecular transfer of the sulfone group as shown in Scheme 2.7.



**Scheme 2.7.** Rearrangement of  $^{18}\text{O}$ -,  $^{34}\text{S}$ -, and  $^2\text{H}$ -labelled **53**, **55** and **56**. Top:  $^{18}\text{O}$ -scrambling experiment. Bottom: Crossover experiment.<sup>[26]</sup>

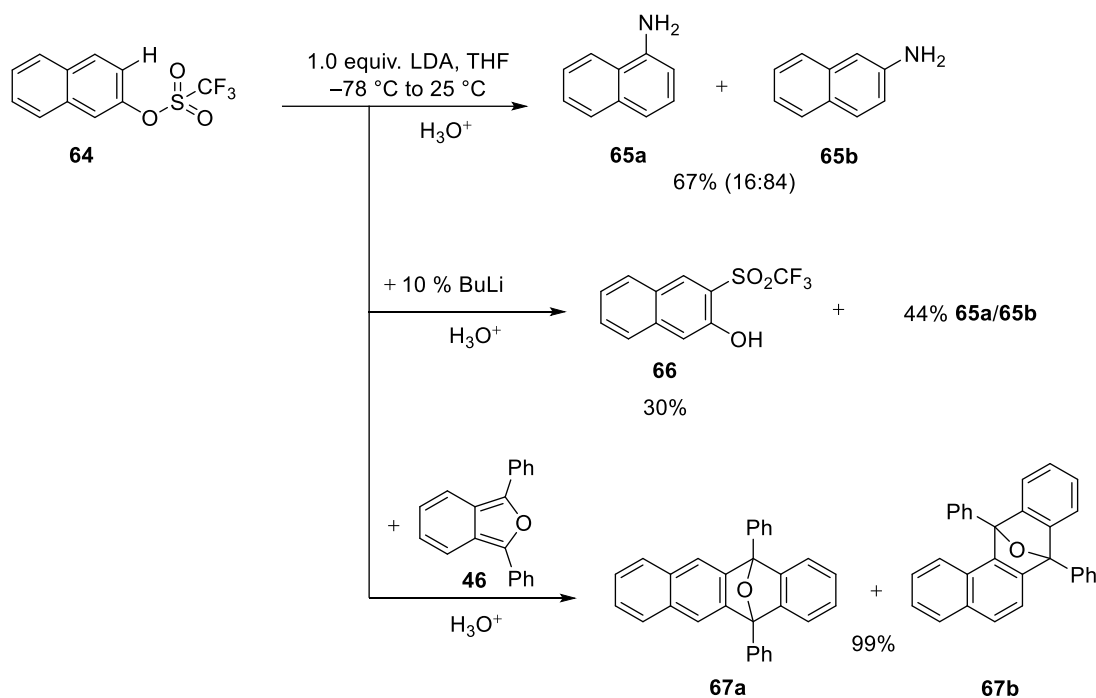
A further isotopic labelling experiment showed that an intramolecular attack of an *ortho* anionic triflate at the sulfonyl oxygen atom via **59** and **60** was not plausible (Scheme. 2.8). Sulfonates are known for being highly reactive and undergo rearrangement to sulfones under non-hydroxylic conditions.<sup>[28]</sup> If this were the case, there would be isomerization of **61**, but instead, only the isomer **62** was obtained, excluding a sulfinate-based mechanism.<sup>[26]</sup>



**Scheme 2.8.** Probing for a sulfinate based mechanism.<sup>[26]</sup>

Lloyd-Jones and et al. also cogitate that the free concentration of DIPA affects the partition between rearrangement and elimination pathways.<sup>[10,26]</sup> Both routes generate DIPA from the

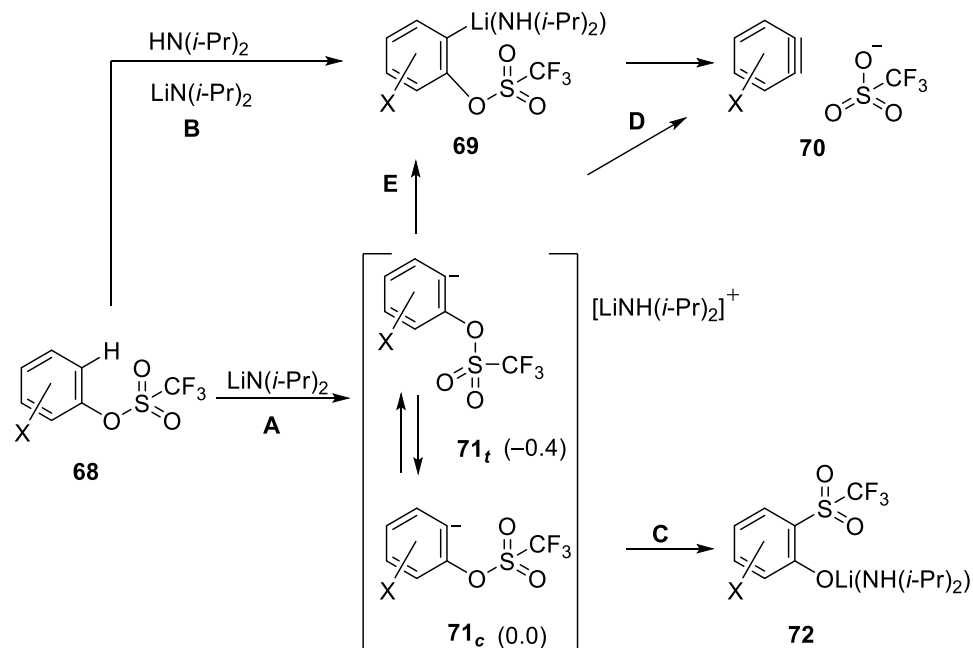
reaction of LDA with aryl triflate,<sup>[10,26]</sup> which remains strongly complexed to the lithium atom in the rearrangement product or reacts with the aryne to generate aryl diisopropylamine.<sup>[10]</sup> Reaction of 2-naphthyl triflate **64** with one equivalent of LDA delivers only 1-naphthylamine **65a** and 2-naphthylamine **65b** (Scheme 2.9). However, the anionic thia-Fries considerably competes upon addition of extra 10 % BuLi, which consumes free DIPA, and **66** is obtained in 30% yield.<sup>[10,26]</sup> To oblige the increase in DIPA concentration bypassing the former consumption trapping generated aryne, 1,3-diphenyl-isobenzofuran (**46**) was added. The addition of the trapping reagent **46** suppresses the formation of the rearranged product and affords 99% yield of naphthalene-DPIBF adducts, as shown in Scheme 2.9.<sup>[10,26]</sup> This reinforces again the solvent's influence on the rearrangement/elimination distribution and suggests that DIPA catalyses aryne generation.<sup>[10,26]</sup>



**Scheme 2.9.** Influence of DIPA and excess of butyllithium governing rearrangement and/or elimination.<sup>[10,26]</sup>

To rationalize all their observations, Lloyd-Jones et al. summarized their finds according to the reactions model in Scheme 2.10, which is subdivided into anionic (**A**: **68** → **72**) and a DIPA-catalysed metalation pathway (**B**: **68** → **70**).<sup>[26]</sup> In pathway **A**, the low activation barriers for the sulfonyl group migration (**C**) and elimination (**D**) shows that the conformation of anion **71** plays

a key role. The intermediate **71<sub>c</sub>** can interconvert to **71<sub>t</sub>** leading to elimination directly heading to **70** or via **69** (**E**). However, Lloyd-Jones et al.<sup>[26]</sup> concluded that aryne is always generated when the triflate is *ortho* lithiated irrespective of the route.



**Scheme 2.10.** Mechanisms models for elimination and rearrangement. The values given for **71** are the relative energies of the transoid and cisoid conformations. Subscripts refers to the anion **71** conformations: *t* = transoid and *c* = cisoid.<sup>[26]</sup>

Much to everyone's surprise, in pursuit of ferrocynes (**75**) and ferrocene-1,1'-diyne (**76**), ferrocene species equivalent of benzyne (**73**) (Figure 2.3), Butenschön et al. reported the first anionic thia-Fries rearrangement at ferrocene in 2010.<sup>[17]</sup> Ferrocene (**74**) is electron rich, and this transformation defies some of Lloyd-Jones et al. conclusions. Ferrocenyl triflate (**79**) was prepared via transesterification of ferrocenyl acetate<sup>[29]</sup> (**77**) with KOH followed by neutralization using hydrochloric acid forming the corresponding triflate **79** in 90 % yield upon reaction with triflic anhydride in the presence of pyridine (Scheme 2.11). 1,1'-ferrocenediyl ditriflate (**80**) was prepared in the same way as the latter (Scheme 2.11).<sup>[17]</sup>

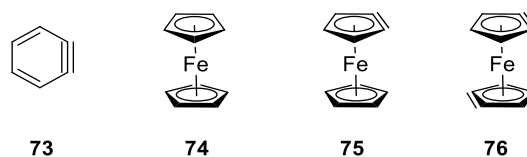
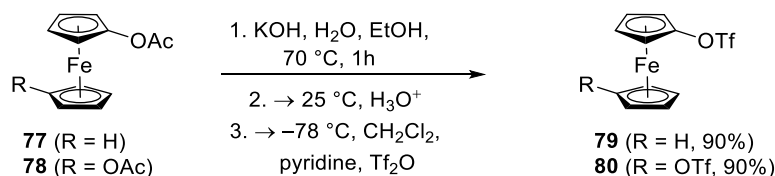
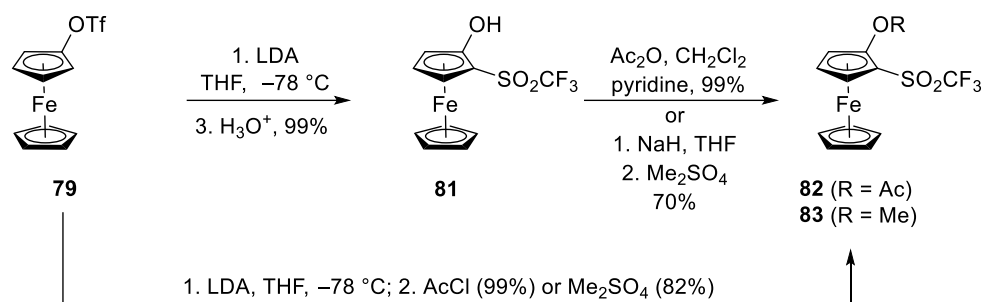


**Figure 2.3.** Benzyne or 1,2-didehydrobenzene (**73**), ferrocene (**74**), ferrocene or 1,2-didehydroferrocene (**75**) and ferrocenediynes or 1,2,1',2'-tetrahydroferrocene (**76**).<sup>[17]</sup>



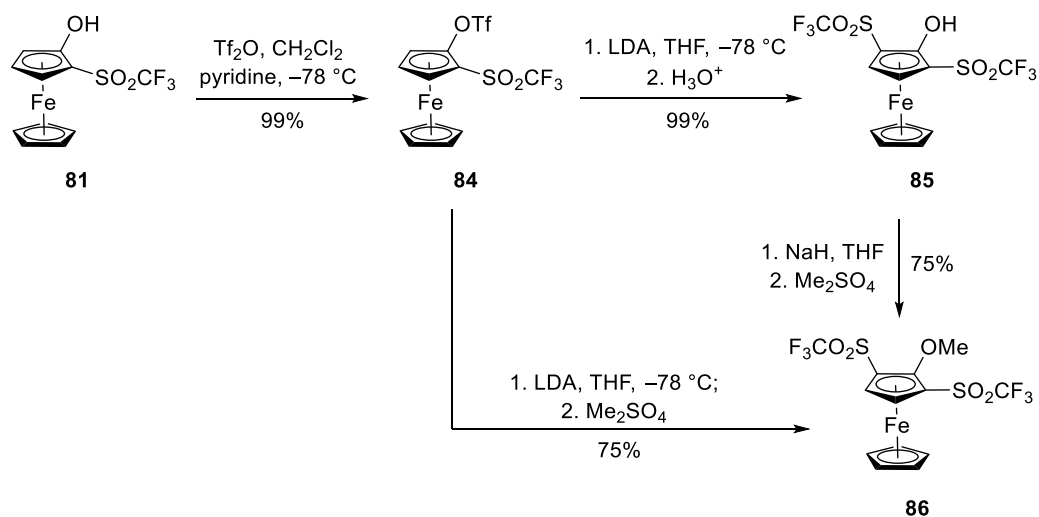
**Scheme 2.11.** Synthesis of ferrocenyl triflate (**79**) and 1,1'-ferrocenediyl ditriflate (**80**) (OTf = SO<sub>2</sub>CF<sub>3</sub>).<sup>[17]</sup>

To avoid a nucleophilic attack on the triflate sulfur atoms, lithium diisopropylamide was chosen as a non-nucleophilic base for the attempted deprotonation and desired ferrocene generation. In the presence of trapping reagents (such as furan, 2,5-dimethylfuran, 1,3-diphenylisobenzofuran (**46**), anthracene, 2,3,4,5-tetraphenylcyclopentadienone), ferrocenyl triflate (**79**) was treated with LDA at  $-78\text{ }^{\circ}\text{C}$  followed by aqueous work-up affording 2-(trifluoromethylsulfonyl)ferrocenol (**81**) in almost quantitative yield (Scheme 2.12). There was no observation of ferrocene (**75**) or trapping via adduct formation.<sup>[17]</sup> Despite an electron-rich system, ferrocenyl triflate (**79**) undergoes a highly efficient anionic thia-Fries rearrangement rather than triflate elimination, in contradiction to the observations and proposals of Lloyd-Jones et al. The reaction was also successful without trapping reagents as in Scheme 2.12 and at a temperature as low as  $-117\text{ }^{\circ}\text{C}$  after a brief induction period.<sup>[17]</sup> The protected ferrocenols **82** and **83** were prepared directly or via ferrocenol **81** with acetyl chloride or dimethyl sulfate. Ferrocenol **81** was protected due to ferrocenols known sensitivity towards oxygen.<sup>[30]</sup>



**Scheme 2.12.** Anionic thia-Fries rearrangement of ferrocenyl triflate (**79**).<sup>[17]</sup>

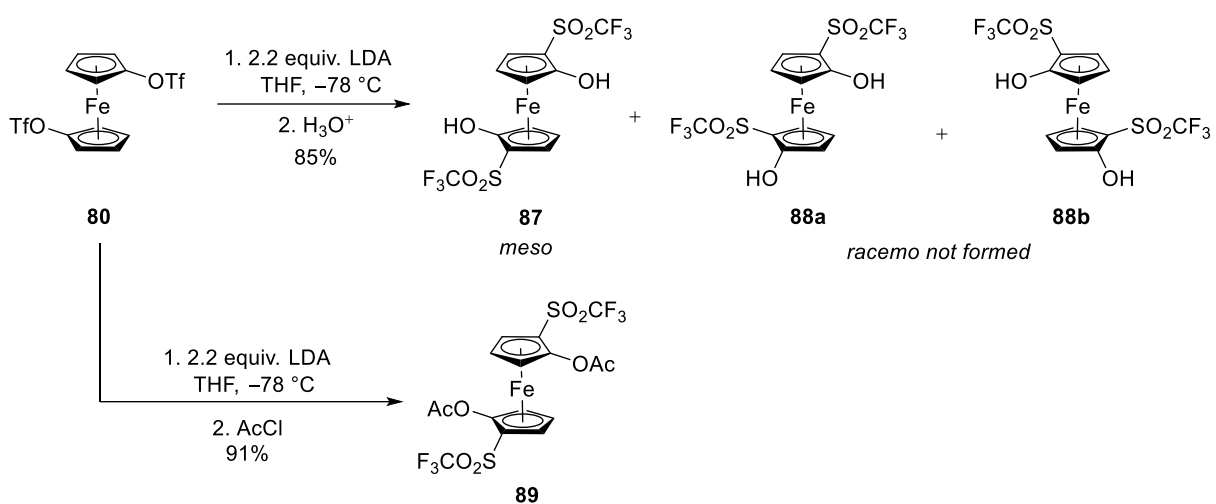
The exceptional facility of this transformation is visualized following the synthesis of **86**, which results from a second rearrangement from the outcome of a first anionic thia-Fries at **79** protected with triflic anhydride (Scheme 2.13). Compound **84** has a diminished electronic density which should help with a second anionic thia-Fries rearrangement at the same ring.<sup>[17]</sup>



**Scheme 2.13.** Twofold anionic thia-Fries rearrangement of ferrocenyl triflate(**79**) via **84**.<sup>[17]</sup>

A double anionic thia-Fries rearrangement was also achieved upon treatment of 1,1'-ferrocenediyl ditriflate (**80**) with 2.2 equivalents of LDA in THF at -78 °C and a remarkable diastereoselectivity was observed (Scheme 2.14). In theory, the two rearrangement products, *meso* **87** and *racemo* **88**, could have been obtained, however, only the *meso* isomer **87** was observed. The configuration was demonstrated via X-ray crystal structure analysis of the

respective diacetate **89**, as shown in Figure 2.4. The compound **89** was afforded in 91% yield by quenching the reaction with acetyl chloride.



**Scheme 2.14.** Double anionic thia-Fries rearrangement at **80**.<sup>[17]</sup>

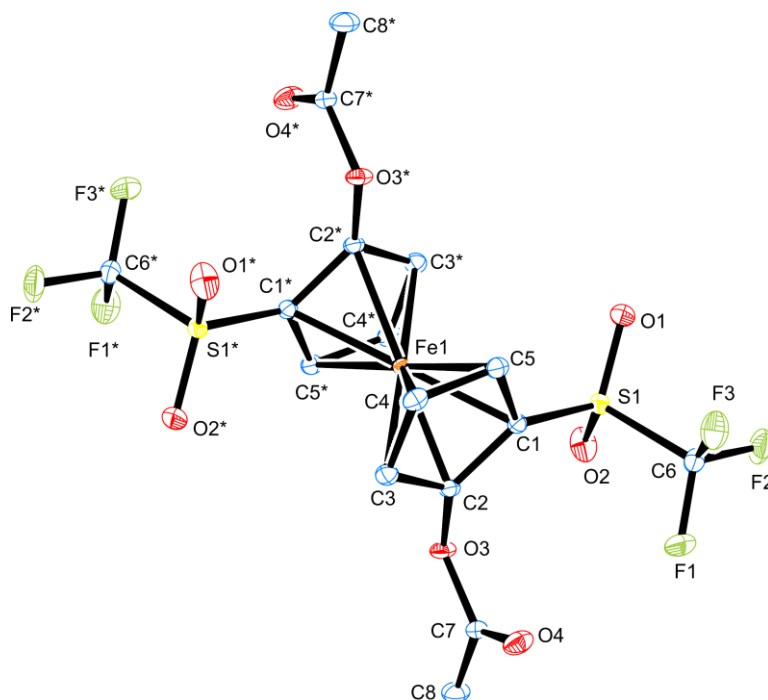
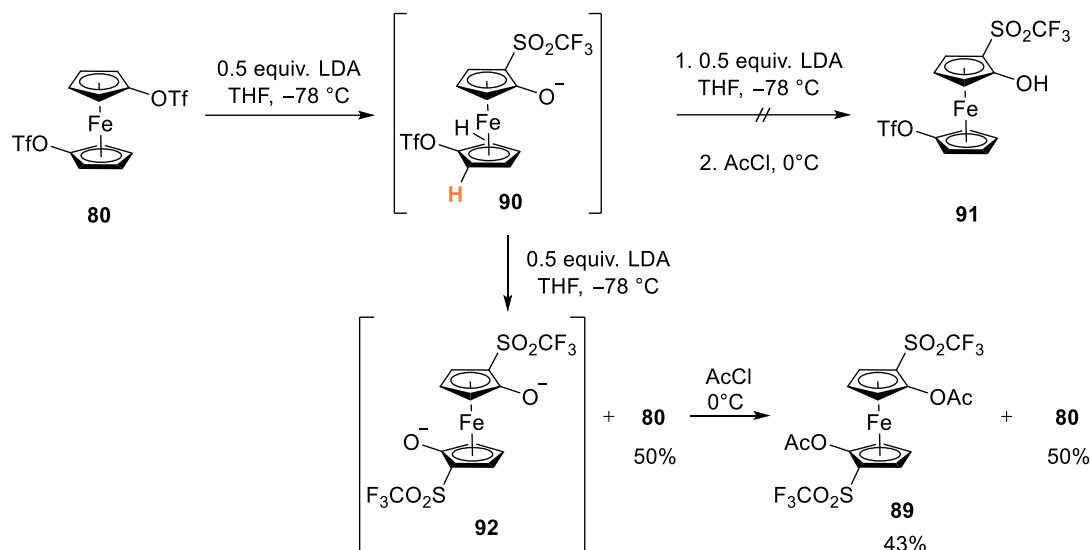


**Figure 2.4.** Crystal structure of **89**. Hydrogen atoms have been omitted for clarity.<sup>[17]</sup>

In an effort to better understand this exceptional diastereoselectivity, Butenschön et al. planned a single thia-Fries rearrangement of **80** by treating it with 1.0 equivalent of LDA (instead of 2.2 equiv.) followed by quenching with acetyl chloride, which did not afford the expected product **91**. Instead, the double thia-Fries rearrangement took place, and **89** was obtained in 43% yield and half of the starting material **80** was recovered (Scheme 2.15).<sup>[17]</sup> This result suggests that the rearrangement at the second cyclopentadienyl ligand is faster than that at the first one.<sup>[17]</sup> The reason for such an impressive stereoinduction is not yet known.



**Scheme 2.15.** Double anionic thia-Fries rearrangement with 1 equivalent of LDA.<sup>[17]</sup>

## 2.2. Results and discussion

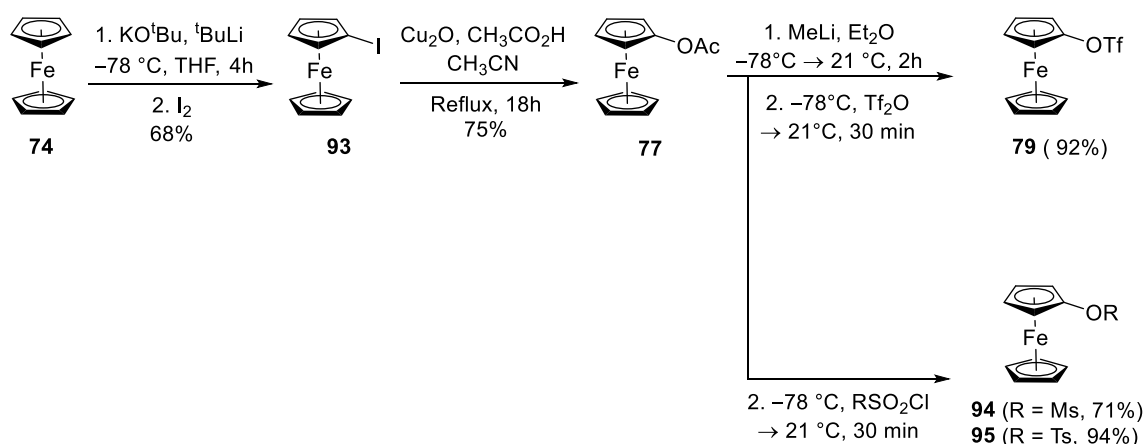
### 2.2.1. Extension of the scope of the anionic thia-Fries rearrangement to other functional groups

In order to broaden the scope of the anionic thia-Fries rearrangement as a synthetic tool for the formation of *ortho* substituted sulfonyl groups, it was decided to investigate whether this strategy could be used for other organosulfonates besides triflates or nonaflates.<sup>[31]</sup> The investigation started with the synthesis of ferrocenyl triflate (**79**),<sup>[17]</sup> ferrocenyl tosylate<sup>[31]</sup> (**95**)



and ferrocenyl mesylate (**94**) (Scheme 2.16). Trifluoromethanesulfonic anhydride is useful for converting alcohols and phenols into triflate groups in the presence of a base (usually pyridine), in an inert solvent (usually dichloromethane). When triflic anhydride and pyridine (**96**) are combined, the pyridium salt **97** is formed immediately, and this salt is an effective esterifying agent, forming the respective triflate **98** and the salt **99** (Scheme 2.17). This approach was used by Butenschön et al. to synthesise **79** starting from hydroxyferrocene (**100**).<sup>[17]</sup> Surprisingly, the synthetic path used by Werner to synthesise ferrocenyl tosylate (**95**)<sup>[31]</sup> worked for ferrocenyl triflate (**79**) too. This last synthetic pathway avoids the handling and laborious work-up of the oxygen sensitive ferrocenol.

The compounds **79**, **94** and **95** were then synthesised from ferrocenyl acetate<sup>[30]</sup> via ferrocenolate, upon addition of methyl lithium followed by trapping with the corresponding sulfonyl chloride/sulfonyl anhydride (Scheme 2.16). Ferrocenyl acetate (**77**) itself is obtained from iodoferrocene (**93**) via a Ullmann type reaction.<sup>[30]</sup> Iodoferrocene (**93**) was obtained from lithiation of ferrocene using Lochmann-Schlosser base followed by electrophilic trapping using iodine.<sup>[32]</sup> The new compound **94** is a yellow air stable solid, which should be stored in a protected atmosphere for long periods. The solid was crystallized at  $-30\text{ }^{\circ}\text{C}$  in DCM and suitable single crystals were obtained for X-ray analysis. Although the crystal structure analysis had a poor quality it was useful to visualise the compound arrangement. The crystal structure analysis shown in Figure 2.5. displays a monoclinic crystal system, space group P 21/c (14). The cyclopentadienyl rings are eclipsed and the dihedral angle C3–C2–C1–O1 of  $-179^{\circ}$  shows that the oxygen atom is co-planar.



**Scheme 2.16.** Synthesis of ferrocenyl triflate (**79**),<sup>[17]</sup> ferrocenyl tosylate(**95**)<sup>[31]</sup> and ferrocenyl mesylate (**94**).



**Scheme 2.17.** Trifluoromethanesulfonylation of alcohols using trifluoromethanesulfonic anhydride and pyridine.<sup>[33]</sup>

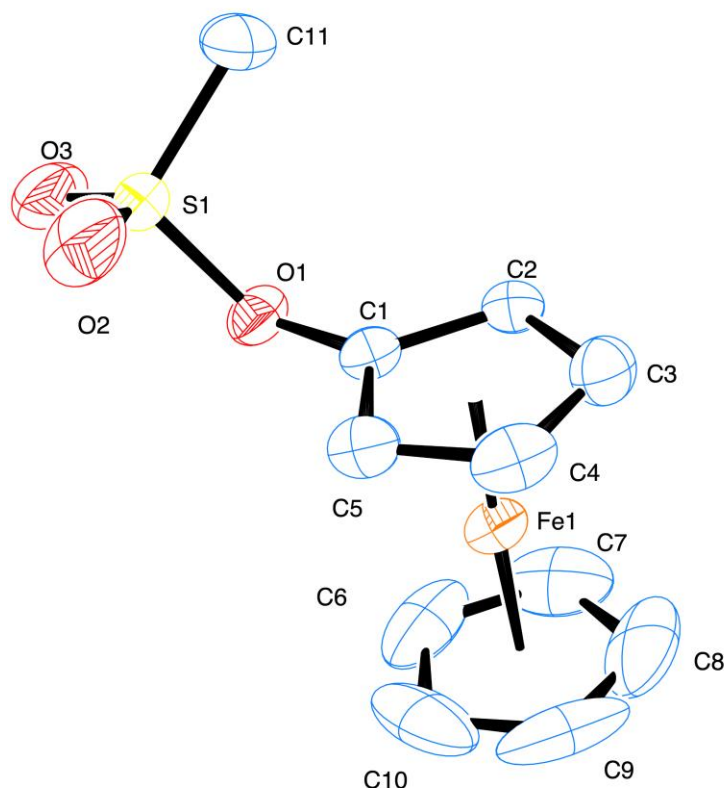


**Figure 2.5.** Crystal structure of **94**. Ellipsoids at 50 % probability level. Hydrogen atoms have been omitted for clarity. Selected bond lengths [pm], angles [°] and dihedral angles [°]: C1–C2 141.4(5), C2–C3 142.1(5), C3–C4 140.3(5), C4–C5 141.6(5), C5–C1 141.8(4), C1–O1 140.1(4), O1–S1 160.1(2), S1–O2 140.7(3), S1–O3 141.3(3), S1–C11 174.0(4); C2–C1–O1 123.2, C1–O1–S1 117.8, O1–S1–C11 103.6, O2–S1–O3 119.8; C3–C2–C1–O1 –179.2.

The compound **95** is not new, however, the crystal structure is not known. The solid of **95** was then crystallized at  $-30\text{ }^{\circ}\text{C}$  in DCM and suitable single crystals were also obtained for X-ray

analysis. Again, the crystal structure analysis had a poor quality, but it is still useful to visualise the compound **95** structure.

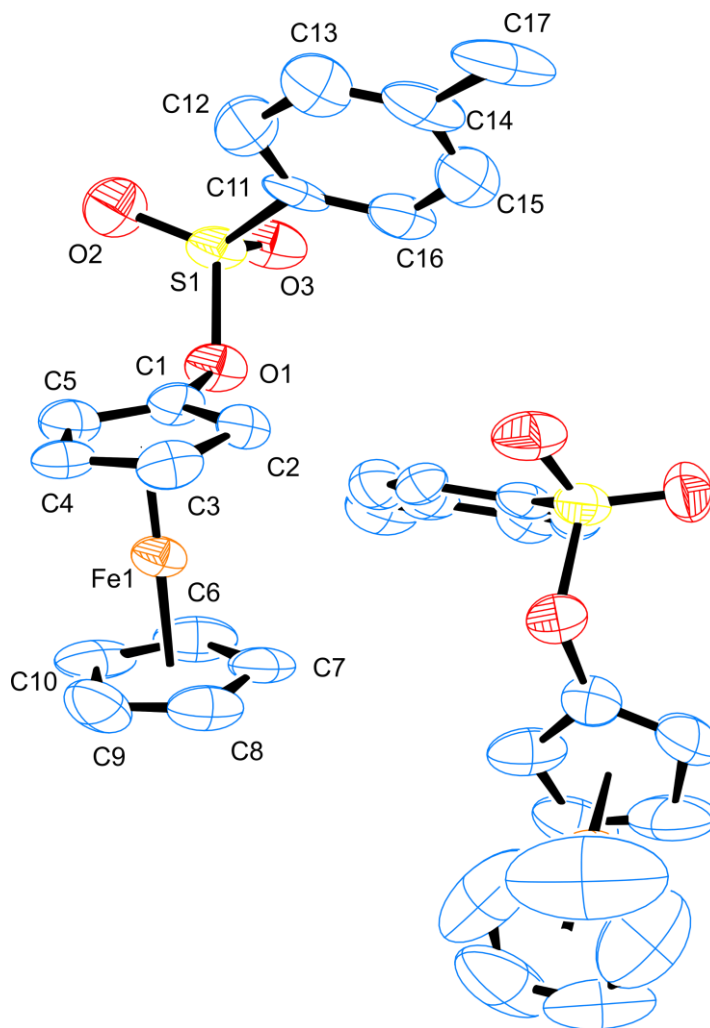
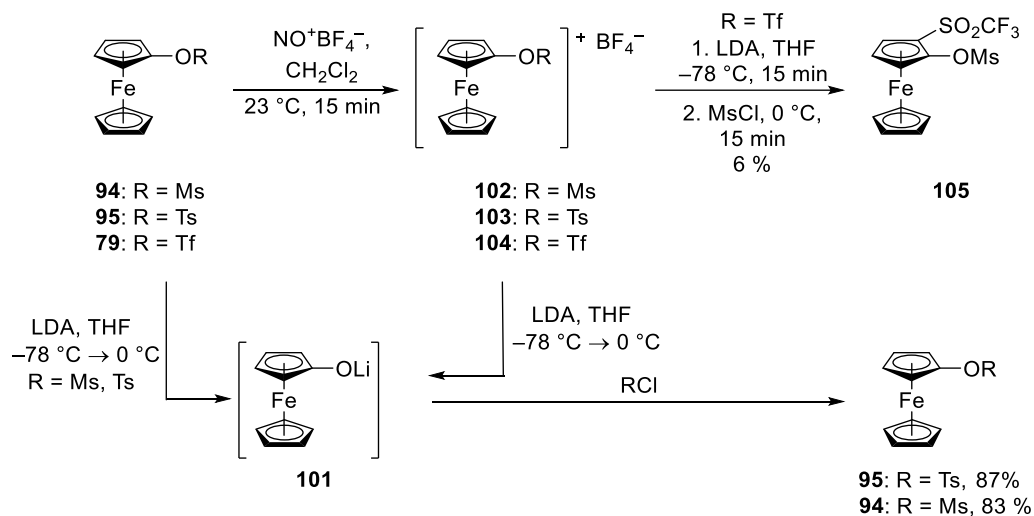


**Figure 2.6.** Crystal structure of **95**. Ellipsoids at 50 % probability level. Hydrogen atoms have been omitted for clarity. Selected bond lengths [pm], angles [°] and dihedral angles [°]: C1–C2 142.3(14), C2–C3 144.4(16), C3–C4 139.3(17), C4–C5 139.3(16), C5–C1 140.5(18), C1–O1 141.9(13), O1–S1 159.4(8), S1–C11 178.0(12), S1–O2 143.2(11), S1–O3 142.0(9); O2–S1–O3 122.2, C2–C1–O1 121.7, C1–O1–S1 118.3, O1–S1–C11 104.4; C3–C2–C1–O1 –179.6.

The ferrocenyl sulfonates **94** and **95** were then treated with LDA in THF affording only lithium ferrocenolate (**101**), which was trapped by addition of mesyl or tosyl chloride to afford **94** and **95** in 83 and 87 % yields, respectively (Scheme 2.18). To increase the acidity of the *ortho* protons, and possibly facilitate a deprotonation and thereby a presumptive anionic thia-Fries

rearrangement, **79**, **94** and **95** were oxidized with nitrosyl tetrafluoroborate to give the ferrocenium salts **102-104** (Scheme 2.18). The new compounds **102-104** were characterized by infrared spectroscopy, by mass spectrometry and a typical change in colour to either blue or green, characteristic of ferrocenium compounds. In the IR spectra of **102**, **103** and **104**, it is possible to see a very strong and broad band around  $1000\text{ cm}^{-1}$ . This band is not present in their neutral equivalents, **94**, **95** and **79**. According to DFT vibrational assignments of 1-ethyl-3-methyl imidazolium tetrafluoroborate, vibrations at  $979$ ,  $1033$ ,  $1047$  and  $1053\text{ cm}^{-1}$  were assigned the  $\text{BF}_4$  anion (asymmetric stretch).<sup>[34]</sup> Further purification was precluded by the sensitivity of these compounds and the compounds were used freshly prepared. Upon treatment with LDA an anionic thia-Fries rearrangement was observed in the case of the triflate **104** giving **105** in only 6 % yield. In contrast to **104**, mesylate **102** and tosylate **103** gave **101** without further addition of a reducing agent.



**Scheme 2.18.** Attempted anionic thia-Fries rearrangement at ferrocenyl mesylate (**94**) and ferrocenyl tosylate (**95**).

The reason for the ferrocenolate **101** formation in detriment of the rearrangement product was not clear. To further investigate the reasons behind it, the molecular orbitals (HOMO to HOMO – 4) and Mulliken charges of **79**, **94** and **95** were calculated and compared, as shown in Figure 2.7 and 2.8. The gas phase calculations were performed using the Gaussian<sup>[35]</sup> software, the functional PBE0<sup>[36–38]</sup> and basis set LANL2DZ<sup>[39–42]</sup> and LANL<sup>[39–42]</sup> for valence and core electrons of iron, respectively. 6-311+G(d,p)<sup>[43–45]</sup> was used for all other atoms.

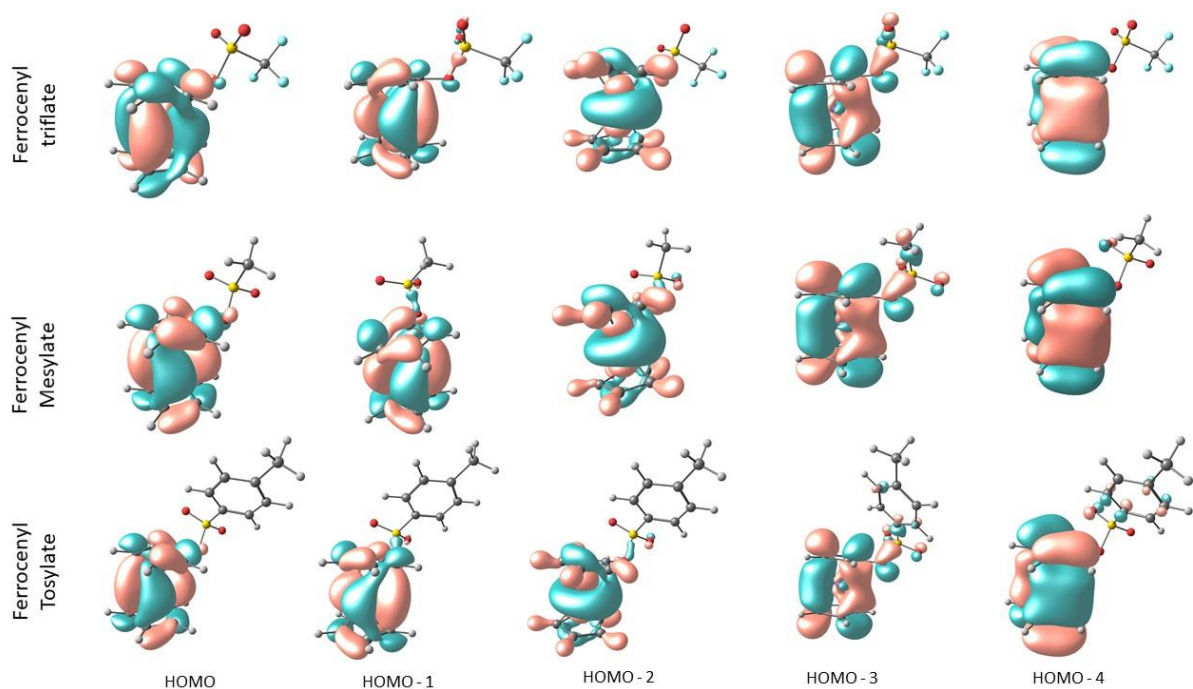


**Figure 2.7.** Calculated molecular orbitals of **79**, **94** and **95**.

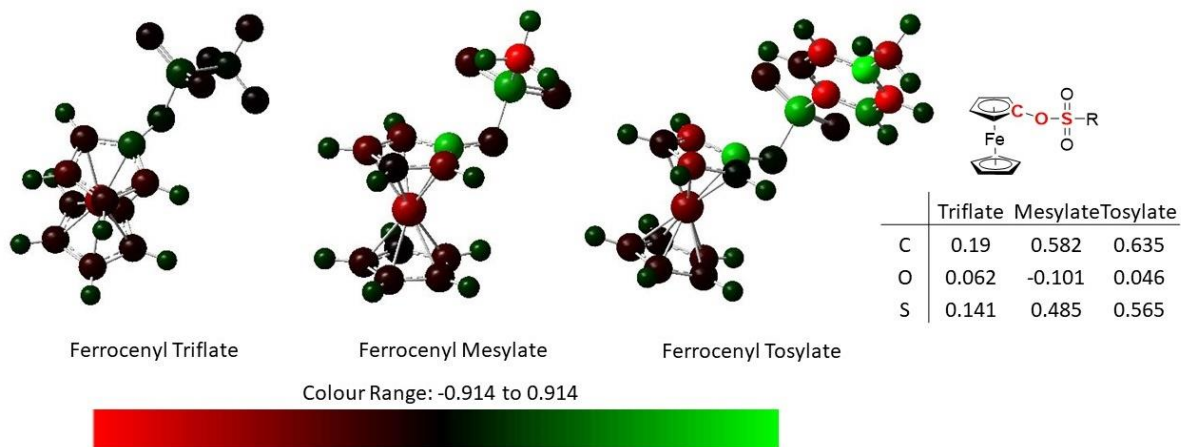


**Figure 2.8.** Mulliken atomic charge ( $e$ ) distribution of **79**, **94** and **95**.

In Figure 2.7 it is possible to see that the orbitals of **79**, **94** and **95** from HOMO to HOMO –4 are similar and therefore was not valuable to explain why the rearrangement did not take place. However, the Mulliken charge distribution looked rather different between the ferrocenyl triflate

(**79**) and the ferrocenyl mesylate (**94**) and tosylate (**95**). The acidity of the *ortho* proton was similar, but it is possible to see in Figure 2.8 that the sulfur atoms and the cyclopentadienyl carbon atoms adjacent to the oxygen atoms at **94** and **95** are much more acidic than those at **79** which might facilitate a nucleophilic attack at the sulfur atom. Nevertheless, this information did not seem to be crucial enough to solve the problem.

It is important to keep in mind that sulfones are among the most powerful of the *ortho* directing groups,<sup>[46]</sup> as shown in Figure 2.9, and this might indicate that a deprotonation did happen, but not on the ferrocenyl side of the molecule.

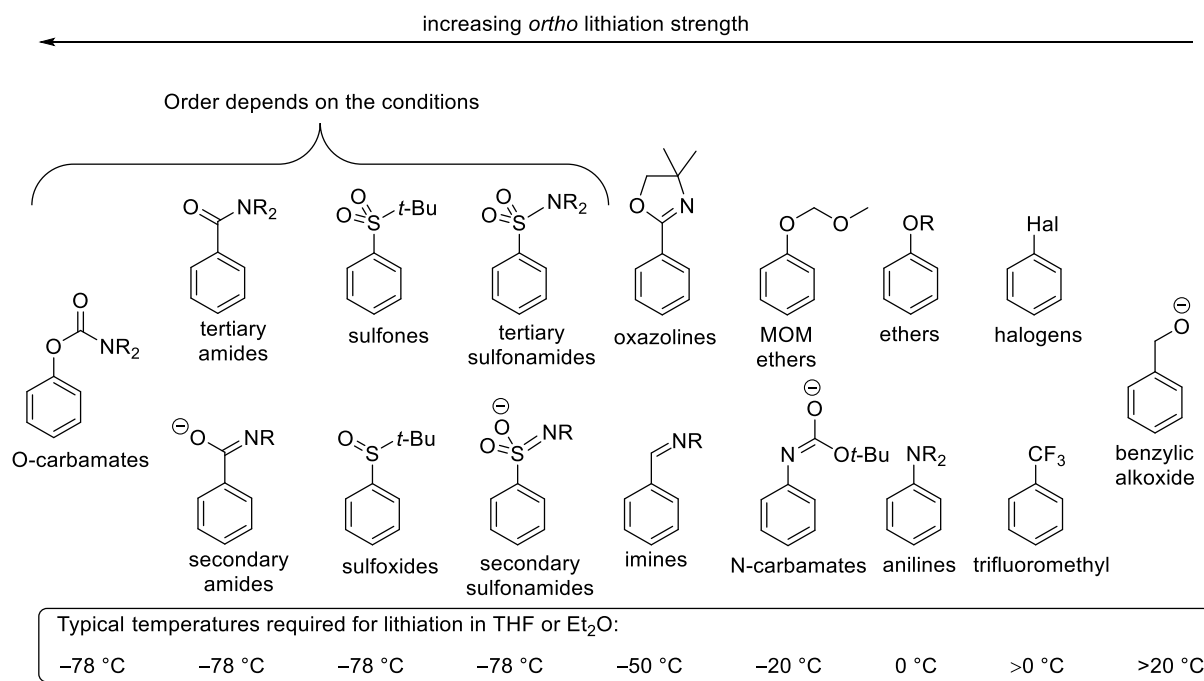
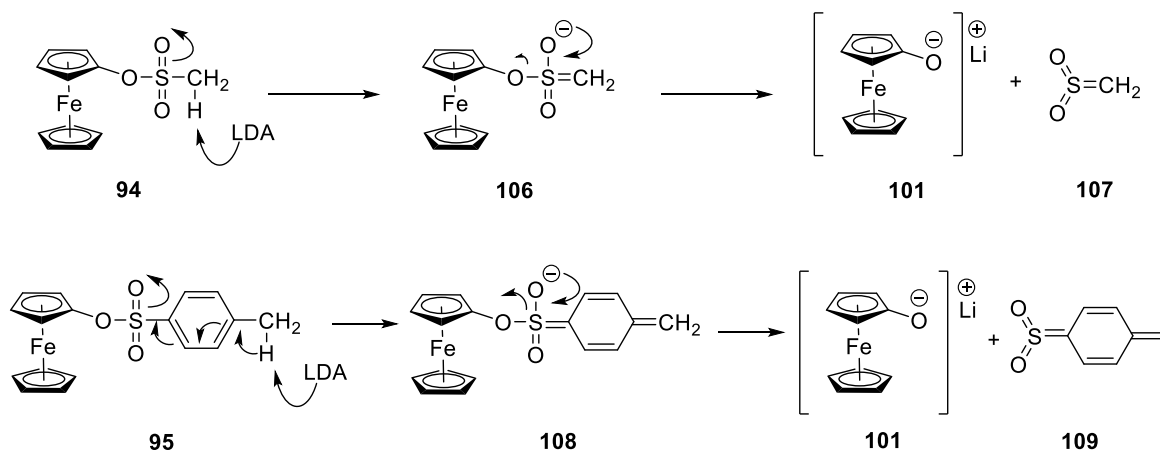


**Figure 2.9.** General overview of *ortho* lithiation directing groups and their relative strength.<sup>[46]</sup>

Presumably, a methyl proton of the mesyl or tosyl group was removed allowing for the formation of the respective sulfenes **107** and **109** and ferrocenolate **101** (Scheme 2.19). In this context it is of interest that Carreira et al. reported the treatment of methanesulfonates with lithium diisopropylamide in THF as a mild chemoselective deprotection method for phenyl mesylates. The reactions were repeated, and furan was added to the reaction in an unsuccessful attempt to trap the putative respective sulfenes.



**Scheme 2.19.** Possible mechanism for the formation of ferrocenolate **101** via sulfene derivative formation upon treatment of **94** and **95** with LDA in THF.

As the nature of the sulfonyl substituent appears to be critical for the course of the reaction, some other ferrocenyl arylsulfonates **110** - **114** were prepared in a similar fashion to the ferrocenyl tosylate (**95**)<sup>[31]</sup> (Table 2.1) and tested for their ability to undergo an anionic thia-Fries rearrangement upon treatment with LDA or with lithium 2,2,6,6-tetramethylpiperidide (LiTMP). However, none of them underwent an anionic thia-Fries rearrangement. While **111**<sup>[29]</sup>, **113** and **114** reacted, with the formation of ferrocenolate **101** as indicated by electrophilic trapping or by TLC/MS analysis spotting hydroxyferrocene (**100**), no reaction was observed with the sterically highly crowded **112**.

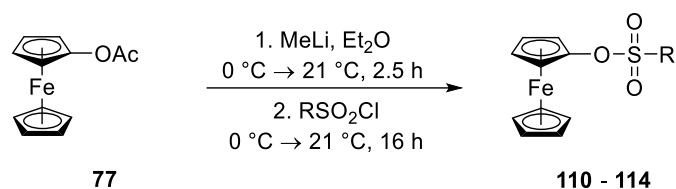


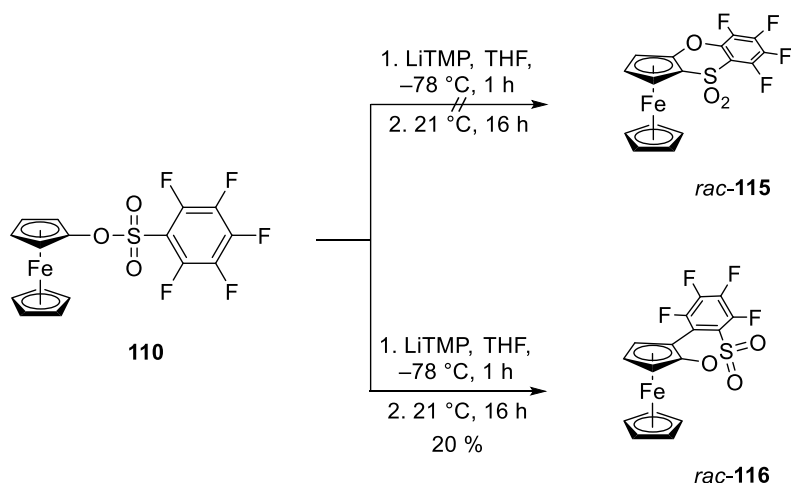
**Table 2.1.** Synthesis of ferrocenyl sulfonates **110 - 114**.

Entry	R	Product	Yield [%]
1		<b>110</b>	50
2		<b>111</b>	83
3		<b>112</b>	93
4		<b>113</b>	90
5		<b>114</b>	67

Ferrocenyl (2,3,4,5,6-pentafluorophenyl)sulfonate (**110**) contains an even more electron withdrawing aryl substituent, and lacks any hydrogen atoms at the sulfonyl substituent which could possibly be abstracted, leading to a sulfene derivative and was expected to undergo anionic thia-Fries rearrangement. When **110** was treated with LiTMP at  $-78$  °C, the yellow solution turned immediately purple. Subsequently, after stirring the solution for 1 h at  $-78$  °C and then warming to 21 °C over 16 h, a stable red solid was obtained. The ferrocene-annulated 1,4-oxathiine-4,4-dioxide *rac*-**115** was thought to be the reaction product resulting from an anionic thia-Fries rearrangement followed by an intramolecular nucleophilic substitution. However, it turned out that after deprotonation, the rearrangement had not taken place, but



instead was directly followed by an intramolecular nucleophilic aromatic substitution affording the ferrocene annelated 6,7,8,9-tetrafluorobenzo[*c,e*]-[1,2]oxathiine 5,5-dioxide *rac*-**116** as a red solid in 20 % yield (Scheme 2.20).



**Scheme 2.20.** Formation of 6,7,8,9-tetrafluorobenzo[*c,e*]-[1,2]oxathiine 1,1-dioxide *rac*-**116**.

Crystallization of *rac*-**116** via slow evaporation of a solution of *rac*-**116** in ethyl acetate rendered single crystals suitable for X-ray analysis. Although only a low-quality X-ray structure analysis was obtained, it confirmed the identity of the compound *rac*-**116** (Figure 2.10). The structure of *rac*-**116** in the crystal displays a pair of enantiomers. It is possible to see that the oxygen atom O1 is above the plane and that the sulfur atom S1 is below the plane. The distance between the C12–C11 is 146 pm, a bit shorter for a carbon-carbon single bond length, indicating a certain degree of conjugation between the cyclopentadienyl ring and the phenyl ring. It can also be observed in the calculated molecular orbitals, HOMO – 8 and HOMO – 2 as shown in Figure 2.11. The gas phase calculations were performed using the Gaussian<sup>[35]</sup> software, the functional PBE0<sup>[36–38]</sup> and basis set LANL2DZ<sup>[39–42]</sup> and LANL<sup>[39–42]</sup> for valence and core electrons of iron, respectively. 6-311+G(*d,p*)<sup>[43–45]</sup> was used for all other atoms.

Fluorinated benzo[*c,e*][1,2]oxathiine 5,5-dioxides are rare, and *rac*-**116** is the first derivative with more than one fluorine substituent. The very small number of monofluorinated derivatives were obtained by radical reactions by Motherwell et al.<sup>[47,48]</sup> In contrast, the formation of *rac*-**116** is explained by an *ortho* lithiation of **110** followed by an intramolecular nucleophilic aromatic substitution with a newly formed carbon-carbon bond.

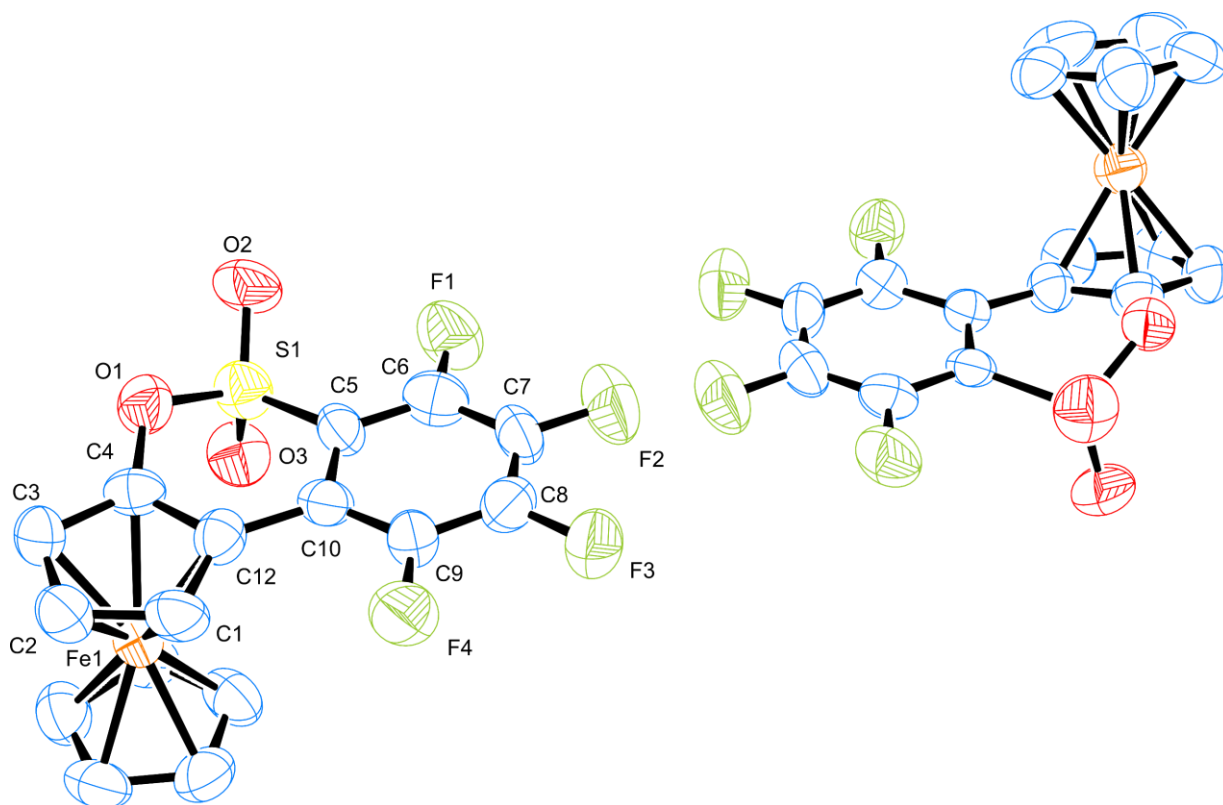


**Figure 2.10.** Crystal of *rac*-**116** featuring the pair of enantiomers. The average C–F bond distance is 134 pm and S=O is 142 pm. Selected bond lengths [pm] and angles [°] and dihedral angles [°]: C1–C2 141.1(8), C1–C12 142.5(8), C12–C11 145.9(8), C2–C3 141.0(8), C3–C4 140.0(8), C4–C12 141.4(8), C4–O1 140.1(7), O1–S1 160.0(4), S1–C6 175.8(6), C6–C11 141.2(8), Fe1–C1 202.8(6), Fe1–C2 204.6(6), Fe1–C3 205.0(6), Fe1–C4 200.2(7), Fe1–C12 203.3(6) pm; C4–O1–S1 119.8, O1–S1–C6 102.0, S1–C6–C11 121.8; C4–C12–C11–C6 –3.7, C12–C11–C6–S1 –7.8, C2–C3–C4–O1 –168.0.

In an attempt to increase the yield of *rac*-**116**, the reaction was repeated, more equivalents of base were used, and the solution was stirred for 5 h at –78 °C before bringing it to room temperature. The yield of red solid obtained did not change, but the NMR spectra showed two different compounds, which could not be separated. The new NMR peaks are similar in shape to the peaks of *rac*-**116**, apart from those at  $\delta = 4.4$  ppm, as shown in Figure 2.12. VT NMR measurements of *rac*-**116** did not show any changes in the spectra. It can only be speculated that the peaks belong to a small amount of *rac*-**115** formed in the reaction.

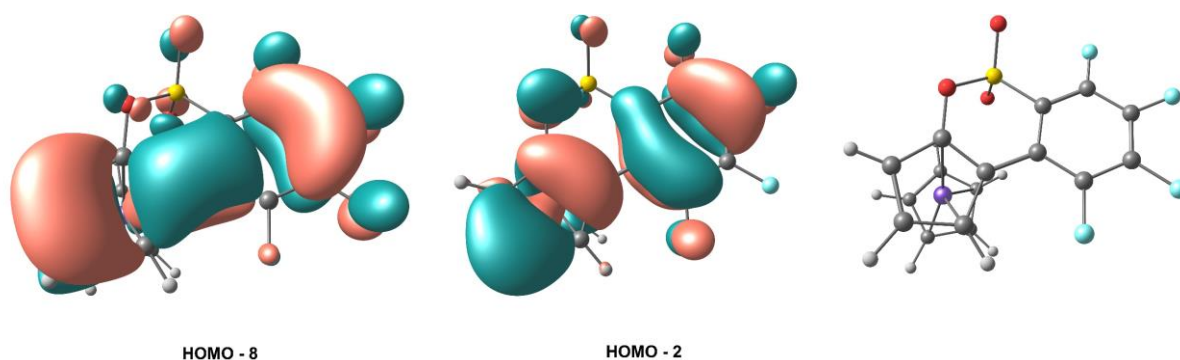


**Figure 2.11.** Calculated molecular orbitals of *rac*-116. The left molecular orbital is HOMO – 8, the centre is the HOMO – 2 and on the right the calculated molecule skeleton of *rac*-116 for correlation is displayed. A racemic mixture was obtained but only one enantiomer is shown (*R*). Grey spheres: carbon atoms; off-white spheres: hydrogen atoms; red spheres: oxygen atoms; purple sphere: iron atom; blue spheres: fluorine atoms.

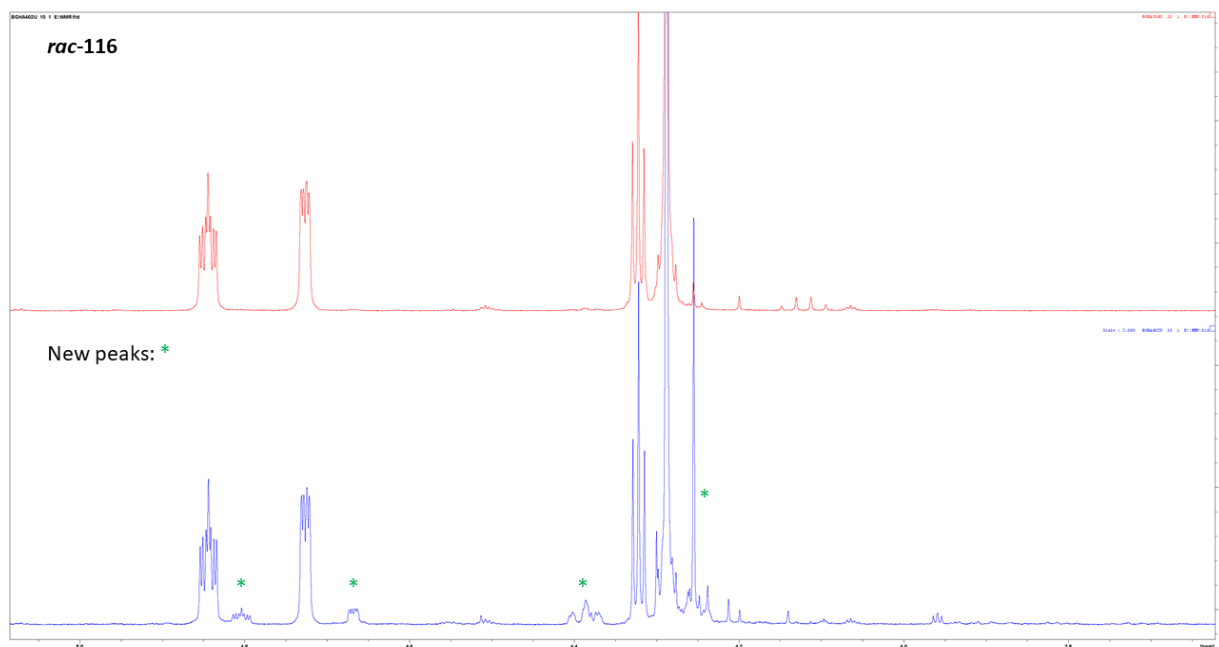


**Figure 2.12.** NMR stacking plot of *rac*-116 and the red solid obtained when prolonging the first step of the reaction in the presence of an increased amount of base.

The new ferrocene annellated oxathiin *rac*-**116** is not only a very interesting compound, but it also possesses an interesting  $^{13}\text{C}$  NMR spectrum, due to the large  $^{19}\text{F} - ^{13}\text{C}$  coupling pattern. The  $^{19}\text{F} - ^{13}\text{C}$  couplings are large, and besides one bond CF coupling constant, the  $^{13}\text{C}$  NMR spectra also shows two, three and even four CF coupling constants (Figures 2.13 to 2.16). The pattern of the CF correlations was already very helpful for the assignment of carbons, but to be sure and to correlate the fluorine atoms, a  $^{19}\text{F} - ^{13}\text{C}$  NMR and  $^{19}\text{F} - ^{13}\text{C}$  HMQC were measured.

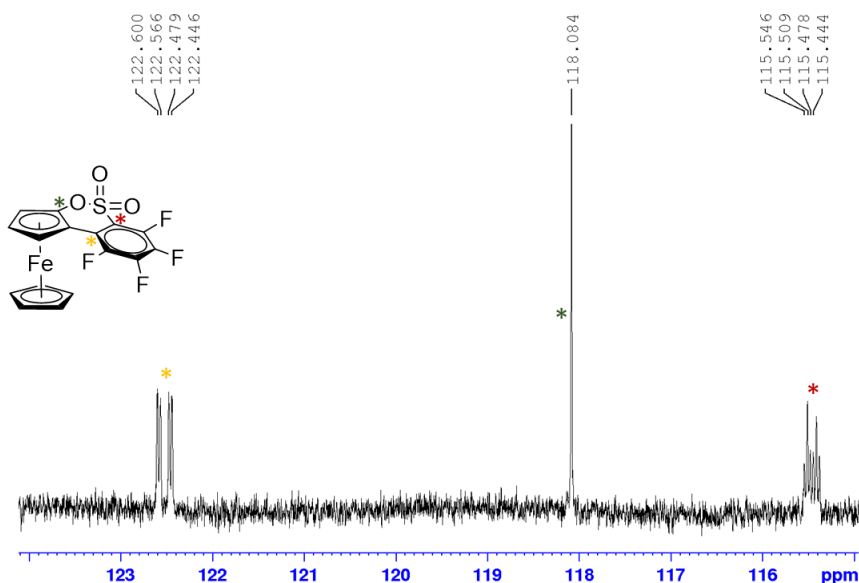


**Figure 2.13.**  $^{13}\text{C}$  NMR of *rac*-**116** displaying long range  $^{19}\text{F} - ^{13}\text{C}$  coupling.

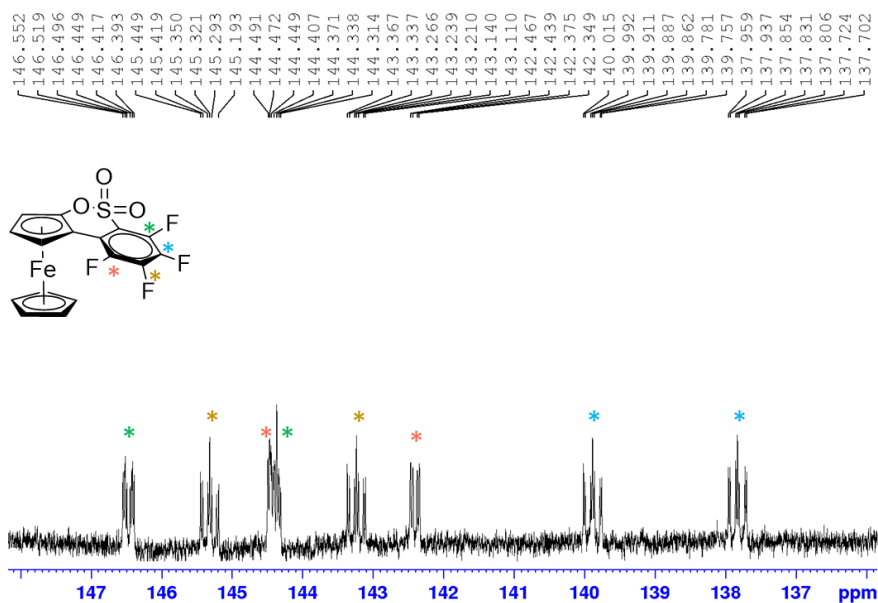


**Figure 2.14.**  $^{13}\text{C}$  NMR of *rac*-**116** displaying short and long range  $^{19}\text{F} - ^{13}\text{C}$  couplings.

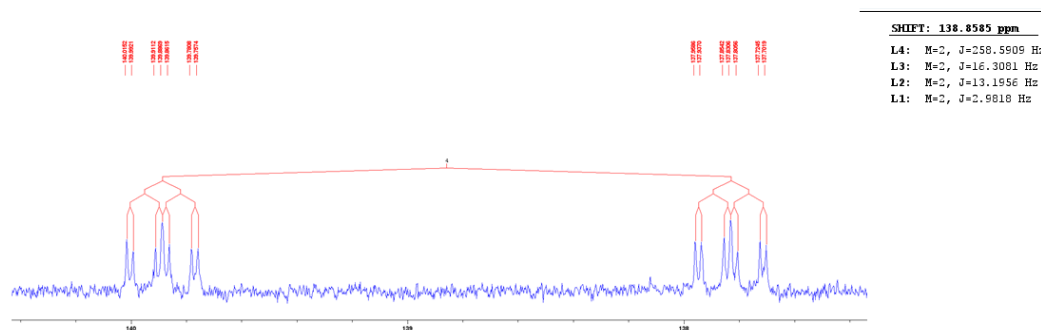


**Figure 2.15.**  $^{13}\text{C}$  NMR extension of *rac*-**116** between 138 ppm and 140 ppm.

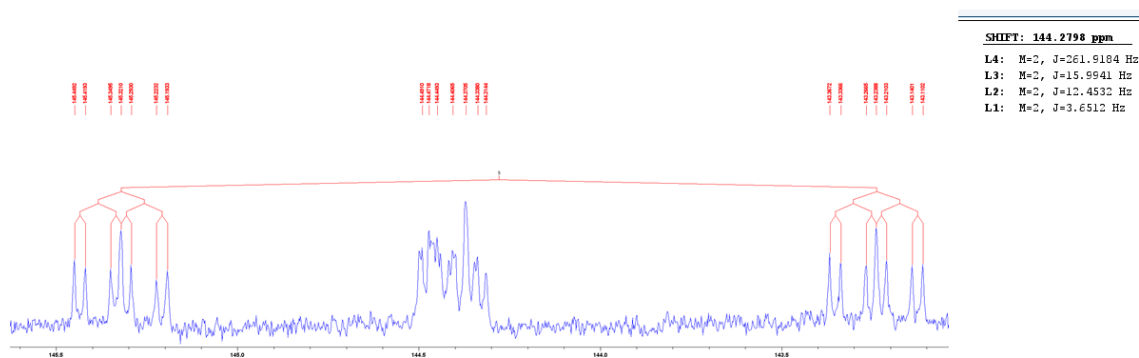


**Figure 2.16.**  $^{13}\text{C}$  NMR extension of *rac*-**116** between 143 ppm and 145 ppm.

A HMQC spectrum was also used to determine the  $^{13}\text{C}$  chemical shift of **110**. The  $^{13}\text{C}$  NMR spectrum of **110** was expected to be similar to the spectrum of 2,3,4,5,6-pentafluorobenzene-sulfonyl chloride (**117**), possessing three large doublets (Figure 2.17). However, the spectrum of **110** shows apparently only two large doublets even though the  $^{19}\text{F}$  NMR clearly shows three distinct peaks. It was suspected that there was an overlap of peaks and to clarify, a decoupled  $^{19}\text{F} - ^{13}\text{C}$  was measured (Figures 2.18 and 2.19). The latter shows three different carbon peaks and two very close together, confirming the overlap. And an HMQC spectrum between  $^{19}\text{F} - ^{13}\text{C}$  helped to assign the peaks (Figure 2.19).

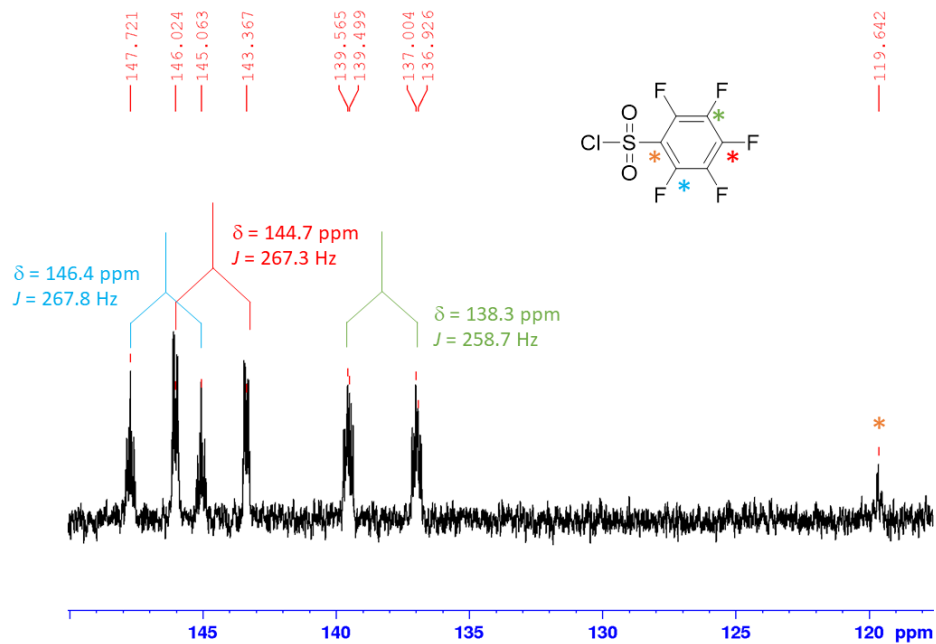


Figure 2.17.  $^{13}\text{C}$  NMR of 2,3,4,5,6-pentafluorobenzenesulfonyl chloride (**117**) in  $\text{CDCl}_3$ .

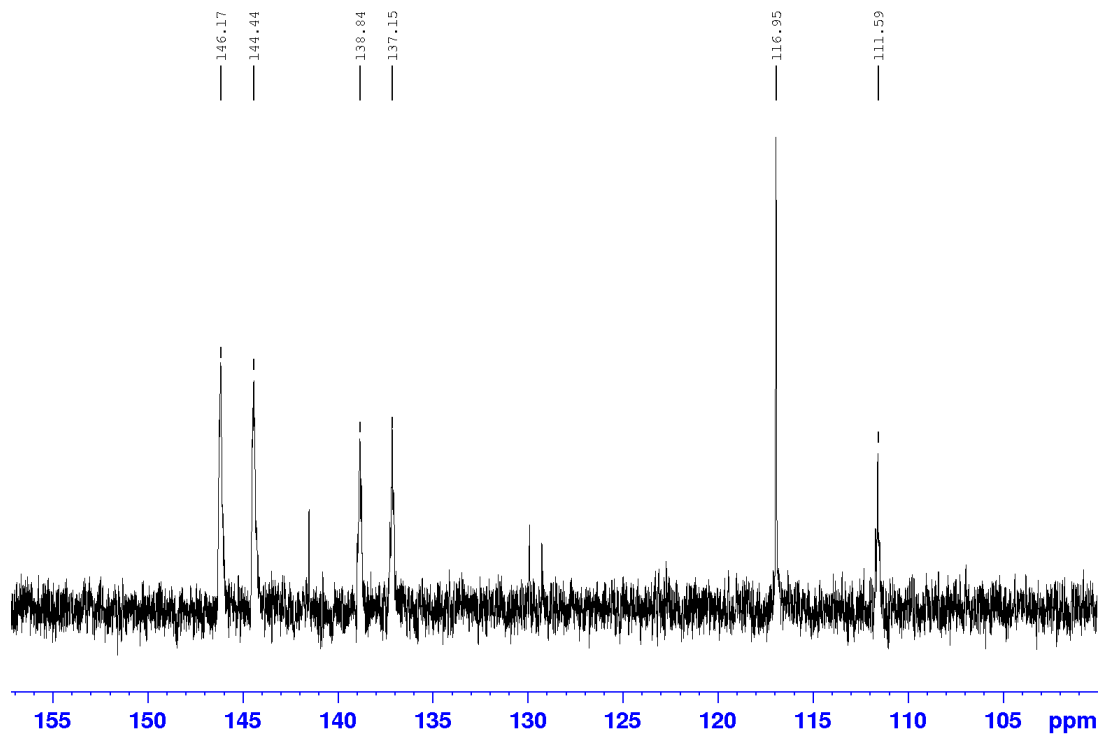


Figure 2.18.  $^{13}\text{C}$  NMR spectrum of **110** obtained at 150.9 MHz.

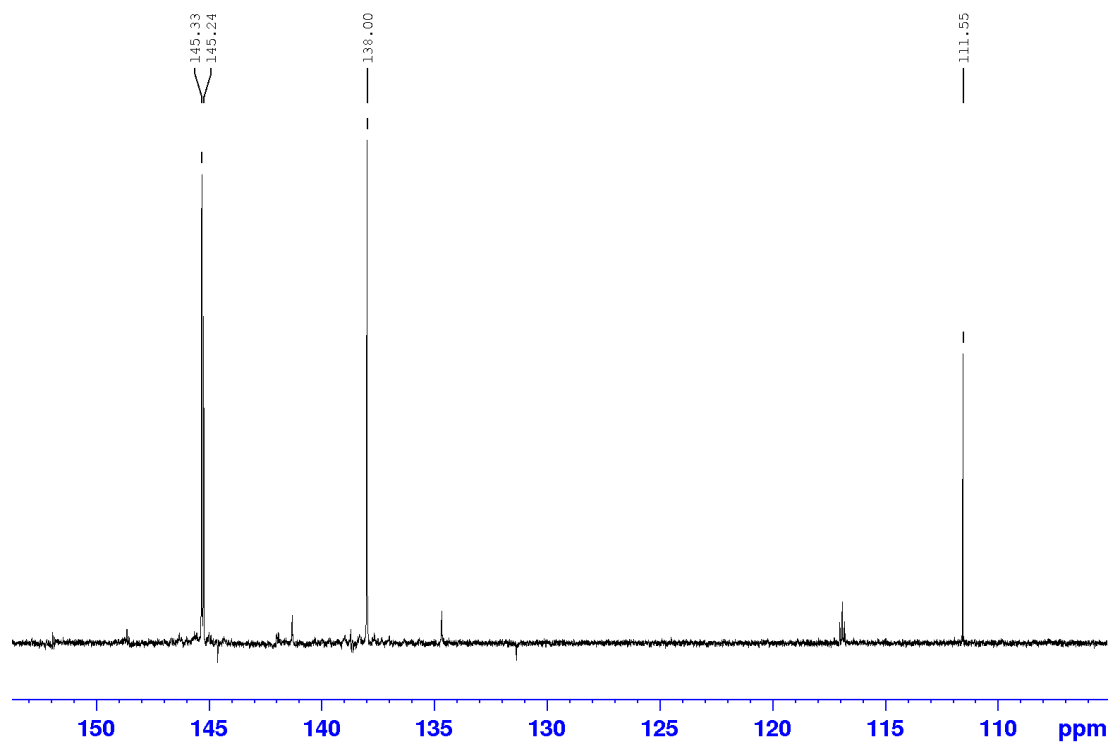


Figure 2.19.  $^{19}\text{F}$  –  $^{13}\text{C}$  NMR spectrum of **110** obtained at 100.6 MHz.

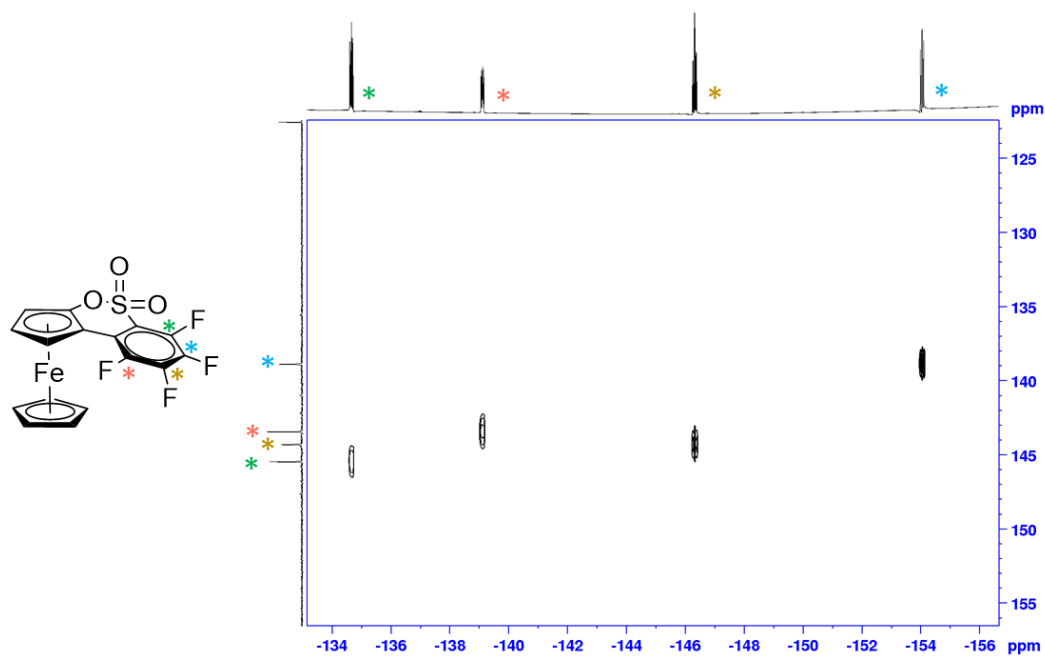
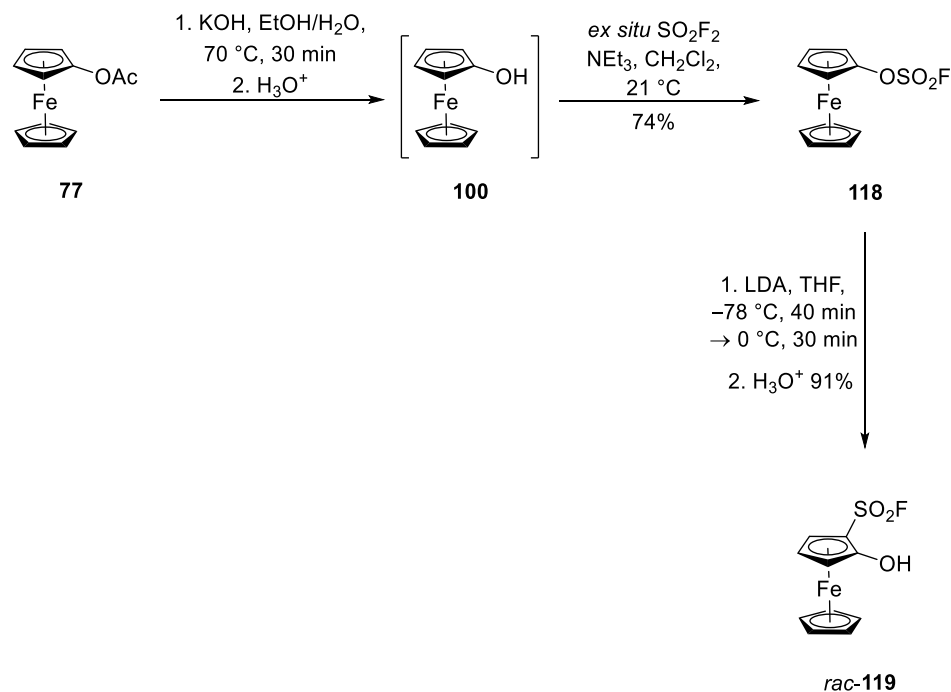


Figure 2.20.  $^{19}\text{F}$  –  $^{13}\text{C}$  HMQC spectra of **110** obtained at 376.5 and 100.6 MHz.

Recently, Barbasiewicz et al. reported the anionic thia-Fries rearrangement of 2-chlorophenyl fluorosulfonate.<sup>[49]</sup> In the context of the earlier investigations on anionic thia-Fries rearrangements at ferrocene,<sup>[17,50]</sup> it was of interest to investigate if the rearrangement also took place at ferrocenyl fluorosulfonate (**118**). Based on Sharpless' sulfur(VI) exchange (SuFex) chemistry,<sup>[51]</sup> De Borggraeve developed a very convenient procedure for the synthesis of aryl fluorosulfonates from phenols in the presence of a base and *ex situ* produced sulfonyl fluoride.<sup>[52]</sup> Following this, ferrocenyl acetate (**77**) was treated with potassium hydroxide in water followed by acid hydrolysis. Without isolation, the intermediate hydroxyferrocene (**100**) was treated with sulfonyl fluoride in the presence of triethylamine affording ferrocenyl fluorosulfonate (**118**) in 74 % yield. The desired anionic thia-Fries rearrangement was finally realized by treatment of **118** with lithium diisopropylamide at  $-78\text{ }^{\circ}\text{C}$  for 40 min followed by warming to  $0\text{ }^{\circ}\text{C}$  over 30 min and hydrolytic workup giving 2-(fluorosulfonyl)ferrocenol (*rac*-**119**) in 91 % yield (Scheme 2.21). This result confirms the propensity of the ferrocene system to undergo anionic thia-Fries rearrangements.

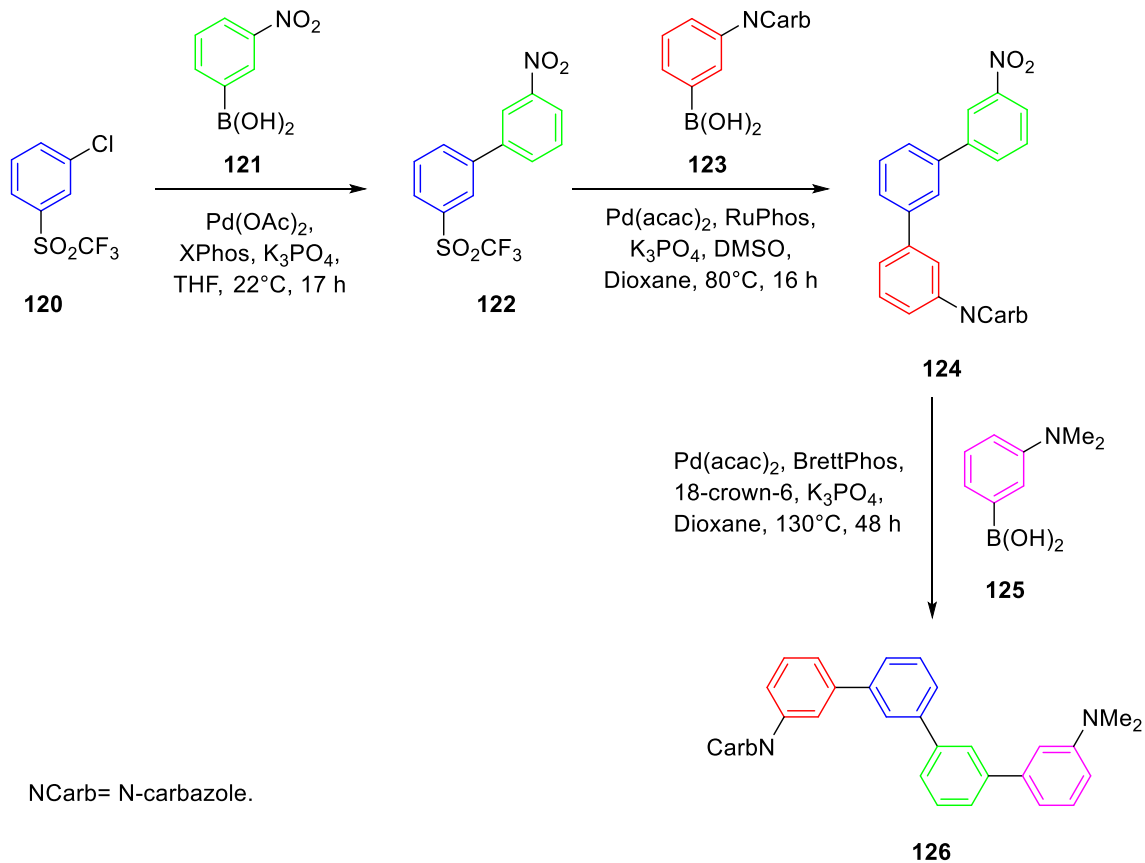


**Scheme 2.21.** Anionic thia-Fries rearrangement of ferrocenyl fluorosulfonate (**118**).



## 2.2.2. Investigation of the potential use of the anionic thia-Fries rearrangement product for Suzuki cross-coupling reaction

The Suzuki-Miyaura reaction was first published in 1979 and consists of a palladium catalysed cross-coupling reaction employing organohalides and boronic acids. At the time, cross-coupling reactions had been developed between organohalides and several different partners, such as organo-magnesium, -zinc, -copper, -aluminium, -mercury, -zirconium and silicon reagents.<sup>[53]</sup> However, the electrophilic partner in cross-coupling reactions did not change very much, consisting basically of aryl halides (-I, -Br, -Cl) and pseudohalides (-OTf). In 2017, Nakao et al. reported for the first time the use of nitroarenes as the electrophilic partner in Suzuki coupling.<sup>[54]</sup> Two years later Moran et al. reported the use of the trifluoromethanesulfonyl group as a new electrophilic partner. The different reactivity of aryl halides, aryl sulfones and nitroarenes, enabled the iterative polyaryl synthesis as shown in Scheme 2.22.<sup>[55]</sup>



**Scheme 2.22.** Sequential synthesis of non-symmetric quaterphenyls (**120** to **126**) by taking advantage of the relative SMC reactivity: chloroarenes > sulfonylarene > nitroarene.<sup>[55]</sup>

Because of the new trifluoromethanesulfonyl electrophilic partner, it was decided to take advantage of the easy formation of this group at ferrocene via anionic thia-Fries rearrangement to investigate a putative Suzuki cross-coupling reaction at ferrocene.

2-(Trifluoromethylsulfonyl)ferrocenol (**81**) is not very easy to handle as it is oxygen sensitive, and therefore the protected ferrocenols **82**<sup>[17]</sup> and **83**<sup>[17]</sup> were chosen as possible coupling partners. The results of the investigation are depicted in Table 2.2. The standard condition used by Moran et al.<sup>[55]</sup> worked only for **83**, affording **132** but in very small yield, only 3%. The exchange of the ligand RuPhos for dppf also worked, but again **132** was obtained in only very small yield, 4%. The use of the sulfone **82** did not work, presumably because the use of base, even though it was a mild one, deprotected the alcohol. At the end of the reaction, most of the starting material was decomposed. The reaction did not work with the boronic acid **127**. A lower temperature was also used for **82** because of faster observed decomposition of starting material at higher temperatures.

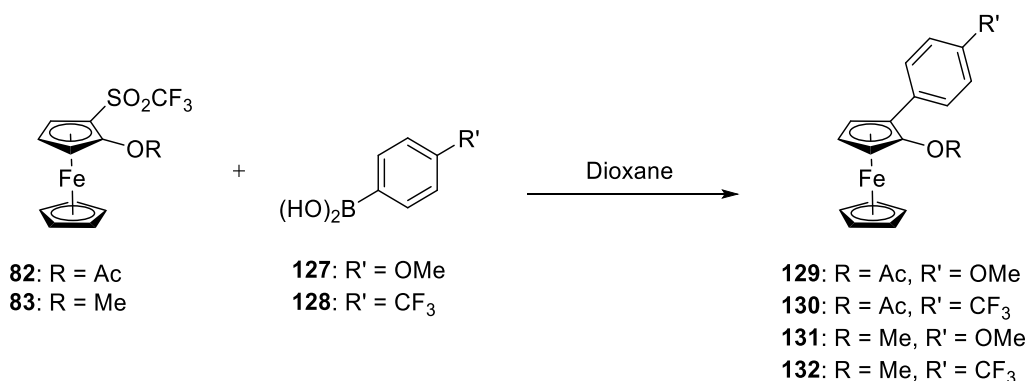


**Table 2.2:** Evaluation of reaction parameters for the Suzuki-Miyaura coupling of the sulfones **82** and **83** with the boronic acids **127** and **128**.

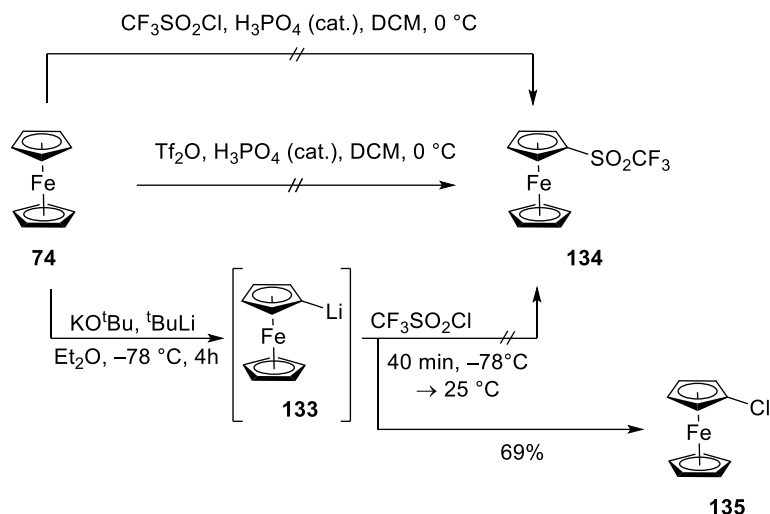
Boronic acid	Sulfone	Pd-catalyst	Ligand	Base	Temperature (oil bath) [°C]	Yield [%]
<b>128</b>	<b>82</b>	Pd(acac) <sub>2</sub>	RuPhos	K <sub>3</sub> PO <sub>4</sub>	80	-
<b>128</b>	<b>82</b>	Pd(acac) <sub>2</sub>	XPhos	K <sub>3</sub> PO <sub>4</sub>	80	-
<b>128</b>	<b>82</b>	Pd(acac) <sub>2</sub>	SPhos	K <sub>3</sub> PO <sub>4</sub>	80	-
<b>128</b>	<b>82</b>	Pd(acac) <sub>2</sub>	dppf	K <sub>3</sub> PO <sub>4</sub>	80	-
<b>128</b>	<b>82</b>	Pd(OAc) <sub>2</sub>	RuPhos	K <sub>3</sub> PO <sub>4</sub>	80	-
<b>128</b>	<b>82</b>	Pd(OAc) <sub>2</sub>	XPhos	K <sub>3</sub> PO <sub>4</sub>	80	-

128	82	Pd(OAc) <sub>2</sub>	SPhos	K <sub>3</sub> PO <sub>4</sub>	80	-
128	82	Pd(OAc) <sub>2</sub>	dppf	K <sub>3</sub> PO <sub>4</sub>	80	-
127	83	Pd(acac) <sub>2</sub>	RuPhos	K <sub>3</sub> PO <sub>4</sub>	80	-
128	83	Pd(acac) <sub>2</sub>	RuPhos	K <sub>3</sub> PO <sub>4</sub>	95	3
128	83	Pd(acac) <sub>2</sub>	XPhos	K <sub>3</sub> PO <sub>4</sub>	80	-
128	83	Pd(acac) <sub>2</sub>	NHC Ipr	K <sub>3</sub> PO <sub>4</sub>	105	-
128	83	Pd(acac) <sub>2</sub>	d <b>t</b> bpf	K <sub>3</sub> PO <sub>4</sub>	105	-
128	83	Pd(acac) <sub>2</sub>	dppf	K <sub>3</sub> PO <sub>4</sub>	80-100	4
128	83	Pd(PPh <sub>3</sub> ) <sub>4</sub>	-	Cs <sub>2</sub> CO <sub>3</sub>	100	-
128	83	Pd(acac) <sub>2</sub>	dppf	Cs <sub>2</sub> CO <sub>3</sub>	80-100	-

In general, the turnover-limiting step in the Suzuki-Miyaura cross-coupling is the oxidative addition step, and according to DFT calculations performed by Moran et al., the oxidative addition into the sulfone C–S bond is indeed the limiting step of the reaction.<sup>[55]</sup> Ferrocene is a very electron rich system, even more than benzene, which might impair the oxidative addition. The presence of an *ortho* oxygen atom is even more detrimental, on the account that although the oxygen atom removes electronic density through the inductive effect, it shifts more electronic density into the system due to resonance. For this reason, the synthesis of the trifluoromethylsulfonyl ferrocene (**134**) was foreseen as an attempt to test the new electrophilic partner at ferrocene without the influence of an *ortho* group.

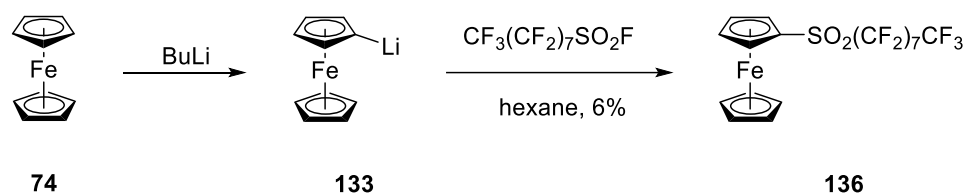
Trifluoromethylsulfonyl ferrocene (**134**), surprisingly, is an unknown compound. Initially, a direct synthesis from ferrocene was attempted, in a similar fashion to Friedel Crafts acylation. Ferrocene (**74**) was dissolved in dichloromethane; a few drops of phosphoric acid were added followed by triflic anhydride. The same was tried with trifluoromethanesulfonyl chloride. Both solutions turned blue immediately, ferrocene (**74**) was oxidized, and no product was formed. Hoping that ferrocenyllithium (**133**) would have a lower oxidation potential than ferrocene, triflic anhydride and trifluoromethanesulfonyl chloride was added to ferrocenyllithium (**133**) (not isolated). Triflic anhydride oxidized ferrocene and promoted the polymerization of the solvent, THF. Trifluoromethanesulfonyl chloride on the other hand, led to an electrophilic chlorination and chloroferrocene (**135**) was formed (Scheme 2.23). Trifluoromethanesulfonyl chloride is a very versatile reagent and has been used for trifluoromethylation, trifluoromethylsufenyl-, sulfinyl- and sulfonylation, but also sparingly as a chlorinating agent.<sup>[56]</sup> Indeed, the synthesis

of **135** via trifluoromethanesulfonyl chloride from ferrocene (**74**) has been reported previously by Metzler-Nolte et al., albeit in much lower yield, 5%.<sup>[57]</sup>



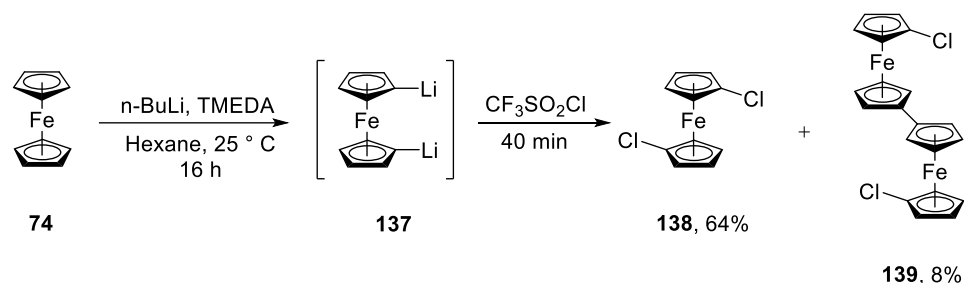
**Scheme 2.23.** Attempts to synthesise **134** and reaction of lithiumferrocene (**133**) with trifluoromethanesulfonyl chloride.

Interestingly, Metzler-Nolte et al.<sup>[57]</sup> succeeded to realize a sulfonation direct from ferrocenyllithium (**133**) and perfluorooctanesulfonyl fluoride forming perfluorooctanesulfonylferrocene (**136**) (Scheme 2.24). Fluorine seems to be a better leaving group.<sup>[57]</sup> This is in agreement with the recent advances in sulfur(VI) fluoride exchange (SuFEx) reactions, which highlights the abilities of the S-F nucleophilic exchange. Trifluoromethanesulfonyl fluoride might be a good alternative for a putative trifluoromethanesulfonylation of ferrocenyllithium (**133**). However, only towards the end of this work, a convenient synthesis for the non-commercially available trifluoromethanesulfonyl fluoride gas published by Luo was found but was not tried.<sup>[58]</sup>



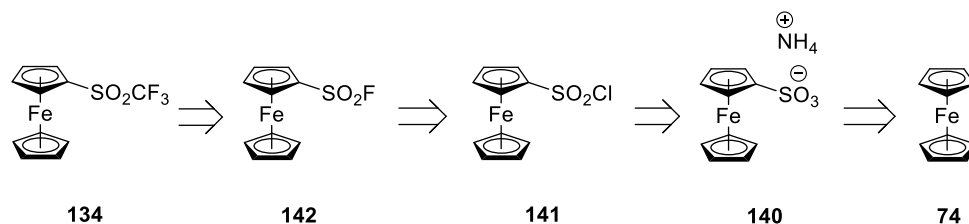
**Scheme 2.24.** Synthesis of perfluorooctanesulfonylferrocene from lithiated ferrocene.<sup>[57]</sup>

Out of curiosity, the 1,1'-dilithioferrocene (**137**) was also reacted with trifluoromethanesulfonyl chloride. 1,1'-Dichloroferrocene (**138**)<sup>[59]</sup> was obtained in 64% yield but it was not the only product. Dichlorinated biferrocenyl derivative **139**<sup>[60]</sup> was also formed in 8% yield (Scheme 2.25).



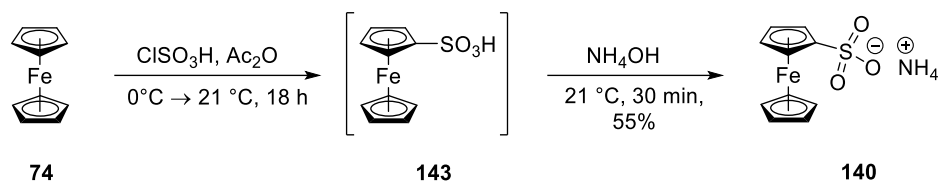
**Scheme 2.25.** Synthesis 1,1'-dichloroferrocene (**138**) from trifluoromethanesulfonyl chloride.

Fortunately, the vast amount of synthetic organic methods available allows, in general, for several different synthetic routes, and therefore, the retrosynthetic path shown in Scheme 2.26 was proposed for the synthesis of **134**.



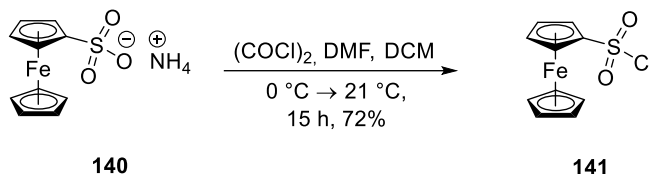
**Scheme 2.26.** Proposed retrosynthetic path to the synthesis of **134**.

The synthetic route up to the ferrocenylsulfonyl chloride (**141**) is known and was conducted according to the literature.<sup>[61–64]</sup> The ferrocene sulfonation forming ammonium ferrocenesulfonate (**140**) was achieved using chlorosulfonic acid in the presence of an excess of acetic anhydride and later addition of a concentrated aqueous ammonia solution to the formed ferrocenesulfonic acid (Scheme 2.27). The salt **140** is used instead of the acid **143** because it is easier to handle.<sup>[61–63]</sup> According to Weinmayr et al., the use of acetic anhydride minimises the oxidation of ferrocene by sulfuric acid and the strategy worked for chlorosulfonic acid too.<sup>[61]</sup>



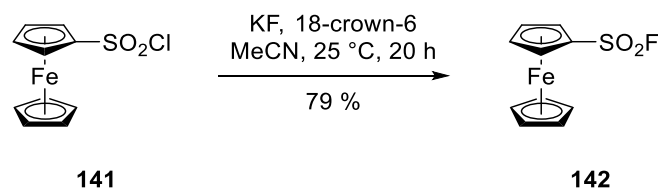
**Scheme 2.27.** Synthesis of ammonium ferrocenesulfonate (**140**).

Whilst Pauson et al.<sup>[62]</sup> reported for the first time the synthesis of ferrocenylsulfonyl chloride (**141**) treating ammonium ferrocenesulfonate (**140**) with phosphorus trichloride, oxalylic chloride was used instead based on an improved synthesis by Ganter et al (Scheme 2.28).<sup>[64]</sup> The purification method employed (extraction with hexane) is easy, straightforward and affords **141** as a very pure red solid.



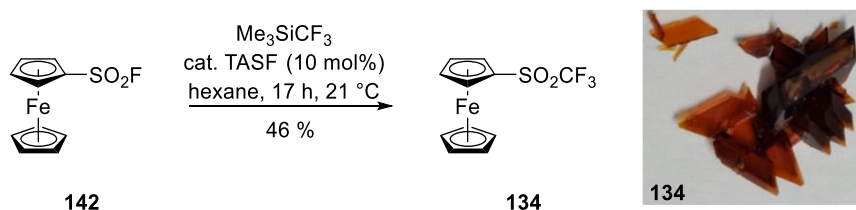
**Scheme 2.28.** Synthesis of ferrocenylsulfonyl chloride (**141**).

Fluorosulfonylferrocene (**142**) is only the third ferrocenesulfonyl fluoride derivative reported so far. Nesmeyanov et al reported 1-carboxy- and 1-methoxycarbonyl-1'-(fluorosulfonyl)ferrocene in 1959.<sup>[65]</sup> These authors obtained the fluorosulfonyl group from the respective chlorosulfonyl derivative by treatment with  $\text{KHF}_2$  in acetic acid. A similar pathway was tested starting from ferrocenylsulfonyl chloride (**141**) in acetonitrile, however, this procedure led only to a very modest yield of 21 % of fluorosulfonylferrocene (**142**). Application of a halogen exchange procedure originally applied for the synthesis of phenylsulfonyl fluoride<sup>[66]</sup> using potassium fluoride in the presence of 18-crown-6 in acetonitrile gave a much better yield of 79 % of **142** (Scheme 2.29), whereas an attempt with tetrabutylammonium fluoride in THF and  $\text{KHF}_2$  in acetonitrile failed. The new compound fluorosulfonylferrocene is an orangish yellow air stable solid and can be crystallized from a solution of **142** in hexane at  $-30^\circ\text{C}$ .



**Scheme 2.29.** Synthesis of fluorosulfonylferrocene (**142**).

The new compound (trifluoromethyl)sulfonylferrocene (**134**) was foreseen to be synthesised from a promising relatively new SuFEx-based procedure by Moses et al. making use of  $\text{KHF}_2$ .<sup>[67]</sup> However, the attempt was unsuccessful. A trifluoromethylation of ferrocenylsulfonyl chloride (**141**) using sodium trifluoroacetate in the presence of copper(I) iodide in DMF failed, too. Finally, **134** was obtained in moderate yield of 46 % following a route by Yagupolski et al.<sup>[68]</sup> by treatment of fluorosulfonylferrocene (**142**) with (trifluoromethyl)trimethylsilane in the presence of a catalytic amount (10 mol%) of tris(dimethylamino)sulfonium difluorotrimethylsilicate (TASF) (Scheme 2.30). The new compound (trifluoromethyl)sulfonylferrocene (**134**) is an orange air stable solid.



**Scheme 2.30.** Synthesis of (trifluoromethylsulfonyl)ferrocene (**134**).

The moderate yield may be explained by difficulties in the purification of **134**. Many attempts to separate residual **142** and **134** by column chromatography failed. Both compounds crystallize from hexane and both compounds sublime at 50 °C / 1.0 mbar. Finally, pure **134** was obtained by stirring the mixture of **142** and **134** in dioxane / water (1:1) in the presence of potassium phosphate for 16 h at 85 °C causing hydrolysis of **142**. Crystals of **134** suitable for a crystal structure analysis were obtained by crystallization from hexane at -30 °C over 7 days (Figure 2.21). (Trifluoromethylsulfonyl)ferrocene (**134**) crystallizes in a monoclinic system [space group  $P2_1/n$  (14)]. The cyclopentadienyl ligands adopt an eclipsed conformation, and the trifluoromethylsulfonyl substituent points away from the unsubstituted cyclopentadienyl ring.

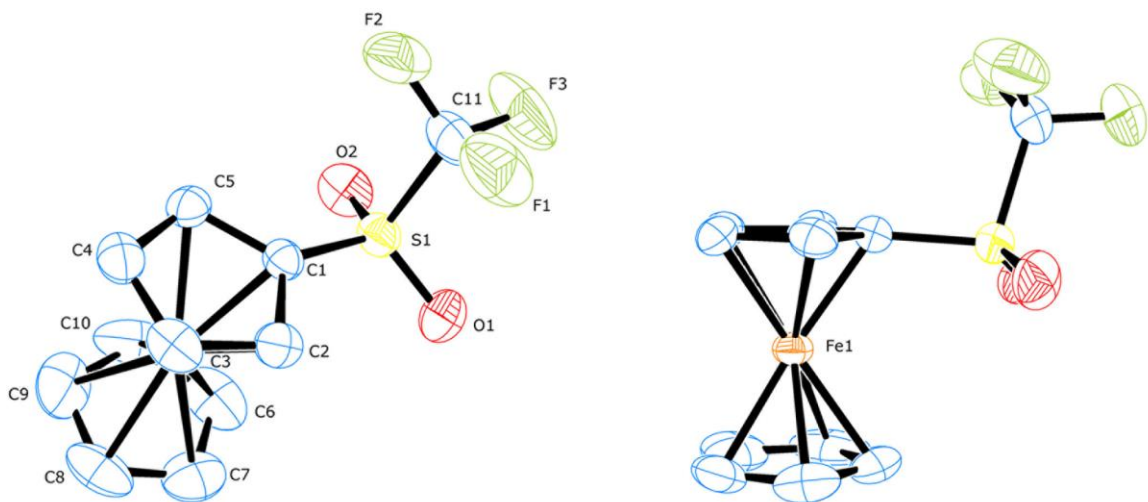
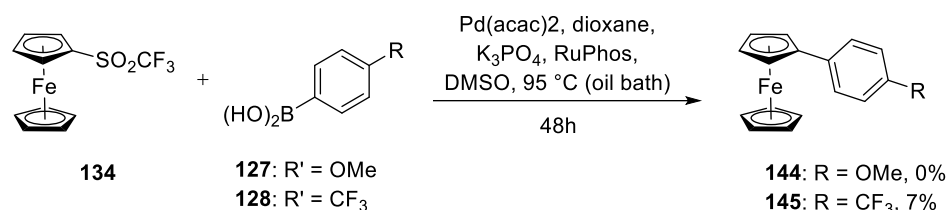


**Figure 2.21.** Structure of **134** in the crystal. Left: Top view; right: Side view. The average C–F bond distance is 131 pm and S–O is 143 pm. Selected bond lengths [pm] and angles [°] and dihedral angles [°]: S1–C11 182.7(4), S1–C1 171.7(3), Fe1–C1 198.9(3), Fe1–C2 203.9(3), Fe1–C3 206.1(3), Fe1–C4 205.9(3), Fe1–C5 203.5(3), Fe1–C6 201.8(4), Fe1–C7 204.7(4), Fe1–C8 204.3(4), Fe1–C9 202.4(4), Fe1–C10 202.2(4) pm; C1–S1–O1 110.3°, C1–S1–C11 102.5°; C2–C1–S1–O1 14.3°.

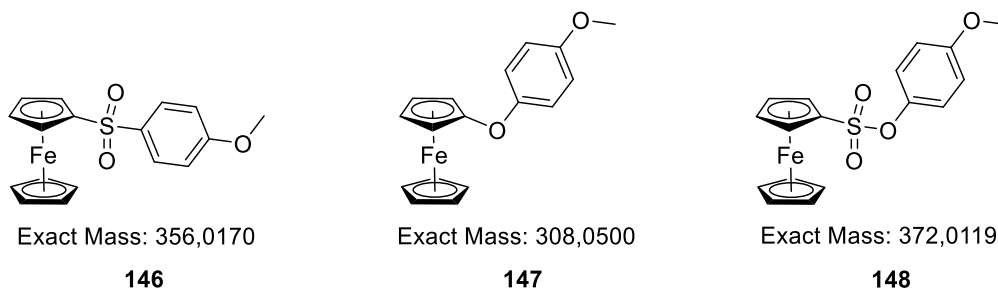
Following the synthesis of **134**, the Suzuki-Miyaura coupling reaction optimized procedure by Moran et al. was used for (trifluoromethylsulfonyl)ferrocene (**134**). The coupling reaction using 4-(trifluoromethyl)phenylboronic acid (**128**) gave only 7% yield and no coupling product was observed with 4-methoxyphenylboronic acid (**127**) (Scheme 2.31). Nevertheless, the coupling using **127** resulted in another product obtained in the form of yellow crystals. The analysis of the  $^1\text{H}$  NMR and  $^{13}\text{C}$  NMR initially indicated this to be the coupling product, but the expected mass was not found. A close analysis of the HMBC spectrum showed that no  $^3J$  coupling was present between the protons of the phenyl ring and the quaternary ferrocenyl carbon atom, or between the ferrocenyl proton and the phenyl quaternary carbon atom. The  $^1\text{H}$  NMR and  $^{13}\text{C}$  NMR of the unknown product do not match the one of **144** in the literature.<sup>[69]</sup> The spectra of the unknown product suggests that “something” was in between the ferrocenyl and phenyl groups, and the structures **146** and **147** were proposed (Scheme 2.32). The high mass of **147** was found and **146** was not. However, the TLC/MS showed a main peak of  $m/z = 372.1$ . Based on the NMR, IR and low mass analysis, the structure **148** was proposed instead (Scheme 2.32).



A closer look at the IR spectrum, showed a strong band at  $1364\text{ cm}^{-1}$ , a typical region for S=O stretching of sulfonates, sulfonyls, sulfonamides, sulfones etc indicating that **148** is likely the product.<sup>[70]</sup> Besides this, the  $^{13}\text{C}$  NMR chemical shift of the unknown product is in the range obtained for the C-S bonds present in the ferrocene rings obtained in this work, ranging between 80 and 100 ppm. All the ferrocenol derivatives have a C-O around 115 ppm at the  $^{13}\text{C}$  NMR, reinforcing the hypothesis that **148** is the correct structure. The respective yield would be 9%.

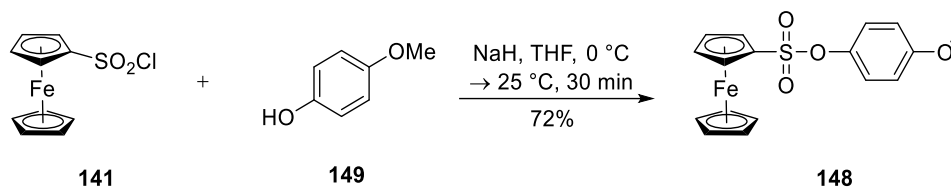


**Scheme 2.31.** Suzuki coupling of (trifluoromethylsulfonyl)ferrocene (**6**). RuPhos = 2-Dicyclohexylphosphino-2',6'-diisopropoxybiphenyl.



**Scheme 2.32.** Proposed structures for the obtained product other than the expected Suzuki coupling **144**.

To obtain stronger supporting evidence for the proposed structure, **148** was synthesised in a different way, from ferrocenylsulfonyl chloride (**141**) and deprotonated mequinol (**149**) (Scheme 2.33). **148** was obtained in 72% yield and both  $^1\text{H}$  NMR and  $^{13}\text{C}$  NMR spectra match that of the product obtained in the attempted cross-coupling reaction.



**Scheme 2.33.** Synthesis of 4-(methoxybenzenesulfonate) ferrocene (**148**).

The boronic acid appearance was a white crystalline solid, but its NMR (Figure 2.22) showed that the reagent was not pure. It is not clear what the impurity is, but it does not seem to correspond to mequinol (**149**) ( $\text{OCH}_3$ : 3.75 ppm,  $\text{C}_{\text{Ph}}\text{H}$ : 6.80 ppm).<sup>[71]</sup> Protonolysis of the boronic acid did not seem to have happened either, because the peaks do not correspond to anisole. Nevertheless, the reaction was repeated with a pure boronic acid and neither the cross-coupling reaction nor the formation of **148** took place, suggesting that the impurity is probably responsible for the obtained product **148**.

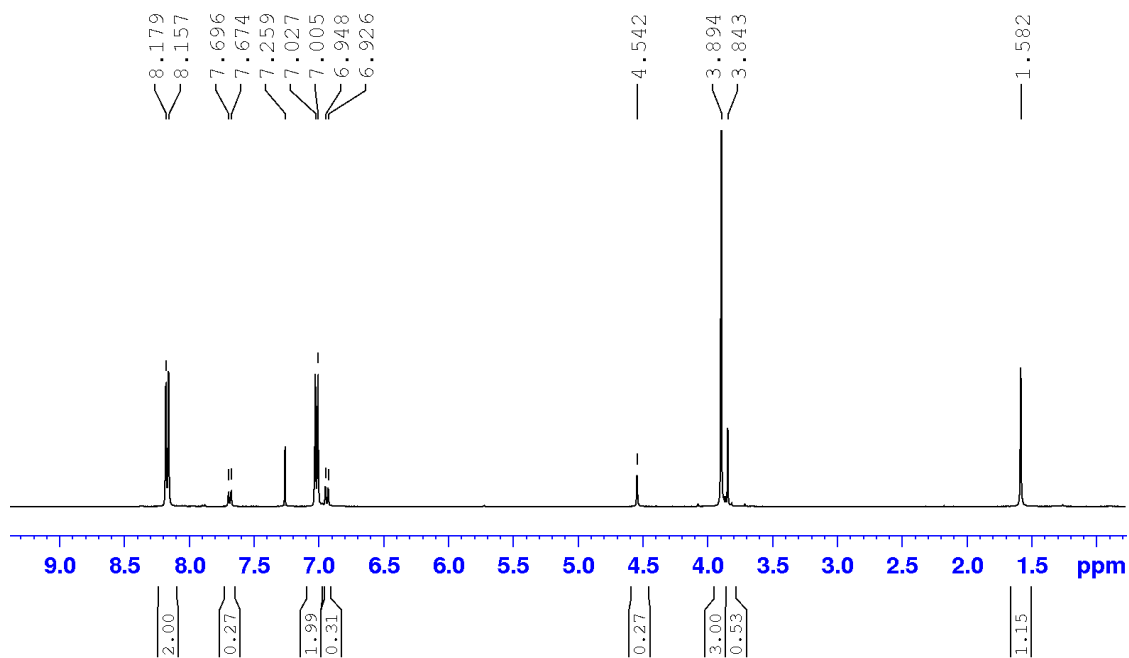


**Figure 2.22.** NMR of impure 4-methoxyphenyl boronic acid (**127**) used for the cross-coupling reaction.

### 2.2.3. *ortho* Lithiation of fluorosulfonylferrocene (**142**) and (trifluoromethylsulfonyl)ferrocene (**134**)

According to Clayden, “lithiation by deprotonation of a C-H bond takes place at a reasonable rate only if the organolithium product displays two features: intramolecular coordination of the electron deficient lithium atom to a heteroatom and stabilization of the electron-rich C-Li bond by a nearby empty orbital or electron-withdrawing group.”<sup>[46]</sup> The crystal structure analysis of (trifluoromethylsulfonyl)ferrocene (**134**) (Figure 2.21), shows that the oxygen atoms of the sulfonyl group are in a very favourable position to coordinate the lithium atom, forming a 5-membered ring upon deprotonation and therefore stabilizing the intermediate aryllithium product formed. The structure also fulfils the second requirement, since ferrocene is bonded to the electron-withdrawing trifluoromethylsulfonyl group.

Among the large number of existing ODGs, those containing sulfur-oxygen double bonds are among the more active ones: sulfones, sulfoxides, secondary and tertiary sulfonamides.<sup>[46]</sup> The use of the (trifluoromethyl)sulfonyl group of some arenes as an ODG was first reported in 2018 by Shibata et al.<sup>[72]</sup> One year later, the first observation of fluorosulfonylarenes to undergo *ortho*-lithiation was reported by Barbasiewicz et al.<sup>[49]</sup> In this context, it was decided to investigate the degree to which fluorosulfonylferrocene (**142**) and (trifluoromethylsulfonyl)ferrocene (**134**) are prone to *ortho* lithiation. Initial experiments with **142** and LiTMP showed that a reaction took place, however, products obtained by quench with acetyl chloride were not stable enough for the isolation of pure products. Replacing acetyl chloride with the less reactive 2,6-dimethoxybenzoyl chloride afforded mono-substitution product *rac*-**150** in 16 % yield with no di-substitution product being observed in addition to 74 % of recovered **142**. Higher yields were achieved with iodomethane as the electrophile. When 1.3 equiv. of LiTMP was used, 60 % of the mono-substitution product *rac*-**151** was obtained in addition to 10 % of di-substitution product **152** and 19 % of starting material **142**. Increasing the amount of LiTMP to 3.0 equiv. afforded an improved yield of *rac*-**151** of 72 % in addition to 9 % of **152** and 10 % of starting material **142** indicating higher chemoselectivity (Table 2.3).

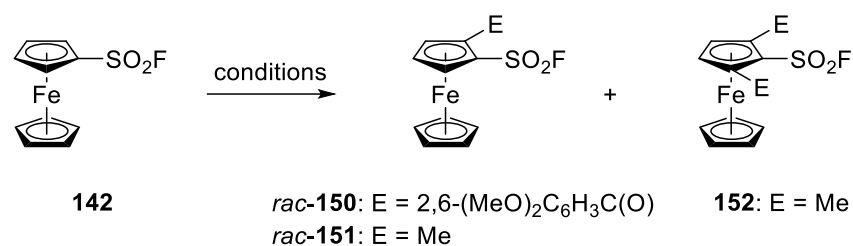
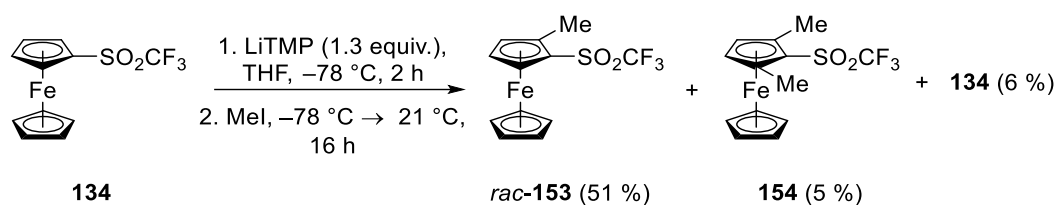


**Table 2.3.** *ortho* Lithiation of fluorosulfonylferrocene (**142**).

Entry	Conditions	Electrophile E	Product (Yield)		Recov. <b>142</b>
			mono-substitution	Product (Yield) di-substitution	
<b>1</b>	LiTMP (1.1 equiv.), THF, -78 °C, 1 h. After electrophile addition -78 °C (15 min) → 22 °C (30 min)		<i>rac-150</i> (16 %)	-	74 %
<b>2</b>	LiTMP (1.3 equiv.), THF, -78 °C, 2 h. After electrophile addition -78 °C (15 min) → 21 °C (30 min)	MeI	<i>rac-151</i> (60 %)	<b>152</b> (10 %)	19 %
<b>3</b>	LiTMP (3.0 equiv.), THF, -78 °C, 2 h. After electrophile addition -78 °C (15 min) → 21 °C (30 min)	MeI	<i>rac-151</i> (72 %)	<b>152</b> (9 %)	10 %

The *ortho* lithiation of (trifluoromethylsulfonyl)ferrocene (**134**) was tested by treatment with 1.3 equiv. of LiTMP and iodomethane as the electrophile and gave the mono-substitution product *rac-153* in 51 % yield in addition to di-substitution product **154** (5 %) and starting material **134** (6 %) (Scheme 2.34). The chromatographic separation of the product mixture was problematic

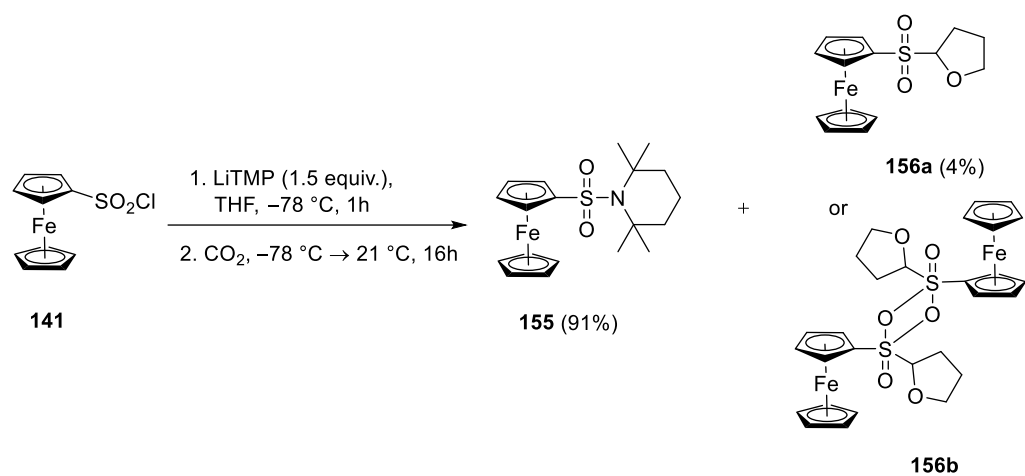
and caused some product loss. It is interesting to note that Shibata et al. did not observe di-substitution products in the respective lithiation of (trifluoromethylsulfonyl)benzene.



**Scheme 2.34.** *ortho* Lithiation of (trifluoromethylsulfonyl)ferrocene (**134**).

In the course of the investigations, it was observed that ferrocenylsulfonyl chloride (**141**) is remarkably resistant against hydrolysis for a sulfonyl chloride, presumably as a result of the electron rich ferrocenyl group. Therefore, it was speculated if this compound could be *ortho* lithiated. Treatment of **141** with LiTMP under the usual reaction conditions with carbon dioxide as the electrophile resulted in the formation of ferrocenyl sulfonamide **155** in 91 % yield in addition to a side product (most likely **156a**, 4% yield) (Scheme 2.35). The reaction shows the remarkable difference in the reactivity of the sulfonyl chloride **141** and the sulfonyl fluoride **142**.

After analysis of the NMR and IR spectra of the side product, structure **156a** was considered. The ESI mass spectrum shows a peak at  $m/z = 344$  corresponding to  $[M + {}^{23}\text{Na}]^+$  for compound **156a**. However, there is also a signal at  $m/z = 663$ , which corresponds to  $[M + {}^{23}\text{Na}]^+$  for cyclodimer **156b**, which cannot easily be distinguished from **156a** by standard NMR measurements. In both cases, the tetrahydrofuranyl substituents can be understood as the result of a lithiation of THF at C2 followed by reaction with **141** forming (ferrocenyl)(2-tetrahydrofuranyl)sulfone (**156a**). A [2+2] cyclodimerization of **156a** leading to **156b** would to our knowledge be unprecedented and might have taken place under the conditions of the mass spectrometric analysis. The initial high mass analysis found only the dimer **156b**, but upon dilution of the sample, **156a** was also found.



**Scheme 2.35.** Formation of sulfonamide **155** and side product **156a** or **156b**.

#### 2.2.4. Asymmetric anionic thia-Fries rearrangement

Planar chirality is a term, defined by IUPAC, used to refer to stereoisomerism resulting from the arrangement of out-of-plane groups with respect to a plane. It is exemplified by the atropisomerism of (*E*)-cyclooctene or monosubstituted paracyclophane.<sup>[73]</sup> Ferrocene (**74**) has a three-dimensional structure and 1,2- or 1,3-disubstituted ferrocene derivatives are also planar chiral, Figure 2.23. In 1967, Schlögl defined symmetry of metallocenes and proposed the CIP convention for planar-chiral metallocenes as shown in Figure 2.23. To denote planar chirality, *p* is subscribed.<sup>[74]</sup>

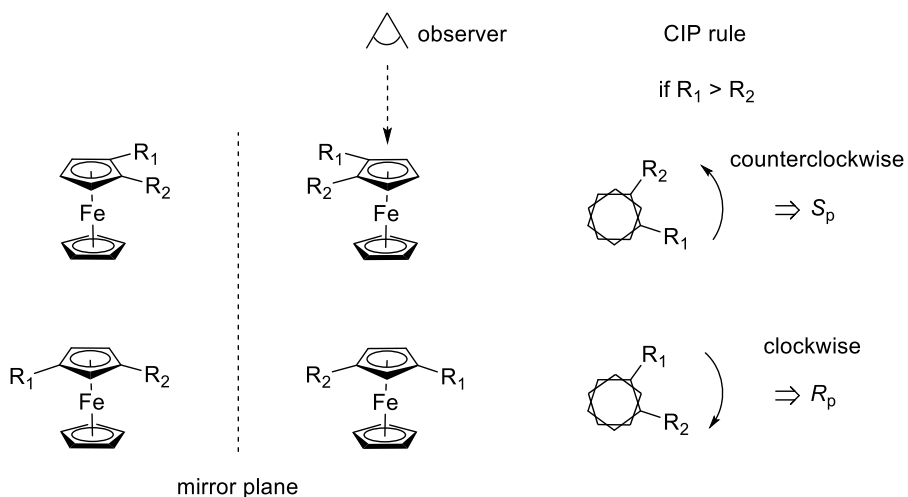
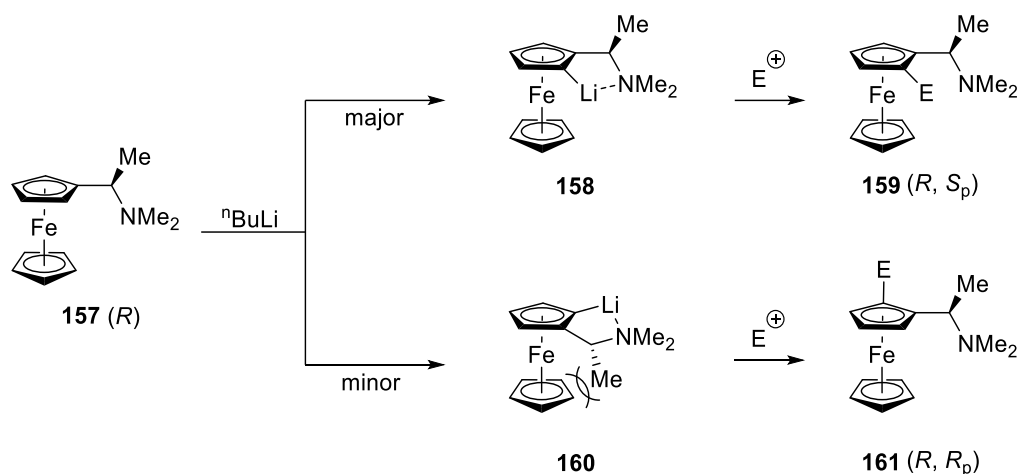


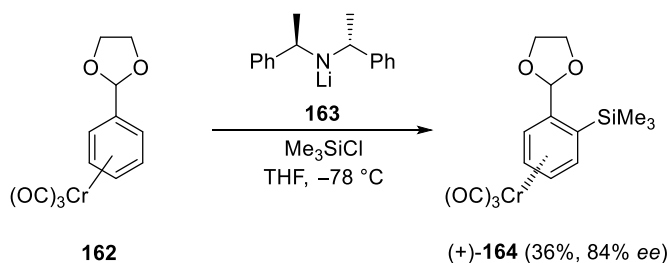
**Figure 2.23.** Planar-chirality of 1,2- or 1,3-disubstituted ferrocene derivatives and their configurations assignment.<sup>[75]</sup>

Due to planar-chirality, ferrocene derivatives can be used as ligands in asymmetric catalysis, however, to function as one, their formation in non-racemic form is necessary. There are several strategies to prepare enantiomerically pure compounds. Among ferrocene chemistry, one of them consists in the use of a monosubstituted ferrocene which contains a chiral centre. A subsequent lithiation, for example, profits from favourable and unfavourable interactions due to the configuration of the chiral substituent, a so called diastereoselective *ortho* lithiation. An example of such a strategy is the use of Ugi's amine **157**. In 1970, Ugi et al., reported the synthesis of both enantiomers of [1-(dimethylamino)ethyl]-ferrocene (**157** - *R* and *S*) in their enantiopure form and their use leading to enantiomerically enriched disubstituted ferrocene (Scheme 2.36).<sup>[76]</sup>



**Scheme 2.36.** Diastereochemical control of direct *ortho* lithiation at Ugi's amine **157**.<sup>[76]</sup>

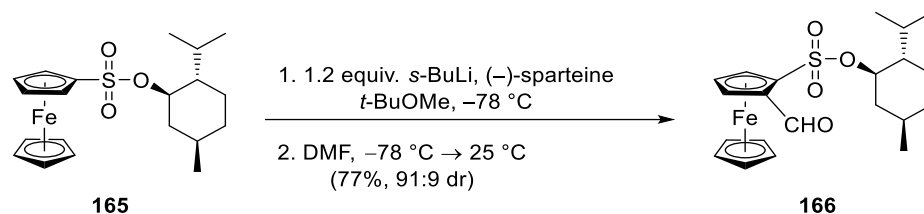
A second common strategy to differentiate enantiotopic *ortho* protons is to make use of a chiral lithium amide, e.g., Simpkins' bases. Simpkins et al. reported in 1994, the enantioselective *ortho* deprotonation of (2-phenyl-1,3-dioxolane)tricarboxylchromium (**162**) using lithium (*R,R*)-di(1-phenylethylamide) (**163**) achieving **164** with a low yield but with a good enantiomeric excess (Scheme 2.37).<sup>[77]</sup>



**Scheme 2.37.** *ortho* Deprotonation of (2-phenyl-1,3-dioxolane)tricarboxylchromium using lithium (*R,R*)-di(1-phenylethylamide).<sup>[77]</sup>

The third way to achieve desymmetrisation is using a chiral ligand. In fact, Snieckus et al. used a chiral ligand and combined it with the first strategy to perform a (–)-sparteine-mediated matched chiral-directed metalation of ferrocenesulfonate **165** using *sec*-butyllithium reaching **166** with a high diastereoisomeric ratio and good yield (Scheme 2.38).<sup>[78]</sup>

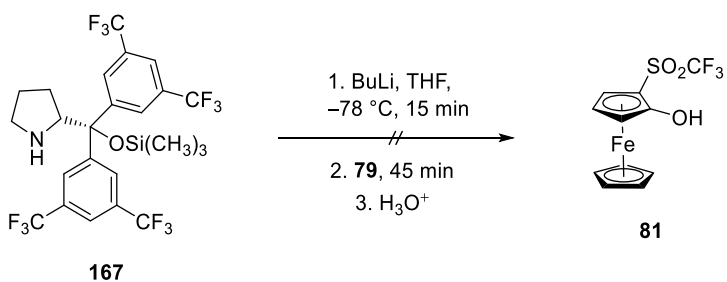




**Scheme 2.38.** Planar chirality induced via a matched chiral-directed metalation group/(-)-sparteine interaction of ferrocenesulfonates.<sup>[78]</sup>

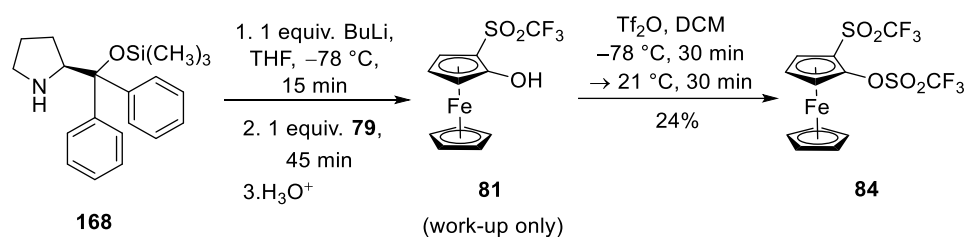
In order to use the ferrocenyl triflate anionic thia-Fries rearrangement product as a ligand in asymmetric catalysis, Werner used the Simpkins base **163** to achieve an enantiotopic *ortho* proton differentiation of ferrocenyl triflate. Whilst the reaction yield was very good, 95%, the enantiomeric excess of 10 % ee was unsatisfactory. He also tried the use of (-)-sparteine combined with butyllithium, but the rearrangement did not take place, and instead only ferrocenol was formed.<sup>[31]</sup> For this reason, it was decided to try a couple more chiral lithium amides in order to differentiate the *ortho* protons.

Available chiral pyrrolidines were chosen to be lithiated and reacted with ferrocenyl triflate (**79**). Chiral pyrrolidines are frequently used as auxiliaries in catalysis, due to their good availability and efficient transfer of chirality via the rigid pyrrolidine scaffold.<sup>[79]</sup> Therefore, it was hypothesized that the use of a chiral lithiated pyrrolidine could differentiate the *ortho* protons and that the rearrangement would follow. The first trial was performed with (*R*)-2-[(bis(3,5-bis(trifluoromethyl)phenyl)]trimethylsilyloxy)methyl]pyrrolidine (**167**). Upon addition of butyllithium to pyrrolidine **167**, the solution immediately turned dark purple and later deep blue, suggesting the lithiation of the pyrrolidine **167**. However, no rearrangement product was observed (Scheme 2.39). A later attempt to isolate and crystallize the lithiated pyrrolidine **167** failed.



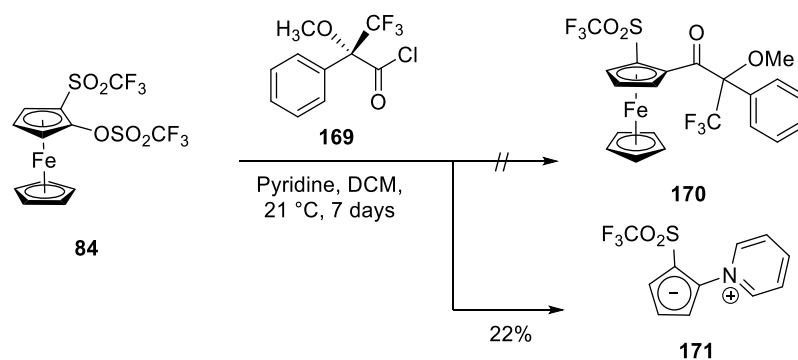
**Scheme 2.39.** Attempted proton differentiation of ferrocenyl triflate (**79**) using a putative chiral lithiated pyrrolidine.

The use of the (*S*)-2-[diphenyl(trimethylsilyloxy)methyl]pyrrolidine (**168**), a similar chiral pyrrolidine to **167** but more electron rich, led to the rearrangement product in 24% yield (Scheme 2.39). The same change of colour was observed upon addition of butyllithium to pyrrolidine **168**: an intense dark purple immediately formed, followed by a deep blue. Ideally, the reaction would be directly quenched with Mosher's acid chloride and the ee of the reaction would be easily determined via NMR. However, the reaction TLC plate showed several spots and the Mosher's acid chloride is too expensive to be wasted quenching a reaction with several by-products. Instead, the reaction was quenched with triflic anhydride and **84**<sup>[17]</sup> was isolated as the anionic thia-Fries rearrangement product. Triflic anhydride was chosen because at the time, incipient computational calculations studying the anionic thia-Fries rearrangement showed that bond between the oxygen and sulfur atom at **79** was somehow labile. And it was thought that **84** could be later directly reacted with the Mosher's acid chloride. Nevertheless, the compound anionic rearrangement product **84** didn't show any optical rotation.



**Scheme 2.39.** Attempted proton differentiation of ferrocenyl triflate (**79**) using a more electron rich putative chiral lithiated pyrrolidine.

Out of curiosity, a very small amount of the Mosher's acid chloride **169** was reacted with an excess of **84** in dichloromethane in the presence of pyridine, to inquiry if the Mosher ester **170** could be obtained directly from **84** without its previous hydrolysis. A new yellow spot was visualized at the TLC plate, but it was not the expected product. Instead, the new stable yellow solid inner salt **171** was formed in 22% (Scheme 2.40). The same result was hoped to be obtained upon repeating the reaction with the exchange of the Mosher's acid chloride for acetyl chloride, but no **171** was formed. The mechanism of this reaction is not clear though, and unfortunately due to time limitations the reaction was not further examined and explored.



**Scheme 2.40.** Unexpected inner salt **171** formation upon reaction of **84** with the Mosher's acid chloride **169**.

The skeleton structure of **171** is known. Cyclopentadienylidene inner salts are relatively common, and several structures of this type are known, e.g., **172** - **176** (Figure 2.24).<sup>[80–84]</sup> The similar pyridinium cyclopentadienylidene (**172**) was first disclosed by Lloyd et al. in 1955.<sup>[82]</sup> **172** was synthesised by the reaction of two equivalents of pyridine and one of dibromocyclopentene (**178**) [itself freshly prepared from cyclopentadiene (**177**) and bromide], leading to the formation of the salt **179**, followed by treatment with alkali (Scheme 2.41).

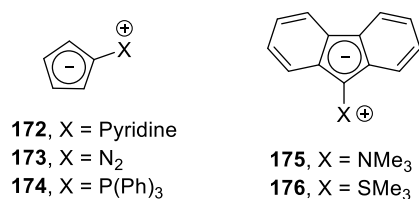
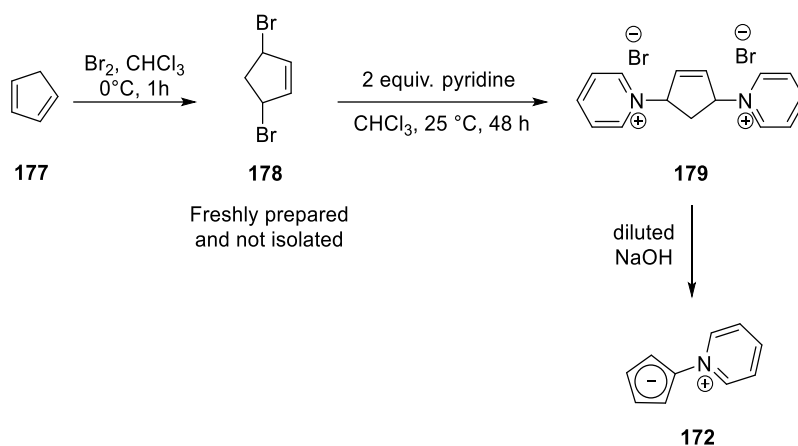
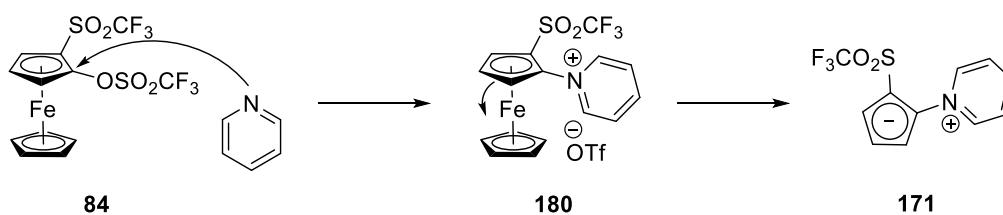


**Figure 2.24.** Some examples of cyclopentadienylidene inner salts.<sup>[80–84]</sup>



**Scheme 2.41.** Synthesis of pyridinium cyclopentadienylide (**172**).<sup>[82]</sup>

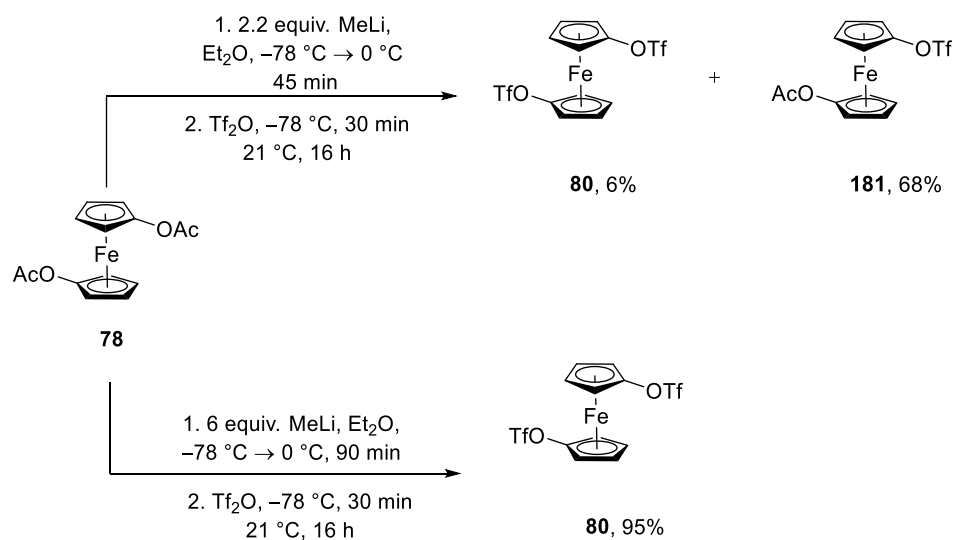
The mechanism of how **171** was obtained is not clear though. But in a similar way that pyridine displaced the bromo atom in Scheme 2.41, the pyridine might displace the pseudo halide triflate group forming the salt **180**. Upon demetallation, possibly aided by the Mosher's acid chloride, the inner salt **171** is formed (Scheme 2.42).



**Scheme 2.42.** Rough depiction of the reaction mechanism of **171**.

The anionic thia-Fries rearrangement of 1,1'-ferrocenediyl ditriflate (**80**), as stated before, led only to the *meso* product **87**. However, the synthesis of the *racemo* product could be of interest as an auxiliary in asymmetric synthesis in a similar fashion to BINAP. But before discussing the double anionic thia-Fries rearrangement, the synthesis of its starting material deserves consideration. 1,1'-Ferrocenediyl ditriflate was not synthesised as reported in the literature (Scheme 2.11)<sup>[17]</sup> but instead was synthesised in a similar way that ferrocenyl tosylate and triflate were, using methyllithium (Scheme 2.17). At the time, the best conditions, e.g., time and temperature, for the ferrocenolate formation using methyllithium were not yet established. 1,1'-Ferrocenediyl diacetate was reacted with methyllithium in diethyl ether and stirred at  $-78^\circ\text{C}$  for

30 minutes. The reaction was not complete though and formed the new compound 1-(acetyloxy)-1'-(trifluoromethanesulfonate)ferrocene (**181**) besides the desired **80**. Increasing the equivalents of base resulted in the very high desired yield of **80**. Although not tested, the use of less base and longer time at room temperature, as performed for ferrocenyl triflate (Scheme 2.17), might lead to similar results. The compound **181** is interesting because it might be used as a precursor for heterodifunctional 1,1'-ferrocenes.



**Scheme 2.43.** Synthesis of **80** and 1-(acetyloxy)-1'-(trifluoromethanesulfonate)ferrocene (**181**).

With the starting material in hand, an attempt to obtain either the *racemo* **88** or a mixture of the *meso* **87** and *racemo* **88** products was pursued using the divalent base magnesium bis(diisopropyl)amide, phosphazane P<sub>2</sub>-t-Bu, dimethyl magnesium and sodium diisopropylamide. The choices were based on the hypothesis that the counter cation could be important for the outcome of the reaction. Treatment of 1,1'-ferrocenediyl ditriflate (**80**) with magnesium bis(diisopropyl)amide unfortunately did not lead to anionic thia-Fries rearrangement, and instead, it was either recovered or led to full and partial deprotection of 1,1'-ferrocenediyl ditriflate (**80**) which was trapped with acetyl chloride affording in some cases **181** and **78** as by-products (Table 2.4).

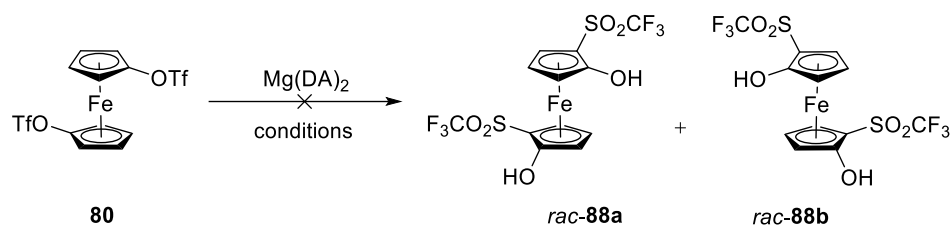


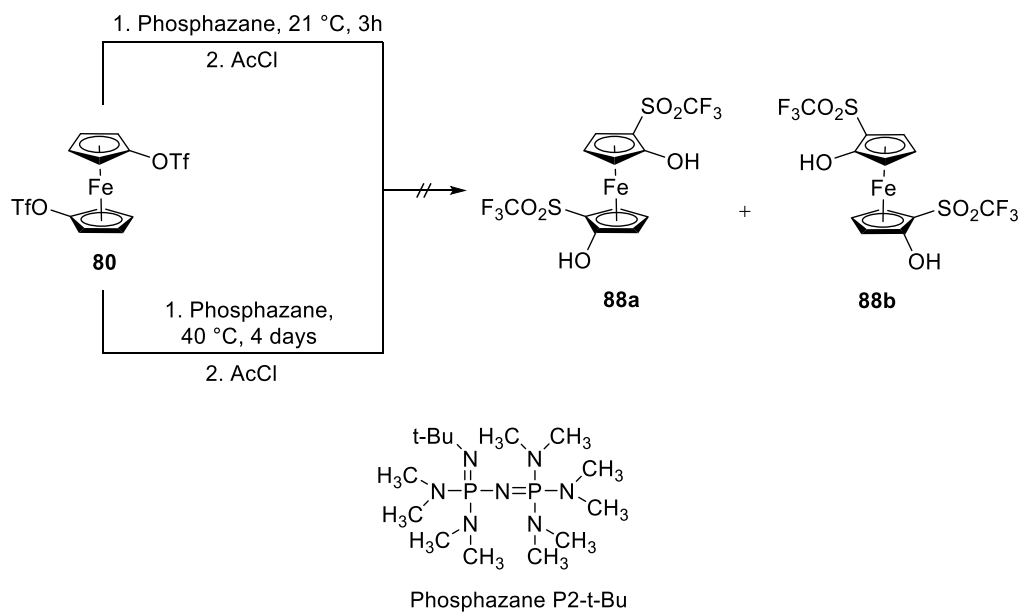
**Table 2.4:** Attempted anionic thia-Fries rearrangement of **80** using the divalent base magnesium bis(diisopropyl)amide.

Entry	Solvent	Conditions	Recovered <b>80</b> (%)	By-products
1	THF	-78 °C, 15 min; 0 °C, 40 min; H <sub>3</sub> O <sup>+</sup>	38	-
2	THF	-78 °C, 45 min, -20 °C, 20 min, 21 °C, 45 min; AcCl, 30 min	34	<b>181</b> (3%) and <b>78</b> (5%)
3	Et <sub>2</sub> O	21 °C, 20 min; AcCl, 30 min	41	<b>181</b> (14%) and <b>78</b> (7%)
4	THF	0 °C, 30 min; AcCl, 30 min	69	<b>78</b> (8%)

Dimethyl magnesium was classically prepared from methylmagnesium bromide by addition of dioxane, which causes precipitation of MgBr<sub>2</sub> as an insoluble dioxane-adduct, shifting the Schlenk equilibrium to the desired dimethyl magnesium.<sup>[85,86]</sup> A solution of dimethyl magnesium in THF was added to **80**, but no anionic thia-Fries rearrangement was observed. **80** was recovered in 31% yield.

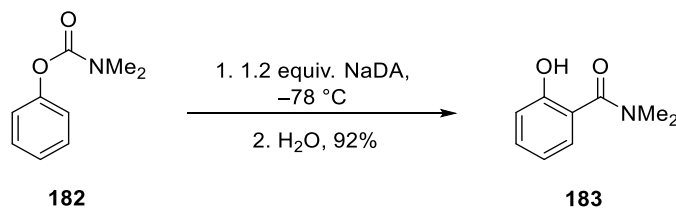
Another attempt to prepare *rac* **88** was performed using the extremely strong and hindered neutral nitrogen phosphazane P2-t-Bu base. Lloyd-Jones successfully used a similar phosphazane (P4-t-Bu) base to deprotonate aryl triflates and induce rearrangement under metal-free conditions.<sup>[26]</sup> Addition of phosphazane P2-t-Bu (phosphazane P4-t-Bu was not commercially available at the time) at 21 °C left stirring for 3 hours, led to the quantitative recovery of starting material. Another attempt was made by increasing the temperature to 40 °C

for 4 days, monitored via TLC plates, and led in the end to total decomposition of the starting material with no rearrangement having taken place.



**Scheme 2.44.** Attempted anionic thia-Fries rearrangement of **80** using the phosphazane P2-t-Bu.

A last attempt to prepare *rac* **88** was performed using the sodium analogue base of LDA, sodium diisopropylamide (NaDA). NaDA can easily be prepared from *N,N*-dimethylethylamine and diisopropylamine without pre-drying and sodium dispersion in toluene. The *ortho* metalation of the phenyl carbamate **182** afforded the anionic Fries rearrangement product **183**.<sup>[87]</sup> However, the product of the reaction was very unstable and was not characterized.



**Scheme 2.45.** Anionic Fries rearrangement of the phenyl carbamate **182** using NaDA.<sup>[87]</sup>

This branch of the project has proved challenging, both to differentiate the enantiotopic proton at ferrocenyl triflate (**79**) and to obtain a racemic mixture upon rearrangement of 1,1'-

ferrocenediyl ditriflate (**80**). The handling of the double anionic thia-Fries product is also very troublesome due to its sensitivity towards oxygen. Hence, this part of the project was withheld. Better results were obtained with the anionic thia-Fries rearrangement at cobaltocenium, and for this reason, more resources were focused on this approach.

### 2.3. Conclusion

The synthesis of several new ferrocenyl sulfonates and sulfonyl ferrocenes have been described. Most of them did not undergo anionic-thia Fries rearrangement. However, the effective *ortho* lithiation of ferrocenyl fluorosulfonate (**118**) allowed the anionic thia-Fries rearrangement at ferrocene to take place in high yields, whilst the *ortho* lithiation at ferrocenyl (2,3,4,5,6-pentafluorobenzene)sulfonate (**110**) followed by intramolecular nucleophilic aromatic substitution led to the formation of a rare ferrocene-annellated oxathiin. Fluorosulfonylferrocene (**142**) proved to be a good *ortho* directing group and will possibly enable future SuFEx reactions at ferrocene. The *ortho* lithiation of (trifluoromethylsulfonyl)ferrocene (**134**) was also demonstrated to be effective. The Suzuki-Miyaura cross-coupling of the latter worked, albeit in only low yields, and the reaction conditions must further be improved. The unexpected inner salt **171** was formed upon reaction of **84** with the Mosher's acid chloride **169**.

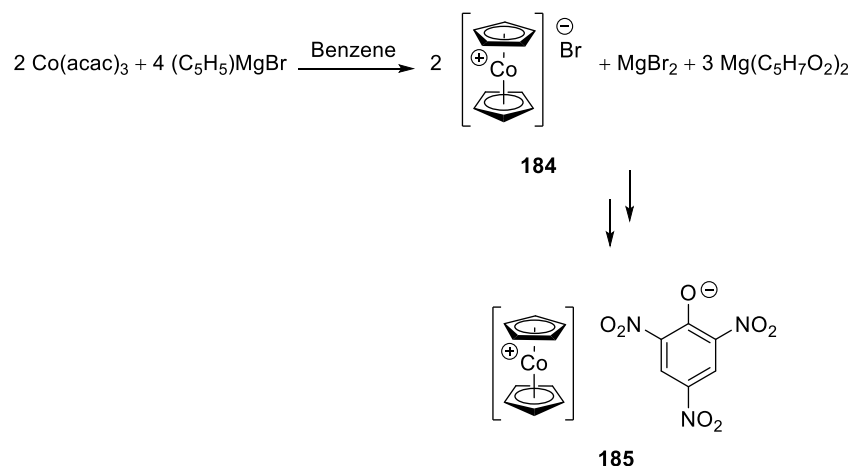


## Chapter 3

# 3. Anionic thia-Fries rearrangement at Cobaltocenium

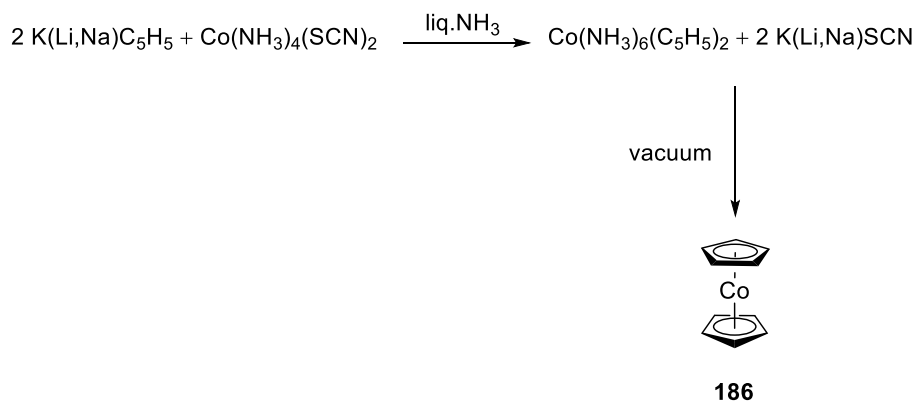
## 3.1 Introduction

Whilst ferrocene chemistry has developed a lot in the last 70 years since its discovery in 1951/2,<sup>[88,89]</sup> the sandwich complexes cobaltocene, reported by Fischer in 1953<sup>[90]</sup>, and cobaltocenium, reported by Wilkinson in 1952<sup>[91]</sup> (also referred to as cobalticenium and quite often as cobalticinium in the past), have not been scrutinized in comparable depth. Wilkinson et al. synthesised cobaltocenium for the first time using cobalt(III) acetylacetonate and cyclopentadienyl magnesium bromide in 1952. The cobaltocenium bromide (**184**) obtained was further reacted to facilitate purification and afforded the pure compound cobaltocenium picrate **185** (Scheme 3.1.). On the other hand, Fischer et al. used a mixture of alkali salts of cyclopentadienide with  $\text{Co}(\text{NH}_3)_4(\text{SCN})_2$  in the presence of liquid ammonia to prepare cobaltocene (**186**) for the first time in 1953 (Scheme 3.2.).



**Scheme 3.1.** Synthesis of cobaltocenium using cobalt(III) acetylacetonate and cyclopentadienylmagnesium bromide by Wilkinson et al. in 1952.<sup>[91]</sup>

Cobaltocene (**186**) is a purple black solid, unstable in air,<sup>[90]</sup> paramagnetic and isostructural with ferrocene, possessing a staggered conformation as shown in Figure 3.1. However, it is not isoelectronic with ferrocene (**74**). It has 19 valence electrons and therefore is easily oxidized to its akin cobaltocenium ion.<sup>[92]</sup> The cobaltocene tendency to lose its “extra” electron is evident in its use as a common one-electron reducing agent in synthesis.<sup>[93]</sup> Cobaltocenium salts on the other hand, are isoelectronic with ferrocene, are air-stable and resistant to attack by strong acids and bases.<sup>[92]</sup>



**Scheme 3.2.** Synthesis of cobaltocene (**186**) by Fischer et al. in 1953.<sup>[90]</sup>

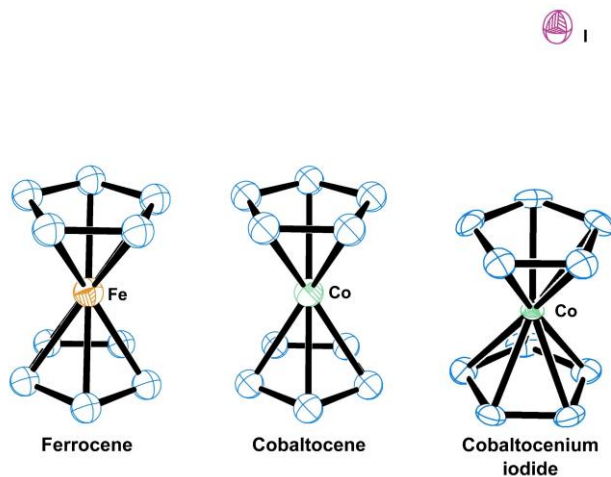
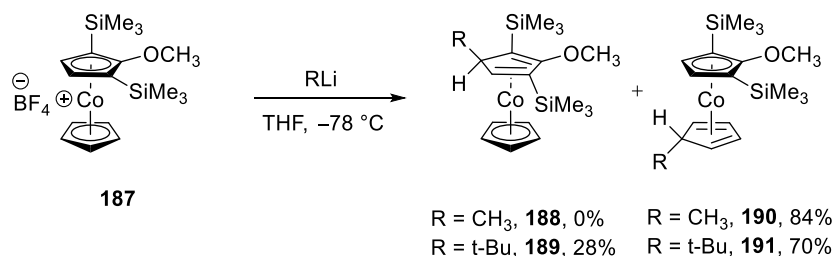
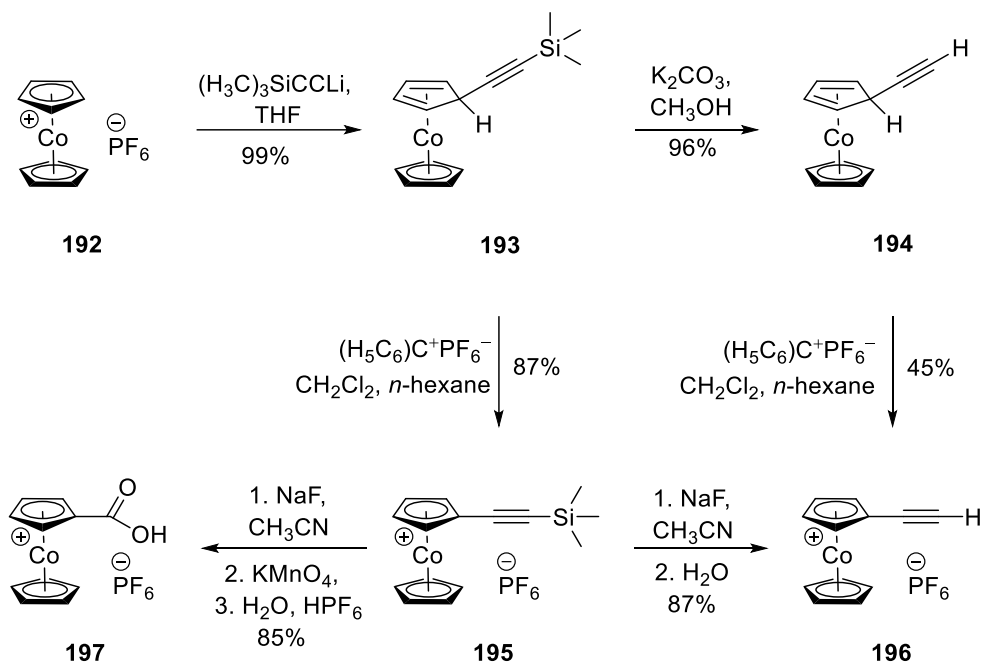


**Figure 3.1.** Crystal structures of ferrocene, cobaltocene and cobaltocenium iodide obtained from Cambridge Database (CCDC numbers: 1154868,1137578,799364).

The chemical behaviour of cobaltocene (**186**) and cobaltocenium salts differs from that of ferrocene (**74**). As an electron rich compound, ferrocene (**74**) is known to undergo electrophilic substitution, such as Friedel-Crafts acylation,<sup>[94]</sup> Vilsmeier<sup>[95]</sup> and Mannich<sup>[96]</sup> reactions among others, much faster than benzene. Acetylation of ferrocene (**74**), for example, is a popular reaction in undergraduate laboratory courses.<sup>[97]</sup> Cobaltocene (**186**) on the other hand, is readily oxidized in the presence of electrophilic reagents and the net positive charge of the cobaltocenium salt repels electrophilic species.<sup>[92]</sup> Nucleophilic reactions can also be carried out to functionalize ferrocene (**74**) upon formation of lithium ferrocene using Schlosser's base.<sup>[98]</sup> To the best of the author's knowledge, direct lithiation was not reported for cobaltocene (**186**) or cobaltocenium salts. Nevertheless, nucleophilic addition seems to be the typical reaction of these two compounds.<sup>[92]</sup> An example is the nucleophilic addition of alkyl lithium species to the cobaltocenium salt **187**, affording the (cyclopentadiene)(cyclopentadienyl)-cobalt(I) **188** – **191** reported by Vollhardt et al. (Scheme 3.3).<sup>[99]</sup> The ring selectivity depended upon the electronic preference to attack the substituted ring and steric factors forcing bulky electrophiles to add to the unsubstituted ring.<sup>[99]</sup> A recent example is illustrated in the first step of the synthetic route to cobaltocenium carboxylic acid hexafluorophosphate (**197**) from cobaltocenium hexafluorophosphate (**192**) upon nucleophilic addition of (trimethylsilyl)-acetylide reported by Bildstein et al. (Scheme 3.4).<sup>[100]</sup>

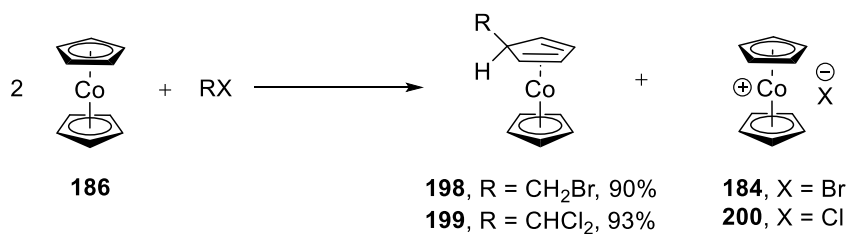


**Scheme 3.3.** Nucleophilic additions to cobaltocenium salt (**187**) forming substituted (cyclopentadienone)(cyclopentadienyl)cobalt(I) **188** – **191**.<sup>[99]</sup>



**Scheme 3.4.** Synthesis of cobaltocenium carboxylic acid hexafluorophosphate (**197**).<sup>[100]</sup>

The reaction of cobaltocene with organic halides forms two products: a substituted (cyclopentadiene)(cyclopentadienyl)cobalt(I) (**198** and **199**) and a cobaltocenium salt (**184** and **200**), as reported by Schwarzer et al. (Scheme 3.5).<sup>[101]</sup>

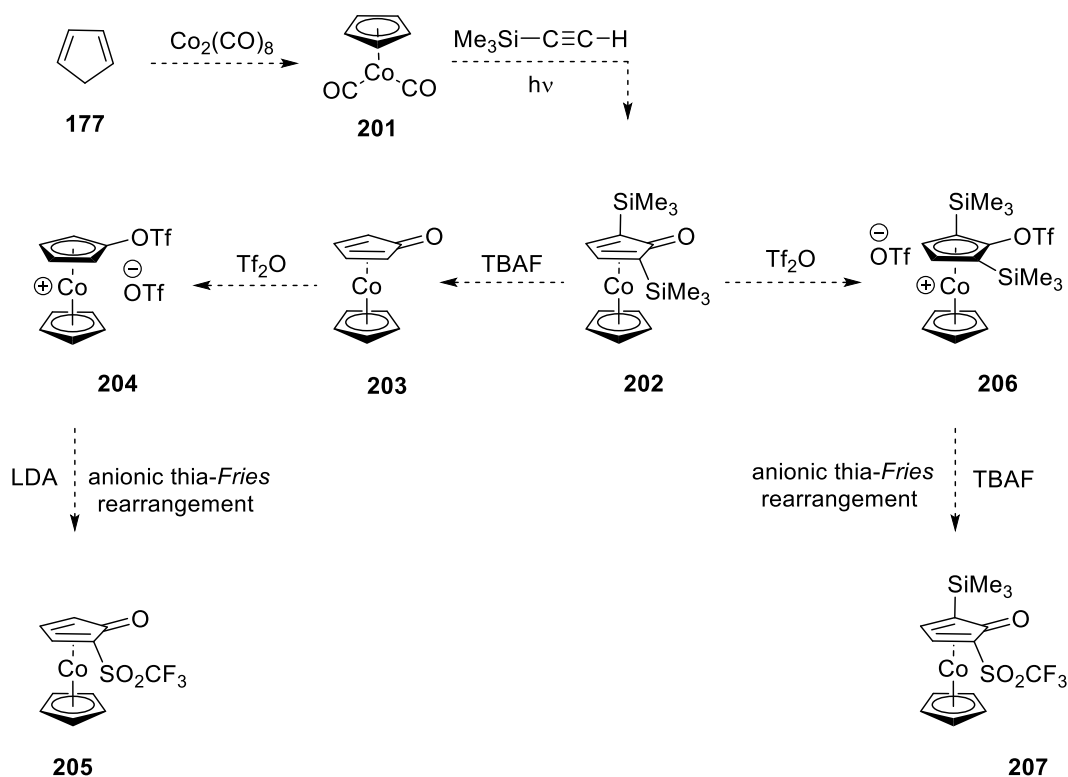


**Scheme 3.5.** Reaction of cobaltocene with a couple of organic halides. The yield of the cobaltocenium salts formed were not given. The reaction conditions vary.<sup>[101]</sup>

As mentioned above, cobaltocenium chemistry is much less developed than ferrocene chemistry, mainly because of the deactivating positive charge of the cobaltocenium moiety, which prevents convenient chemical functionalization by established methods in organic chemistry.<sup>[100]</sup> Quite often, reported cobaltocenium syntheses afford low yield, require

elaborate work-up procedures, harsh conditions, and many synthetic steps.<sup>[102]</sup> Nevertheless, as mentioned above, cobaltocenium is highly stable, diamagnetic, soluble in water and further investigation of these compounds, although challenging, might lead to new applications.

In this context, it was speculated if the anionic thia-Fries also takes place in cobaltocenium. In fact, the *ortho* deprotonation should be facilitated by the positive charge of cobaltocenium. The development of new methodologies for cobaltocenium chemistry allowing for further functionalization might open new frontiers for uses of cobaltocenium as catalyst precursors, ligands in catalysis, or simply as a new building block. To test if the rearrangement takes place, two different precursors, **204** and **206**, were envisaged, and the proposed synthetic routes are shown in Scheme 3.6.

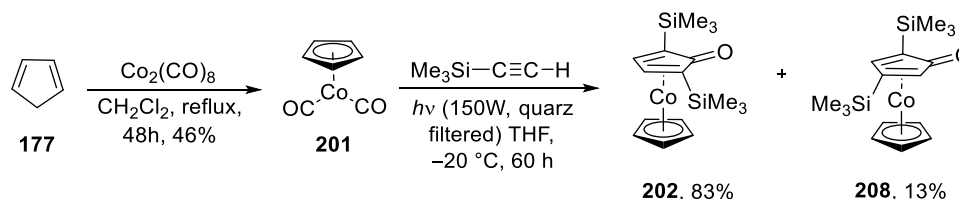


**Scheme 3.6.** Projected syntheses of the precursors **204** and **206** and proposed synthetic routes to the anionic thia-Fries rearrangement at cobaltocenium.

## 3.2 Results and discussion

The synthetic path starts with the synthesis of cyclopentadienylcobalt(I) dicarbonyl. This compound was first reported by Fischer in 1954<sup>[103]</sup> and Wilkinson one year later.<sup>[104]</sup> Fischer afforded the compound via high pressure carbonylation of cobaltocene.<sup>[103]</sup> Wilkinson, on the other hand, synthesised the compound simply by mixing dicobalt octacarbonyl with cyclopentadiene at room temperature.<sup>[104]</sup> In this work, a similar procedure to Wilkinson's method was used based on the work of Rausch et al.<sup>[105]</sup> and Bergman et al.<sup>[106]</sup> The reaction was conducted under reflux in DCM for 48 h and afforded 46% yield, Scheme 3.7., lower than that reported in the literature, 75%.

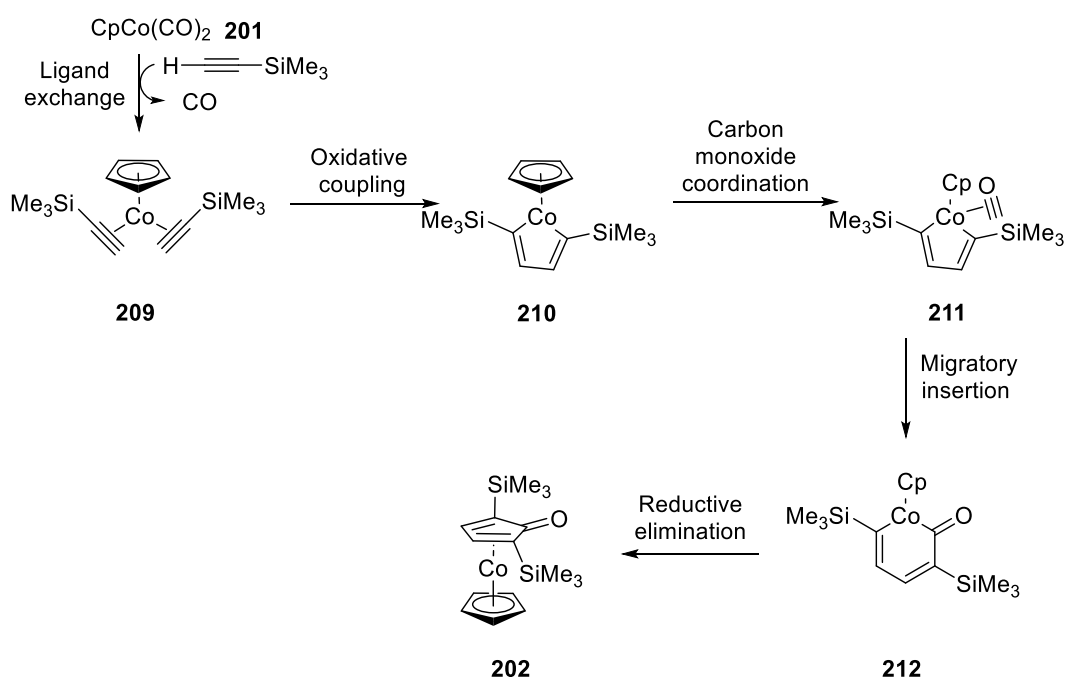
The synthesis of the intermediates **202** and **203** are already known and their synthetic path was developed by Vollhardt et al.<sup>[107]</sup> The synthesis of **202** consists of an elegant [2+2+1] cobalt mediated cyclisation of two alkynes and carbon monoxide. The reaction is conducted under UV light which promotes the dissociation of carbonyl group. It was reported that higher temperatures lead to increasing alkyne cyclotrimerization.<sup>[107]</sup> Vollhardt used a 450 W lamp and the reaction was irradiated for 5 h affording the isomers **202** and **208** in 53% and 17% yields, respectively. In this work, a weaker (150 W) and older UV lamp was used. For this reason, the reaction time was prolonged. Nevertheless, this set up increased the yield and regioselectivity as shown in Scheme 3.7.



**Scheme 3.7.** Synthesis of the (cyclopentadienone)(cyclopentadienyl)cobalt(I) **202** and **208**.<sup>[107]</sup>

To the best of the author's knowledge, the mechanism of [2+2+1] cobalt mediated cycloaddition of alkynes and carbon monoxide is not known. However, the mechanism shown in Scheme 3.8., is likely to be similar to the same generally accepted mechanism proposed for the [2+2+1] cycloaddition of alkyne, alkene and carbon monoxide Pauson-Khand reaction<sup>[108]</sup> and iron mediated [2+2+1] cycloaddition of alkynes and carbon monoxide proposed by Knölker et al.<sup>[109]</sup>

It consists of ligand dissociation and alkyne coordination giving **209**, followed by oxidative addition, forming the  $\eta^4$ -cyclopentadienone cobalt complex **210**. This step is followed by coordination of carbon monoxide (structure **211**) and a migratory insertion forming the cobaltcyclohexadienone **212**. After reductive elimination without dissociation **202** is formed. Nevertheless, the mechanism could also be slightly different. It could start with just one carbon monoxide dissociation followed by alkyne coordination. And the consecutive steps follow the same pattern of the mechanism shown in Scheme 3.8. Possibly, the mechanism could be probed experimentally using a closed vessel with  $^{13}\text{C}$  labelled carbon monoxide.

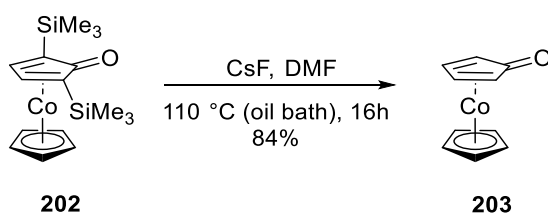


**Scheme 3.8.** Possible mechanism of the synthesis of the (cyclopentadienone)(cyclopentadienyl)cobalt(I) **202**.

In the same work, Vollhardt et al. also synthesized the (cyclopentadienone)(cyclopentadienyl)cobalt(I) **203** via desilylation of **202** using benzyltrimethylammonium fluoride and ethanol.<sup>[107]</sup> As this salt was not available in the laboratory, TBAF and TBAT were tested instead. The desilylation worked, monitored via TLC. However, the purification step via column chromatography proved to be very difficult, especially upon use of TBAF. The purification procedure used by Vollhardt et al. involved sublimation under ultrahigh vacuum, which was

unfortunately unavailable, and chromatography. Before trying benzyltrimethylammonium, it was decided to test an inorganic source of fluoride, e.g., caesium fluoride, which can be easily removed, Scheme 3.9. A mixture of **202** and CsF in DMF was stirred initially at 21 °C and the reaction progress was monitored via TLC. As nothing happened, the temperature was slowly increased. Upon reaching 110 °C, the reaction seemed to have taken place, due to the fact that the starting material had been consumed. The solution was then filtered, and the solvent removed at reduced pressure at 70 °C (oil bath). The product was crystallized from EtOAc affording **202** in 84%. Mistakenly, no ethanol as a proton source was used in the reaction. Nevertheless, the reaction worked well and there was no crystal water. The proton source is not known. Even though CsF can be obtained as an anhydrous reagent, it is very hygroscopic, and it might have had some water in it, despite the used reagent flask being relatively new and the powder having no clumps. The solvent used, DMF, is known for being a non-innocent solvent in several reactions, although it is not common for being a source of protons.<sup>[110]</sup> However, near its boiling point, DMF undergoes decarbonylation forming dimethylamine, which is a proton source. But for this reason, the reaction was repeated at a smaller scale using deuterated DMF to test this hypothesis. However, the NMR does not show incorporation of deuterium in the molecule.

Vollhardt et al. reported **203** as a monohydrate,<sup>[107]</sup> but the use of caesium fluoride, together with the purification procedure proposed, enabled the obtention of **203** without any crystal water. This proved to be advantageous for the next step of the synthesis, which uses triflic anhydride.



**Scheme 3.9.** Synthesis of the (cyclopentadienone)(cyclopentadienyl)cobalt(I) (**203**).

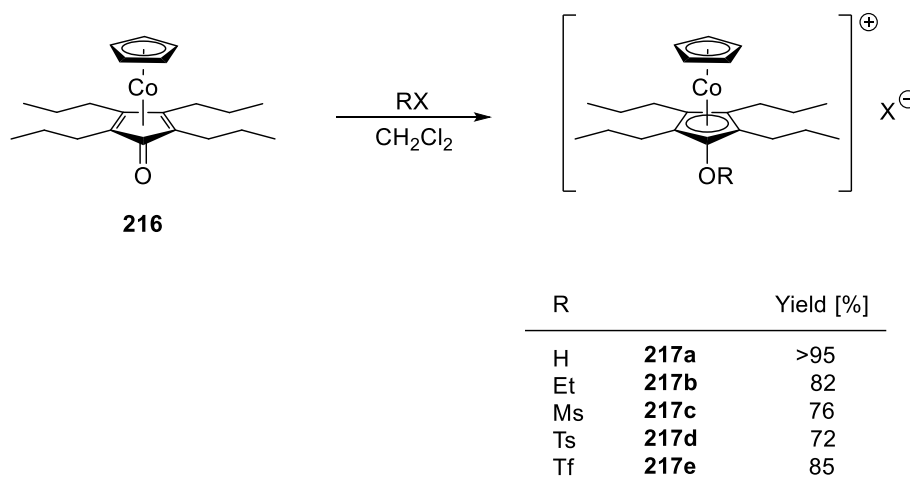
**203** is very hygroscopic. In the NMR it was possible to see that there was no water peak. However, the IR could not be measured under protected atmosphere, and a broad band at 3300 cm<sup>-1</sup> was present due to water. The band got stronger the longer the sample was left exposed to air (Figure 3.2).



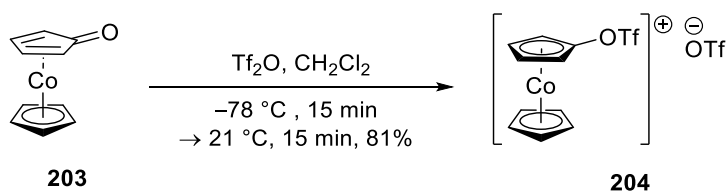


represented by deprotonated hydroxycobaltocenium zwitterions (**214a – d**) resonance form.<sup>[111]</sup>

Gleiter et al. explored the electronic properties of **216** to synthesise compounds **217 a – e** as shown in Scheme 3.11.<sup>[112]</sup> The same strategy was considered for the synthesis of **204**. Upon addition of triflic anhydride to a solution of (cyclopentadienone)(cyclopentadienyl)cobalt(I) (**203**) in DCM, the red/orange solution immediately changed to yellow (Scheme 3.12). After purification, the new cobaltocenium salt **204** was afforded in 81 % yield as a yellow air stable solid. The compound **204** is a good potential candidate to palladium cross-coupling, since the positive charge of the cobalt might facilitate the oxidative addition step.



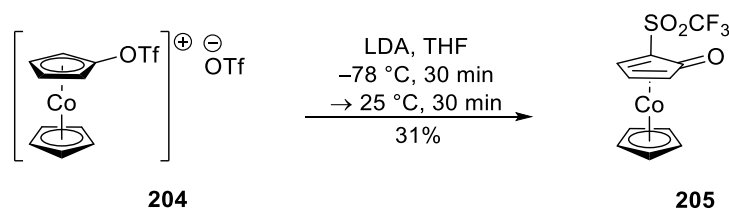
**Scheme 3.11.** Synthesis of the cobaltocenium salts **217 a – e**.



**Scheme 3.12.** Synthesis of the [(trifluoromethylsulfonyl)oxy]cobaltocenium trifluoromethanesulfonate (**204**).

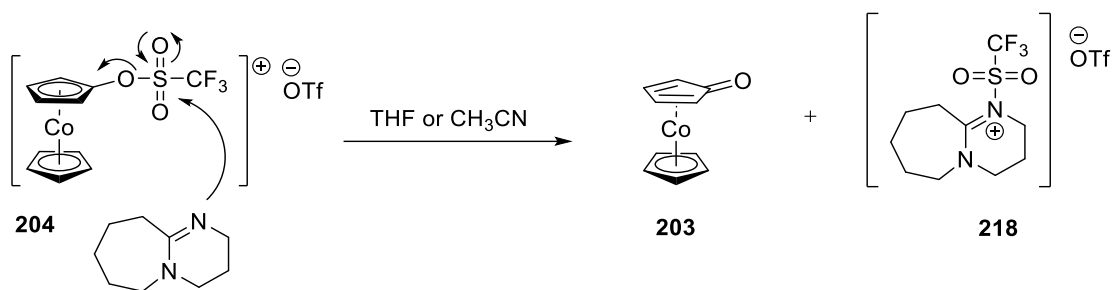
Fortunately, by reacting the cobaltocenium salt **204** with the non-nucleophilic hindered base LDA, the anionic thia-Fries rearrangement took place forming the new compound **205** (Scheme 3.13). The product **205** is an air stable red/orange solid. The reaction seemed to proceed well,

but the yield was low, at only 31%. There was no sign of the starting material though. It is still not known if the compound is lost during the purification or if there was partial decomposition/demetallation. Nevertheless, the reaction is the first case of an anionic thia-Fries rearrangement at a cobalt complex. So far, the rearrangements at ferrocene<sup>[17]</sup> and at (arene)tricarbonylchromium<sup>[15]</sup> were the only examples of the rearrangement at metal complexes.



**Scheme 3.13.** Anionic thia-Fries rearrangement of the cobaltocenium salt **204**.

Cobaltocenium salts are less electron rich than ferrocene, and thus, the cyclopentadienyl protons should be more acidic. Accordingly, the anionic thia-Fries rearrangement at cobaltocenium was sought using a weaker organic base such 1,8-diazabicyclo[5.4.0]undec-7-ene (DBU). DBU was added to **204** in THF at 25 °C. The yellow solution changed immediately to red, but an inspection via TLC showed only **203** (**204** in silica/alumina goes back to **203**), the base and no product **205**. The reaction was then stirred for 1 h, but there was still no sign of the product. The solution was then brought to reflux for 16 h and an extra red spot was visualized in the TLC. The retention time did not correspond to the one of product **205**, and a TLC/MS afforded a mass of  $m/z = 455.1$ . An attempt to isolate the new compound via column chromatography (deactivated silica) failed since the product perished in the column, but there was no visual sign of decomposition. DBU has a  $pK_a$  of 24 in acetonitrile, higher than in THF, with a  $pK_a$  of 17.<sup>[113]</sup> DBU was also added to **204** in acetonitrile at 25 °C and the solution again promptly turned red, too. The solution was stirred for 1 h at 25 °C, but no product **205** was formed. DBU is a sterically hindered tertiary amine base, however, it has been demonstrated that DBU can be nucleophilic.<sup>[114]</sup> Consequently, it is possible the DBU attacked the electrophilic sulfur forming **203** and **218**, which fragmented at the silica of the TLC (Scheme 3.14).



**Scheme 3.14.** Possible nucleophilic attack of DBU at **204** in THF and acetonitrile.

Single crystals suitable for X-ray crystal structure analysis were obtained from slow solvent evaporation of **205** in a solution of EtOAc. The crystal structure analysis (Figure 3.3.) displays a racemic mixture of **205** and a water molecule coordinated to both carbonyl groups, in a monoclinic crystal system, space group *Cc* (9). The cyclopentadienyl rings are not perfectly eclipsed. The angle between the cobalt atom, the centroid on the substituted cyclopentadienyl ring and the carbonyl carbon is 100° and elevated above the plane, clearly showing that the cyclopentadienone ring is not planar and that the hapticity changed from  $\eta^5$ -cyclopentadienyl to  $\eta^4$ -cyclopentadienone.

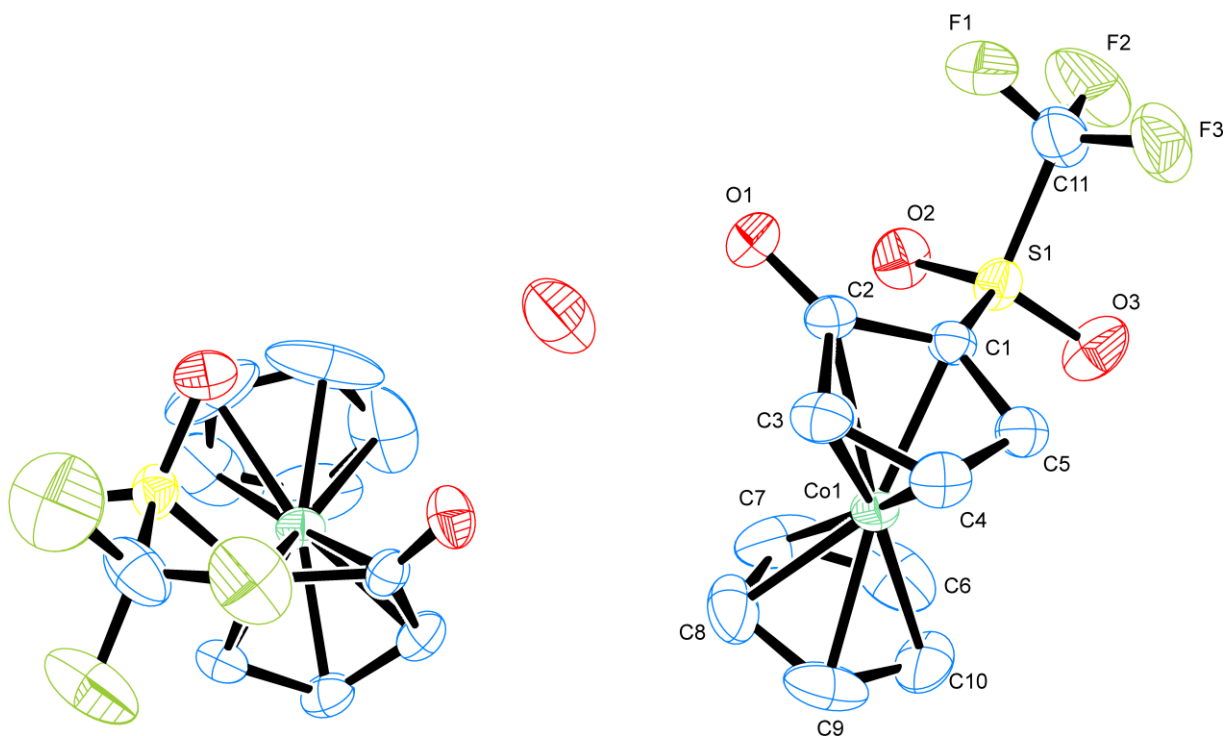


**Figure 3.3.** Crystal structure analysis of **205**. Ellipsoids at 50 % probability level. Hydrogen atoms have been omitted for clarity. Selected bond lengths [pm] and angles [°]: Co1–C1 202.2(6), Co1–C2 227.3(6), Co1–C3 206.3(6), Co1–C4 201.3(5), Co1–C5 198.2(6), Co1–C6 201.9 (9), Co1–C7 202.5 (9), Co1–C8 202.4(9), Co1–C9 203.3 (7), Co1–C10 204.9 (7), C1–O2 172.5 (5), C2–O1 124.4 (7), S1–O2 142.6 (5), S1–O3 143.4 (5), S1–C11 183.6 (7), C11–F1 131.3 (9), C11–F2 133.0(8), C11–F3 131.6(9), C2–C1–S1 125.4(4), Co1–C1–S1 117.5(3), Co1–C2–O1 134.8(4).

The anionic thia-Fries rearrangement of **204** affords a very dark brown mixture after initially turning red. In an attempt to obtain better yields by changing the purification process from column chromatography to crystallization, the triflic anhydride was changed to trifluoromethanesulfonyl chloride. The reaction should result in a rearranged product, DIPA and LiCl, and should therefore be easier to be purified. The more electron rich **208** was chosen to do the tests and should better react than the less electron rich **203**, according to Sheats et al. observations. However, when the isomer **208** was treated with trifluoromethanesulfonyl chloride, a full conversion did not take place, as can be seen in the NMR spectrum (Figure 3.4). Unfortunately, it was not possible to separate product from starting material. Trifluoromethanesulfonyl chloride has a boiling point of 32 °C, and it seems like the starting material is in equilibrium with the product in solution. Due the low boiling point of trifluoromethanesulfonyl chloride, it might slowly evaporate, shifting the equilibrium to the starting material after a long reaction time as shown in Figure 3.4. It is also interesting to note that the NMR peaks of the starting material **208** change, possibly depending on the concentration and interaction with the product. This was also observed upon reaction of **203** with trifluoromethanesulfonyl chloride (Figure 3.5).

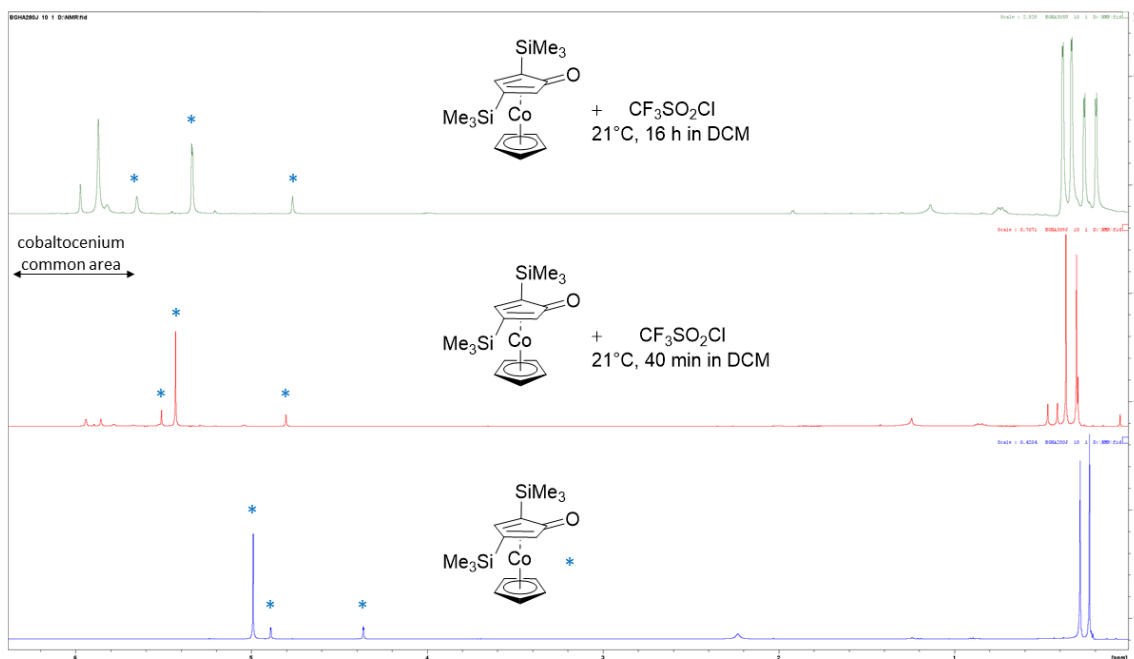


**Figure 3.4.** Stacking  $^1\text{H}$  NMR plots of **208** and its reaction with trifluoromethanesulfonyl chloride after 40 min and after 16 h. The second  $^1\text{H}$  NMR spectrum shows an increase of **208**.

Interested to know if the anion could be exchanged, the reaction to prepare **204** was repeated, and after it was brought to room temperature, silver tetrafluoroborate was added. After evaporation of the solvent, diethyl ether was added and a yellow precipitate was formed. Unfortunately, the replacement did not take place and only **204** was present. This was to some extent anticipated. Silver tetrafluoroborate is expected to replace halide anions. The formed insoluble silver halide precipitates and shifts the reaction, but in this case, the soluble silver triflate would have been formed instead. Curiously though, not even a mixture of **204** and **202** was observed. For this reason, silver tetrafluoroborate was added to the reaction forming **220**, but it did not work either.

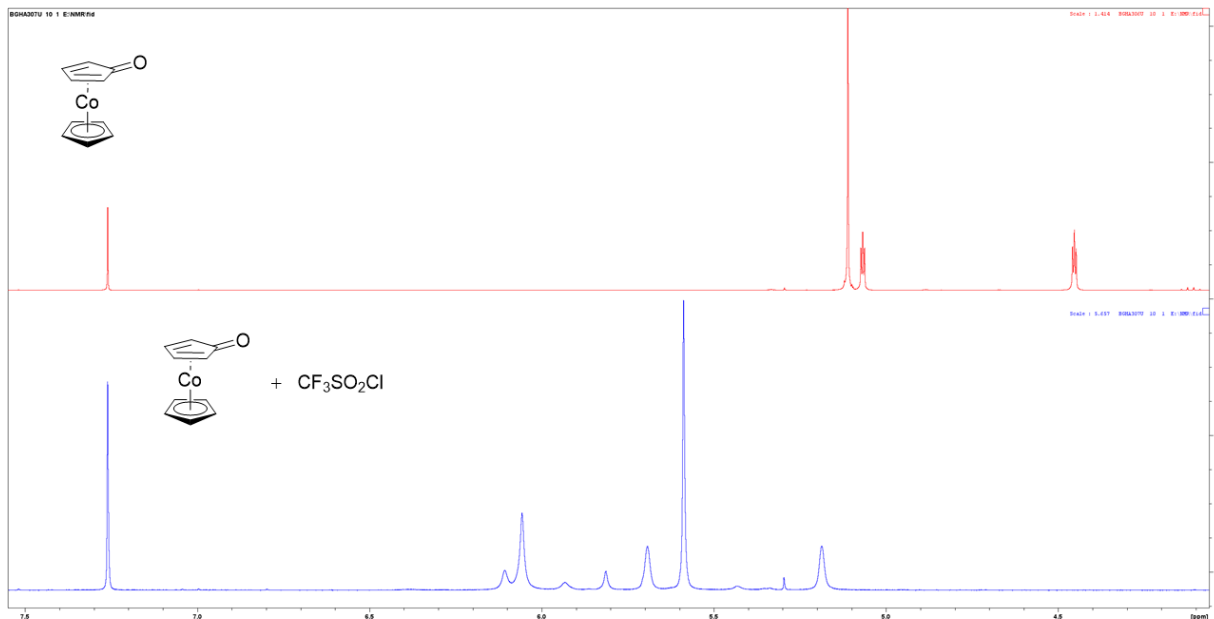
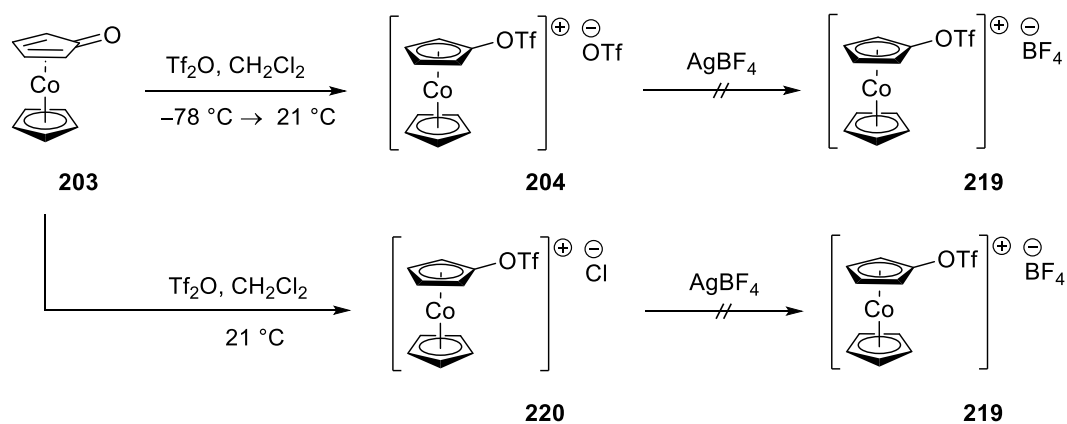


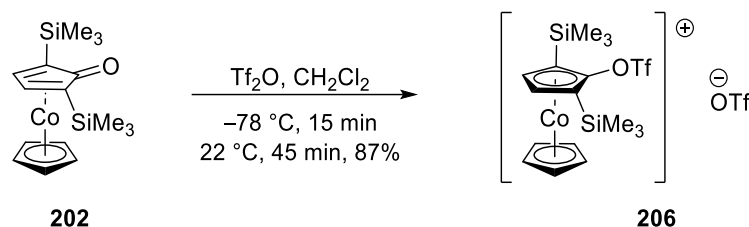
**Figure 3.5.** NMR of **203** (top NMR spectrum) and its reaction with trifluoromethanesulfonyl chloride (bottom NMR spectrum).



**Scheme 3.15.** Anion exchange attempt of the cobaltocenium salts **204** and **220** using silver tetrafluoroborate.

Meanwhile, the second proposed route synthesis was conducted in parallel. The preparation

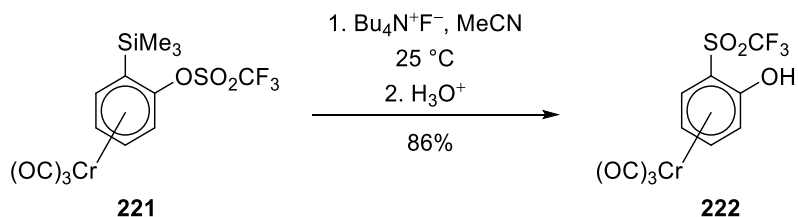
of the cobaltocenium salt **206** obtained from **202** before desilylation, was synthesized in good yield (Scheme 3.16). The reaction conditions were the same used for the synthesis of **204**. The reaction worked very well, there was no equilibrium, and the new air stable compound **206** was crystallized as a yellow solid.



**Scheme 3.16.** Synthesis of the 1-[(trifluoromethylsulfonyl)oxy]-2,5-bis(trimethylsilyl)cobaltocenium trifluoromethanesulfonate (**206**).

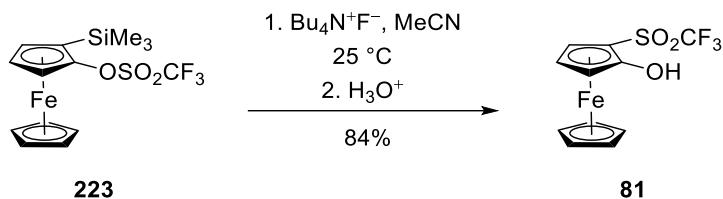
Sheats et al. assessed the effects of substituents on the acidities of hydroxycobaltocenium salts. They concluded that the acidity increases with increasing electronegativity of the substituent at the cyclopentadienyl ring and decreases with the addition of methyl groups on either cyclopentadienyl ring.<sup>[111]</sup> This tendency of cobalt to remain as cobalt (III) seems to apply also to this case.

Kobayashi prepared arynes in 1983 using fluoride ion to remove the trimethylsilyl group which was followed by triflate elimination and benzyne formation.<sup>[115]</sup> However, an attempt to use this strategy to generate aryne tricarbonylchromium complex in 2010 and ferrocene in 2013 led to the anionic thia-Fries rearrangement (Schemes 3.17 and 3.18).<sup>[15,50]</sup>



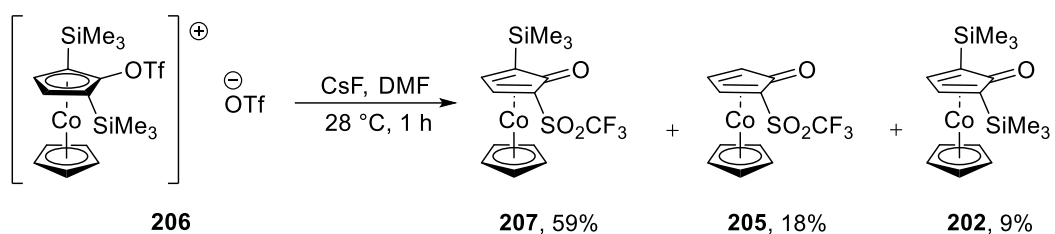
**Scheme 3.17.** Anionic thia-Fries rearrangement at an (aryl triflate)tricarbonylchromium complex via desilylation.<sup>[15]</sup>





**Scheme 3.18.** Anionic thia-Fries rearrangement at the ferrocenyl triflate derivative **223** via desilylation.<sup>[50]</sup>

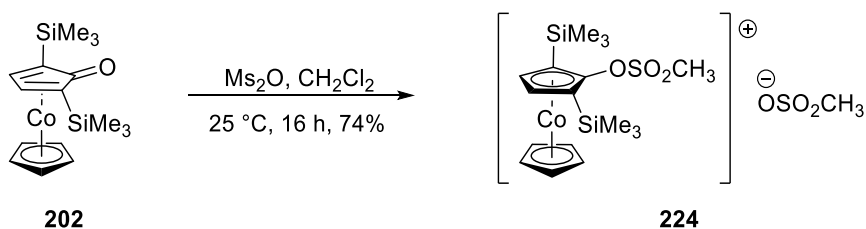
With the compound **206** in hand, **206** was then treated with CsF in DMF at 28 °C, and the yellow solution of the starting material turned red immediately, affording the new compound **207** as an air stable red/orange solid in 59% yield, besides 18% of **205** and 9% of **202** (Scheme 3.19). The obtained yield for **207** is much better than that obtained for **205** and its purification through column chromatography is much easier. Besides this, compound **207** is less polar and easier to handle. Compound **205** for example, seems to be more easily retained in silica and/or alumina upon purification.



**Scheme 3.19.** Fluoride induced anionic thia-Fries rearrangement at **206**.

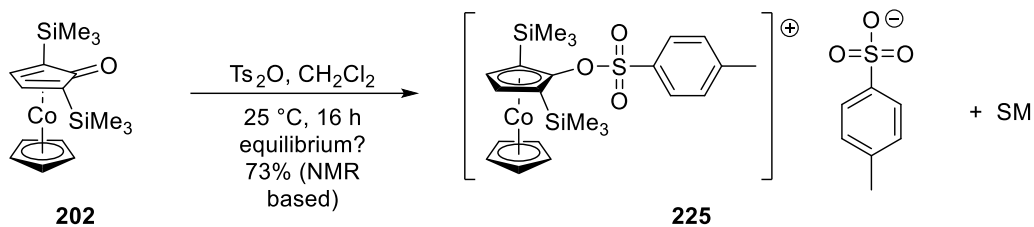
The new anionic thia-Fries rearrangement product **207** obtained via desilylation led to a trisubstituted compound, which possibly can be further modified due to the remaining silyl group. The product **207** may also potentially be a valuable source of substituted cyclopentadienone synthons since (cyclopentadienone)(cyclopentadienyl)cobalt(I) complexes can in general be de-metalated in the presence of ceric ammonium nitrate in a two solvent system as reported by Vollhardt et al. in 1980.<sup>[107]</sup> The product **207** could also be further reacted with triflic anhydride and be submitted to a second anionic thia-Fries rearrangement via desilylation.

The presence of the silyl group at the *ortho* position of the ketone at **207** might be quite strategic in allowing for an anionic thia-Fries rearrangement at mesyl- and tosyl- cobaltocenium derivatives and therefore their syntheses were envisaged. **202** was then treated with methanesulfonic anhydride in dichloromethane at 25 °C (Scheme 3.20). The reaction has to be conducted at higher temperatures when compared with triflic anhydride, and the observed solution change in colour, from red to yellow, did not happen immediately as it was observed for the reaction of **202** with triflic anhydride. As methanesulfonic anhydride is not as strong an electrophile as triflic anhydride, the reaction time was extended in comparison with the reaction described in scheme 3.16. After the reaction was finished, the solvent was evaporated, washed with cold diethyl ether, and crystallized from dichloromethane and diethyl ether. The new compound **224** was obtained as an air stable, hygroscopic yellow crystalline solid, but which might not have been obtained in a pure form according to the NMR spectrum. The NMR spectrum showed a small percentage of the starting material, but it is not clear if the starting material is an impurity or if reagent and reactants are in equilibrium in solution.



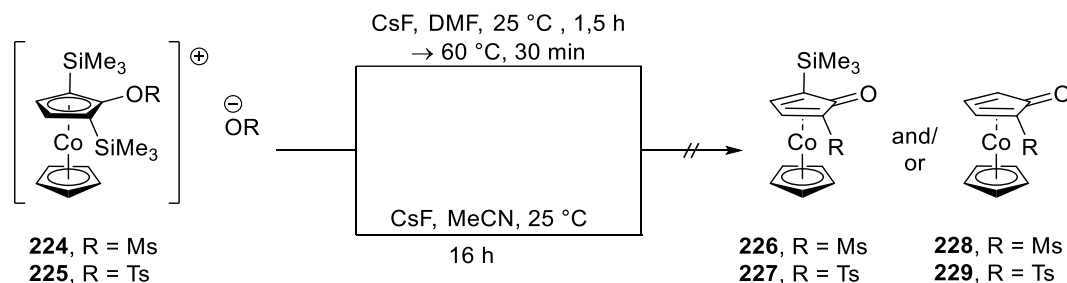
**Scheme 3.20.** Synthesis of 1-[(methanesulfonyl)oxy]-2,5-bis(trimethylsilyl)cobaltocenium methanesulfonate (**224**).

A similar behaviour was observed when **202** was treated with *p*-toluenesulfonic anhydride. The colour started to change to orange only after two hours, and only after long more hours it was yellow. After removal of the solvent and washing with diethyl ether, the remaining yellow solid was dissolved in dichloromethane, and after addition of diethyl ether, it was left in the fridge to crystallize. The crystallization was not successful, though. An NMR measurement of the solid was done, and a mixture of the product and the reagents was observed.



**Scheme 3.21.** Synthesis of the 1-[(*p*-toluenesulfonyl)oxy]-2,5-bis(trimethylsilyl)cobaltocenium *p*-toluenesulfonate (**225**).

Nevertheless, **224** and **225** as obtained, were reacted with caesium fluoride in dimethylformamide (Scheme 3.22) but no anionic thia-Fries rearrangement took place. None of the products **226** to **229** were observed. The reactions were repeated in acetonitrile at 25 °C but no rearrangement took place, either.

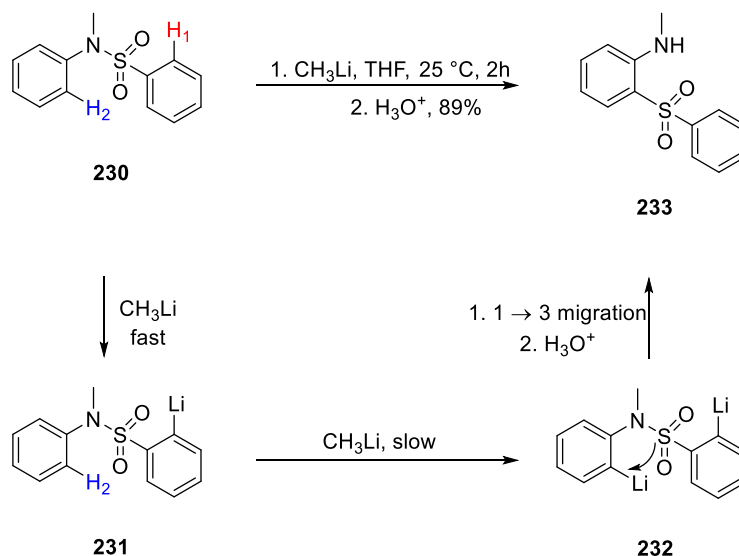


**Scheme 3.22.** Misassumed anionic thia-Fries rearrangement at **224** and **225**.

The reason why the anionic thia-Fries rearrangement takes place at **206** but do not take place at **224** and **225** is not very clear but it might be due to a nucleophilic attack at the sulfur atom instead at the silicon atom. **202** is deep red in colour and it looks like that the fluoride anion is attacking the sulfonyl group instead of displacing the trimethylsilyl group. During our chemistry courses we always hear that silicon-fluorine bond is a very strong one. The dissociation energy of Si-F is 552 kJ/mol<sup>[116]</sup> whilst S-F is 340 kJ/mol<sup>[117]</sup>. The high strength of silicon-fluorine bond is behind the use of fluoride sources as desilylation reagents and therefore, it would be expected that the fluoride would attack the trimethylsilyl group instead of the sulfur atom. The DFT calculations for ferrocenyl triflate (**79**), mesylate (**94**) and tosylate (**95**) presented in chapter 2 (Figure 2.8), shows different electronic density distribution between the ferrocenyl triflate (**79**),

which undergoes anionic thia-Fries rearrangement, from the mesylate (**94**) and tosylate (**95**), which do not undergo the rearrangement. In figure 2.8, it is possible to see that the charge density in the sulfur atom at the mesylate (**94**) and tosylate (**95**) are smaller and that they are more acidic than the sulfur atom at **79**. This might be a reason for the fluoride nucleophilic attack at the sulfur atom instead of the silicon atom

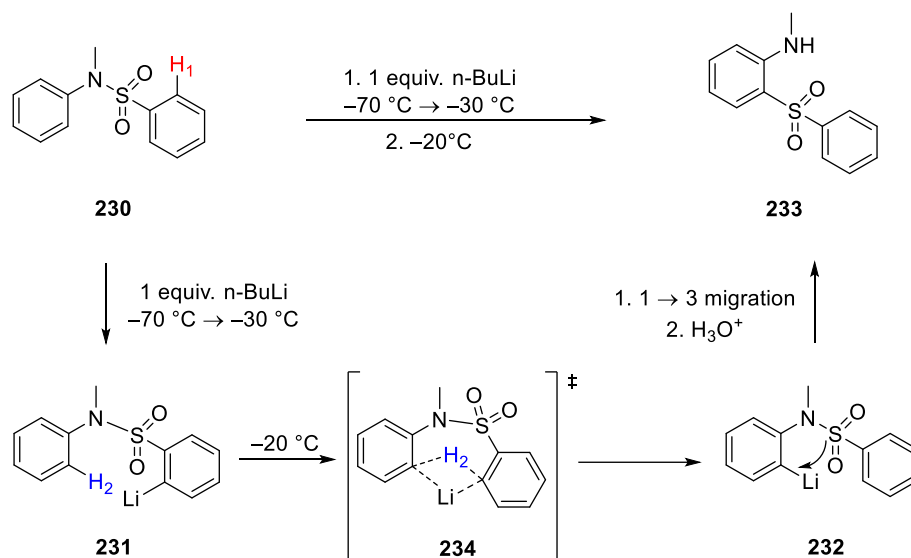
Anionic thia-Fries rearrangement of phenyl sulfonyl derivatives is rare but the homologous 1,3 N→C migration disclosed by Closson et al.<sup>[118]</sup> has been known for a long time and shows that it also should be possible for sulfonyl esters (Scheme 3.23) to undergo rearrangement. The major structural requirement of the sulfonamide for rearrangement was for the nitrogen atom to be completely substituted, however, this is not an issue for sulfonyl esters. The proposed mechanism is bit different, though. Crossover experiments showed that the rearrangement is intramolecular and that the *ortho* proton to the sulfonyl group (**230**, H<sub>1</sub>) is first removed and only if an excess of alkyllithium is used, the rearrangement take place. It suggests that the *ortho* deprotonation to the nitrogen group (**231**, H<sub>2</sub>) happens only after, forming **232**, allowing for the rearrangement to take place, leading to the product **233** (Scheme 3.23).



**Scheme 3.23.** Base-promoted rearrangement of sulfonamides and its mechanism proposed by Closson et al in 1975.<sup>[118]</sup>

However, the investigations conducted by Hellwinkel et al. proposed that after the *ortho* lithiation to the sulfonyl group (**230**, H<sub>1</sub>), there would be a hydrogen metal exchange leading to

the transition state **234**, which undergoes the rearrangement (Scheme 3.24).<sup>[119]</sup> Nevertheless, both mechanisms show that as soon as the *ortho* position to the nitrogen atom is lithiated, the rearrangement happens, and that probably **224** and **225** were not desilylated, but rather underwent a nucleophilic attack at the sulfur atom.



**Scheme 3.24.** Base-promoted rearrangement of sulfonamides and its mechanism proposed by Hellwinkel et al. in 1976.<sup>[119]</sup>

### 3.3 Conclusion

In conclusion, it was demonstrated for the first time that the anionic thia-Fries rearrangement is also feasible at cobaltocenium salt complexes broadening the scope of this chemistry. The rearrangement takes place in the presence of lithium amide base as well as via mild desilylation at room temperature. The desilylation pathway has the advantage of leading to a product that can be more easily purified. Besides this, the synthesis and purification of **203** was improved, and **203** can now be obtained in an anhydrous form. The new cobaltocenium salts **224** and **225** were prepared, but they did not undergo rearrangement, putatively because the fluoride anion attacked the sulfur atom leading to **202**.

## Chapter 4

# 4. Computational studies

### 4.1. Introduction

Quantum mechanics fundamental equation was postulated by Erwin Schrödinger and named after him. The Schrödinger equation (eq. 1), which describes the behaviour of subatomic particles, is

$$\hat{H}\Psi = E\Psi \quad \text{Eq. 1}$$

where  $\hat{H}$  is the Hamiltonian operator,  $\psi$  a wave function and  $E$  the energy. Typically, the Hamiltonian operator takes into account five different contributions to the total energy of a system (e.g. molecule) which are the kinetic energy of the electrons and nuclei, the attraction of the electrons to the nuclei, and the interelectronic and internuclear repulsion. The Hamiltonian is composed of kinetic energy and potential energy terms and the mathematical notation is represented in Eq. 2,

$$H = -\sum_i \frac{\hbar^2}{2m_e} \nabla_i^2 - \sum_k \frac{\hbar^2}{2m_k} \nabla_k^2 - \sum_i \sum_k \frac{e^k Z_k}{r_{ik}} + \sum_{i<j} \frac{e^2}{r_{ij}} + \sum_{k<l} \frac{e^2 Z_k Z_l}{r_{kl}} \quad \text{Eq. 2}$$

where  $i$  and  $j$  run over electrons,  $k$  and  $l$  run over nuclei,  $\hbar$  is the Planck's constant divided by  $2\pi$ ,  $m_e$  is the mass of the electron,  $m_k$  is the mass of the nucleus  $k$ ,  $\nabla^2$  is the Laplacian operator,  $e$  is the charge on the electron,  $Z$  is the atomic number.<sup>[120]</sup>

Accurate wave functions for many-particle molecular systems are extremely difficult to express because of the correlated motion of particles. To try to simplify and solve the wavefunctions,

Born-Oppenheimer approximation may be used. Basically, it assumes that the motions of atomic nuclei and the electrons in a molecule can be decoupled, because the nuclei move much more slowly than the electrons (protons and neutrons have approx. 1800 times the mass of an electron).<sup>[120]</sup>

Several different ways to solve the Schrödinger equation have emerged and the most prominent are the *ab initio* Hartree-Fock (HF), the post-Hartree-Fock *ab initio* Møller–Plesset perturbation theory (MP), which are based on wavefunction, Density Functional Theory (DFT) based on electronic density, which was used in this work.<sup>[120]</sup>

### *Density Functional Theory*

The motivation to develop DFT was the difficulty to solve the wavefunctions used in HF and it is rooted in the Hohenberg-Kohn theorems.<sup>[121]</sup> The Hohenberg-Kohn existence theorem states that electrons interact with one another and with an “external potential” (nuclear potential), and that the total energy is a unique functional of the electron density. The Hohenberg-Kohn variational theorem shows that the density obeys a variational principle.<sup>[120]</sup>

In 1965, Kohn-Sham made a breakthrough simplifying the expression of the Hamiltonian operator as one for a *non-interacting* system of electrons, e.g., as a sum of one-electron operators. The energy functional can be expressed as

$$E[\rho(\mathbf{r})] = T_{ni}[\rho(\mathbf{r})] + V_{ne}[\rho(\mathbf{r})] + V_{ee}[\rho(\mathbf{r})] + \underbrace{\Delta T[\rho(\mathbf{r})] + \Delta_{ee}[\rho(\mathbf{r})]}_{E_{xc}[\rho(\mathbf{r})]} \quad \text{Eq. 3}$$

where the term on the right-hand side refers, respectively, to the kinetic energy of the non-interacting electrons, the nuclear-electron interaction, the classical electron-electron repulsion, the correction to the kinetic energy deriving from the interacting nature of the electrons, and all non-classical corrections to the electron-electron repulsion energy.<sup>[120]</sup> Since then, the use of DFT models has seen a huge rise and became very popular. It has proved to be a very robust and powerful tool to explore and unravelled reaction mechanisms in the past decades. A quick search of “DFT” in Scifinder, returns more the 440 thousand hits, for example.

### *CPMD*

In 1985 Car and Parrinello developed the Car-Parrinello molecular dynamics method (CPMD)<sup>[122]</sup> to describe atomic and molecular motion. “Molecular Dynamics” generally means that the nuclei are described classically (Newtonian dynamics) as point charges. CPMD on the

other hand, treats the movement of electron quantum mechanically.<sup>[123]</sup> The basis set for the coding of CPMD are usually plane waves. The formulation is an extension of a classical molecular dynamics Lagrangian, in which the electronic degrees of freedom (wavefunctions) are added to the system, along with any other dynamical variable.<sup>[124]</sup>

$$\begin{aligned} \mathcal{L}^{CP} = & \frac{1}{2} \sum_I M_I \dot{R}_I^2 + \sum_i \mu \int |\psi(x)|^2 d^3x + \frac{1}{2} \sum_\alpha \eta_\alpha \dot{q}_\alpha^2 - E^{KS}[\rho, \{R_I\}, q_\alpha] \\ & + \sum_{ij} \lambda_{ij} \left( \int d^3x \psi_i^*(x) \psi_j(x) - \delta_{ij} \right) \end{aligned} \quad \text{Eq. 4}$$

The first term on the right-hand side of the equation is the kinetic energy of the nuclei, the second one the fictitious kinetic energy of the electrons representing the update of the wavefunctions during the dynamics, the third one the kinetic term of any further dynamical variable used in the sense specified above, the fourth one is the DFT total energy, and the last addendum is the orthonormality constraint for the wavefunctions. The kinetic energy for the electronic degrees of freedom is the main novelty of the CPMD approach: A strategy to update on-the-fly the wavefunctions when ions undergo a dynamical displacement, avoiding expensive iterative diagonalization required by the BO approach at each time step.<sup>[124]</sup>

## 4.2. Results and discussion

As presented in the Chapter 2, Butenschön et al. published the anionic thia-Fries rearrangement at ferrocenyl triflate (**79**) and 1,1'-ferrocenediyl ditriflate (**80**) and observed an unprecedented stereoinduction of the later affording only the *meso* product **87** (Schemes 2.12 and 2.14).<sup>[17]</sup> The origin of the selective formation of the *meso* product **87** trapped as diacetate **89** with no *racemo* product **88a/88b** being obtained is still unknown. To understand the reaction mechanisms and unravel the observed diastereoselectivity, experimental and computational investigations of the anionic thia-Fries rearrangement at ferrocenyl triflate (**79**) and 1,1'-ferrocenediyl ditriflate (**80**) were realized.

Several different bases for the rearrangement of **79** were screened in order to obtain a better insight into the importance of the counter cation and the solvent (Table 4.1). Furthermore, it was hoped that the formation of 1,2-dehydroferrocene (ferrocene, **75**) would be observed,



which was, unfortunately, not the case. The use of lithium diisopropylamide (LDA) in the presence of 12-crown-4 did not change the result nor the yield of the reaction. Using the sodium analogue of LDA, NaDA,<sup>[87]</sup> also led to the rearrangement product, albeit in a lower yield. However, significantly lower yields were observed when either sodium or potassium bis(trimethylsilyl)amide were used suggesting that the counter cation charge density might indeed play an important role.

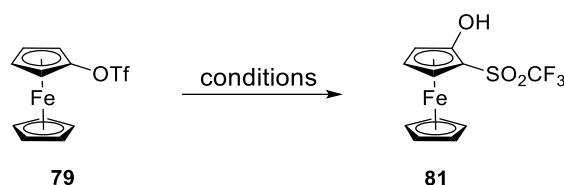


**Table 4.1.** Screening of different bases for the anionic thia-Fries rearrangement of ferrocenyl triflate (**79**).

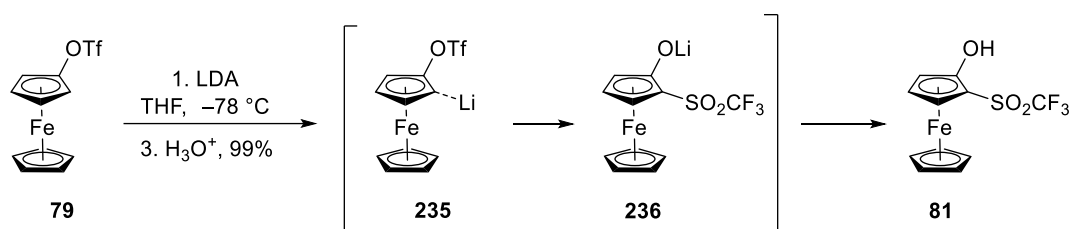
Base (1 equiv.)	Conditions	Yield of <b>81</b> (%)	Recov. <b>79</b> (%)
LDA <sup>a</sup>	THF, -78 °C → 23 °C, 30 min	99	–
LDA/12-crown-4	THF, -78 °C → 23 °C, 30 min	99	–
LDA	DIPA, -78 °C → 23 °C, 30 min	75	13
NAH	THF, 23 °C, 16 h	– <sup>[b]</sup>	–
KH	THF, 23 °C, 16 h	– <sup>[b]</sup>	–
NaDA <sup>[5]</sup>	THF, -78 °C, 40 min	81 <sup>[c]</sup>	–
NaN[Si(CH <sub>3</sub> ) <sub>3</sub> ] <sub>2</sub>	0 °C → 23 °C, 16 h	62	–
KN[Si(CH <sub>3</sub> ) <sub>3</sub> ] <sub>2</sub>	0 °C → 23 °C, 16 h	13	67
Phosphazene P2-tBu	THF, -78 °C → 0 °C, 30 min	– <sup>[d]</sup>	61
Mg(DA) <sub>2</sub>	THF, -78 °C → 0 °C, 30 min	– <sup>[e]</sup>	29

<sup>[a]</sup> Benchmark<sup>[17]</sup>. <sup>[b]</sup> Hydroxyferrocene formed. <sup>[c]</sup> Product quenched with AcCl. <sup>[d]</sup> 24% Hydroxyferrocene quenched with AcCl. <sup>[e]</sup> 4% Hydroxyferrocene quenched with AcCl.

The use of diisopropylamine (DIPA) instead of THF as the solvent led to a lower yield, but only the rearrangement product **81** was formed. Based on the conclusions of Lloyd-Jones et al.,<sup>[10]</sup> the use of DIPA was expected to cause the elimination of the triflate group with the formation

of 1,2-dehydroferrocene (**75**). The use of hydride bases, NaH and KH, led to a nucleophilic attack with the formation of hydroxyferrocene.

Although many more bases could have been tested to better understand the complex system formed between ferrocenyl triflates and amide bases, detailed computational studies seemed to be a more promising approach. Meanwhile, the primary thia-Fries rearrangement product **81** (putatively via the intermediate **235**, Scheme 4.1), before hydrolysis was isolated in 96% yield as the highly air and moisture sensitive red solid **236** (Figure 4.1). Crystals suitable for an X-ray crystal structure analysis were obtained through solvent diffusion. In addition to being an interesting aggregate in itself, its crystal structure provided a good way to benchmark the theoretical analysis.



**Scheme 4.1.** Anionic thia-Fries rearrangement of ferrocenyl triflate (**79**) including intermediates.

Lithium has a high charge density compared to larger cations and shows a tendency to form contact ion pairs,<sup>[125]</sup> which explains the self-assembly observed in the X-ray crystallographic analysis. In this structure, the lithium atoms are strongly bound to the alkoxide and one of the sulfonyl oxygen atoms forming a six-membered chelate ring. The O–Li moiety originating from the migration of the sulfonyl group interacts strongly with two other O–Li moieties forming a heterocubane structure of four lithium and four oxygen atoms (Li<sub>4</sub>O<sub>4</sub>). While this motif is quite common for alkali metal alkoxides with bulky substituents,<sup>[126]</sup> there are only few structures known, which involve ferrocene moieties.<sup>[127,128]</sup>

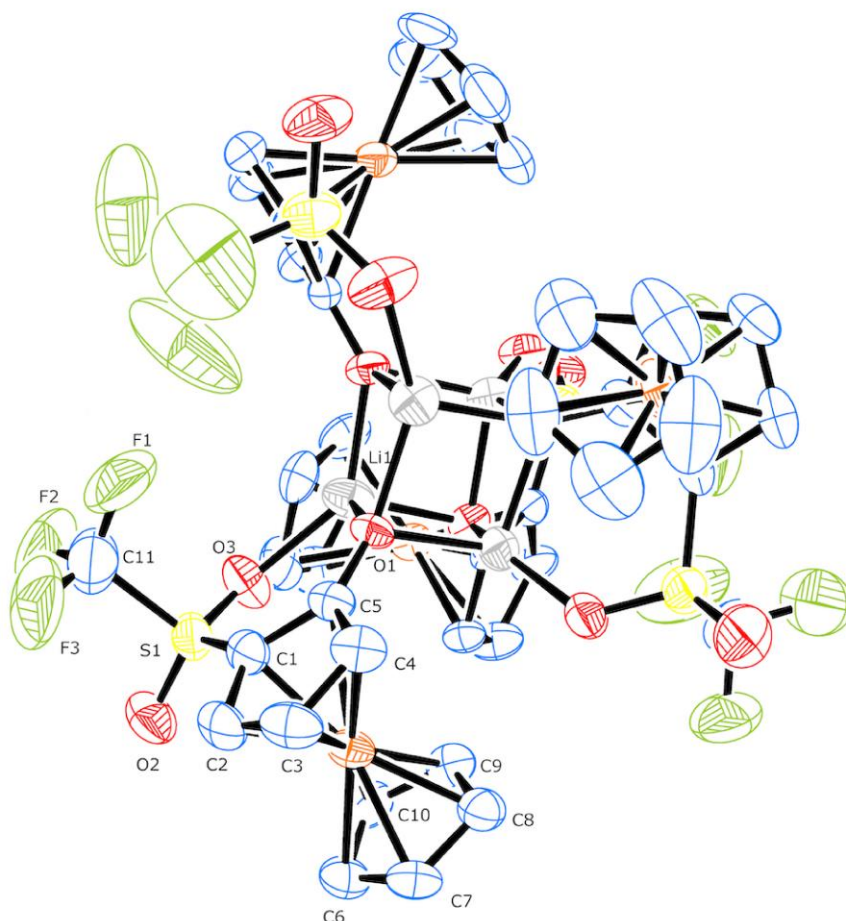


**Figure 4.1.** Structure of **236** in the crystal. Ellipsoids at 50 % probability level. Hydrogen atoms have been omitted for clarity. Within the formed cube, the Li–O bond distances vary from 192.8(9) pm to 196.2(9) pm; the O–Li–O angles range from 91.3(3)° to 96.6(4)° and Li–O–Li from 83.3(4)° to 97.7(4)°. Selected bond lengths [pm]: Fe1–C1 201.0(5), Fe1–C2 201.4(5), Fe1–C3 204.7(5), Fe1–C4 208.8(5), Fe1–C5 212.6(5), Fe1–C6 206.4(5), Fe1–C7 204.5(6), Fe1–C8 205.3(5), Fe1–C9 205.2(5), Fe1–C10 204.3(5), C1–S1 171.4(5), S1–O2 142.2(4), S1–O3 143.3(4), S1–C11 184.1(8), C11–F1 128.9(8), C11–F2 131.3(8), C11–F3 133.2(9), C5–O1 130.0(5), O1–Li1 195.9(8), Li1–O3 198.2(9). CCDC-2046411 contains the supplementary crystallographic data for this article.

Molecular dynamic simulations were carried out using the CPMD method<sup>[122]</sup> and software package.<sup>[129]</sup> The functionals, basis set and pseudopotential were chosen accordingly to benchmarks performed for both CPMD and Gaussian software using the X-ray crystal structure of **236** for comparison.

For the CPMD benchmark, the whole unit cell containing 16 ferrocene units comprising 448 atoms was calculated. The full direct comparison table of the bond lengths is too large to be displayed here and is available in the appendix. Car-Parrinello molecular dynamics were benchmarked using the functionals Becke-Lee-Yang-Parr<sup>[130,131]</sup> and Perdew-Burke-Ernzerhof<sup>[36]</sup> with and without Grimme's dispersion correction D2.<sup>[132]</sup> For BLYP, Goedecker pseudopotentials<sup>[133]</sup> were used for all the atoms, and for PBE, Troullier–Martins pseudopotentials<sup>[134]</sup> were chosen for all the atoms except lithium, for which the Goedecker functional was utilized. The best matching functional, PBE, without Grimme's dispersion correction, was used to perform further calculations.

PBE gave better results than BLYP as shown in Figure 4.2. The use of Grimme's dispersion correction D2 did not improve the results. A threshold of 2% between simulation and measurement was defined as the maximum acceptable error in bond length.

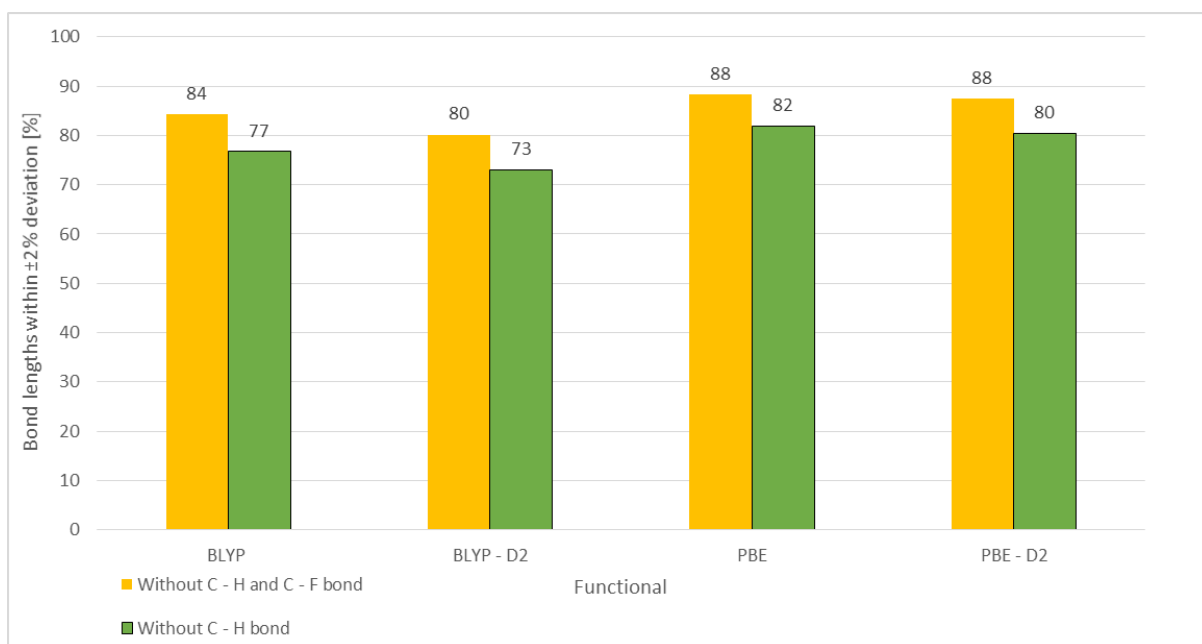


**Figure 4.2.** Comparison of calculated and measured bond lengths (structure **236**) using CPMD. 100% corresponds to exact match.

C–Fe distances were computed with high accuracy, not only by PBE, but by all the functionals. C–H bond lengths were not considered since hydrogen atoms are hardly accurately detected by X-ray crystallography.<sup>[135]</sup> Not all C–C bonds are accurately predicted, but a high proportion

were within the 2% limit. S–O and S–C bonds did not fit as well as the C–Fe bonds, but in general they stayed within a maximum difference of 3 to 4 percent. However, there was a big difference in the C–F bonds in the trifluoromethyl units, not only for all functionals for CPMD, but also for all Gaussian results. This might be due to the very large displacement parameters of fluorine atoms within the –CF<sub>3</sub> group due to its large thermal vibration. This can easily be visualized in programs like ORTEP which include anisotropic thermal parameters in the molecule. Trifluoromethyl groups are known to be one of the most disordered chemical groups,<sup>[136]</sup> which might explain some of the shorter than expected C–F bond lengths.

The best geometry match was obtained using PBE Troullier-Martin pseudopotentials chosen for all the atoms except lithium, for which Goedecker pseudopotential was utilized. This protocol was used for further CPMD calculations. A visual representation of the PBE modelling fitting the measured crystal structure of **236** is presented in Figure 4.3. Obviously, the differences are hardly visible.

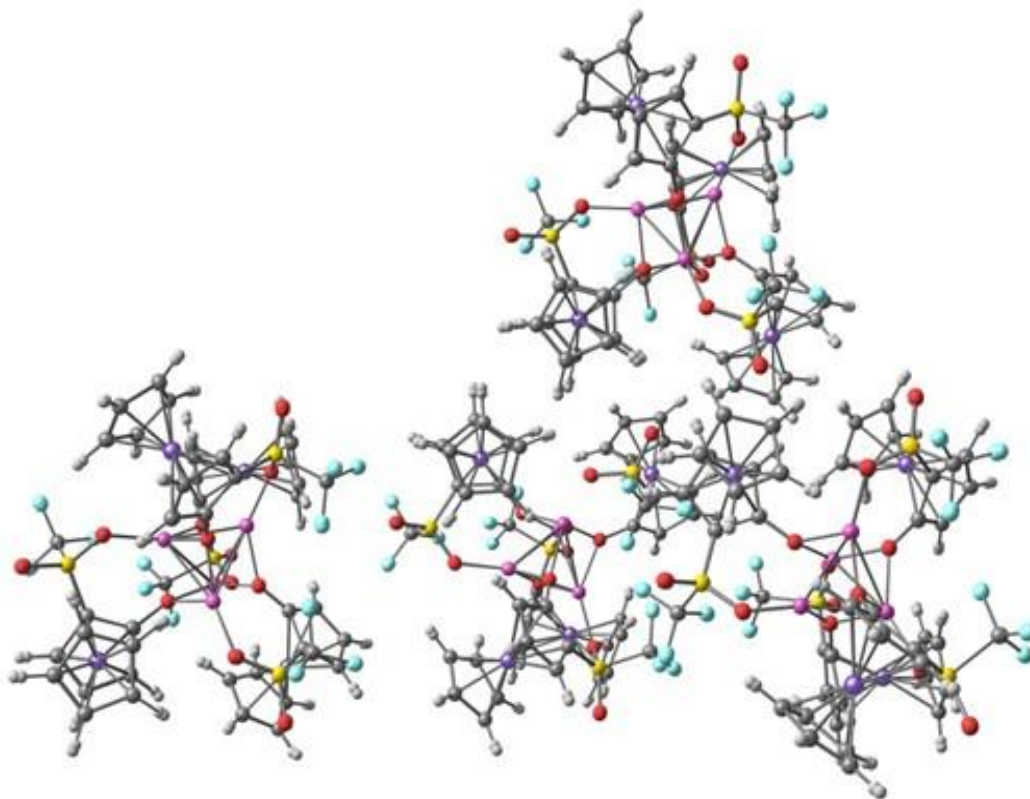


**Figure 4.3.** Superposition of X-ray measurement and calculated crystal structure of **236** showing small variation between them.

For the Gaussian benchmark, a tetramer unit containing 4 ferrocene moieties was initially used. The following GGA and hybrid functionals were benchmarked (Grimme's dispersion with Becke-Johnson damping GD3BJ29 added was marked with D3 abbreviation); BLYP,<sup>[130,131]</sup> BLYP-D3,<sup>[130,131,137]</sup> B3LYP,<sup>[130,131,138]</sup> B3LYP-D3,<sup>[130,131,137,138]</sup> B3LYP-D3,<sup>[130,131,137,138]</sup> PBE0,<sup>[36-38]</sup> PBE0-D3,<sup>[36-38,137]</sup> wB97XD,<sup>[139]</sup> PBE<sup>[36]</sup> and M06.<sup>[140]</sup> LANL2DZ<sup>[39-42]</sup> and LANL,<sup>[39-42]</sup> were used for valence and core electrons of iron, respectively. 6-311+G(d,p)<sup>[43-45]</sup> was used for all other atoms. However, the frequency calculation indicated that the structure did not converge, even though the optimization completed successfully (displacement not converged) for all except for PBE-D3 including diffuse function. After re-optimization and a second frequency calculation, there were still failed convergence criteria.

Analysis of the output files showed that for each functional the geometry lay on a flat surface, indicated by the more than 20 small frequencies in the files. Using a finer grid would probably lead to full frequency conversion, but due to the exceptionally large size of the system, that would be very computational costly. Some frequency calculations alone took more than a thousand hours. Even though the structures found do not correspond to a true minimum, in general they are very close to it, and a benchmark shown in Figure 4.4 was created comparing the functionals used.

To support the benchmark trend, the optimization of the smaller monomeric unit of the crystal structure of **236** containing one ferrocene moiety was performed. This has the advantage of being computationally cheaper, however, it also has the disadvantage that the Li-O bonds of the cube were not taken into account, and as such, were not completely representative of the larger molecule. The calculations for the monomeric unit for all the functionals fully converged, and a stationary point was found. The benchmark trend was identical to that presented in Figure 4.4, with the exception of M06, which performed better for the monomeric unit than for the whole tetramer.

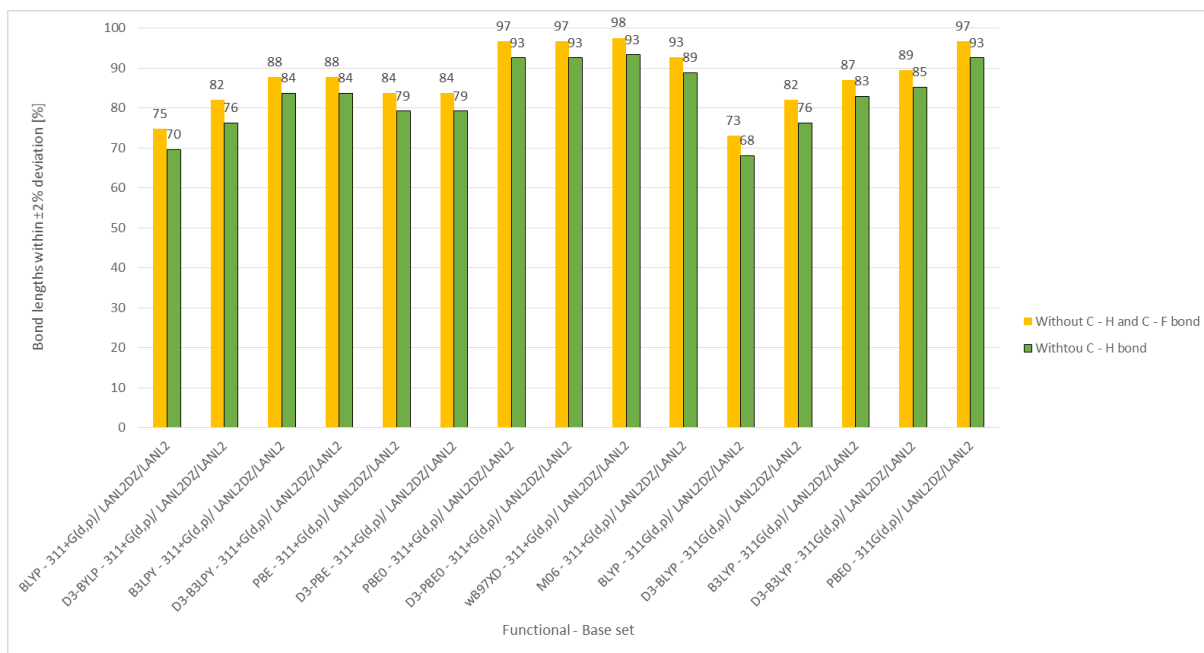


**Figure 4.4.** Comparison of calculated and measured bond lengths in **236** using Gaussian. 100% corresponds to exact match.

The best geometry match to the crystal structure was obtained using the hybrid functionals PBE0 and wB97XD. The wB97XD functional was slightly better than PBE0 but it used a significantly larger CPU time (ca. 3 times) to complete the geometry optimization, and therefore it was decided to use PBE0. The diffuse function had no effect on the result. Nevertheless, the function was included because of the negative charges developed during the thia-Fries rearrangement simulation. Grimme's dispersion function with Becke and Johnson damping GD3BJ did not alter the result either and was therefore not used.

LDA was included in the Gaussian model of the mono- and double rearrangements. An implicit solvent and a molecule of THF were additionally included in the mono rearrangement model. This was not possible for the double rearrangement, as some steps in the reaction pathway were not found when the continuum solvent and a molecule of THF were present. This differs from the work of Lloyd-Jones et al.,<sup>[26]</sup> which used no base, an already *ortho* deprotonated phenyl triflate and an implicit solvent. Although the base increases complexity, it better models the intricate pathways and intermediate organolithium structures of the reaction.

The strategy devised in this study to obtain the transition state structures in Gaussian, was to

perform a relaxed scan, followed by an optimization of the structures at the highest point of the curve. After finding the desired structures, it was verified that only one imaginary negative vibrational frequency was present (saddle point), and the corresponding eigenvector visualized to check for consistency with the expected chemical reaction. An intrinsic reaction coordinate (IRC) calculation was performed afterwards to verify if the obtained transition state led to the desired product and back to the reactant connecting both of them.

Based on the calculations, the mechanism of the anionic thia-Fries rearrangement of ferrocenyl triflate (**79**) is proposed as shown in Figure 4.5. Calculations using two explicit THF molecules were performed for the starting structure **A** and transition state **B** but did not lead to significant differences. Calculations for intermediate **C** using two THF molecules did not converge. The modelling of this reaction shows a strong coordination between reactant, lithium base and solvent, forming a pre-complex **A** as shown in the energy diagram (Figure 4.5). It is interesting to note, that the lithium atom is coordinated to THF and the sulfonyl oxygen atoms. The transition structure **B** reveals a low barrier with a small activation energy of 34.7 kJ/mol and has a geometry very similar to that of **A**, except that the amide now interacts with the *ortho* proton. The angle N–H–C involved in the proton transfer step is 168°.



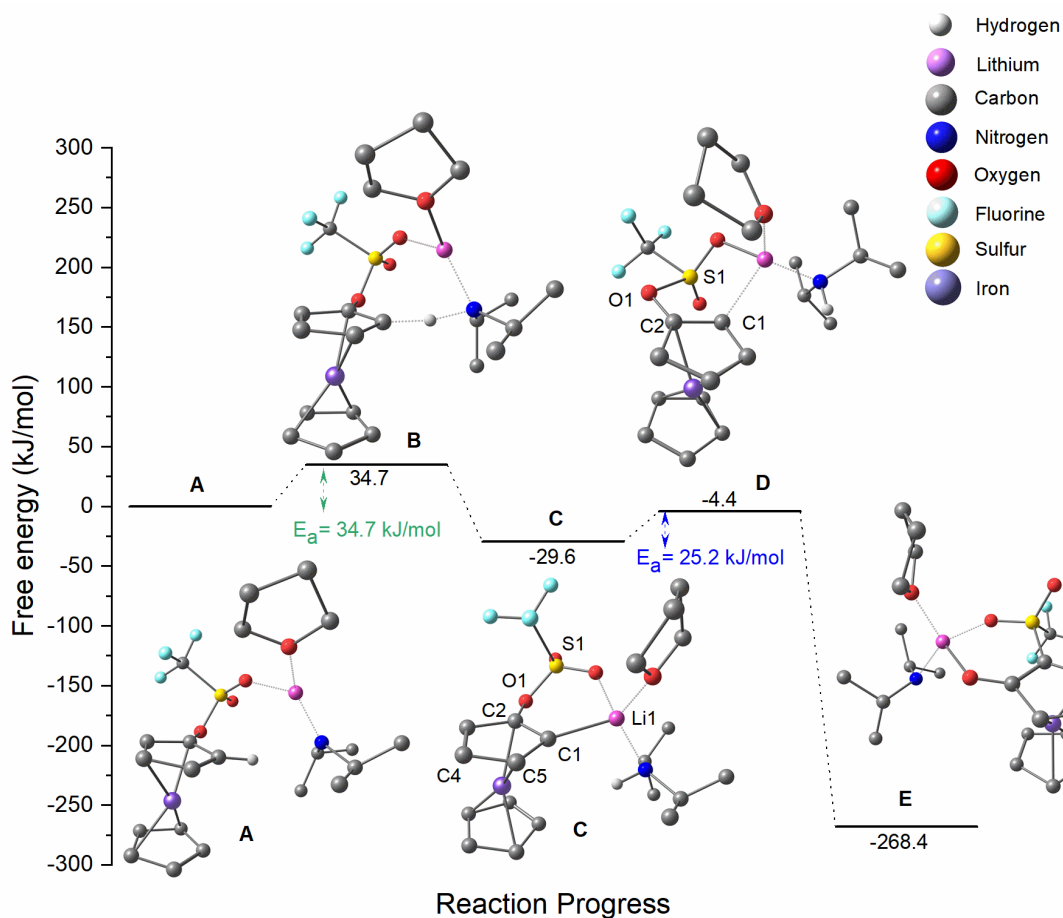


**Figure 4.5.** Relative free-energy scheme for the deprotonation and rearrangement of ferrocenyl triflate (**79**) at the PBE0/[LANL2DZ/LANL2/6-311+ G(d,p)] level of theory. Most of the hydrogen atoms have been omitted for clarity.

The intermediate structure **C** found shows an intramolecular chelation of the lithium ion with one of the oxygen atoms of the triflate group, and coordinates to THF and to the previously formed diisopropylamine. The energy released is only 29.6 kJ/mol, being mildly exothermic. Lloyd-Jones et al. decouple deprotonation from metalation and concluded that metalation *ortho* to a triflate group results in elimination and deprotonation alone to thia-Fries rearrangement.<sup>[26]</sup> Following this reasoning, Butenschön and Werner tested how far *ortho* lithiation instead of *ortho* deprotonation in ferrocene could shift the results. 2-Tributylstannylferrocenyl triflate was treated with butyllithium in the presence of 1,3-diphenylisobenzofuran, which should have been followed by metal exchange and expected to undergo elimination forming ferrocene (**75**). Instead, the anionic thia-Fries rearrangement immediately took place.<sup>[50]</sup> There was also no

sign of elimination and formation of ferrocene (**75**), when **79** was treated with LDA;<sup>[17]</sup> however, **C** does suggest *ortho* metalation. The bond distance C1–Li1 is 210 pm, smaller than the distance C–Li of 231 pm in methyllithium,<sup>[141]</sup> and smaller than the sum of the atomic radii of **C** (70 pm) and Li (145 pm), 215 pm.<sup>[142]</sup> The dihedral angle Li1–C1–C5–C4 is 161°. The HOMO of **C** was also analysed, and a bonding interaction along the C1–Li1 distance was observed as shown in Figure 4.6.

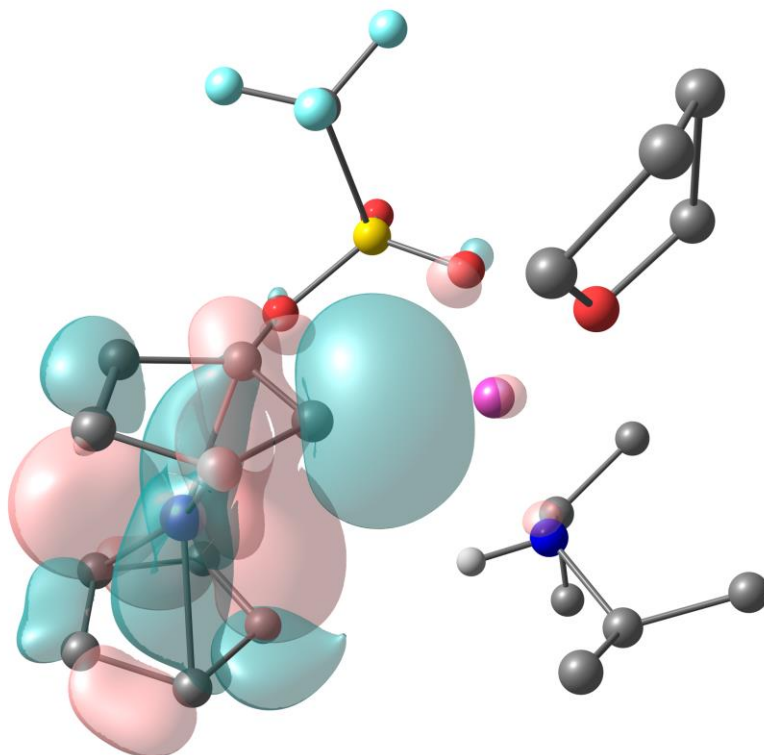


**Figure 4.6.** HOMO of the intermediate **C**. For atom colour code, see Figure 4.5. Most of the hydrogen atoms have been omitted for clarity. The colour of the isosurface refers to the sign/phase: Positive for red and negative for green.

Maximally localized Wannier Functions (MLWF) were also calculated using CPMD software package.<sup>[129]</sup> These localized orbitals allow to analyse the electronic structure. A localised orbital was found between C1 and Li1 suggesting a putative heavily polarized covalent bond (Figure 4.7).

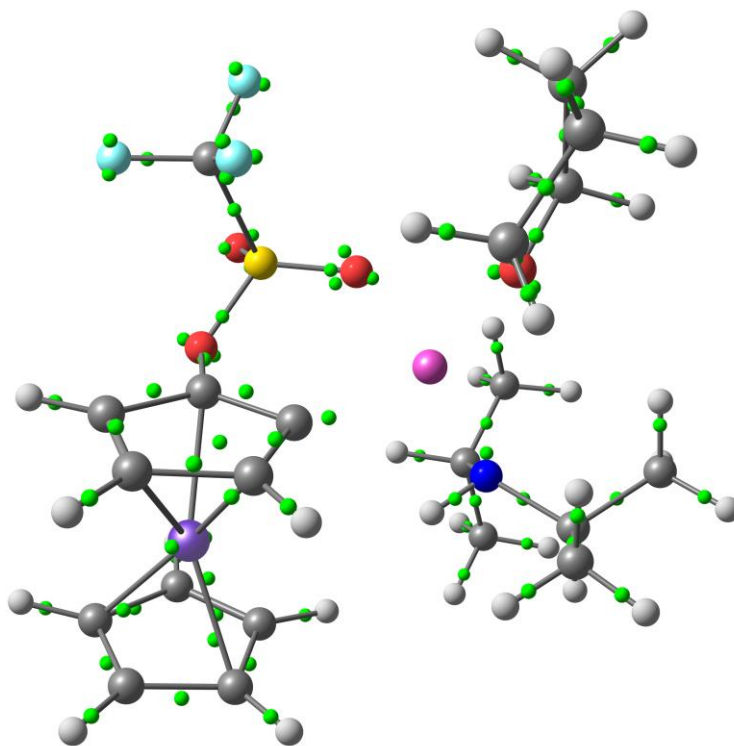


**Figure 4.7.** MLWF of intermediate **C**. For atom colour code see Figure 4.5. Green spheres represent localized orbitals centres.

The rearrangement transition state proceeds through (1,3- $O_{Ar} \rightarrow C_{Ar}$ ) sulfonyl migration with an average activation energy of 58.3 kJ/mol. The reaction is highly exothermic (238.7 kJ/mol). The transition structure **D** shows a dihedral angle C1–C2–O1–S1 of 3°, which is close to planarity. The distance C2–O1 decreases to 137 pm compared to 144 pm in **C**, whilst O1–S1 increases to 172 pm compared to the corresponding distance of 157 pm in **C**. The distance S1–C1 changes a lot, partially due to the change in conformation, from 327 pm in **C** to 230 pm in the transition state **D**. The product **E**, although still coordinated to THF and diisopropylamine, shows a structure remarkably similar to the subunits of the tetramer revealed in the X-ray crystal analysis (Figure 4.1).

The mechanistic studies of the double anionic thia-Fries rearrangement of 1,1'-ferrocenediyl ditriflate (**80**) using LDA as the base are subdivided into two potential energy diagrams including calculated structures of reactants, intermediates, transition states and product in a stepwise

fashion. The first one, shown in Figure 4.8, represents the computational results regarding the first deprotonation, followed by the first rearrangement at one of the cyclopentadienyl rings. The second one, shown in Figure 4.9, reveals the second deprotonation followed by the second rearrangement. A concerted mechanism was considered, but no respective transition state was found.

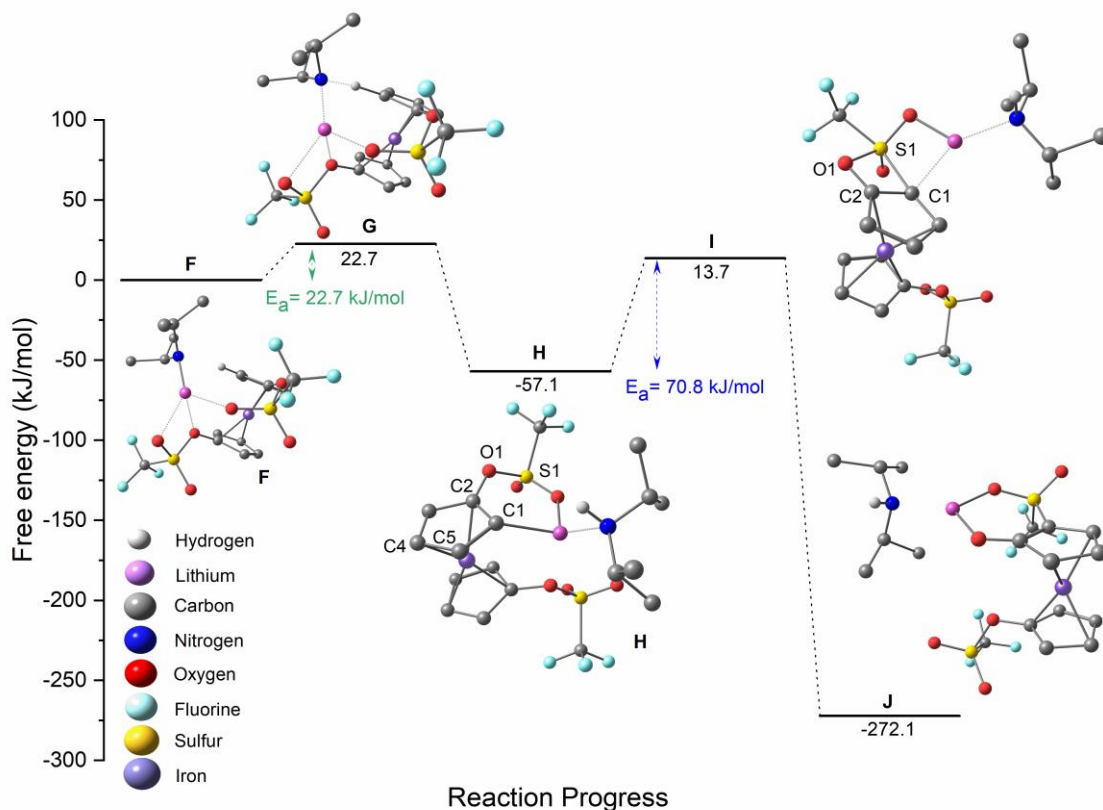
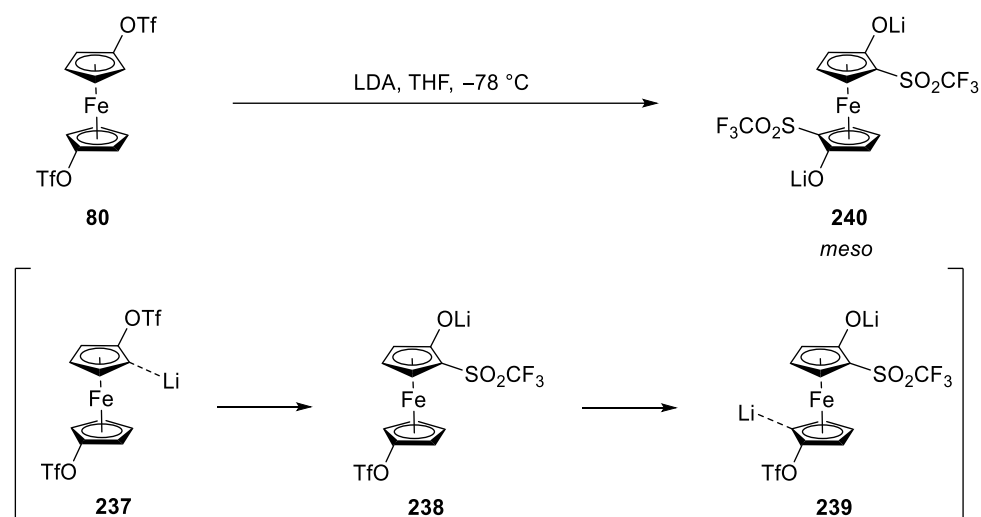


**Figure 4.8.** Relative free-energy scheme for the first deprotonation and rearrangement of 1,1'-ferrocenediyl ditriflate (**80**) at PBE0/[LANL2DZ/LANL2/ 6-311+ G(d,p)] level of theory. Most of the hydrogen atoms have been omitted for clarity.

The model used for the double anionic thia-Fries rearrangement of **80** to **240** through **237–239** (Scheme 4.2) did not use implicit solvent and a molecule of THF as described for the mono rearrangement. The transition states of the rearrangement steps were not found using implicit solvent and were even less successful with a molecule of THF. The reason why it was difficult to find it, is probably due to a very low imaginary vibrational frequency ( $-131$   $\text{cm}^{-1}$  for **I** and  $-171$   $\text{cm}^{-1}$  for **O**), which means that it lies on a very flat potential energy surface (second

derivative corresponds to curvature) and that the addition of solvent adds more degrees of freedom making it more difficult to find the desired structure.



**Scheme 4.2.** Double anionic thia-Fries rearrangement of 1,1'-ferrocenediyl ditriflate (**80**).

The calculations for the first transition state and rearrangement of **80** depicted in Figure 4.8, starts with 1,1'-ferrocenediyl ditriflate (**80**) also as a pre-complex **F**, strongly coordinated to LDA. The transition state structure **G** has a geometry similar to that of **F** and a very small activation barrier of 22.7 kJ/mol. The proton transfer angle N–H–C is 172°. In the intermediate structure **H** it is possible to see that an *ortho* metalation does not seem to have taken place as in the case of the mono triflate **79**. Rather, the lithium atom is chelated between the oxygen atoms of both triflate groups and the previously formed diisopropylamine. The relative free energy of 57.1 kJ/mol released is not very high.

The rearrangement transition state following after depicts a very similar structure to the mono case (cf. Figure 4.5), proceeding through (1,3-O<sub>Ar</sub>→C<sub>Ar</sub>) sulfonyl migration with a medium activation energy of 70.8 kJ/mol. The reaction is highly exothermic. The transition state **I** shows a dihedral angle C1–C2–O1–S1 of 0.4° corresponding to planarity. The distance C2–O1 decreases to 136 pm compared to 143 pm in **H**, whilst the distance O1–S1 increased to 177 pm compared to 158 pm in **H**. The distance S1–C1 changed a lot from 332 pm in **H** to 218 pm in the transition state **I**.

The modelling of the reaction step for the second cyclopentadienyl ligand (Figure 4.9) started

with the pre-complex structure **K**, optimized from structure **J** without previously formed DIPA but including an additional LDA. Gratifyingly, the conformation of the formed structure **K** already gave us a clue of the reason for the diastereoselective formation of the *meso* product **87**. Two transition state structures were found for the deprotonation step, both leading to the observed *meso* product. The main difference between transition state structures **M** and **L** is the degree of intramolecular chelation of lithium atoms. In the first, the lithium atom from LDA is bound only to one of the oxygen atoms of the sulfonyl group of the bottom cyclopentadienyl ring, whilst the second is also chelated by the olate oxygen atom. The difference in energy between them of 38.7 kJ/mol is quite significant and the latter, **L**, most stable, will be considered for this study.

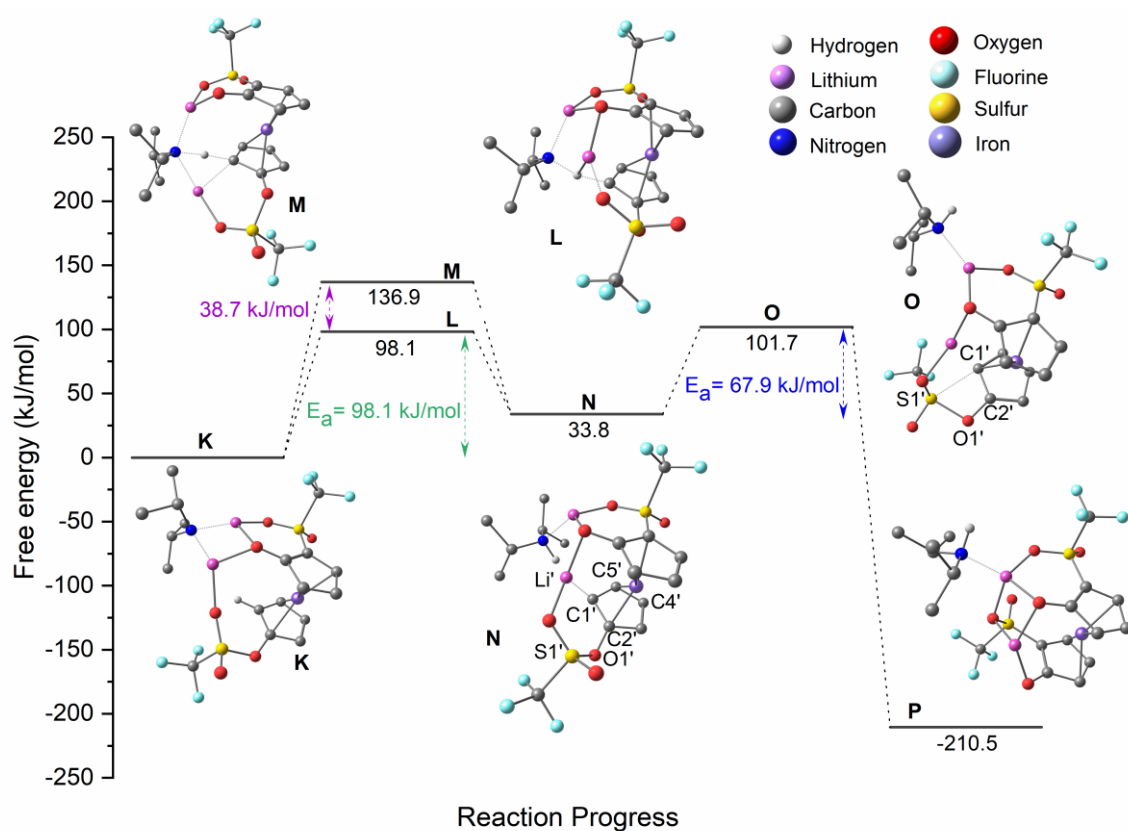


**Figure 4.9.** Relative free-energy scheme for the second deprotonation and rearrangement of 1,1'-ferrocenediyl ditriflate (**80**) at PBE0/[LANL2DZ/ LANL2/6-311+ G(d,p)] level of theory. Most of the hydrogen atoms have been omitted for clarity.

The activation energy of 98.1 kJ/mol for the second deprotonation is much higher than that observed for the first deprotonation,  $E_a = 22.7$  kJ/mol (Figure 4.8). The intermediate **N** has a

higher energy than **K**, and this reaction step is mildly endothermic. In the intermediate **N**, the distance C1'–Li' is 208 pm, surprisingly the same distance obtained for structure **H**. The dihedral angle Li'–C1'–C5'–C4' is 117°, also far from planarity. It is again inconclusive if metalation occurs, or if the lithium atom is just coordinated between the alcoholate, one of the oxy-gen atoms of the remaining triflate group and the newly formed diisopropylamine.

The rearrangement transition structure is very similar to its precedent intermediate **N**. It proceeds again through (1,3-O<sub>Ar</sub>→C<sub>Ar</sub>) sulfonyl migration with an average activation energy of 67.9 kJ/mol. The reaction is highly exothermic. The transition structure **O** shows a dihedral angle C1–C2–O1–S1 of 2°, which is close to planarity. The distance C2–O1 decreases to 134 pm compared to 143 pm in **N**, whilst the distance O1–S1 increased to 177 pm compared to 158 pm in **N**. The distance S1–C1 significantly changed from 338 pm in **N** to 244 pm in the transition state **O**.

The structure of the transition state leading to the *racemo* product **Q** was calculated and compared. Figure 4.10 shows that the planar chirality of the intermediate molecule leads to two different deprotonation transition state geometries. Each diastereomer has a distinctive degree of chelation leading to an impressive difference in energy between them: 59 kJ/mol. This explains the exclusive formation of the *meso* product **87**.

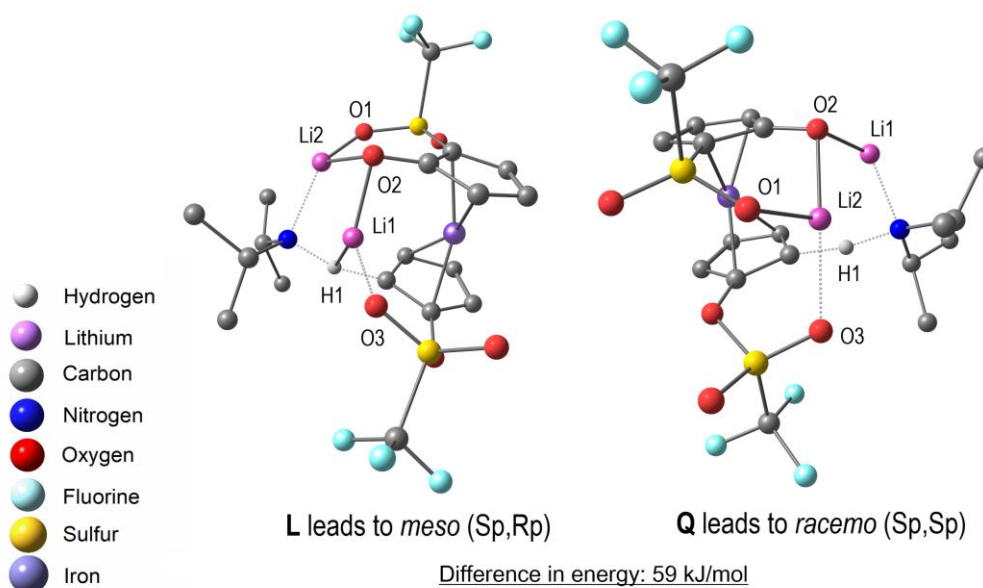


**Figure 4.10.** *meso* vs. *racemo*: Transition state of the second deprotonation in the double anionic thia-Fries rearrangement of 1,1'-ferrocenediyl ditriflate (**80**). Most of the hydrogen atoms have been omitted for clarity.



### Molecular dynamics

In the beginning of the computational work, there were not many clues to explain the diastereoselectivity of the reaction displayed in Figure 2.14. The investigation started with the initial model, **R**, which was relatively simple. It did not include any base or solvent and comprised of the transition state structure of the first rearrangement starting from deprotonated 1,1'-ferrocenediyl ditriflate (**80**) as shown in Figure 4.11. Interestingly, the Mulliken charges of the *ortho* hydrogen atoms to the triflate group in the second cyclopentadienyl ring in the structure **R** were not the same. The proton on the left which, upon removal, leads to the observed product **87**, seemed to be more acidic (0.149 e). The HOMO of the structure **R** shows an electronic density going from one cyclopentadienyl ring to the second through the iron atom, seemingly making the right *ortho* proton more electron rich than the other as shown in Figure 4.11. It was thought then, that an interannular stereoinduction might have been responsible for the selective deprotonation observed.

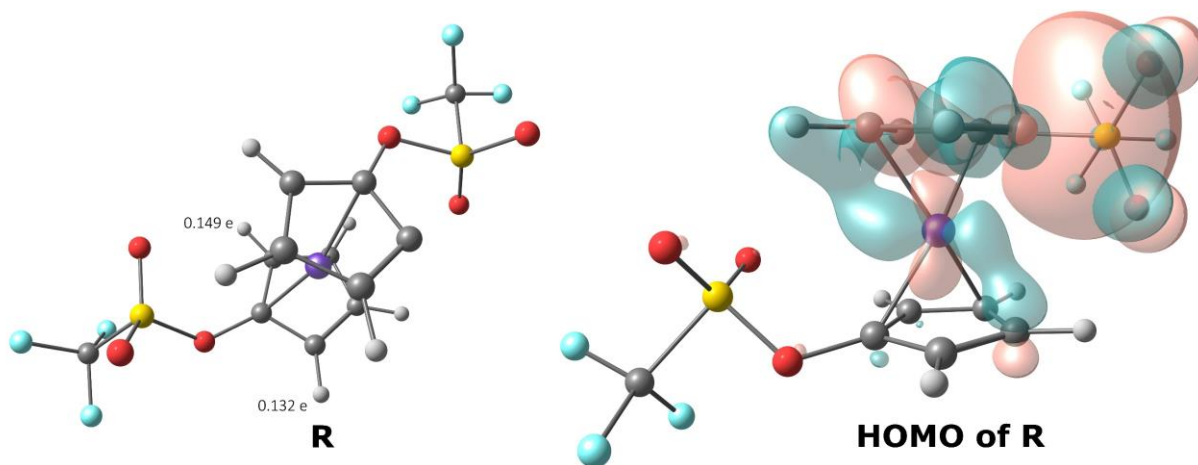


**Figure 4.11.** Structure of **R** and its HOMO obtained from a Gaussian calculation.

Accordingly, MD (molecular dynamics) calculations seemed the appropriate way to go. The transition state structure **R**, obtained from Gaussian, plus a lithium atom placed far from the molecule, was used as starting point for CPMD calculations. The lithium atom was added to avoid dealing with a non-neutral system. The MD successfully simulated the rearrangement but unfortunately it gave us no idea as to why one proton is deprotonated preferentially



compared to the other. Some steps of the MD are shown in Figure 4.12. Curiously, the bond between the oxygen and sulfur atoms in the triflate at the second cyclopentadienyl group broke (Figure 4.12, Step 3991).

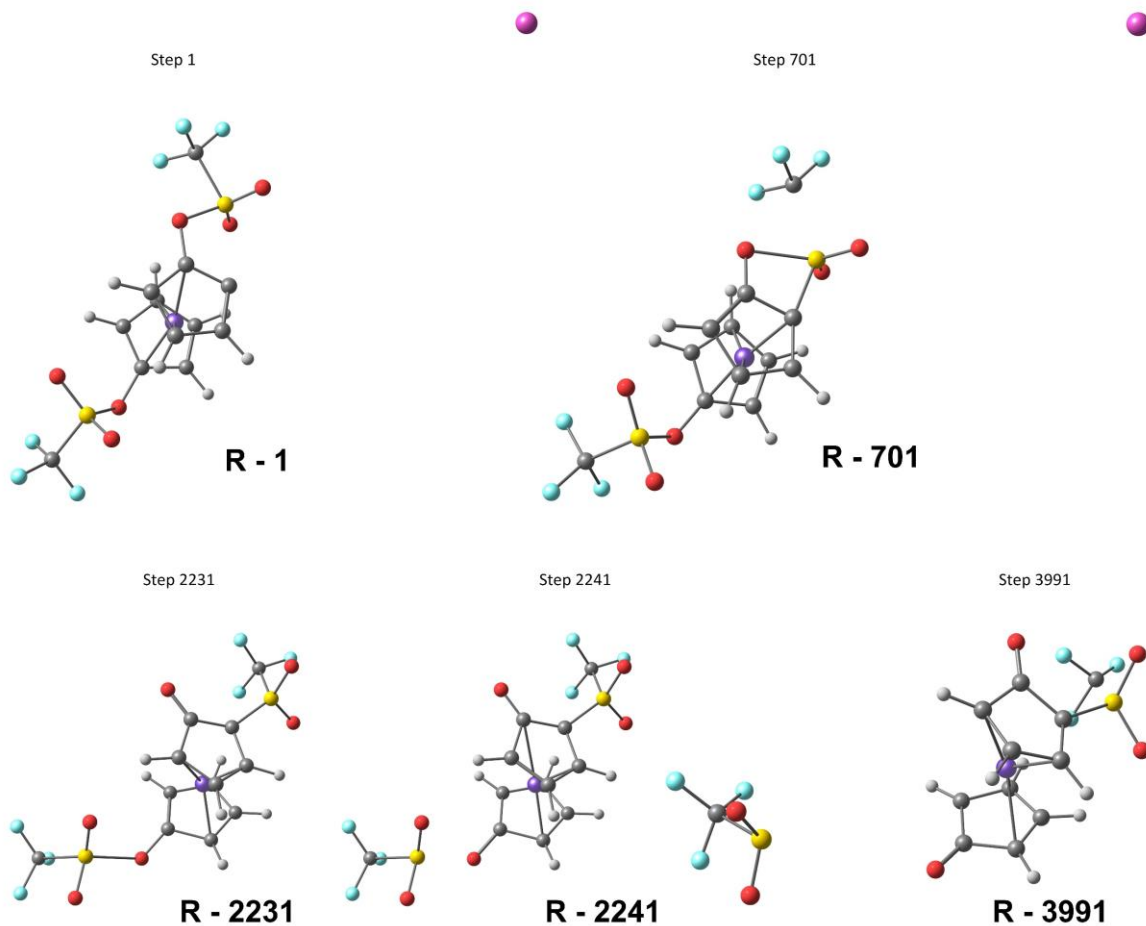


**Figure 4.12** MD calculation using a single *ortho* deprotonated 1,1'-ferrocenediyl ditriflate (**80**) structure starting from the transition state structure **R** obtained from Gaussian calculations.

At this point, it was decided to simulate the second deprotonation hoping for a lead to help explain the only formation of the *meso* product **87**. The deprotonation transition state structure **S**, shown in Figure 4.13 and calculated from Gaussian, was used as a starting point for a MD calculation. At this point, only a transition state structure similar to **M** had been found. The structure **L** was not known at that time. A small less complex base than LDA, the hydroxyl

group, was explicitly introduced to the system. The hydroxyl groups were placed in a similar way close to both sides of the triflate group at the bottom cyclopentadienyl ring to avoid preferable coordination to some of the oxygen atoms and possibly favouring one deprotonation over the other forming the structure **T**, shown in Figure 4.14, step 1. Three lithium atoms far from the molecule were also used to achieve a neutral system. Surprisingly, the deprotonation took place as shown in Figure 4.14. The expected proton was removed, and the hypothesis of an interannular stereinduction seemed possible.

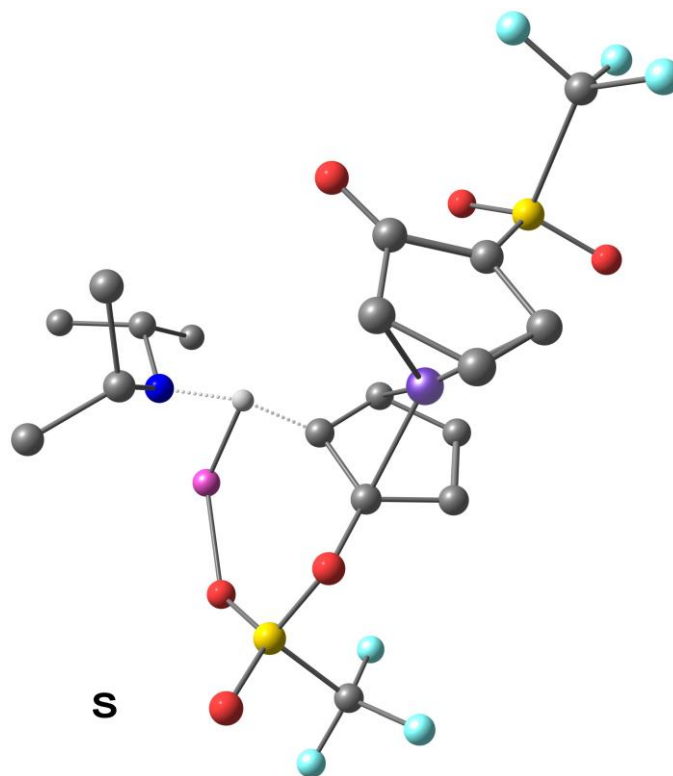


**Figure 4.13.** Transition state structure **S** obtained for the second deprotonation using LDA as a base.

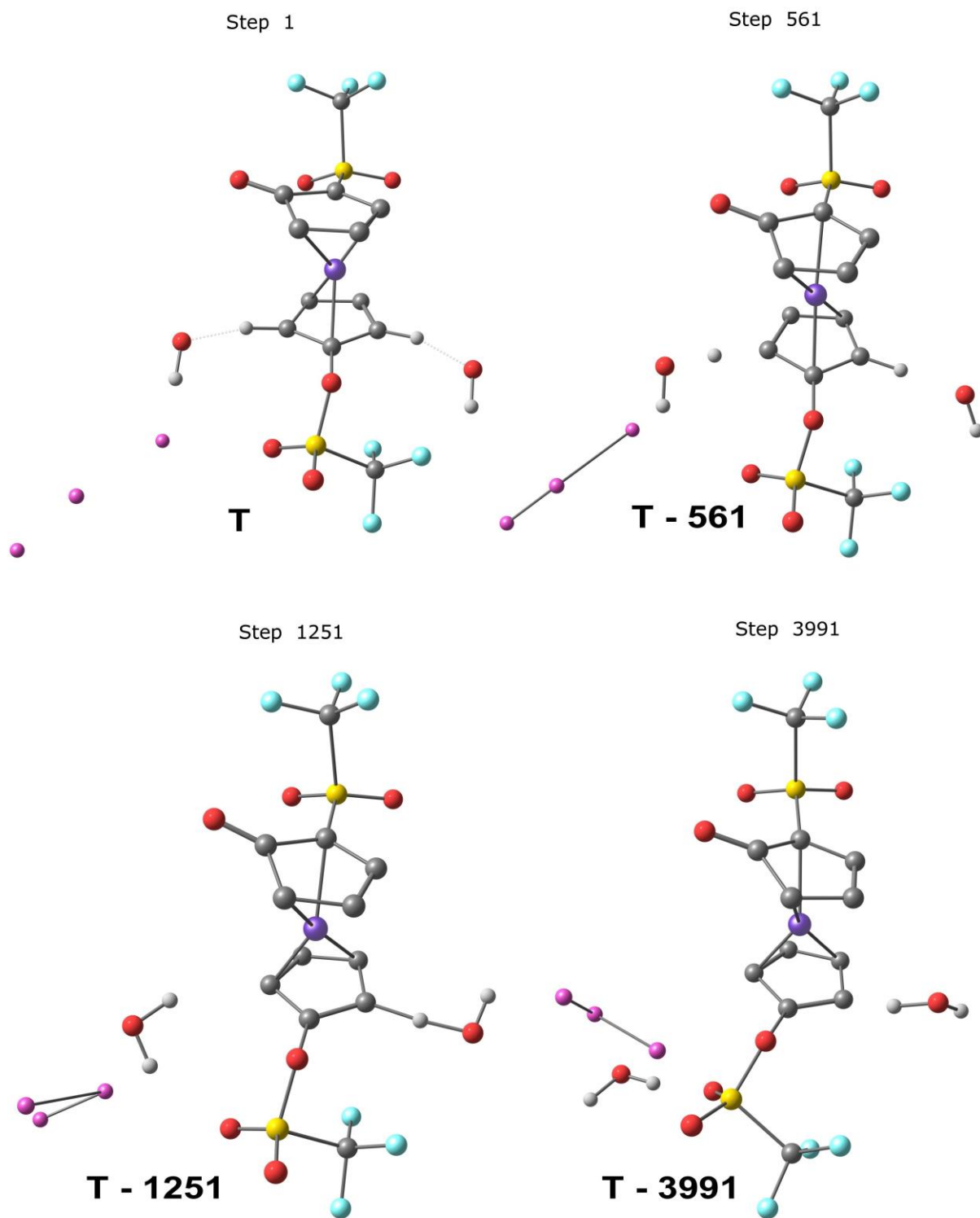


**Figure 4.14.** MD calculation starting from structure T.

The hypothesis of a concerted mechanism was also considered and simulated. The structure **U** was built from the association of the structures **R** and **S**, besides the addition of two OH groups oriented towards the two *ortho* protons at the second cyclopentadienyl ring. The resulting MD showed the deprotonation of both protons, the first proton also being the one leading to the *meso* product **87** (Figure 4.15). Although the MD shows what was hoped for, the results were still not sufficient to draw a solid conclusion.

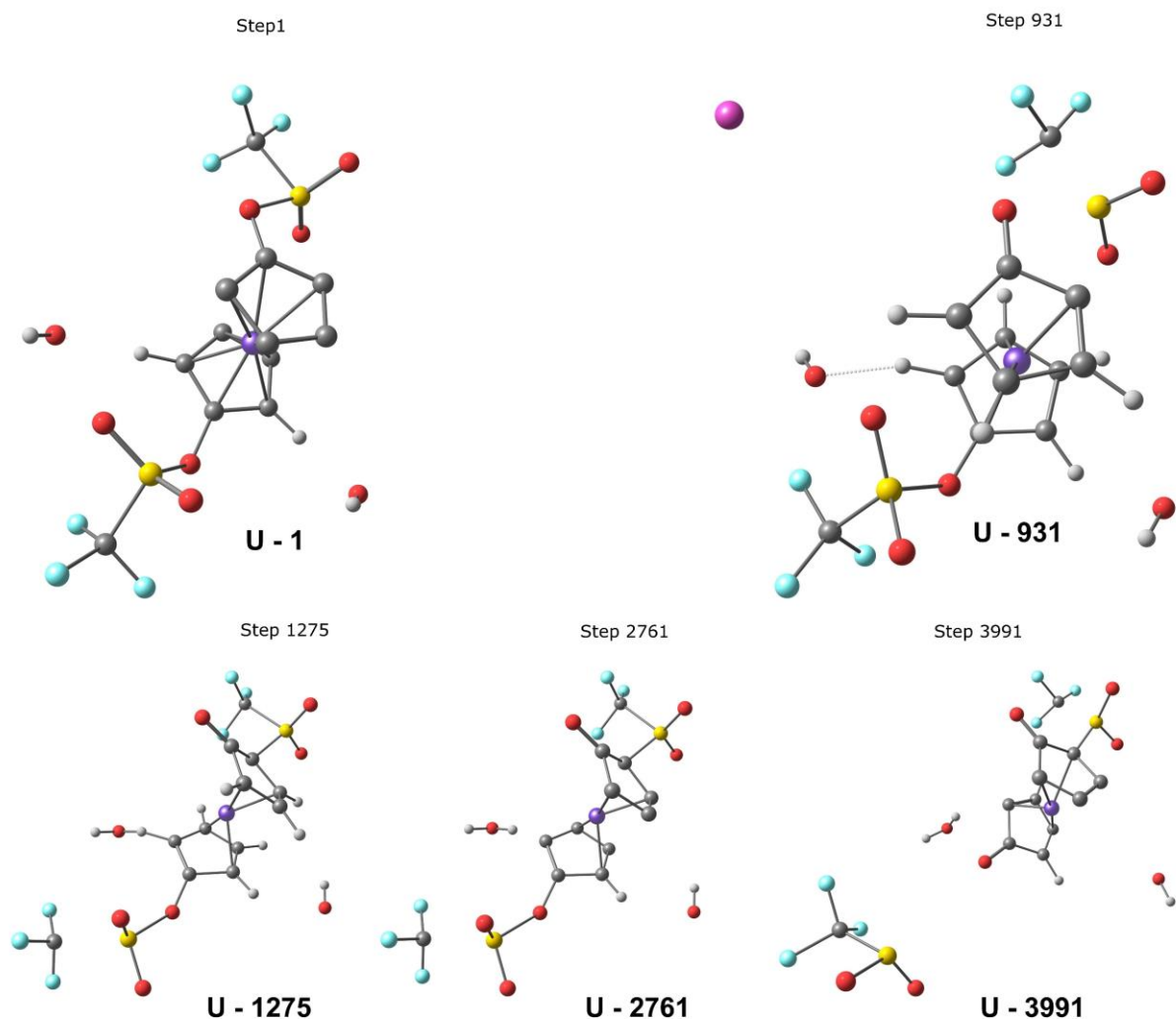


**Figure 4.15.** MD calculation starting from structure **U** featuring two hydroxy groups oriented in the direction of both *ortho* protons to the triflate group.

A last MD calculation was done using structure **V** built using structure **U** upon replacement of

the hydroxy groups for Figure 4.16, step 1. One extra lithium atom far from the molecule was also used to have a neutral system, however, it is not shown in Figure 4.16 because of the perspective chosen. Nevertheless, nothing of the expected happened (Figure 4.16, Step 2991). Not even the rearrangement at the top cyclopentadienyl ring took place.

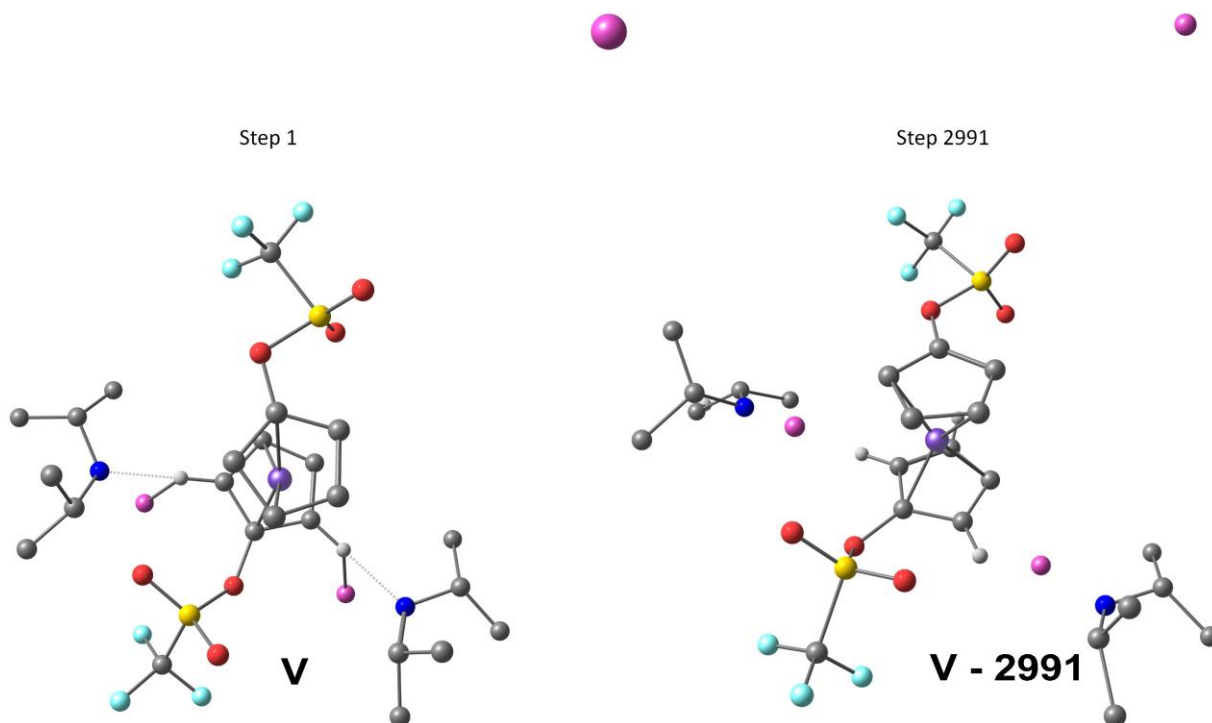


**Figure 4.16.** MD of the structure **V** featuring two LDA oriented in the direction of both *ortho* protons to the triflate group.

The uncertain results obtained with MD led to further Gaussian studies that ended up mapping the energy diagram of the double deprotonation and rearrangement of 1,1'-ferrocenediyl ditriflate (**80**) (Fig. 4.8 and 4.9) and later the calculation of the structure **Q** that revealed a significantly lower degree of coordination with the lithium and a surprisingly high difference in energy between **L** and **Q** which explained the observed diastereoselectivity of the reaction.

### 4.3. Conclusion

In conclusion, the detailed mechanisms of the anionic thia-Fries rearrangement of ferrocenyl triflate (**79**) as well as that of the double anionic thia-Fries rearrangement of 1,1'-ferrocendiyl ditriflate (**80**) have been investigated by DFT calculations using Gaussian and CPMD programs. The functionals, basis set and pseudopotentials applied were selected on the basis of the crystal structure analysis of the prime product **236** of the reaction of **79** before hydrolysis. The unprecedented *meso* diastereoselectivity of the double anionic thia-Fries rearrangement of **80** is a result of coordinating interactions of the lithium cations with oxygen atoms of the product and the diisopropylamine nitrogen atom.

This study also highlights the importance of lithium coordination in simulations. Additionally, it demonstrates the capabilities of computational chemistry helping experimental chemists to investigate reaction mechanisms through modelling and simulation.

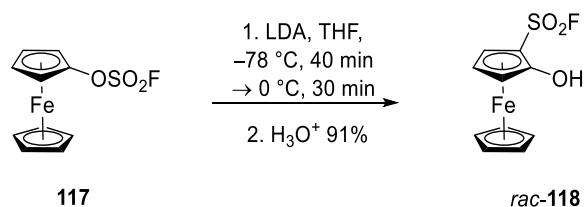
## Chapter 5

### 5. Summary and future work

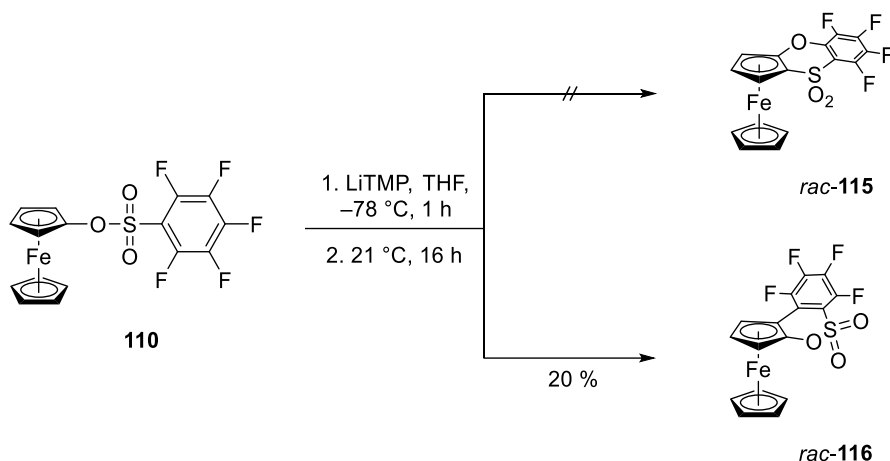
The goals of this project were very broad, curiosity driven and, in some aspects, very challenging. It involved a series of experimental and theoretical investigations to expand and understand the chemistry of the anionic thia-Fries rearrangement at metallocenes.

Chapter 2 was dedicated to the expansion of the anionic thia-Fries rearrangement to different functional group besides the triflate and exploring the potential to use the anionic thia-Fries rearrangement product as an electrophilic partner in Suzuki-Miyaura cross-coupling reaction and as a possible ligand in catalysis.

The anionic thia-Fries rearrangement was successfully extended to ferrocenyl fluorosulfonate (**117**) (Scheme 5.1), whilst *ortho* deprotonation of ferrocenyl (2,3,4,5,6-pentafluorophenyl)sulfonate (**110**) led to the formation of the rare ferrocene annelated oxathiin *rac*-**116** via nucleophilic aromatic substitution (Scheme 5.2) instead of a rearrangement. The other ferrocenyl sulfonyl compounds **94**, **95**, **111**, **113** and **114** led to the formation of ferrocenolate upon treatment with LDA, whilst no transformation was observed for the bulky **112**.

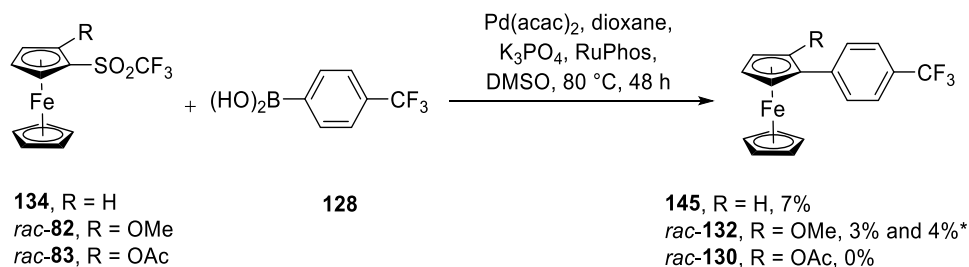


**Scheme 5.1.** Anionic thia-Fries rearrangement of ferrocenyl fluorosulfonate (**117**).



**Scheme 5.2.** Attempted anionic thia-Fries rearrangement of ferrocenyl (2,3,4,5,6-pentafluorophenyl)sulfonate (**110**) leading instead to the formation of the ferrocene annelated *rac*-**116**.

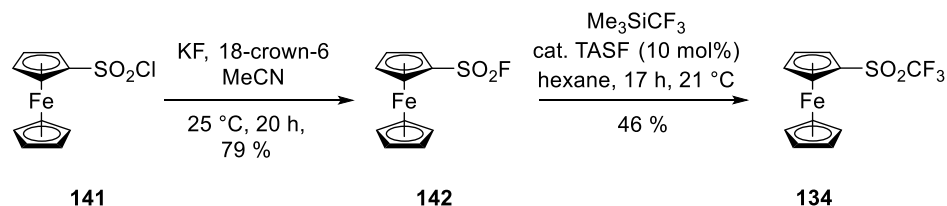
The potential value of the ferrocenyl triflate anionic thia-Fries rearrangement product was explored as an electrophilic counter partner for Suzuki-Miyaura cross-coupling according to a new method disclosed by Moran et al.<sup>[55]</sup> The reaction worked but only in low yield. Ferrocene is more electron rich than benzene, and this might explain the poorer yields obtained in the Suzuki-Miyaura cross-coupling (SMC). In addition, not only a more electron rich aromatic system was used, but **132** also contains a methoxy group *ortho* to the triflyl group, which pushes electron density to the system via resonance, making the system even more electron rich, which does not help the rate-determining oxidative addition step. To better evaluate the chances to use this system in SMC, trifluoromethylsulfonyl ferrocene (**134**) was synthesised too. But unfortunately, the yield was not improved much.



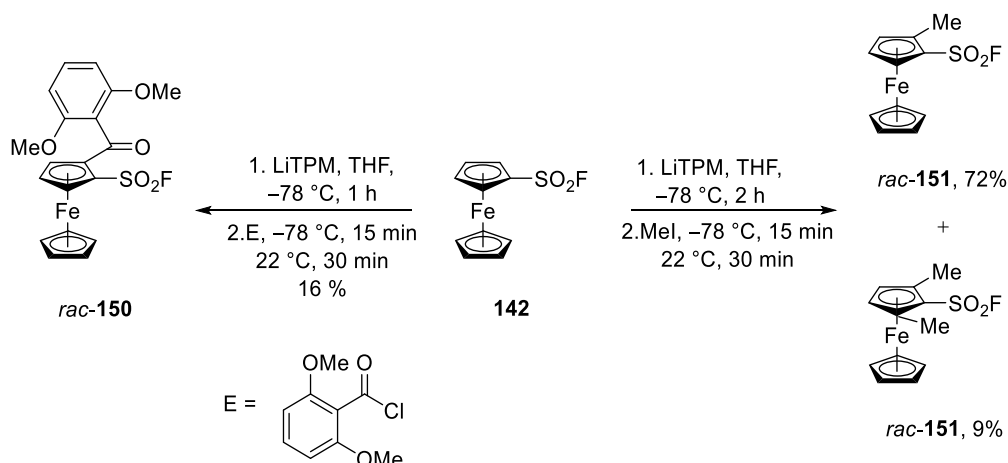
**Scheme 5.3.** Suzuki coupling of (trifluoromethylsulfonyl)ferrocene derivatives. RuPhos = 2-Dicyclohexylphosphino-2',6'-diisopropoxybiphenyl. \*dppf as ligand instead of RuPhos.



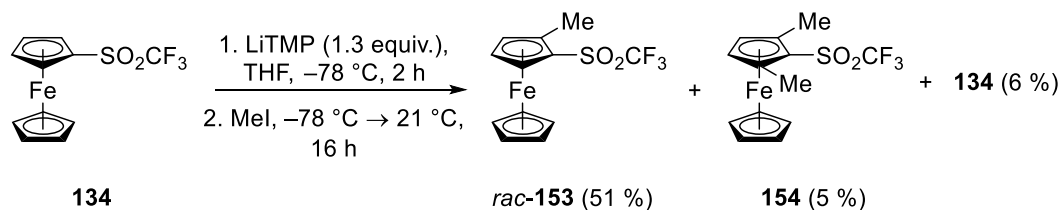
Nevertheless, the synthetic path to **134** led to the synthesis of the so far unreported fluorosulfonyl ferrocene (**142**) (Scheme 5.4), which might be used in the future as a versatile reagent in SuFEx reactions. The abilities of the two new compounds **134** and **142** as direct *ortho* metalation groups were explored. The *ortho* metalations worked very well using LiTMP in THF leading to mono and double *ortho* lithiation (Scheme 5.5 and 5.6).



**Scheme 5.4.** Syntheses of fluorosulfonylferrocene (**142**) and (trifluoromethylsulfonyl)ferrocene (**134**).

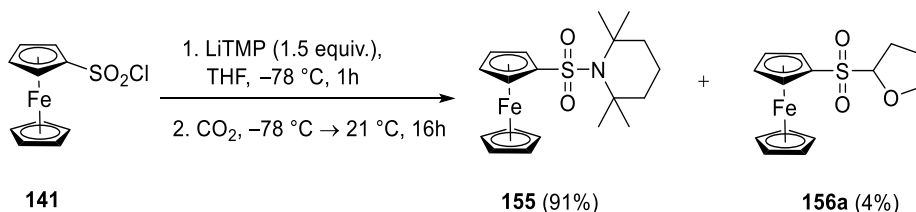


**Scheme 5.5.** Direct *ortho* metalation of the ferrocenyl sulfonyl **142**.



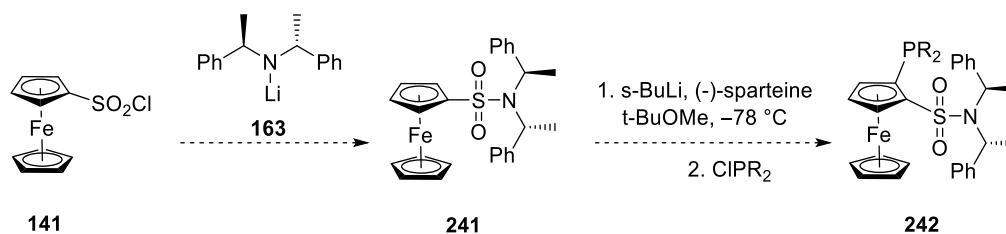
**Scheme 5.6.** Direct *ortho* metalation of the ferrocenyl sulfonyl **134**.

Chlorosulfonylferrocene (**141**) was surprisingly stable for a sulfonyl chloride derivative, probably because of the electron rich ferrocenyl group. For this reason, it was wondered if **141** had also the ability to be *ortho* lithiated. It did not work though, but instead, the bulky sulfonamide **155** and the sulfone **156a** were formed (Scheme 5.7).



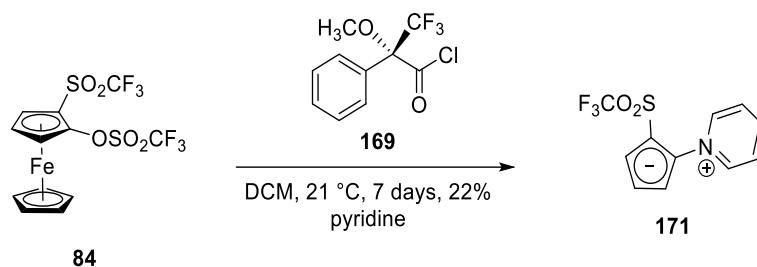
**Scheme 5.7.** Attempted *ortho* lithiation of **141** using LiTMP which led instead to the formation of the sulfonamide **155** and the ferrocene sulfonyl derivative **156a**.

In this context, it would be interesting to explore the synthesis of a chiral ferrocenyl sulfonamide derivatives, for example, via reaction with Simpkin's base **163** with ferrocenyl sulfonyl chloride (Scheme 5.8). The putative ferrocenyl sulfonamide **241** could later be used to induce planar chirality as accomplished by Snieckus et al.<sup>[78]</sup> (Scheme 2.38). If a chlorophosphine were used as an electrophile, the putative formed planar chiral ferrocenyl sulfonamide **242** could be used as a bidentated chiral ligand in asymmetric catalysis.



**Scheme 5.8.** Synthesis of the putative chiral ferrocenyl sulfonamide **241** and its use to induce a chiral planarity in **242**.

Pursuing the synthesis of a chiral ligand derived from the anionic thia-Fries rearrangement product, it is essential to have an enantiopure form of 2-(trifluoromethylsulfonyl)ferrocenol (**81**) or its derivative. Chiral lithiated pyrrolidines were used to perform an asymmetric anionic thia-Fries rearrangement but it failed. Nevertheless, during the studies the unexpected inner salt **171** was obtained (Scheme 5.9). The mechanism is not clear though.

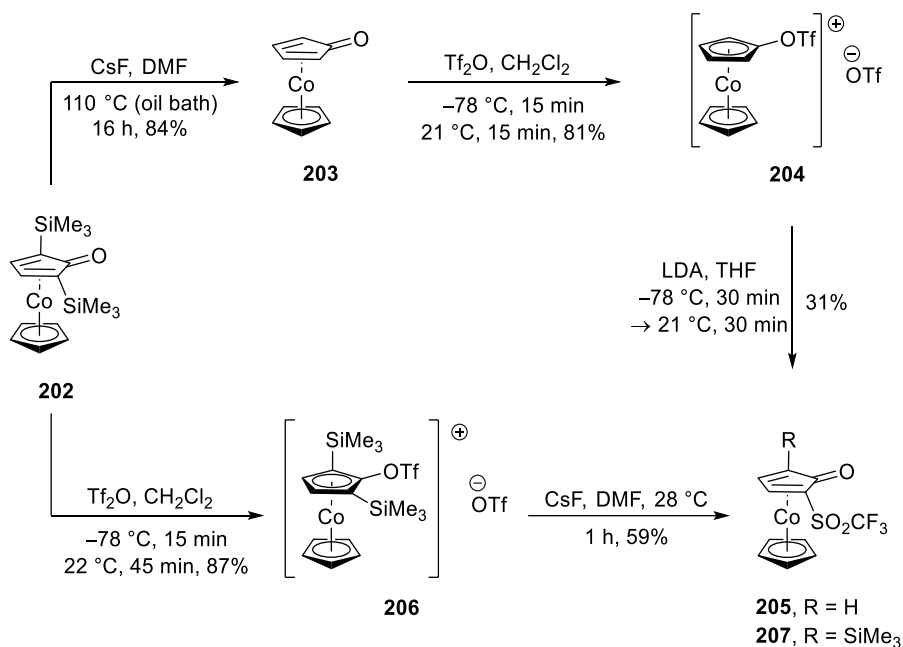


**Scheme 5.9.** Unexpected inner salt **171** formation upon reaction of **84** with Mosher's acid chloride **169**.

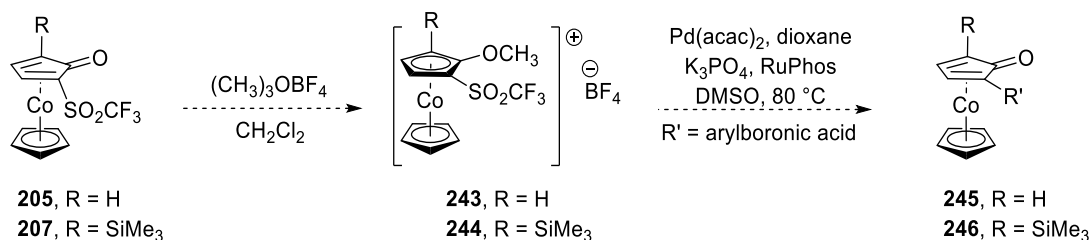
Chapter 3 was dedicated to expanding the anionic thia-Fries rearrangement to another metallocene system other than ferrocene and it was successfully developed for cobaltocenium salts.

From the known synthesised cyclopentadienonecobalt(I) complex **202**, the new derivatives **204** and **206** were successfully prepared and the anionic thia-Fries rearrangement was achieved through two different routes (Scheme 5.10). In the first, LDA was used as base to *ortho* deprotonate **204**, affording **205** in 31% yield. The purification was not easy, de-metalation might have taken place. Although the yield obtained was only modest, this is the first case of an anionic thia-Fries rearrangement at a cobalt complex. The second route took advantage of the pre-installed silyl groups to accomplish the desired rearrangement using caesium fluoride as a desilylation agent, affording **207** in 59% yield. The reaction path has the advantage of being shorter, giving a higher yield, and **207** is also easier to purify than **205**. Another advantage is that the second route leads to a trisubstituted cyclopentadienone, with a remaining silyl group that might further be modified.

The products **205** and **207** of the anionic thia-Fries rearrangements were not exploited in this thesis. Nevertheless, it would be interesting to test for example, if they are a good partner in cross-coupling reactions using the trifluoromethanesulfonyl group as electrophilic partner as proposed by Moran et al.<sup>[55]</sup> If **205** and **207** were transformed into their respective cobaltocenium complexes using trimethyloxonium tetrafluoroborate for example, the new structures **243** and **244** should be more electron poor than ferrocene and accordingly, facilitate oxidative addition, which is, in general, the rate determining step of Suzuki-Miyaura cross-couplings, leading to compounds **245** and **246** (Scheme 5.11).



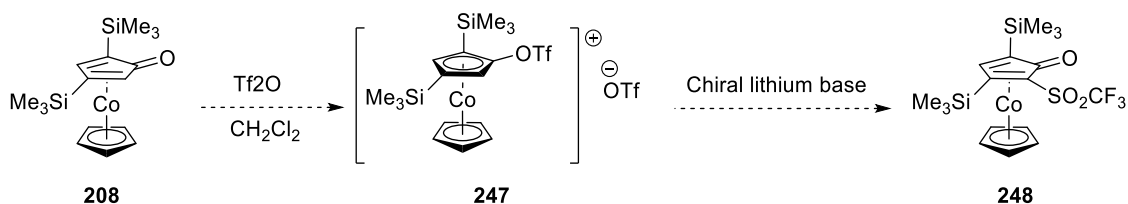
**Scheme 5.10.** Synthetic routes to realize anionic thia-Fries rearrangement at a cobalt complex.



**Scheme 5.11.** Proposed synthesis of cobaltocenium derivatives **243** and **244**, from **205** and **207** and their uses as electrophilic partner in Suzuki cross-coupling reaction.

Due to the different electronic properties between ferrocene and cobaltocenium salts, it is probably worth to try an asymmetric anionic thia-Fries rearrangement at the latter. A good candidate for this, would be the cobaltocenium salt **247** derived from **208**, because the potentially more electron rich product **248** might be easier to purify than **205** (Scheme 5.12).

The cobaltocenium salts anionic thia-Fries rearrangement products **205** and **207** are more stable than their ferrocene related 2-(trifluoromethylsulfonyl)ferrocenol (**81**). In case the desymmetrisation works, the putative chiral ligand can easily be recovered. Due to titanium oxophilicity, **248** could be used as a ligand in reactions where  $\text{TiCl}_4$  is required, and an asymmetric synthesis is desired, for example.



**Scheme 5.12.** Proposed asymmetric anionic thia-Fries rearrangement at a cobalt complex.

In chapter 4, experimental and computational studies led to the development of a benchmark database using both the Gaussian and CPMD software programs. Detailed mechanism of the anionic thia-Fries rearrangement of ferrocenyl triflate (**79**) and 1,1'-ferrocendiyl ditriflate (**80**) were proposed based on DFT calculations using Gaussian and CPMD software programs. Finally, a reasoning for the unprecedented *meso* diastereoselectivity of the double anionic thia-Fries rearrangement was proposed, based on the high difference in energy between the transition states leading to the obtained *meso* or to the *racemo* products which were not obtained. The pronounced difference in energy is due to the *meso* transition state structure having more favourable coordination interactions of the lithium cations with oxygen atoms of the product and the nitrogen atom at the base.

## Chapter 6

# 6. Experimental and theoretical method section

## 6.1. Theoretical Method Section

### *CPMD Calculations*

Car-Parrinello molecular dynamics were benchmarked using the functionals Becke-Lee-Yang-Parr (BLYP)<sup>[130,131]</sup> and Perdew-Burke-Ernzerhof (PBE)<sup>[36]</sup> with and without Grimme's dispersion correction D2.<sup>[132]</sup> For BLYP, Goedecker pseudopotentials<sup>[133]</sup> were used for all the atoms, and for PBE, Troullier-Martins pseudopotentials<sup>[134]</sup> were chosen for all the atoms except lithium, for which the Goedecker functional was utilized. The best matching functional, PBE, without Grimme's dispersion correction, was used to perform further calculations.

### *Benchmark*

The wavefunction was optimized to the Born-Oppenheimer surface and the geometry was relaxed using TEMPCONTROL option: the ionic velocities were set back to zero, whenever the temperature exceeded 100 K. The time step chosen was 4 a.u. (~0.1 fs). The plane-wave cutoff determining the basis set size was set to 70 Rydberg. The simulation cell size was set to same size of the crystal unit cell: 14.9657×15.2558× 22.9370 Å<sup>3</sup> and  $\alpha$ ,  $\beta$  and  $\gamma$  were set to 90°.

### *MLWF of Intermediate C.*

The PBE<sup>[36]</sup> functional and the pseudopotentials cited previously were used to perform molecular dynamics calculations starting from Gaussian optimized structure C. The system was optimized to the Born-Oppenheimer surface and a molecular dynamics run was performed for 200 steps. Maximally localized Wannier functions were calculated (keywords: DIPOLE DYNAMICS<sup>[143-145]</sup> WANNIER SAMPLE<sup>[146-148]</sup>). The simulation cell size was set to 22×22×22 Å<sup>3</sup> and  $\alpha$ ,  $\beta$  and  $\gamma$  were set to 90°.

## Simulations

Perdew–Burke–Ernzerhof (PBE),<sup>[36]</sup> was used to perform molecular dynamics calculations starting from the transition state geometry I found in Gaussian. Troullier-Martins<sup>[134]</sup> pseudopotentials were used for the nitrogen atoms.

## Gaussian calculations.<sup>[35]</sup>

For the Gaussian calculations, the following GGA and hybrid functionals were benchmarked (Grimme's dispersion with Becke-Johnson damping GD3BJ<sup>[137]</sup> added was marked with D3 abbreviation); BLYP,<sup>[130,131]</sup> BLYP-D3,<sup>[130,131,137]</sup> B3LYP,<sup>[130,131,138]</sup> B3LYP-D3,<sup>[130,131,137,138]</sup> PBE0,<sup>[36–38]</sup> PBE0-D3,<sup>[36,37,137]</sup> wB97XD,<sup>[139]</sup> PBE<sup>[36]</sup> and M06.<sup>[140]</sup> We used LANL2DZ<sup>[39–42]</sup> and LANL,<sup>[39–42]</sup> for valence and core electrons of iron, respectively. 6-311+G(d,p)<sup>[43–45]</sup> was used for all other atoms.

## 6.2. Experimental section

### 6.2.1 General Considerations

All procedures which required manipulation of air sensitive compounds carried out in an inert atmosphere (Argon) using the Schlenk technique. Reaction apparatuses were heated using a heat gun under vacuum and flushed with argon. This cycle was repeated three times. Anhydrous and oxygen free solvents were prepared as following: THF, diethyl ether and hexane were dried at reflux over sodium/benzophenone, dichloromethane by stirring over calcium hydride. Diisopropylamine, triethylamine and tetramethylethylenediamine were distilled from potassium hydroxide in a still under nitrogen atmosphere. All solvents were freshly distilled before use. When necessary, deuterated chloroform was dried by heating at reflux over CaH<sub>2</sub> and distilled in an inert atmosphere. CD<sub>2</sub>Cl<sub>2</sub> was first dried over molecular sieves (4Å) for 24 h followed by reflux over CaH<sub>2</sub> and distillation under argon atmosphere collected in a Schlenk flask with molecular sieves (4Å). Anhydrous acetonitrile, dimethyl sulfoxide, dimethylformamide, ethanol and methanol were purchased from commercial suppliers and used without further purification. If stated, solvents were degassed by three or more freeze-

pump-thaw cycles. Chiral compounds were obtained as racemate.

### **Preparative column chromatography**

Silica gel with particle size from 40 to 63  $\mu\text{m}$  (Silica M) from MACHEREY-NAGEL was used for flash chromatography separation. For the chromatography of air sensitive compounds, the silica gel was degassed, and flame dried with a heat gun under vacuum and settled under normal pressure with argon. All the solvents used for column chromatography under protected atmosphere were distilled over drying agents and purged with argon for *circa* 20 min by flushing with a constant argon stream. The silica gel was neutralized with the solvents containing 3% triethylamine. If stated, neutral aluminium oxide 90 (activity grade I) from MACHEREY-NAGEL was used instead.

### **Thin layer chromatography**

Thin layer chromatography (TLC) was performed on aluminium TLC plates ALUGRAM® Xtra SIL G/UV254 from MACHEREY-NAGEL. The detection of substances was done using a UV lamp of a wavelength of 254 nm.

### **NMR Spectra**

The multiplicity of the peaks was abbreviated as s (singlet), d (doublet), t (triplet), q (quartet), m (multiplet), br (broad). 2D NMR measurement methods (COSY, HSQC, HMBC, NOESY, HMQC) were used to help to elucidate structures and chemical shift assignment. Cp' refers to the unsubstituted cyclopentadienyl ligand ( $\text{C}_5\text{H}_5$ ) and Py to pyridine.

**$^1\text{H-NMR}$**  spectra were measured using the instruments Bruker Ascend (400 MHz) with Avance III Console besides Bruker Ascend (400 MHz) with Avance IIIHD Console, Ultrashield (500 MHz) with Avance-III HD console and Bruker Ascend (600 MHz) with Avance NEO Console at 298 K. The chemical shifts of the residual solvent signals of the deuterated solvents ( $\text{CDCl}_3$ ,  $\delta = 7.26$  ppm,  $\text{CD}_2\text{Cl}_2$ ,  $\delta = 5.32$  ppm,  $\text{CD}_3\text{OD}$ ,  $\delta = 3.31$  ppm,  $\text{C}_6\text{D}_6$ ,  $\delta = 7.16$  ppm) were used as internal standards.

**$^{13}\text{C-NMR}$**  spectra were measured using the instruments Bruker Ascend (100.6 MHz) with Avance III Console besides Bruker Ascend (100.6 MHz) with Avance IIIHD Console, Ultrashield (500 MHz) with Avance-III HD console and Bruker Ascend (151 MHz) with Avance NEO Console at 298 K. The chemical shifts of the residual solvent signals of the deuterated solvents ( $\text{CDCl}_3$ ,  $\delta = 77.16$  ppm;  $\text{CD}_2\text{Cl}_2$ ,  $\delta = 54.00$  ppm;  $\text{CD}_3\text{OD}$ ,  $\delta = 49.00$  ppm;  $\text{C}_6\text{D}_6$ ,  $\delta =$



128.06 ppm) were used as internal standards.

**<sup>19</sup>F NMR** spectra were measured using the instruments Bruker Ascend (100.6 MHz) with Avance IIIHD Console and Bruker Ascend (376.5 MHz) with Avance NEO Console at 298 K. Spectrometer frequency for <sup>1</sup>H was multiplied by 0.94094008 and the resulting value entered as the spectrometer frequency for <sup>19</sup>F according to the IUPAC convention.<sup>[149]</sup>

### **High resolution mass spectra**

High resolution electron ionization (HR-EI) mass spectra were measured using a Micromass GCT spectrometer with direct insertion probe, 70 eV electron energy and 250 °C source temperature. High resolution electrospray ionization (HR-ESI) mass spectra were measured using a Waters LCT Premier with Alliance 2695 HPLC (Waters), 2700 V capillary voltage, 650 l/h desolvation gas and 250 °C desolvation temperature. Samples (5 µL, 10 µg/mL in methanol) were injected in a constant flow of methanol (400 µL/min) infused in the mass spectrometer without further chromatographic purification. All values are given in atomic units of mass per elemental charge (*m/z*).

### **Infrared spectra**

IR spectra were recorded with the Fourier transform infrared spectrophotometer IRAffinity-1S from Shimadzu with quest ATR unit (32 scans). The signal intensities were abbreviated as follows: strong (s), medium (m), weak (w), broad (br).

### **Melting Point**

Melting points (m. p.) were measured using Electrothermal™ IA 9000 Series Melting Point Apparatus.

### **Medium pressure liquid chromatography (MPLC)**

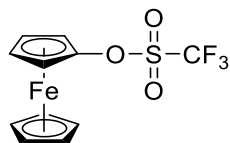
Büchi Chromatography Pump 688, Büchi gradient Former B687, Büchi Fraction collector B684 and a Knauer UV detector K-2501.

### **Single crystal X-ray Diffraction analysis**

Single X-ray diffraction analysis were measure with KAPPA APEX II CCD and Typ Smart X2S diffractometer from Bruker.

## 6.2.2 Synthesised compounds

### 6.2.2.1 Ferrocenyl triflate (**79**)<sup>[17]</sup>

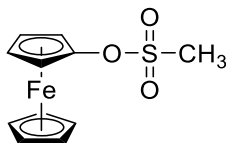


**79**

At  $-78\text{ }^{\circ}\text{C}$  a solution of methyllithium in hexane (1.6 M, 5.3 mL, 8.4 mmol) was added to ferrocenyl acetate<sup>[29]</sup> (**77**, 2050 mg, 8.4 mmol) in diethyl ether (80 mL). The reaction mixture was slowly warmed to  $22\text{ }^{\circ}\text{C}$  and stirred for 2h. The solution was cooled  $-78\text{ }^{\circ}\text{C}$  and trifluoromethanesulfonic anhydride (3.20 mL, 19.1 mmol) was added dropwise, and the solution was stirred for 30 min. The mixture was slowly brought to  $22\text{ }^{\circ}\text{C}$  and further stirred for 30 min. After quenching with water, the mixture was extracted with dichloromethane (3 x 80 mL). The collected organic layers were dried with magnesium sulfate and the solvent removed at reduced pressure. After purification by column chromatography [3 x 30 cm,  $\text{SiO}_2$  (deactivated with  $\text{NEt}_3$ ), petroleum ether / dichloromethane 4:1] ferrocenyl triflate (**79**, 2594 mg, 7.8 mmol, 92%) was obtained as a yellow oil. (Not directly comparable with the literature because the authors recorded the spectra using acetone- $d_6$ ).

$^1\text{H}$  NMR (400.1 MHz,  $\text{CDCl}_3$ ):  $\delta$  = 4.04 (AA'BB',  $J$  = 2.0 Hz, 2 x 2H, Cp), 4.33 (s, 5H, Cp'), 4.52 (AA'BB',  $J$  = 1.8 Hz, 2 x 2H, Cp) ppm.  $^{13}\text{C}$  NMR (100.6 MHz,  $\text{CDCl}_3$ , HSQC, HMBC):  $\delta$  = 61.3 ( $\text{C}_{\text{CpH}}$ ), 64.3 ( $\text{C}_{\text{CpH}}$ ), 70.4 (Cp'), 118.6 (q,  $^1J_{\text{F,C}}$  = 321.1 Hz,  $\text{CF}_3$ ), 119.2 ( $\text{C}_{\text{CpO}}$ ) ppm. HRMS (EI): Calcd. for  $\text{C}_{11}\text{H}_9\text{F}_3\text{FeO}_3\text{S}$  [ $\text{M}^+$ ] 333.9574, found 333.9576.

#### 6.2.2.2. Ferrocenyl methanesulfonate (**94**)

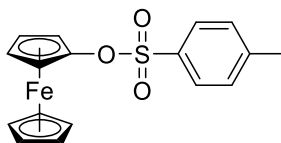


**94**

At  $-78\text{ }^{\circ}\text{C}$  a solution of methyllithium in hexane (1.6 M, 3.1 mL, 6.2 mmol) was added to ferrocenyl acetate<sup>[29]</sup> (**77**, 500 mg, 2.1 mmol) in diethyl ether (10 mL). The reaction mixture was stirred for 30 min and warmed to  $0\text{ }^{\circ}\text{C}$ . Methanesulfonyl chloride (0.48 mL, 6.2 mmol) was added dropwise, and the solution was stirred for 30 min. After warming to  $21\text{ }^{\circ}\text{C}$  the mixture was stirred for another 30 min. After addition of water (25 mL) the mixture was extracted with ethyl acetate (3 x 40 mL). The collected organic layers were dried with magnesium sulfate and the solvent removed at reduced pressure. After purification by column chromatography (3 x 30 cm, SiO<sub>2</sub>, petroleum ether / dichloromethane 9:1] ferrocenyl methanesulfonate (**94**, 410 mg, 1.5 mmol, 71%) was obtained as an orange/yellow solid (m.p.  $63\text{-}64\text{ }^{\circ}\text{C}$ ).

<sup>1</sup>H NMR (400.1 MHz, CDCl<sub>3</sub>):  $\delta$  = 3.00 (s, 3H, CH<sub>3</sub>), 4.01 + 4.48 (AA'BB',  $J$  = 1.8 Hz, 2 x 2H, CpH), 4.30 (s, 5H, Cp') ppm. <sup>13</sup>C NMR (100.6 MHz, CDCl<sub>3</sub>, HSQC, HMBC):  $\delta$  = 36.5 (CH<sub>3</sub>), 61.6 (C<sub>Cp</sub>H), 64.2 (C<sub>Cp</sub>H), 70.1 (Cp'), 116.7 (C<sub>Cp</sub>O) ppm. IR:  $\tilde{\nu}$  = 3113 (w), 3037 (w), 2941 (w), 1436 (m), 1375 (m), 1170 (s), 1018 (m), 921 (m), 806 (s), 761 (m), 592 (m), 522 (m), 482 (s) cm<sup>-1</sup>. HRMS (ESI, MeCN): Calcd. for C<sub>11</sub>H<sub>12</sub>FeO<sub>3</sub>S [M<sup>+</sup>] 279.9857, found 279.9849.

#### 6.2.2.3. Ferrocenyl (4-methylphenyl)sulfonate (**95**)<sup>[31]</sup>



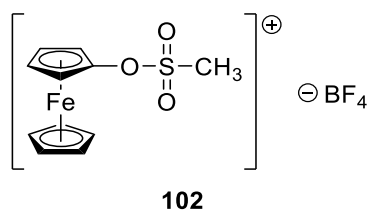
**95**

At  $-78\text{ }^{\circ}\text{C}$  a solution of methyllithium in hexane (1.6 M, 3.1 mL, 6.2 mmol) was added to ferrocenyl acetate<sup>[29]</sup> (**77**, 607 mg, 2.5 mmol) in diethyl ether (15 mL) and stirred at  $-78\text{ }^{\circ}\text{C}$  for 5 min. After slowly warming to  $21\text{ }^{\circ}\text{C}$  the mixture was stirred for another 2 h. At  $0\text{ }^{\circ}\text{C}$ , a solution

of 4-toluenesulfonyl chloride (711 mg, 3.7 mmol) in THF (5 mL) was added dropwise, the solution was slowly warmed to 21 °C and stirred for 30 min. After addition of water (15 mL) the mixture was extracted with dichloromethane (3 x 20 mL). The collected organic layers were dried with magnesium sulfate, and the solvent removed at reduced pressure. After purification through column chromatography (3 x 30 cm, SiO<sub>2</sub>, petroleum ether / dichloromethane 8:2) ferrocenyl tosylate (**95**, 835 mg, 2.3 mmol, 94%) was obtained as an orange solid (m. p. 95 - 96 °C), identified by comparison with literature data (<sup>1</sup>H NMR, <sup>13</sup>C NMR, MS).<sup>[31]</sup>

<sup>1</sup>H NMR (400.1 MHz, CDCl<sub>3</sub>): δ = 2.43 (s, 3H, CH<sub>3</sub>), 3.87 + 4.17 (AA'BB', J = 2.0 Hz, 2 x 2H, CpH), 4.23 (s, 5H, Cp'), 7.29 + 7.66 (AA'BB', J = 8.2 Hz, 2 x 2H, C<sub>6</sub>H<sub>4</sub>) ppm. <sup>13</sup>C NMR (100.6 MHz, CDCl<sub>3</sub>, HSQC, HMBC): δ = 21.8 (CH<sub>3</sub>), 62.0 (C<sub>Cp</sub>H), 63.9 (C<sub>Cp</sub>H), 69.9 (Cp'), 116.5 (C<sub>Cp</sub>O), 128.7 (C<sub>Ar</sub>H), 129.7 (C<sub>Ar</sub>H), 132.1 (C<sub>Ar</sub>S), 145.3 (C<sub>Ar</sub>CH<sub>3</sub>). HRMS (ESI, MeCN): Calcd. for C<sub>17</sub>H<sub>16</sub>FeO<sub>3</sub>SNa [M+Na] 379.0067, found 379.0067.

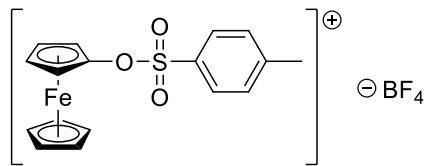
#### 6.2.2.4. (Methylsulfonyl)ferrocenium tetrafluoroborate (**102**)



At 21 °C nitrosyl tetrafluoroborate (83 mg, 0.7 mmol) was added to a yellow solution of ferrocenyl mesylate (**94**, 200 mg, 0.7 mmol) in dichloromethane (5 mL). The solution immediately turned green and was stirred for 15 min at 21 °C. The solvent was removed at reduced pressure affording **13** an air sensitive green solid (Yield was not quantified and compound was further used without any purification).

IR:  $\tilde{\nu}$  = 3487 (w), 3122 (w), 1928 (w), 1847 (w), 1637 (w), 1460 (w), 1365 (w), 972 (s), 794 (m), 516 (s) cm<sup>-1</sup>. HRMS (ESI, MeCN): Calcd. for C<sub>11</sub>H<sub>12</sub>FeO<sub>3</sub>S [M<sup>+</sup>] 279.9857, found 279.9746; Calcd. for BF<sub>4</sub><sup>-</sup> [M<sup>-</sup>] 87.0029, found 87.0027.

6.2.2.5. [(4-Methylphenyl)sulfonyl]ferrocenium tetrafluoroborate (**103**)

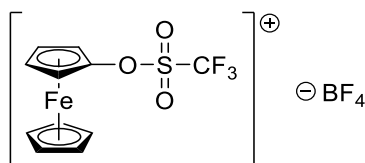


**103**

At 21 °C nitrosyl tetrafluoroborate (28 mg, 0.2 mmol) was added to a yellow solution of ferrocenyl tosylate (**95**, 86 mg, 0.2 mmol) in dichloromethane (5 mL). The solution immediately turned green and was stirred for 15 min at 21 °C. The solvent was removed at reduced pressured affording **103** as an air sensitive green solid (Yield was not quantified and compound was further used without any purification).

IR:  $\tilde{\nu}$  = 3525 (w), 3120 (w), 2339 (W), 1928 (w), 1849 (s), 1624 (w), 1496 (w), 1369 (w), 1294 (w), 999 (s), 856 (m), 688 (m), 547 (m), 518 (m)  $\text{cm}^{-1}$ . HRMS (ESI, MeCN): Calcd. for  $\text{C}_{17}\text{H}_{16}\text{FeO}_3\text{S}$  [ $\text{M}^+$ ] 356.0170, found 356.0168; Calcd. for  $\text{BF}_4^-$  [ $\text{M}^-$ ] 87.0029, found 87.0029.

6.2.2.6. [(Trifluoromethyl)sulfonyl]ferrocenium tetrafluoroborate (**104**)



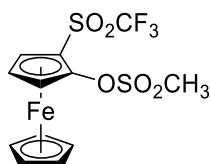
**104**

At 21 °C nitrosyl tetrafluoroborate (98 mg, 0.8 mmol) was added to a yellow solution of ferrocenyl triflate<sup>[17]</sup> (**79**, 280 mg, 0.8 mmol) in dichloromethane (5 mL). The solution immediately turned green and was stirred for 15 min at 21 °C. The solvent was removed at reduced pressure affording **104** as an air sensitive green solid (Yield was not quantified and compound was further used without any purification).

IR:  $\tilde{\nu}$  = 3510 (w), 3122 (w), 1930 (w), 1849 (w), 1433 (m), 1367 (m), 1220 (m), 1128 (s), 1020 (s), 925 (s), 823 (m), 765 (m), 682 (m), 609 (m), 516 (m)  $\text{cm}^{-1}$ . HRMS (EI): Calcd. for

C<sub>11</sub>H<sub>9</sub>FeF<sub>3</sub>O<sub>3</sub>S [M<sup>+</sup>] 333.9574, found 333.9573; HRMS (ESI, MeCN): Calcd. for BF<sub>4</sub><sup>-</sup> [M<sup>-</sup>] 87.0029, found 87.0028.

6.2.2.7. *rac*-2-[(Trifluoromethyl)sulfonyl]ferrocenyl methanesulfonate (*rac*-**105**)

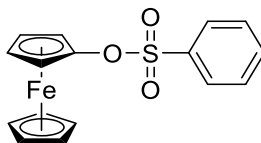


*rac*-**105**

At  $-78\text{ }^{\circ}\text{C}$  THF (10 mL) was added to [(trifluoromethyl)sulfonyl]ferrocenium tetrafluoroborate (**104** (353 mg, 0.8 mmol; addition at  $21\text{ }^{\circ}\text{C}$  caused decomposition). Lithium diisopropylamide [prepared from 2.5 M butyllithium (0.12 mL, 0.8 mmol) in hexane and diisopropylamine (0.12 mL, 2.5 mmol)] was added dropwise at  $-78\text{ }^{\circ}\text{C}$ . The solution was stirred for 30 min at  $-78\text{ }^{\circ}\text{C}$  and warmed to  $0\text{ }^{\circ}\text{C}$ . Methanesulfonyl chloride (0.23 mL, 2.9 mmol) was added at  $0\text{ }^{\circ}\text{C}$ , and the solution was stirred for 30 min. After addition of water (10 mL) the mixture was extracted with dichloromethane (3 x 20 mL). The collected organic layers were dried with magnesium sulfate, and the solvent was removed at reduced pressure. After purification by column chromatography [20 x 2 cm, SiO<sub>2</sub>, petroleum ether / ethyl acetate 9:1] *rac*-**105** (58 mg, 0.14 mmol, 17%) was obtained as a brown oil. *rac*-**105** turned out to be air-sensitive, and after column chromatography in inert atmosphere [20 x 2 cm, SiO<sub>2</sub>, Hexane / Dichloromethane 9:1] *rac*-**105** (21 mg, 0.05 mmol, 6 %) was isolated as an orange/yellow oil.

<sup>1</sup>H NMR (400.1 MHz, CDCl<sub>3</sub>):  $\delta$  = 3.20 (s, 3H, CH<sub>3</sub>), 4.55 (t, <sup>3</sup>J = 2.9 Hz, 1H, CpH), 4.63 (s, 1H, CpH), 4.64 (s, 5H, Cp'), 5.08 (s, 1H, CpH) ppm. <sup>13</sup>C NMR (150.9 MHz, CDCl<sub>3</sub>, HSQC, HMBC):  $\delta$  = 38.9 (CH<sub>3</sub>), 67.0 (C<sub>CpH</sub>), 68.1 (C<sub>CpH</sub>), 68.1 (C<sub>CpH</sub>), 68.2 (q, <sup>3</sup>J<sub>F,C</sub> = 2.22 Hz, C<sub>CpS</sub>), 73.6 (Cp'), 115.7 (C<sub>CpO</sub>), 119.5 (q, <sup>1</sup>J<sub>F,C</sub> = 327 Hz, CF<sub>3</sub>) ppm. <sup>19</sup>F NMR (376.5 MHz, CDCl<sub>3</sub>):  $\delta$  =  $-78.7$  (CF<sub>3</sub>) ppm. IR:  $\tilde{\nu}$  = 2954 (m), 2992 (m), 2852 (m), 1460 (w), 1429 (m), 1357 (m), 1259 (m), 1219 (m), 1201 (m), 1029 (m), 970 (m), 800 (s), 752 (m), 626 (m), 569 (m), 491 (m), 405 (w) cm<sup>-1</sup>. HRMS (ESI, MeCN): Calcd. for C<sub>12</sub>H<sub>11</sub>F<sub>3</sub>FeO<sub>5</sub>S<sub>2</sub> [M<sup>+</sup>] 412.9347, found 411.9349.

6.2.2.8. Ferrocenyl benzenesulfonate (**111**)<sup>[29]</sup>

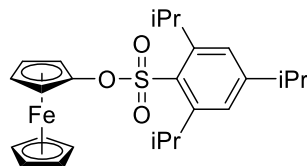


**111**

At 0 °C methyllithium in hexane (1.6 M, 0.90 mL, 1.5 mmol) was added to ferrocenyl acetate<sup>[29]</sup> (**77**, 294 mg, 1.2 mmol) in diethyl ether (10 mL). The reaction mixture was slowly warmed to 22 °C and stirred for 2.5 h. At 0 °C, benzenesulfonyl chloride (254 mg, 1.5 mmol) in diethyl ether (5 mL) was added dropwise, and the solution was slowly warmed to 22 °C and stirred for 16 h. After addition of water (10 mL) the mixture was extracted with dichloromethane (3 x 10 mL). The collected organic layers were dried with magnesium sulfate and the solvent removed at reduced pressure. After purification by column chromatography (3 x 30 cm, SiO<sub>2</sub>, petroleum ether / ethyl acetate 95:5 to 8:2) ferrocenyl benzenesulfonate (**111**, 342 mg, 1.0 mmol, 83%) was obtained as a yellow solid (m. p. 89 °C).

<sup>1</sup>H NMR (400.1 MHz, CDCl<sub>3</sub>):  $\delta$  = 3.87 (s, 2H, C<sub>Cp</sub>H), 4.16 (s, 2H, C<sub>Cp</sub>H), 4.23 (s, 5H, Cp'), 7.50 (m, 2H, SCCCH), 7.64 (m, 1H, SCCCH), 7.78 (m, 2H, SCCH) ppm. <sup>13</sup>C NMR (100.6 MHz, CDCl<sub>3</sub>, HSQC, HMBC):  $\delta$  = 61.9 (C<sub>Cp</sub>H), 64.0 (C<sub>Cp</sub>H), 69.9 (Cp'), 116.6 (C<sub>Cp</sub>O), 128.7 (C<sub>Ph</sub>H), 129.1 (C<sub>Ph</sub>H), 134.2 (C<sub>Ph</sub>H), 135.1 (SC) ppm. IR:  $\tilde{\nu}$  = 3105 (w), 3082 (w), 1448 (m), 1441 (m), 1398 (w), 1371(s), 1337 (w), 1310(w), 1227 (w), 1182 (s), 1173 (s), 1105 (w), 1090 (m), 1024 (m), 1001 (m), 926 (s), 831 (w), 795 (s), 754 (s), 733 (s), 704 (m), 682 (s), 613 (s), 575 (s), 550 (s), 498 (s), 486 (s), 424 (w) cm<sup>-1</sup>. HRMS (EI): Calcd. for C<sub>16</sub>H<sub>14</sub>FeO<sub>3</sub>S [M<sup>+</sup>] 342.0013, found 342.0018.

6.2.2.9. Ferrocenyl (2,4,6-triisopropylbenzene)sulfonate (**112**)



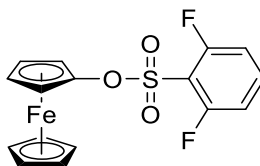
**112**

At 0 °C methyllithium in hexane (1.6 M, 2.00 mL, 3.2 mmol) was added to ferrocenyl acetate<sup>[29]</sup> (**77**, 517 mg, 2.1 mmol) in diethyl ether (15 mL). The reaction mixture was slowly warmed to 22 °C and stirred for 2.5 h. At 0 °C 2,4,6-triisopropylbenzenesulfonyl chloride (962 mg, 3.18 mmol) in Et<sub>2</sub>O (5 mL) was added dropwise, the solution was slowly warmed to 21 °C and stirred for 2 h. After addition of water (25 mL) the mixture was extracted with dichloromethane (3 x 25 mL). The collected organic layers were washed with water (25 mL) and dried with magnesium sulfate. The solvent was removed at reduced pressure. After purification by column chromatography [20 x 3 cm, SiO<sub>2</sub> (deactivated with Et<sub>3</sub>N), *tert*-butyl methyl ether] 2,4,6-triisopropylbenzenesulfonyl ferrocene (**112**, 921 mg, 2.0 mmol, 93%) was obtained as a yellow solid (m. p. 144 °C).

<sup>1</sup>H NMR (400.1 MHz, CDCl<sub>3</sub>):  $\delta$  = 1.21 (d, <sup>3</sup>J = 6.8 Hz, 12H, SCCCHCH<sub>3</sub>), 1.27 (d, <sup>3</sup>J = 6.9 Hz, 6H, SCCCHCCHCH<sub>3</sub>), 2.92 (sept, <sup>3</sup>J = 6.9 Hz, 1H, SCCCHCCHCH<sub>3</sub>), 3.87 + 4.10 (AA'BB', J = 1.9 Hz, 2 x 2H, C<sub>Cp</sub>H), 4.04 (sept, <sup>3</sup>J = 6.8 Hz, 2H, SCCCHCH<sub>3</sub>), 4.23 (s, 5H, Cp'), 7.17 (s, 2H, SCCCH) ppm. <sup>13</sup>C NMR (100.6 MHz, CDCl<sub>3</sub>, HSQC, HMBC):  $\delta$  = 23.5 (SCCCHCCHCH<sub>3</sub>), 24.6 (SCCCHCCHCH<sub>3</sub>), 29.6 (SCCCHCH<sub>3</sub>), 34.2 (SCCCHCCHCH<sub>3</sub>), 62.0 (C<sub>Cp</sub>H), 63.9 (C<sub>Cp</sub>H), 69.7 (Cp'), 115.8 (C<sub>Cp</sub>O), 123.7 (SCCCH), 129.2 (SC), 151.3 (SCC), 154.1 (SCCCHC) ppm. IR:  $\tilde{\nu}$  = 2957 (w), 2926 (w), 1595 (w), 1439 (w), 1425 (w), 1410 (w), 1226 (w), 1180 (s), 1107 (w), 1038 (w), 922 (m), 777 (s), 756 (m), 721 (m), 663 (m), 559 (m), 550 (m), 482 (s) cm<sup>-1</sup>. HRMS (ESI, MeCN): Calcd. for C<sub>25</sub>H<sub>32</sub>FeO<sub>3</sub>S [M<sup>+</sup>] 468.1422, found 468.1422; calcd. for C<sub>25</sub>H<sub>32</sub>FeO<sub>3</sub>Na [M<sup>+</sup>+Na] 491.1319, found 491.1317.



6.2.2.10. Ferrocenyl (2,6-difluorobenzene)sulfonate (**113**)

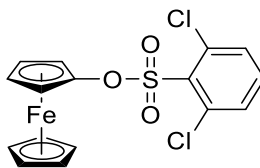


**113**

At 0 °C methyllithium in hexane (1.6 M, 2.20 mL, 3.5 mmol) was added to ferrocenyl acetate<sup>[29]</sup> (**77**, 860 mg, 3.5 mmol) in diethyl ether (15 mL). At 0 °C 2,6-difluorobenzenesulfonyl chloride (0.48 mL, 749 mg, 3.5 mmol) was added dropwise, and the reaction mixture was slowly warmed to 21 °C and stirred for 2 h. After addition of water (25 mL) the mixture was extracted with dichloromethane (3 x 25 mL). The collected organic layers were washed with water (25 mL) and dried with magnesium sulfate. The solvent was removed at reduced pressure. After purification by column chromatography [3 x 20 cm, SiO<sub>2</sub> (deactivated with Et<sub>3</sub>N), petroleum ether / ethyl acetate 100:0 gradient to 6:4] ferrocenyl (2,6-difluorobenzene)sulfonate (**113**, 1194 mg, 3.2 mmol, 90%) was obtained as an orange solid (m. p. 114 °C).

<sup>1</sup>H NMR (400.1 MHz, CDCl<sub>3</sub>):  $\delta$  = 3.91 + 4.34 (AA'BB',  $J$  = 2.0 Hz, 2 x 2H, C<sub>Cp</sub>H), 4.27 (s, 5H, Cp'), 7.04 (ABB'XX',  $J$  = 8.4 Hz, 2H, SCCCH), 7.59 (ABB'XX',  $J$  = 8.5,  $J$  = 5.8, 1H, SCCCHCH) ppm. <sup>13</sup>C NMR (100.6 MHz, CDCl<sub>3</sub>, HSQC, HMBC):  $\delta$  = 61.3 (C<sub>Cp</sub>H), 64.1 (C<sub>Cp</sub>H), 70.1 (Cp'), 113.3 (m, SCCCHCH), 116.7 (C<sub>Cp</sub>O), 136.4 (t, <sup>3</sup>J<sub>F,C</sub> = 11 Hz, SCCCH), 160.23 (dd, <sup>1</sup>J<sub>F,C</sub> = 263 Hz, <sup>3</sup>J<sub>F,C</sub> = 3 Hz, CF) ppm. <sup>19</sup>F NMR (376.5 MHz, CDCl<sub>3</sub>):  $\delta$  = -104.3 (s) ppm. IR:  $\tilde{\nu}$  = 3113 (w), 3082 (w), 1609 (m), 1587 (m), 1564 (w), 1470 (s), 1440 (m), 1412 (w), 1391 (s), 1292 (w), 1242 (m), 1229 (w), 1188 (s), 1105 (m), 1053 (w), 1024 (m), 1005 (s), 928 (m), 816 (s), 795 (s), 772 (m), 716 (m), 644 (m), 600 (m), 557 (m), 540 (s), 501 (m), 482 (s), 426 (w), 411 (w) cm<sup>-1</sup>. HRMS (ESI, MeCN): Calcd. for C<sub>16</sub>H<sub>12</sub>F<sub>2</sub>FeO<sub>3</sub>SNa [M<sup>+</sup>+Na] 400.9722, found 400.9728.

6.2.2.11. Ferrocenyl (2,6-dichlorobenzene)sulfonate (**114**)

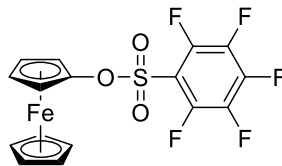


**114**

At 0 °C methyllithium in hexane (1.6 M, 2.22 mL, 3.6 mmol) was added to ferrocenyl acetate<sup>[29]</sup> (**77**, 866 mg, 3.6 mmol) in diethyl ether (30 mL). The reaction mixture was slowly warmed to 21 °C and stirred for 2.5 h. At 0 °C 2,6-dichlorobenzenesulfonyl chloride (871 mg, 3.6 mmol) in diethyl ether (5 mL) was added dropwise, and the solution was slowly warmed to 21 °C and stirred for 2 h. After addition of water (30 mL) the mixture was extracted with dichloromethane (3 x 30 mL). The collected organic layers were washed with water (30 mL) and dried with magnesium sulfate, and the solvent was removed at reduced pressure. After purification by column chromatography [3 x 20 cm, SiO<sub>2</sub> (deactivated with Et<sub>3</sub>N), petroleum ether / ethyl acetate 100:0 gradient to 6:4] ferrocenyl (2,6-dichlorobenzene)sulfonate (**114**, 958 mg, 2.3 mmol, 67%) was obtained as a yellow solid (m. p. 117 °C).

<sup>1</sup>H NMR (400.1 MHz, CDCl<sub>3</sub>):  $\delta$  = 3.90 (s, 2H, C<sub>Cp</sub>H), 4.27 (s, 5H, Cp'), 4.32 (s, 2H, C<sub>Cp</sub>H), 7.39 (m, 1H, SCCCHCH), 7.47 (m, 2H, SCCCH) ppm. <sup>13</sup>C NMR (150.9 MHz, CDCl<sub>3</sub>, HSQC, HMBC):  $\delta$  = 61.2 (C<sub>Cp</sub>H), 64.1 (C<sub>Cp</sub>H), 70.1 (Cp'), 116.6 (C<sub>Cp</sub>O), 131.5 (SCCCH), 131.9 (SC), 133.9 (SCCCHCH), 136.7 (SCCCI) ppm. IR:  $\tilde{\nu}$  = 3102 (w), 1560 (m), 1427 (s), 1410 (m), 1383 (s), 1368 (m), 1223 (w), 1188 (s), 1159 (w), 1132 (w), 1105 (w), 1028 (m), 1020 (m), 920 (m), 835 (m), 802 (m), 783 (s), 741 (m), 714 (m), 613 (s), 584 (s), 557 (m), 511 (m), 498 (m), 480 (s), 442 (m), 407 (m) cm<sup>-1</sup>. HRMS (ESI, MeCN): Calcd. for C<sub>16</sub>H<sub>12</sub>Cl<sub>2</sub>FeO<sub>3</sub>SNa [M<sup>+</sup>+Na] 432.9131, found 432.9129.

6.2.2.12. Ferrocenyl (2,3,4,5,6-pentafluorobenzene)sulfonate (**110**)

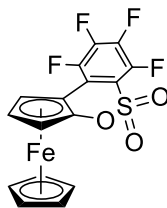


**110**

At 0 °C methyllithium in hexane (1.6 M, 1.65 mL, 2.6 mmol) was added to ferrocenyl acetate<sup>[29]</sup> (**77**, 645 mg, 2.6 mmol) in diethyl ether (30 mL). The reaction mixture was slowly warmed to 21 °C and stirred for 2.5 h. At 0 °C 2,3,4,5,6-pentafluorobenzenesulfonyl chloride (0.39 mL, 704 mg, 2.6 mmol) was added dropwise, and the solution was slowly warmed to 21 °C and stirred for 2 h. After addition of water (30 mL) the mixture was extracted with dichloromethane (3 x 30 mL). The collected organic layers were washed with water (30 mL) and dried with magnesium sulfate. The solvent was removed at reduced pressure. After purification by column chromatography eluted with PE:EtOAc [3 x 20 cm, SiO<sub>2</sub> (deactivated with Et<sub>3</sub>N), petroleum ether / ethyl acetate 8:2] ferrocenyl 2,3,4,5,6-pentafluorobenzenesulfonate (**110**, 571 mg, 1.3 mmol, 50%) was obtained as a yellow solid (m. p. 132 °C).

<sup>1</sup>H NMR (400.1 MHz, CDCl<sub>3</sub>):  $\delta$  = 3.97 + 4.38 (AA'BB',  $J$  = 2.0 Hz, 2 x 2H, C<sub>Cp</sub>H), 4.31 (Cp') ppm. <sup>13</sup>C NMR (150.9 MHz, CDCl<sub>3</sub>, HSQC, HMBC):  $\delta$  = 61.2 (C<sub>Cp</sub>H), 64.5 (C<sub>Cp</sub>H), 70.3 (Cp'), 111.6 (m, SC), 117.0 (C<sub>Cp</sub>O), 138.0 (AA'BB'C, <sup>1</sup>J<sub>C,F</sub> = 256.8 Hz, *meta*), 145.2 (AA'BB'C, <sup>1</sup>J<sub>C,F</sub> = 261.2 Hz, *para*) ppm, 145.3 (AA'BB'C, <sup>1</sup>J<sub>C,F</sub> = 261.2 Hz, *ortho*) ppm. <sup>19</sup>F NMR (376.5 MHz, CDCl<sub>3</sub>):  $\delta$  = -132.9 (m, SCCF, *ortho*), -142.0 (m, SCCCCF, *para*), -157.7 (m, SCCCF, *meta*) ppm. IR:  $\tilde{\nu}$  = 3103 (w), 1643 (m), 1522 (m), 1501 (s), 1435 (m), 1404 (m), 1304 (m), 1219 (m), 1184 (s), 1105 (s), 1020 (m), 993 (s), 922 (s), 868 (m), 810 (s), 698 (m), 608 (s), 588 (s), 575 (m), 488 (s), 438 (m) cm<sup>-1</sup>. HRMS (ESI, MeCN): Calcd. for C<sub>16</sub>H<sub>12</sub>Cl<sub>2</sub>FeO<sub>3</sub>SNa [M<sup>+</sup>Na] 431.9542, found 431.9541.

6.2.2.13. Ferrocene annelated 6,7,8,9-tetrafluorobenzo[*c,e*]-[1,2]oxathiine 5,5-dioxide (*rac*-**116**)

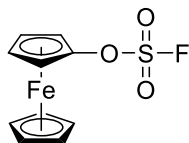


*rac*-**116**

At  $-78\text{ }^{\circ}\text{C}$  LiTMP [prepared from butyllithium in hexane (2.5 M, 0.26 mL, 0.6 mmol) and 2,2,6,6-tetramethylpiperidine (0.16 mL, 1.0 mmol) in THF (1.5 mL)] was added dropwise to ferrocenyl 2,3,4,5,6-pentafluorobenzenesulfonate (**110**, 278 mg, 0.6 mmol) in THF (70 mL). The initially yellow solution immediately turned purple. The solution was stirred for 2 h at  $-78\text{ }^{\circ}\text{C}$  and then slowly warmed to  $21\text{ }^{\circ}\text{C}$ . After stirring for 16 h water (70 mL) was added, and the solution was extracted with ethyl acetate (3 x 70 mL). The collected organic layers were dried with magnesium sulfate and the solvent removed at reduced pressure. After purification by column chromatography [3 x 30 cm,  $\text{SiO}_2$  (deactivated with  $\text{Et}_3\text{N}$ ), petroleum ether / ethyl acetate 95:5 gradient to 65:35] ferrocene annelated 6,7,8,9-tetrafluorobenzo[*c,e*]-[1,2]oxathiine 5,5-dioxide (*rac*-**116**, 54 mg, 0.2 mmol, 20%) was obtained as a red solid [m. p.  $160\text{ }^{\circ}\text{C}$  (dec.)].

$^1\text{H}$  NMR (400.1 MHz,  $\text{CDCl}_3$ ):  $\delta$  = 4.29 (Cp'), 4.32 (t,  $^3J$  = 2.8 Hz, 1H,  $\text{C}_{\text{CpH}}$ ), 4.73 (m, 1H,  $\text{C}_{\text{CpH}}$ ), 4.84 (m, 1H,  $\text{C}_{\text{CpH}}$ ) ppm.  $^{13}\text{C}$  NMR (125.8 MHz,  $\text{CDCl}_3$ , HSQC, HMBC, HMQC):  $\delta$  = 59.3 ( $\text{C}_{\text{CpH}}$ ), 60.8 (m,  $\text{C}_{\text{CpCPh}}$ ), 63.3 (d,  $J_{\text{C-F}}$  = 8.9 Hz,  $\text{C}_{\text{CpH}}$ ), 64.6 (d,  $J_{\text{C-F}}$  = 1.8 Hz,  $\text{C}_{\text{CpH}}$ ), 72.1 (Cp'), 115.5 (dt,  $J_{\text{C-F}}$  = 12.6 Hz,  $J_{\text{C-F}}$  = 4.3 Hz,  $\text{C}_{\text{qPh}}$ ), 118.1 ( $\text{C}_{\text{CpO}}$ ), 122.5 (dd,  $J_{\text{C-F}}$  = 15.8 Hz,  $J_{\text{C-F}}$  = 4.3 Hz,  $\text{C}_{\text{qPh}}$ ), 138.9 (dddd,  $J_{\text{C-F}}$  = 258.6 Hz,  $J_{\text{C-F}}$  = 16.3 Hz,  $J_{\text{C-F}}$  = 13.2 Hz,  $J_{\text{C-F}}$  = 2.9 Hz,  $\text{C}_{\text{FPh}}$ ), 143.4 (ddd,  $J_{\text{C-F}}$  = 254.5 Hz,  $J_{\text{C-F}}$  = 11.7 Hz,  $J_{\text{C-F}}$  = 3.9 Hz,  $\text{C}_{\text{FPh}}$ ), 144.3 (dddd,  $J_{\text{C-F}}$  = 261.9 Hz,  $J_{\text{C-F}}$  = 16.0 Hz,  $J_{\text{C-F}}$  = 12.5 Hz,  $J_{\text{C-F}}$  = 3.6 Hz,  $\text{C}_{\text{FPh}}$ ), 145.4 (dddd,  $J_{\text{C-F}}$  = 261.3 Hz,  $J_{\text{C-F}}$  = 13.0 Hz,  $J_{\text{C-F}}$  = 3.7 Hz,  $J_{\text{C-F}}$  = 3.2 Hz,  $\text{C}_{\text{FPh}}$ ) ppm.  $^{19}\text{F}$  NMR (376.5 MHz,  $\text{CDCl}_3$ ):  $\delta$  =  $-134.7$  (m,  $\text{C}_{\text{ArF}}$ ),  $-139.1$  (m,  $\text{C}_{\text{ArF}}$ ),  $-146.3$  (m,  $\text{C}_{\text{ArF}}$ ),  $-154.1$  (m,  $\text{C}_{\text{ArF}}$ ) ppm. IR:  $\tilde{\nu}$  = 3121 (w), 1632 (w), 1603 (w), 1504 (s), 1466 (m), 1418 (s), 1385 (s, C–F), 1368 (m), 1300 (m), 1248 (w), 1188 (s, C–F), 1125 (m), 1098 (m), 1049 (m), 999 (s), 866 (s), 827 (s), 806 (m), 783 (s), 768 (m), 689 (s), 608 (m), 579 (s), 523 (m), 490 (s), 461 (s), 436 (m)  $\text{cm}^{-1}$ . HRMS (EI): Calcd. for  $\text{C}_{16}\text{H}_8\text{F}_4\text{FeO}_3\text{S}$  [ $\text{M}^+$ ] 411.9480, found 411.9479.

#### 6.2.2.14. Ferrocenyl fluorosulfonate (**118**)



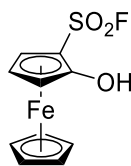
**118**

Water (40 mL) was added to a solution of ferrocenyl acetate<sup>[29]</sup> (**77**, 737 mg, 3.0 mmol) in ethanol (5 mL) followed by addition of potassium hydroxide (847 mg, 15.1 mmol). The mixture was stirred for 30 min at 70 °C. After cooling to 21 °C, the mixture was acidified by addition of oxygen free 37% aq. HCl under pH control until pH 6. Dichloromethane (3 x 40 mL) was added, and the mixture was intensely stirred for 2 min. After phase separation, the organic layers were collected with a syringe and filtered into a Schlenk flask (250 mL) through a P4 frit covered with a 5 cm thick layer of magnesium sulfate. After solvent removal at reduced pressure the remaining solid was redissolved in dichloromethane (60 mL), and triethylamine (0.84 mL, 611 mg, 6.0 mmol) was added. The Schlenk flask was connected through its side arm to another Schlenk flask (25 mL) containing 1,1-sulfonyldiimidazole (898 mg, 4.5 mmol) and potassium fluoride (702 mg, 12.1 mmol). With stirring, trifluoroacetic acid (3.0 mL) was added. Immediate sulfuryl fluoride gas formation was observed. Both Schlenk flasks were stirred for 16 h. Then the small Schlenk flask was exchanged for another one, containing more 1,1-sulfonyldiimidazole (299 mg, 1.5 mmol) and potassium fluoride (351 mg, 6.0 mmol). With stirring, trifluoroacetic acid (1.0 mL) was added, and both flasks were stirred for 16 h.<sup>[52]</sup> The stoppers were removed to release the residual pressure and the Schlenk flasks were stirred for more 15 min to ensure that all sulfuryl fluoride had evaporated into to the fume hood. The content of the bigger Schlenk flask was transferred to a round bottomed flask, and Celite® (approx. half the volume of a 250 mL flask) was added. After solvent removal at reduced pressure the crude product was purified by column chromatography [3 x 25 cm, SiO<sub>2</sub> (deactivated with Et<sub>3</sub>N), petroleum ether / ethyl acetate 9:1] affording ferrocenyl fluorosulfonate (**118**) as a yellow oil (632 mg, 2.2 mmol, 74%), which solidified upon standing over night (m. p. 38 °C).

<sup>1</sup>H NMR (400.1 MHz, CDCl<sub>3</sub>):  $\delta$  = 4.06 + 4.55 (AA'BB',  $J$  = 2.0 Hz, 2 x 2H, C<sub>Cp</sub>H), 4.34 (Cp') ppm. <sup>13</sup>C NMR (100.6 MHz, CDCl<sub>3</sub>, HSQC, HMBC):  $\delta$  = 60.8 (d, <sup>4</sup>J<sub>C,F</sub> = 0.8 Hz, C<sub>Cp</sub>H), 64.3 (C<sub>Cp</sub>H), 70.4 (Cp'), 119.8 (C<sub>Cp</sub>O) ppm. <sup>19</sup>F NMR (376.5 MHz, CDCl<sub>3</sub>):  $\delta$  = 35.1 (s, OSO<sub>2</sub>F) ppm.

IR:  $\tilde{\nu}$  = 3109 (w), 1456 (s), 1431 (s), 1366 (w), 1234 (s), 1207 (s), 1105 (m), 1020 (m), 1001 (m), 926 (s), 874 (s), 835 (s), 800 (s), 791 (s), 716 (m), 604 (m), 567 (m), 544 (m), 488 (s), 463 (s), 440 (m), 420 (m)  $\text{cm}^{-1}$ . HRMS (EI): Calcd. for  $\text{C}_{10}\text{H}_9\text{FFeO}_3\text{S}$  [ $\text{M}^+$ ] 283.9606, found 283.9605.

#### 6.2.2.15. 2-Hydroxyferrocenesulfonyl fluoride (*rac*-**119**)



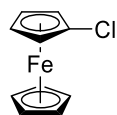
*rac*-**119**

At  $-78\text{ }^\circ\text{C}$  LDA [prepared from butyllithium (2.5 M, 0.26 mL, 0.7 mmol) in hexane and diisopropylamine (0.28 mL, 2.0 mmol)] in THF (3 mL) was added dropwise to ferrocenyl fluorosulfonate (**118**, 187 mg, 0.7 mmol) in THF (5 mL). The initially yellow solution slowly turned orange. The solution was stirred for 40 min at  $-78\text{ }^\circ\text{C}$ , warmed to  $0\text{ }^\circ\text{C}$  and stirred for another 30 min. The orange solution slowly turned red. The solution was acidified by addition of oxygen free 37% aq. HCl under pH control until pH 6. Water (15 mL) and dichloromethane (3 x 20 mL) were added, and the mixture was intensely stirred for 2 min. After phase separation, the organic layers were collected with a syringe and filtered into a Schlenk flask through a P4 frit covered with a 5 cm thick layer of magnesium sulfate. The solvent was removed at reduced pressure, and the remaining yellow oil was redissolved in hexane (3 x 20 mL) and transferred into another Schlenk flask. The solvent was removed at reduced pressure affording 2-hydroxyferrocenesulfonyl fluoride (*rac*-**119**, 171 mg, 0.6 mmol, 91%) as an air sensitive yellow solid (m. p.  $60\text{ }^\circ\text{C}$ , dec.).

$^1\text{H}$  NMR (400.1 MHz,  $\text{CDCl}_3$ ):  $\delta$  = 4.29 (s, 1H,  $\text{C}_{\text{Cp}}\text{H}$ ), 4.42 (s, 5H, Cp'), 4.51 (s, 1H,  $\text{C}_{\text{Cp}}\text{H}$ ), 4.64 (s, 1H,  $\text{C}_{\text{Cp}}\text{H}$ ), 5.06 (br. s, 1H, OH) ppm.  $^{13}\text{C}$  NMR (100.6 MHz,  $\text{CDCl}_3$ , HSQC, HMBC):  $\delta$  = 61.0 ( $\text{C}_{\text{Cp}}\text{H}$ ), 62.4 ( $\text{C}_{\text{Cp}}\text{H}$ ), 63.5 (d,  $^2J_{\text{C-F}}$  = 38.5 Hz,  $\text{C}_{\text{Cp}}\text{S}$ ), 65.6 ( $\text{C}_{\text{Cp}}\text{H}$ ), 72.4 (Cp'), 122.3 ( $\text{C}_{\text{Cp}}\text{O}$ ) ppm.  $^{19}\text{F}$  NMR (376.5,  $\text{CDCl}_3$ ):  $\delta$  = 68.9 (s,  $\text{SO}_2\text{F}$ ) ppm. IR:  $\tilde{\nu}$  = 3505 (m), 3107 (w), 2924 (w), 2853 (w), 1495 (m), 1414 (w), 1383 (s), 1346 (m), 1287 (m), 1219 (m), 1190 (s), 1161 (s), 1109 (m), 1092 (m), 1030 (m), 1007 (m), 908 (w), 829 (m), 802 (m), 748 (s), 683 (m), 646 (s), 613 (s),

544 (s), 486 (s), 473 (s), 419 (m)  $\text{cm}^{-1}$ . HRMS (EI): Calcd. for  $\text{C}_{10}\text{H}_9\text{FFeO}_3\text{S}$  [ $\text{M}^+$ ] 283.9606, found 283.9599.

#### 6.2.2.16. Chloroferrocene (**135**)

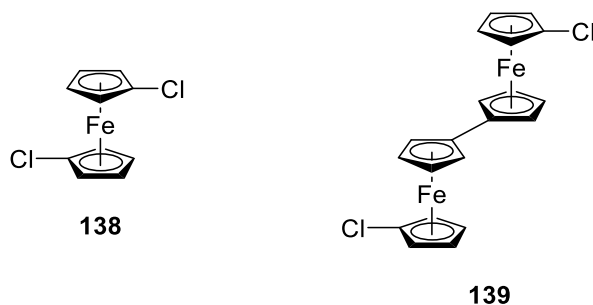


**135**

A schelenk flask was charged with ferrocene (**74**, 200 mg, 1.1 mmol),  $\text{KO}^t\text{Bu}$  (13 mg, 0.1 mmol) and THF (10 mL). The solution was cooled to  $-78\text{ }^\circ\text{C}$  and tert-butyllithium (1.9 M in  $\text{Et}_2\text{O}$ , 1.40 mL, 2.7 mmol) was added dropwise while stirring. After 3 h stirring at  $-78\text{ }^\circ\text{C}$ , trifluoromethane-sulfonyl chloride (0.30 mL, 2.7 mmol) was added dropwise (the orange suspension turned into a translucent brown solution) and it was stirred for 30 min  $-78\text{ }^\circ\text{C}$ . The solution was slowly brought to  $21\text{ }^\circ\text{C}$  and stirred for more 40 min. After addition of water (20 mL) the mixture was extracted with dichloromethane (3 x 20 mL). The collected organic layers were dried with magnesium sulfate, and the solvent was removed under reduced pressure. After purification by column chromatography [3 x 30 cm,  $\text{SiO}_2$  (deactivated with  $\text{Et}_3\text{N}$ ), petroleum ether / ethyl acetate 100:0 gradient to 7:3 (v:v)] chloroferrocene (**135**, 163 mg, 0.7 mmol, 69%) was obtained as an orange crystalline solid, identified by comparison with literature data ( $^1\text{H}$  NMR,  $^{13}\text{C}$  NMR, MS).<sup>[59]</sup>

$^1\text{H}$  NMR (400.1 MHz,  $\text{CDCl}_3$ ):  $\delta = 4.05 + 4.38$  (AA'BB',  $J = 1.9$  Hz, 2 x 2H,  $\text{C}_{\text{Cp}}\text{H}$ ), 4.23 (s, 5H, Cp') ppm.  $^{13}\text{C}$  NMR (100.6 MHz,  $\text{CDCl}_3$ , HSQC, HMBC):  $\delta = 66.1$  ( $\text{C}_{\text{Cp}}\text{H}$ ), 68.0 ( $\text{C}_{\text{Cp}}\text{H}$ ), 70.4 (Cp'), 92.5 ( $\text{C}_{\text{Cp}}\text{Cl}$ ) ppm. HRMS (EI): Calcd. for  $\text{C}_{10}\text{H}_9\text{ClFe}$  [ $\text{M}^+$ ] 219.9742, found 219.9743.

6.2.2.17. 1,1'-Dichloroferrocene (**138**)<sup>[59]</sup> and 1,1'-dichlorobiferrocenyl (**139**)<sup>[60]</sup>



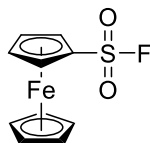
A mixture of ferrocene (**74**, 200 mg, 1.1 mmol), TMEDA (0.40 mL, 312 mg, 2.7 mmol) and n-hexane (20 mL) was cooled to 0 °C. n-Butyllithium [(2.5 M, 1.10 mL, 2.7 mmol) in hexane] was added dropwise while stirring. The suspension was slowly raised to 21 °C and stirred for 16 h. The resulting bright orange suspension was cooled to -78 °C and trifluoromethanesulfonyl chloride (0.30 mL, 2.7 mmol) was added dropwise. The solution was slowly brought to 21 °C and stirred for more 40 min. After addition of water (20 mL) the mixture was extracted with dichloromethane (3 x 20 mL). The collected organic layers were dried with magnesium sulfate, and the solvent was removed under reduced pressure. Column chromatography [3 x 30 cm, SiO<sub>2</sub> (deactivated with Et<sub>3</sub>N), petroleum ether / ethyl acetate 100:0 gradient to 7:3 (v:v)] afforded two products, identified by comparison with literature data (<sup>1</sup>H NMR, <sup>13</sup>C NMR, MS).

I: **138** (175 mg, 0.7 mmol, 64%), orange solid.<sup>[59]</sup> <sup>1</sup>H NMR (400.1 MHz, CDCl<sub>3</sub>): δ = 4.13 (AA'BB', J = 1.8 Hz, 4H, C<sub>Cp</sub>H), 4.41 (AA'BB', J = 1.8 Hz, 4H, C<sub>Cp</sub>H) ppm. <sup>13</sup>C NMR (100.6 MHz, CDCl<sub>3</sub>, HSQC, HMBC): δ = 68.5 (C<sub>Cp</sub>H), 70.1 (C<sub>Cp</sub>H), 93.3 (C<sub>Cp</sub>Cl) ppm. HRMS (EI): Calcd. for C<sub>10</sub>H<sub>8</sub>Cl<sub>2</sub>Fe [M<sup>+</sup>] 253.9352, found 253.9347.

II: **139** (19 mg, 0.04 mmol, 8%), orange solid. <sup>1</sup>H NMR (400.1 MHz, CDCl<sub>3</sub>): δ = 3.89 (AA'BB', J = 1.8 Hz, 4H, C<sub>Cp</sub>H), 4.14 (AA'BB', J = 1.8 Hz, 4H, C<sub>Cp</sub>H), 4.28 (AA'BB', J = 1.8 Hz, 4H, C<sub>Cp</sub>H), 4.41 ppm (AA'BB', J = 1.8 Hz, 4H, C<sub>Cp</sub>H) ppm. <sup>13</sup>C NMR (100.6 MHz, CDCl<sub>3</sub>, HSQC, HMBC): δ = 67.4 (C<sub>Cp</sub>H), 68.7 (C<sub>Cp</sub>H), 69.3 (C<sub>Cp</sub>H), 70.3 (C<sub>Cp</sub>H), 84.7 (C<sub>Cp</sub>-C<sub>Cp</sub>), 92.9 (C<sub>Cp</sub>Cl) ppm. IR:  $\tilde{\nu}$  = 3100 (w), 1655 (w), 1412 (m), 1383 (m), 1352 (m), 1175 (m), 1165 (m), 1111 (m), 1045 (m), 1036 (m), 1022 (m), 1009 (m), 1001 (m), 881 (m), 864 (m), 851 (m), 837 (m), 824 (m), 804 (s), 729 (w), 608 (w), 592 (w), 498 (s), 474 (s) cm<sup>-1</sup>. HRMS (EI): Calcd. for C<sub>20</sub>H<sub>16</sub>Cl<sub>2</sub>Fe<sub>2</sub> [M<sup>+</sup>] 437.9328, found 437.9321.



6.2.2.18. Fluorosulfonylferrocene (**142**)

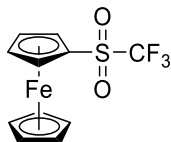


**142**

Ferrocenesulfonyl chloride<sup>[64]</sup> (**141**, 533 mg, 1.8 mmol), anhydrous potassium fluoride (435 mg, 7.5 mmol) and 18-crown-6 (15 mg, 0.06 mmol) in anhydrous acetonitrile (7 mL) were vigorously stirred for 20 h. After addition of water (20 mL) the mixture was extracted with dichloromethane (3 x 20 mL). The collected organic layers were dried with magnesium sulfate, and the solvent was removed under reduced pressure. After purification by column chromatography [3 x 30 cm, SiO<sub>2</sub> (deactivated with Et<sub>3</sub>N), petroleum ether / ethyl acetate 7:3] fluorosulfonylferrocene (**142**, 398 mg, 1.5 mmol, 79%) was obtained as an orange/yellow solid (m. p. 77 °C).

<sup>1</sup>H NMR (400.1 MHz, CDCl<sub>3</sub>):  $\delta$  = 4.44 (s, 5H, Cp'), 4.58 + 4.83 (AA'BB',  $J$  = 2.0 Hz, 2 x 2H, C<sub>Cp</sub>H) ppm. <sup>13</sup>C NMR (100.6 MHz, CDCl<sub>3</sub>, HSQC, HMBC):  $\delta$  = 70.0 (C<sub>Cp</sub>H), 71.7 (Cp'), 72.6 (C<sub>Cp</sub>H), 77.9 (d, <sup>2</sup>J<sub>C-F</sub> = 39.2 Hz, CSO<sub>2</sub>F) ppm. <sup>19</sup>F NMR (376.5 MHz, CDCl<sub>3</sub>):  $\delta$  = 68.2 (s, SO<sub>2</sub>F) ppm. IR:  $\tilde{\nu}$  = 3121 (w), 1396 (s), 1383 (m), 1213 (s), 1161 (s), 1109 (w), 1018 (m), 899 (w), 868 (w), 772 (m), 721 (s), 642 (s), 623 (m), 611 (s), 525 (m), 471 (s), 417 (w) cm<sup>-1</sup>. HRMS (EI): Calcd. for C<sub>10</sub>H<sub>9</sub>FFeO<sub>2</sub>S [M<sup>+</sup>] 267.9657, found 267.9653.

6.2.2.19. (Trifluoromethyl)sulfonylferrocene (**134**)



**134**

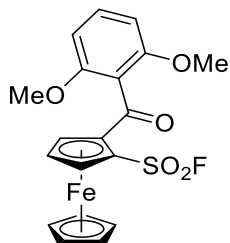
(Trifluoromethyl)trimethylsilane (269 mg, 0.28 mL, 1.9 mmol) in hexane (10 mL) was slowly added dropwise to a mixture of ferrocenylsulfonyl fluoride (**142**, 507 mg, 1.9 mmol) and tris(dimethylamino)sulfonium difluorotrimethylsilicate (TASF, 52 mg, 0.19 mmol) in hexane (25 mL). The mixture was stirred at 21 °C for 17 h and filtered through a patch of silica. This

procedure was repeated two more times with the resulting mixture of **134** and **142** not being separable by chromatography, crystallization, or sublimation. The mixture of **134** and **142** was dissolved in 1,4-dioxane (10 mL). After addition of water (10 mL) and K<sub>3</sub>PO<sub>4</sub> (803 mg, 3.78 mmol), the mixture was stirred at 85 °C (oil bath temperature) for 16 h. The mixture was extracted with petroleum ether (3 x 10 mL). After drying the collected organic layers with magnesium sulfate the solvent was evaporated at reduced pressure. After purification by column chromatography [3 x 20 cm, SiO<sub>2</sub> (deactivated with Et<sub>3</sub>N), petroleum ether / ethyl acetate 85:15] (trifluoromethyl)sulfonylferrocene (**134**, 278 mg, 0.9 mmol, 46%) was obtained as an orange solid (m. p. 69 °C).

<sup>1</sup>H NMR (400.1 MHz, CDCl<sub>3</sub>): δ = 4.51 (s, 5H, Cp'), 4.66 + 4.80 (AA'BB', J = 1.9 Hz, 2 x 2H, C<sub>Cp</sub>H) ppm. <sup>13</sup>C NMR (100.6 MHz, CDCl<sub>3</sub>, HSQC, HMBC): δ = 71.4 (Cp'), 71.7 (d, <sup>4</sup>J<sub>C,F</sub> = 0.5 Hz, C<sub>Cp</sub>H), 73.7 (C<sub>Cp</sub>H), 76.6 (q, <sup>3</sup>J<sub>C,F</sub> = 2.1 Hz, C<sub>Cp</sub>S), 119.40 (q, <sup>1</sup>J<sub>C,F</sub> = 325.2 Hz, CF<sub>3</sub>) ppm. <sup>19</sup>F NMR (376.5 MHz, CDCl<sub>3</sub>): δ = -79.5 (s, SO<sub>2</sub>CF<sub>3</sub>) ppm. IR:  $\tilde{\nu}$  = 3121 (w), 1414 (w), 1350 (s), 1211 (s), 1192 (s), 1175 (s), 1103 (s), 1061 (w), 1034 (m), 1018 (m), 899 (w), 826 (s), 760 (m), 642 (m), 621 (s), 554 (m), 532 (w), 480 (s), 434 (s) cm<sup>-1</sup>. HRMS (EI): Calcd. for C<sub>11</sub>H<sub>9</sub>F<sub>3</sub>FeO<sub>2</sub>S [M<sup>+</sup>] 317.9625, found 317.9625.

Crystal structure analysis: Single crystals suitable for X-ray crystallographic analysis were obtained by crystallization from hexane at -30 °C over 7 d. C<sub>11</sub>H<sub>9</sub>F<sub>3</sub>FeO<sub>2</sub>S, prismatic orange crystal, M<sub>r</sub> = 318.09 g.mol<sup>-1</sup>, crystal system monoclinic, space group P 1 2<sub>1</sub>/n 1, a = 9.8033(13) Å, b = 9.2232(14) Å, c = 13.541 (2) Å, α = 90°, β = 102.494(5)°, γ = 90°. V = 1195.4(3) Å<sup>3</sup>, Z = 4, d<sub>calc</sub> = 1.768 g.cm<sup>-3</sup>, μ = 1.464 mm<sup>-1</sup>, crystal size 0.43x0.29x0.28 mm<sup>3</sup>, F(000) = 640, Bruker SMART X2S diffractometer, graphite crystal monochromator, T = 200 K, Mo-Kα radiation (λ = 0.71073 Å), 2.69 ≤ θ ≤ 27.54°, index ranges -12 ≤ h ≤ 12, -11 ≤ k ≤ 11, -17 ≤ l ≤ 17, reflections collected/unique 2754/2003, numerical absorption correction, structure solution and refinement with SHELXL-2018/3,<sup>[150]</sup> parameters/restraints 163/0, R<sub>1</sub> = 0.0523 [I > 2σ(I)], wR<sub>2</sub> = 0.1062 (all data), S = 1.060, final maximum/minimum difference electron density 0.424/-0.458 eÅ<sup>-3</sup>.

6.2.2.20. *rac*-2-(2,6-Dimethoxybenzoyl)ferrocenesulfonyl fluoride (*rac*-**150**)

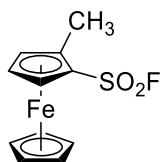


*rac*-**150**

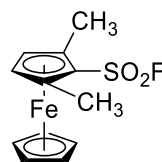
At  $-78\text{ }^{\circ}\text{C}$  LiTMP [prepared from butyllithium in hexane (2.5 M, 0.52 mL, 1.3 mmol) and 2,2,6,6-tetramethylpiperidine (0.24 mL, 201 mg, 1.4 mmol)] in THF (3 mL) was added dropwise to a solution of ferrocenesulfonyl fluoride (**142**, 318 mg, 1.2 mmol) in THF (7 mL). The initial yellow colour changed immediately to orange/red. After stirring for 1 h at  $-78\text{ }^{\circ}\text{C}$ , 2,6-dimethoxybenzoyl chloride (286 mg, 1.42 mmol) was added at  $-78\text{ }^{\circ}\text{C}$ , and the solution was stirred for 15 min before it was slowly warmed to  $22\text{ }^{\circ}\text{C}$  followed by stirring for 30 min. After addition of water (10 mL), dichloromethane (3 x 10 mL) was added, and the mixture was intensely stirred for 2 min. After phase separation, the organic layers were collected with a syringe and filtered through a P4 frit covered with a 5 cm thick layer of magnesium sulfate into a Schlenk flask. The solvent was removed at reduced pressure. After purification by column chromatography (30 x 3 cm, SiO<sub>2</sub> (deactivated with Et<sub>3</sub>N), petroleum ether / ethyl acetate 6:4) *rac*-2-(2,6-dimethoxybenzoyl)ferrocenesulfonyl fluoride (*rac*-**150**, 82 mg, 0.2 mmol, 16%) was obtained as an orange solid (m. p.  $90\text{ }^{\circ}\text{C}$ , dec.).

<sup>1</sup>H NMR (400.1 MHz, CDCl<sub>3</sub>):  $\delta$  = 3.78 (s, 6H, OCH<sub>3</sub>), 4.52 (s, 5H, Cp'), 4.71, (t, <sup>3</sup>J = 2.8 Hz, 1H, C<sub>Cp</sub>H), 4.92 (m, 1H, C<sub>Cp</sub>H), 5.18 (m, 1H, C<sub>Cp</sub>H), 6.60 (d, <sup>3</sup>J = 8.4 Hz, 2H, C<sub>Ar</sub>H), 7.34 (t, <sup>3</sup>J = 8.4 Hz, 1H, C<sub>Ar</sub>H) ppm. <sup>13</sup>C NMR (100.6 MHz, CDCl<sub>3</sub>, HSQC, HMBC):  $\delta$  = 55.9 (OMe), 72.6 (C<sub>Cp</sub>H), 73.6 (Cp'), 76.6 (d, <sup>3</sup>J<sub>C,F</sub> = 0.9 Hz, C<sub>Cp</sub>H), 78.2 (d, <sup>4</sup>J<sub>C,F</sub> = 1.3 Hz, C<sub>Cp</sub>H), 78.9 (d, <sup>2</sup>J<sub>C,F</sub> = 37.1 Hz, CSO<sub>2</sub>F), 81.9 (C<sub>Cp</sub>C), 104.2 (C<sub>Ar</sub>H), 118.8 (C<sub>Ar</sub>CO), 131.5 (C<sub>Ar</sub>H), 157.6 (C<sub>Ar</sub>O), 194.9 (C=O) ppm. <sup>19</sup>F NMR (376.5 MHz, CDCl<sub>3</sub>):  $\delta$  = 65.8 (s, SO<sub>2</sub>F) ppm. IR:  $\tilde{\nu}$  = 3123 (w), 3013 (w), 2926 (w), 2845 (w), 1661 (s), 1595 (s), 1472 (s), 1443 (s), 1391 (s), 1373 (m), 1341 (m), 1285 (m), 1246 (s), 1206 (s), 1105 (s), 1049 (m), 1030 (m), 1016 (m), 1005 (m), 907, (w), 876 (m), 837 (m), 827 (m), 779 (s), 752 (s), 741 (s), 718 (s), 650 (m), 629 (s), 604 (m), 571 (m), 532 (m), 507 (m), 463 (s), 420 (m) cm<sup>-1</sup>. HRMS (ESI, MeCN): Calcd. for C<sub>19</sub>H<sub>17</sub>FFeO<sub>5</sub>SNa [M<sup>+</sup>Na] 455.0028, found 455.0037.

6.2.2.21. *rac*-2-Methylferrocenesulfonyl fluoride (*rac*-**151**) and 2,5-dimethylferrocenesulfonyl fluoride (**152**)



*rac*-**151**



**152**

At  $-78\text{ }^{\circ}\text{C}$  LiTMP [prepared from butyllithium in hexane (2.5 M, 1.04 mL, 2.6 mmol) and 2,2,6,6-tetramethylpiperidine (0.47 mL, 391 mg, 2.8 mmol)] in THF (3 mL) was added dropwise to ferrocenesulfonyl fluoride (**142**, 232 mg, 0.9 mmol) in THF (5 mL). The yellow colour changed immediately to red. After stirring at  $-78\text{ }^{\circ}\text{C}$  for 2 h iodomethane (2.0 M solution in *tert*-butyl methyl ether, 1.38 mL, 2.8 mmol) was added, and the solution was slowly warmed to  $21\text{ }^{\circ}\text{C}$  and stirred for another 1 h. After addition of water (10 mL) the solution was extracted with ethyl acetate (3 x 10 mL). After drying the collected organic layers with magnesium sulfate the solvent was removed at reduced pressure. Column chromatography [MPLC, Büchi, 20 x 3 cm, SiO<sub>2</sub>, petroleum ether / ethyl acetate 100:0 gradient to 45:55 (v:v) in 60 min, flow: 20 mL/min] afforded two products.

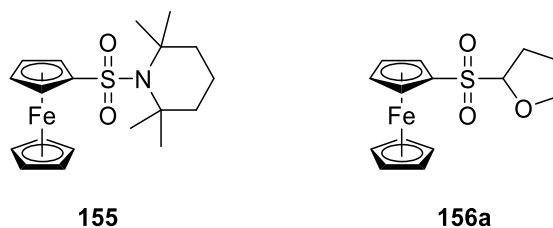
I: **152** (24 mg, 0.08 mmol, 9%), yellow solid (m.p.  $133\text{-}134\text{ }^{\circ}\text{C}$ ). <sup>1</sup>H NMR (400.1 MHz, CDCl<sub>3</sub>):  $\delta$  = 2.21 (s, 6H, CH<sub>3</sub>), 4.27 (s, 5H, Cp'), 4.34 (s, 2H, C<sub>Cp</sub>H) ppm. <sup>13</sup>C NMR (100.6 MHz, CDCl<sub>3</sub>, HSQC, HMBC):  $\delta$  = 13.8 (CH<sub>3</sub>), 72.0 (C<sub>Cp</sub>H), 72.6 (Cp'), 76.5 (d, <sup>2</sup>J<sub>C,F</sub> = 36.8 Hz, CSO<sub>2</sub>F), 86.7 (C<sub>Cp</sub>CH<sub>3</sub>) ppm. <sup>19</sup>F NMR (376.5 MHz, CDCl<sub>3</sub>):  $\delta$  = 70.4 (s, SO<sub>2</sub>F) ppm. IR:  $\tilde{\nu}$  = 2997 (w), 2967 (w), 2853 (w), 1452 (m), 1414 (w), 1393 (s), 1375 (s), 1341 (m), 1196 (s), 1107 (m), 1088 (m), 1042 (m), 1003 (m), 966 (w), 856 (w), 839 (m), 827 (m), 737 (s), 654 (s), 629 (m), 557 (s), 525 (m), 486 (s), 471 (s) cm<sup>-1</sup>. HRMS (EI): Calcd. for C<sub>12</sub>H<sub>13</sub>FFeO<sub>2</sub>S [M<sup>+</sup>] 295.9970, found 295.9972.

II: *rac*-**151** (175 mg, 0.6 mmol, 72%), yellow solid (m. p.  $71\text{ }^{\circ}\text{C}$ ). <sup>1</sup>H NMR (400.1 MHz, C<sub>6</sub>D<sub>6</sub>):  $\delta$  = 1.98 (s, 3H, CH<sub>3</sub>), 3.71 (ABX, *J* = 2.6 Hz, 1H, C<sub>Cp</sub>H), 3.78 (ABX, 1H, C<sub>Cp</sub>H), 3.96 (s, 5H, Cp'), 4.51 (ABX, *J* = 2.7, 1.6 Hz) ppm. <sup>13</sup>C NMR (100.6 MHz, C<sub>6</sub>D<sub>6</sub>):  $\delta$  = 12.9 (CH<sub>3</sub>), 69.8 (C<sub>Cp</sub>H), 70.5 (C<sub>Cp</sub>H), 72.1 (Cp'), 74.3 (C<sub>Cp</sub>H), 77.6 (d, <sup>2</sup>J<sub>C,F</sub> = 39.0 Hz, CSO<sub>2</sub>F), 85.8 (C<sub>Cp</sub>CH<sub>3</sub>) ppm. <sup>19</sup>F NMR (376.5 MHz, C<sub>6</sub>D<sub>6</sub>):  $\delta$  = 69.0 (s, SO<sub>2</sub>F) ppm. IR:  $\tilde{\nu}$  = 3125 (w), 2965 (w), 2924 (w), 1452 (w), 1393 (s), 1371 (m), 1337 (w), 1244 (m), 1200 (s), 1171 (w), 1107 (w), 1090 (w), 1034 (w),



II: *rac*-**153** (75 mg, 0.2 mmol, 51%), yellow oil.  $^1\text{H}$  NMR (600.3 MHz,  $\text{CDCl}_3$ ):  $\delta$  = 2.18 (s, 3H,  $\text{CH}_3$ ), 4.43 (s, 5H, Cp'), 4.52 (ABX,  $J$  = 2.6 Hz, 1H,  $\text{C}_{\text{Cp}}\text{H}$ ), 4.55 (ABX, 1H,  $\text{C}_{\text{Cp}}\text{H}$ ), 4.71 (ABX,  $J$  = 2.6, 1.6 Hz, 1H,  $\text{C}_{\text{Cp}}\text{H}$ ) ppm.  $^{13}\text{C}$  NMR (150.9 MHz,  $\text{CDCl}_3$ , HSQC, HMBC):  $\delta$  = 12.9 ( $\text{CH}_3$ ), 71.2 ( $\text{C}_{\text{Cp}}\text{H}$ ), 71.9 (Cp'), 72.3 ( $\text{C}_{\text{Cp}}\text{H}$ ), 75.0 (q,  $^3J$  = 2.0 Hz,  $\text{C}_{\text{Cp}}\text{S}$ ), 75.6 ( $\text{C}_{\text{Cp}}\text{H}$ ), 87.9 ( $\text{C}_{\text{Cp}}\text{CH}_3$ ), 119.64 (q,  $^1J_{\text{C,F}}$  = 325.3 Hz,  $\text{CF}_3$ ) ppm.  $^{19}\text{F}$  NMR (376.5,  $\text{CDCl}_3$ ):  $\delta$  = -79.7 (s,  $\text{SO}_2\text{CF}_3$ ) ppm. IR:  $\tilde{\nu}$  = 3102 (w), 2928 (w), 1450 (w), 1377 (w), 1352 (s), 1242 (s), 1211 (s), 1126 (s), 1109 (m), 1082 (s), 1036 (m), 1018 (m), 1005 (m), 964 (w), 829 (m), 812 (m), 760 (m), 664 (m), 644 (m), 613 (s), 557 (s), 534 (w), 484 (s), 444 (m)  $\text{cm}^{-1}$ . HRMS (EI): Calcd. for  $\text{C}_{12}\text{H}_{11}\text{F}_3\text{FeO}_2\text{S}$  [ $\text{M}^+$ ] 331.9781, found 331.9770.

#### 6.2.2.23. 2,2,6,6-Tetramethyl-1-(ferrocenylsulfonyl)piperidine (**155**) and **156a**



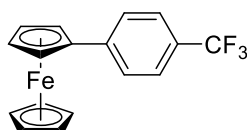
At  $-78\text{ }^\circ\text{C}$  LiTMP [prepared from butyllithium in hexane (2.5 M, 0.61 mL, 1.5 mmol) and 2,2,6,6-tetramethylpiperidine (0.30 mL, 252 mg, 1.8 mmol)] in THF (4 mL) was added dropwise to chlorosulfonylferrocene (**141**, 363 mg, 1.3 mmol) in THF (8 mL). The orange/brown solution changed very quickly and shortly to green upon addition of LiTMP and then changed to yellow. The solution was stirred at  $-78\text{ }^\circ\text{C}$  for 1 h. A small piece of dry ice was added to the solution at  $-78\text{ }^\circ\text{C}$  and it was slowly warmed to  $21\text{ }^\circ\text{C}$ . The mixture was stirred for 1 h. After addition of water (20 mL) the solution was extracted with ethyl acetate (3 x 30 mL). After drying the collected organic layers with magnesium sulfate, the solvent was removed at reduced pressure. Column chromatography [MPLC, Büchi, 20 x 3 cm,  $\text{SiO}_2$ , petroleum ether / ethyl acetate 100:0 gradient to 0:100 (v:v) in 40 min, flow: 30 mL/min] afforded two fractions.

I: **155** (452 mg, 1.2 mmol, 91%), yellow solid (m. p.  $139\text{ }^\circ\text{C}$ ).  $^1\text{H}$  NMR (400.1 MHz,  $\text{CDCl}_3$ ):  $\delta$  = 1.47 (m, 4H,  $\text{NCCH}_2$ ), 1.53 (m, 2H,  $\text{NCCH}_2\text{CH}_2$ ), 1.59 (s, 12H,  $\text{CH}_3$ ), 4.28 + 4.67 (AA'BB',  $J$  = 1.9 Hz, 2x2H,  $\text{C}_{\text{Cp}}\text{H}$ ), 4.36 (s, 5H, Cp') ppm.  $^{13}\text{C}$  NMR (100.6 MHz,  $\text{CDCl}_3$ ):  $\delta$  = 16.7 ( $\text{NCCH}_2$ ), 31.2 ( $\text{CH}_3$ ), 44.5 ( $\text{NCCH}_2\text{CH}_2$ ), 60.5 (NC), 69.2 ( $\text{C}_{\text{Cp}}\text{H}$ ), 69.2 ( $\text{C}_{\text{Cp}}\text{H}$ ), 71.0 (Cp'), 96.3 ( $\text{C}_{\text{Cp}}\text{S}$ ) ppm. IR:  $\tilde{\nu}$  = 3013 (w), 2970 (w), 2940 (w), 2866 (w), 1466 (w), 1443 (w), 1410 (w), 1387 (w), 1360 (w),

1321 (s), 1240 (m), 1184 (m), 1126 (s), 1105 (m), 1092 (w), 988 (m), 970 (m), 912 (s), 889 (m), 847 (w), 826(m), 816 (m), 777 (m), 652 (s), 627 (s), 573 (m), 505 (m), 490 (m), 473 (s), 442 (m)  $\text{cm}^{-1}$ . HRMS (ESI, MeCN): Calcd. for  $\text{C}_{19}\text{H}_{27}\text{FeNO}_2\text{SNa}$  [ $\text{M}^+\text{Na}$ ] 412.1010, found 412.1007.

II: **156a** (17 mg, 0.05 mmol, 4%), yellow solid (m. p. 60 °C).  $^1\text{H}$  NMR (500.1 MHz,  $\text{CDCl}_3$ ):  $\delta$  = 1.90 (m, 1H,  $\text{CH}_2$ ), 2.05 (m, 1H,  $\text{CH}_2$ ), 2.24 (m, 1H,  $\text{CH}_2$ ), 2.54 (m, 1H,  $\text{CH}_2$ ), 3.95 (m, 1H, O- $\text{CH}_2$ ), 4.03 (m, 1H, O- $\text{CH}_2$ ), 4.45 (s, 5H, Cp'), 4.46 (m, 1H,  $\text{C}_{\text{Cp}}\text{H}$ ), 4.48 (m, 1H,  $\text{C}_{\text{Cp}}\text{H}$ ), 4.64 (m, 1H,  $\text{C}_{\text{Cp}}\text{H}$ ), 4.71 (m, 1H,  $\text{C}_{\text{Cp}}\text{H}$ ), 4.76 (dd,  $J$  = 8.2 Hz,  $J$  = 3.9 Hz, 1H, OCHS) ppm.  $^{13}\text{C}$  NMR (125.8 MHz,  $\text{CDCl}_3$ ):  $\delta$  = 25.1 ( $\text{CH}_2$ ), 26.4 ( $\text{CH}_2$ ), 70.16 ( $\text{C}_{\text{Cp}}\text{H}$ ), 70.7 (Cp'), 71.0 (O- $\text{CH}_2$ ), 71.2( $\text{C}_{\text{Cp}}\text{H}$ ), 71.5 ( $\text{C}_{\text{Cp}}\text{H}$ ), 71.7 ( $\text{C}_{\text{Cp}}\text{H}$ ), 84.1 ( $\text{C}_{\text{Cp}}\text{S}$ ), 94.2 (OCHS) ppm. IR:  $\tilde{\nu}$  = 3111 (w), 2986 (w), 2882 (w), 1447 (w), 1410 (w), 1364 (w), 1290 (s), 1231 (w), 1186 (m), 1123 (m), 1107 (w), 1088 (w), 1061 (s), 1028 (m), 1020 (m), 1005 (w), 951 (w), 923 (w), 901 (w), 883 (w), 851 (w), 822 (s), 768 (m), 712 (w), 677 (m), 646 (m), 592 (w), 552 (m), 511 (m), 482 (s), 467 (s), 447 (s)  $\text{cm}^{-1}$ . HRMS (ESI, MeCN): Calcd. for  $\text{C}_{28}\text{H}_{32}\text{Fe}_2\text{O}_6\text{S}_2$  (**156a**) [ $\text{M}^+$ ] 320.0170, found 320.0175. (**32b**) [ $\text{M}^+\text{Na}$ ] 663.0237, found 663.0235.

#### 6.2.2.24. [4-(Trifluoromethyl)phenyl]ferrocene (**145**)<sup>[151]</sup>

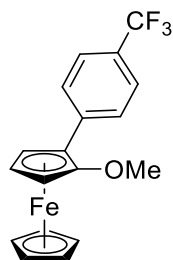


**145**

Trifluoromethylsulfonyl ferrocene (**134**) (203 mg, 0.6 mmol), 4-(trifluoromethyl)phenylboronic acid (**128**, 182 mg, 1.0 mmol),  $\text{K}_3\text{PO}_4$  (408 mg, 1.9 mmol), palladium(II) acetylacetonate ( $\text{Pd}(\text{acac})_2$ ) (9 mg, 0.03 mmol) and 2-dicyclohexylphosphino-2',6'-diisopropoxybiphenyl ( $\text{RuPhos}$ ) (61 mg, 0.1 mmol) were suspended in 1,4-dioxane (2 mL). Dimethyl sulfoxide (0.03 mL) was added, and the mixture was stirred for 48 h at 80 °C. After addition of water (10 mL) the mixture was extracted with dichloromethane (8 x 10 mL). After drying the collected organic layers with magnesium sulfate, the solvent was removed at reduced pressure. After purification by column chromatography (30 x 3 cm,  $\text{SiO}_2$ , petroleum ether / ethyl acetate 9:1) 4-(trifluoromethyl)phenyl ferrocene (**145**, 15 mg, 0.05 mmol, 7%) was obtained as a red solid. (m. p. 140 °C).

$^1\text{H}$  NMR (400.1 MHz,  $\text{CDCl}_3$ ):  $\delta$  = 4.05 (s, 5H, Cp'), 4.38 + 4.69 (AA'BB',  $J$  = 1.5 Hz, 2 x 2H,  $\text{C}_{\text{Cp}}\text{H}$ ), 7.54 (AA'BB',  $J$  = 13.8 Hz,  $J$  = 8.6 Hz, 4H,  $\text{C}_{\text{Ph}}\text{H}$ ) ppm.  $^{13}\text{C}$  NMR (100.6 MHz,  $\text{CDCl}_3$ , HSQC, HMBC):  $\delta$  = 67.0 ( $\text{C}_{\text{Cp}}\text{H}$ ), 69.8 ( $\text{C}_{\text{Cp}}\text{H}$ ), 69.9 (Cp'), 83.4 ( $\text{C}_{\text{Cp}}\text{-C}_{\text{Ph}}$ ), 124.6 (q,  $^1J$  = 271.6 Hz,  $\text{CF}_3$ ), 125.4 (q,  $^3J$  = 3.9 Hz,  $\text{C}_{\text{Ph}}\text{H}$ ), 126.1 ( $\text{C}_{\text{Ph}}\text{H}$ ), 127.8 (q,  $^2J$  = 32.3 Hz,  $\text{C}_{\text{Ph}}\text{CF}_3$ ), 143.9 (d,  $^5J$  = 1.4 Hz,  $\text{C}_{\text{Ph}}\text{-C}_{\text{Cp}}$ ) ppm.  $^{19}\text{F}$  NMR (376.5,  $\text{CDCl}_3$ ):  $\delta$  = -62.4 (s,  $\text{CF}_3$ ) ppm. IR:  $\tilde{\nu}$  = 1614 (m), 1518 (w), 1531 (w), 1420 (m), 1391 (w), 1325 (s), 1283 (m), 1192 (m), 1157 (m), 1105 (s), 1090 (s), 1063 (s), 1038 (m), 1015 (m), 1001 (m), 957 (w), 889 (m), 856 (m), 841 (s), 812 (s), 687 (m), 644 (m), 592 (m), 501 (s), 480 (m), 447 (s)  $\text{cm}^{-1}$ . HRMS (EI): Calcd. for  $\text{C}_{17}\text{H}_{13}\text{F}_3\text{Fe}$  [ $\text{M}^+$ ] 330.0319, found 330.0319.

#### 6.2.2.25. *rac*-2-Methoxy-1-[4-(trifluoromethyl)phenyl]ferrocene (*rac*-**132**)



**132**

#### Method 1:

2-Methoxy-1-(trifluoromethylsulfonyl) ferrocene<sup>[17]</sup> (**83**) (75 mg, 0.2 mmol), 4-(trifluoromethyl)phenylboronic acid (**128**, 60 mg, 0.3 mmol),  $\text{K}_3\text{PO}_4$  (136 mg, 0.6 mmol), palladium(II) acetylacetonate ( $\text{Pd}(\text{acac})_2$ ) (3 mg, 0.01 mmol) and 2-dicyclohexylphosphino-2',6'-diisopropoxybiphenyl (RuPhos) (19 mg, 0.04 mmol) were suspended in 1,4-dioxane (2 mL). Dimethyl sulfoxide (0.01 mL) was added, and the mixture was stirred for 72 h at 95 °C. The reaction mixture was filtered over Celite® and rinsed with dichloromethane (20 mL). After removing the solvent at reduced pressure, the crude was purified by column chromatography (30 x 3 cm,  $\text{SiO}_2$ , petroleum ether / ethyl acetate 10:1) and 2-methoxy-1-(4-(trifluoromethyl)phenyl) ferrocene (*rac*-**132**, 2 mg, 0.01 mmol, 3%) was obtained as an orange-red solid (m. p. 76 °C).

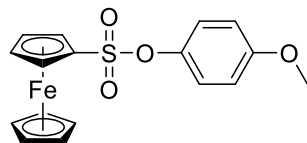


## Method 2:

2-Methoxy-1-(trifluoromethylsulfonyl) ferrocene (**83**) (104 mg, 0.3 mmol), 4-(trifluoromethyl)phenylboronic acid (**128**, 81 mg, 0.4 mmol),  $K_3PO_4$  (196 mg, 0.9 mmol), palladium(II) acetylacetonate ( $Pd(acac)_2$ ) (5 mg, 0.02 mmol) and 1,1'-bis(diphenylphosphino)ferrocene (dppf) (31 mg, 0.06 mmol) were suspended in 1,4-dioxane (1 mL). Dimethyl sulfoxide (0.01 mL) was added, and the mixture was stirred for 72 h at 95 °C. The reaction mixture was filtered over Celite® and rinsed with dichloromethane (20 mL). After removing the solvent at reduced pressure, the crude was purified by column chromatography [30 x 3 cm,  $SiO_2$ , petroleum ether / ethyl acetate gradient 100:0 to 5:5 (v:v)] and 2-methoxy-1-(4-(trifluoromethyl)phenyl)ferrocene (*rac*-**37**, 4 mg, 0.01 mmol, 4%) was obtained as an orange-red solid (m. p. 76 °C).

$^1H$  NMR (400.1 MHz,  $CDCl_3$ ):  $\delta$  = 3.79 (s, 3H,  $OCH_3$ ), 4.02 (ABC,  $J$  = 2.7 Hz, 1H,  $C_{Cp}H$ ), 4.26 (ABC,  $J$  = 2.5 Hz,  $J$  = 1.7 Hz 1H,  $C_{Cp}H$ ), 4.36 (ABC,  $J$  = 2.5 Hz,  $J$  = 1.7 Hz 1H,  $C_{Cp}H$ ), 7.54 (d,  $J$  = 8.2 Hz, 2H,  $C_{Cp}H$ ), 7.81 (d,  $J$  = 8.2 Hz, 2H,  $C_{Cp}H$ ) ppm.  $^{13}C$  NMR (100.6 MHz,  $CDCl_3$ , HSQC, HMBC):  $\delta$  = 54.2 ( $C_{Cp}H$ ), 58.0 ( $OCH_3$ ), 61.5 ( $C_{Cp}H$ ), 62.7 ( $C_{Cp}H$ ), 70.2 ( $Cp'$ ), 72.5 ( $C_{Cp}C$ ), 124.7 (q,  $^1J$  = 271.6 Hz,  $CF_3$ ), 125.1 7 (q,  $^3J$  = 3.8 Hz,  $C_{Ph}H$ ), 125.7 ( $C_{Cp}O$ ), 127.5 ( $C_{Ph}H$ ), 127.6 (q,  $^2J$  = 32.2 Hz,  $C_{Ph}CF_3$ ), 142.8 (q,  $^5J$  = 1.3 Hz,  $C_{Ph}C_{Cp}$ ) ppm.  $^{19}F$  NMR (376.5,  $CDCl_3$ ):  $\delta$  = -62.4 (s,  $CF_3$ ) ppm. IR:  $\tilde{\nu}$  = 3092 (w), 2934 (w), 2860 (w), 1713 (w), 1614 (m), 1572 (w), 1531 (w), 1481 (m), 1452 (w), 1423 (w), 1406 (m), 1321 (s), 1300 (m), 1227 (m), 1161 (m), 1117 (s), 1103 (s), 1069 (s), 1047 (m), 1016 (m), 1001 (m), 953 (w), 845 (m), 818 (m), 799 (m), 775 (w), 700 (m), 642 (m), 604 (m), 525 (m), 496 (m), 465 (m), 442 (m)  $cm^{-1}$ . HRMS (EI): Calcd. for  $C_{18}H_{15}F_3FeO$  [ $M^+$ ] 360.0424, found 360.0422.

6.2.2.26. 4-(Methoxybenzenesulfonate) ferrocene (**148**)

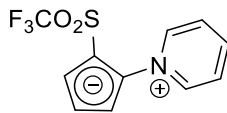


**148**

A solution of 4-methoxyphenol (**149**, 186 mg, 1.5 mmol) in THF (4 mL) was added to a suspension of NaH [60% dispersion in paraffin, 55 mg, 1.4 mmol, washed with hexane (3 x 5 mL)] in THF (1 mL) at 0 °C. The suspension was brought to 25 °C and stirred for 30 min. A solution of ferrocenylsulfonyl chloride (**141**, 328 mg, 1.2 mmol) in THF (10 mL) was added and the suspension was stirred at 25 °C for 72 h. The mixture was cooled to 0 °C and quenched with 30 mL of water. The mixture was extracted with ethyl acetate (3 x 30 mL). After drying the collected organic layers with magnesium sulfate, the solvent was removed at reduced pressure. After purification by column chromatography [30 x 3 cm, SiO<sub>2</sub>, petroleum ether / ethyl acetate gradient 9:1 to 8:2 (v:v)] 4-(methoxybenzenesulfonate)ferrocene (**148**, 309 mg, 0.8 mmol, 72%) was obtained as an orange crystalline solid.

<sup>1</sup>H NMR (400.1 MHz, CDCl<sub>3</sub>): 3.76 (OCH<sub>3</sub>), 4.40 (s, 5H, Cp'), 4.43 + 4.57 (AA'BB', *J* = 2.0 Hz, 2 x 2H, C<sub>Cp</sub>H), 6.76 + 6.90 (AA'BB', *J* = 9.2 Hz, *J* = 6.0 Hz) ppm. <sup>13</sup>C NMR (100.6 MHz, CDCl<sub>3</sub>, HSQC, HMBC):  $\delta$  = 55.7 (OCH<sub>3</sub>), 70.0 (C<sub>Cp</sub>H), 71.2 (Cp'), 71.5 (C<sub>Cp</sub>H), 81.5 (C<sub>Cp</sub>S), 114.4 (C<sub>Ph</sub>H), 123.6 (C<sub>Ph</sub>H), 143.4 (C<sub>Ph</sub>O), 158.2 (C<sub>Ph</sub>OCH<sub>3</sub>) ppm. IR:  $\tilde{\nu}$  = 3109 (w), 3098 (w), 3017 (w), 2968 (w), 2932 (w), 2841 (w), 1595 (w), 1499 (m), 1456 (w), 1441 (m), 1414 (m), 1396 (w), 1364 (s), 1300 (w), 1250 (m), 1207 (m), 1182 (m), 1159 (m), 1138 (w), 1105 (m), 1061 (w), 1028 (m), 1022 (m), 1005 (m), 930 (w), 897 (w), 856 (m), 833 (s), 822 (s), 785 (s), 729 (m), 692 (s), 648 (m), 637 (s), 606 (m), 569 (m), 532 (w), 521 (s), 500 (s), 486 (s), 469 (s), 434 (w), 426 (w) cm<sup>-1</sup>. HRMS (EI): Calcd. for C<sub>17</sub>H<sub>16</sub>FeO<sub>4</sub>S [M<sup>+</sup>] 372.0119, found 372.0120.

6.2.2.27. 1-Trifluoromethanesulfonyl-2-pyridinium-cyclopentadienylide (**171**)

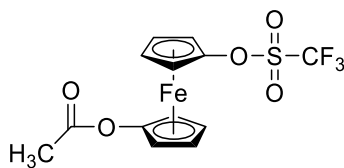


**171**

To a solution of 2-(trifluoronethylsulfonyl) ferrocenyl triflate<sup>[17]</sup> (**84**, 78 mg, 0.2 mmol) and (*R*)-(-)- $\alpha$ -methoxy-(trifluoromethyl)phenylacetate (*R*)-(-) Mosher's acid chloride) (29 mg, 0.1 mmol) in dichloromethane (4 mL), was added pyridine (30  $\mu$ L, 28 mg, 0.4 mmol) at 22 °C. The solution was stirred for 7 days at 22 °C. After addition of water (4 mL) the mixture was extracted with dichloromethane (3 x 10 mL). The collected organic layers were dried with magnesium sulfate, and the solvent removed at reduced pressure. After purification by column chromatography [3 x 20 cm, SiO<sub>2</sub>, ethyl acetate] 1-trifluoromethanesulfonyl-2-pyridinium-cyclopentadienylide (**171**, 7 mg, 0.03 mmol, 22%) was obtained as a yellow solid (m. p. 135 °C, dec).

<sup>1</sup>H NMR (400.1 MHz, CDCl<sub>3</sub>): 6.18 (dd, *J* = 4.5 Hz, *J* = 3.5 Hz, 1H, C<sub>Cp</sub>H), 6.37 (dd, *J* = 3.5 Hz, *J* = 2.4 Hz, 1H, C<sub>Cp</sub>H), 6.79 (dd, *J* = 4.5 Hz, *J* = 2.4 Hz, 1H, C<sub>Cp</sub>H), 7.86 (AA'BB'C, *J* = 7.2 Hz, 2H, Py), 8.27 (AA'BB'C, *J* = 11.7 Hz, *J* = 1.3 Hz, 1H, Py), 8.78 (AA'BB'C, 2H, Py) ppm. <sup>13</sup>C NMR (100.6 MHz, CDCl<sub>3</sub>, HSQC, HMBC):  $\delta$  = 94.7 (C<sub>Cp</sub>S), 111.5 (C<sub>Cp</sub>H), 113.1 (C<sub>Cp</sub>H), 119.8 (C<sub>Cp</sub>H), 121.0 (q, <sup>1</sup>*J*<sub>C,F</sub> = 326.3 Hz, CF<sub>3</sub>), 126.0 (C<sub>Py</sub>H), 126.9 (C<sub>Cp</sub>N), 141.9 (C<sub>Py</sub>H), 145.6 (C<sub>Py</sub>H) ppm. <sup>19</sup>F NMR (376.5, CDCl<sub>3</sub>):  $\delta$  = -80.6 (s, CF<sub>3</sub>) ppm. IR:  $\tilde{\nu}$  = 3117 (w), 3090 (w), 2959 (w), 2922 (w), 2851 (w), 1622 (m), 1468 (m), 1427 (m), 1389 (m), 1362 (m), 1327 (s), 1283 (m), 1260 (m), 1206 (s), 1173 (s), 1155 (s), 1059 (m), 1043 (s), 1024 (m), 955 (m), 874 (w), 860 (w), 847 (w), 779 (s), 756 (m), 718 (s), 679 (s), 652 (w), 625 (s), 600 (s), 573 (s), 521 (s), 457 (m) cm<sup>-1</sup>. HRMS (ESI, MeOH): Calcd. for C<sub>11</sub>H<sub>8</sub>F<sub>3</sub>NO<sub>2</sub>S [M<sup>+</sup>H] 276.0306, found 276.0307.

6.2.2.28. 1-Trifluoromethanesulfonate-1'-acetoxyferrocene (**181**)

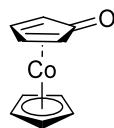


**181**

At  $-78\text{ }^{\circ}\text{C}$  a solution of methyllithium in hexane (1.6 M, 2.3 mL, 6.2 mmol) was added to 1,1'-diferrocenediyl diacetate<sup>[29]</sup> (**78**, 500 mg, 1.7 mmol) in diethyl ether (40 mL) with stirring. The reaction mixture was slowly brought to  $0\text{ }^{\circ}\text{C}$  and further stirred for 45 min. The mixture was cooled to  $-78\text{ }^{\circ}\text{C}$  and trifluoromethanesulfonic anhydride (0.6 mL, 1028 mg, 3.6 mmol) was added dropwise. The reaction was stirred for 30 min at  $-78\text{ }^{\circ}\text{C}$ , brought to  $21\text{ }^{\circ}\text{C}$  and stirred for 16 h. After addition of water (40 mL) the mixture was extracted with dichloromethane (3 x 40 mL). The collected organic layers were dried with magnesium sulfate and the solvent removed at reduced pressure. After purification by column chromatography [3 x 30 cm, SiO<sub>2</sub>, petroleum ether / dichloromethane gradient 100:0 to 5:5 (v:v)] 1-trifluoromethanesulfonate-1'-acetoxy-ferrocene (**181**, 444 mg, 1.1 mmol, 68%) was obtained as a yellow oil.

<sup>1</sup>H NMR (600.3 MHz, CDCl<sub>3</sub>):  $\delta$  = 2.19 (s, 3H, CH<sub>3</sub>), 4.09 + 4.10 + 4.59 + 4.62 (AA'BB',  $J$  = 2.0 Hz, 2H, C<sub>Cp</sub>H) ppm. <sup>13</sup>C NMR (150.9 MHz, CDCl<sub>3</sub>): 20.9 (CH<sub>3</sub>), 62.2 (C<sub>Cp</sub>H), 62.5 (C<sub>Cp</sub>H), 65.1 (2 x C<sub>Cp</sub>H), 116.1 (C<sub>Cp</sub>OCO), 118.3 (q, <sup>1</sup> $J$  = 321.9 Hz, CF<sub>3</sub>), 118.6 (C<sub>Cp</sub>OSO<sub>2</sub>), 168.8 (CO) ppm. <sup>19</sup>F NMR (376.5, CDCl<sub>3</sub>):  $\delta$  =  $-72.8$  (s, CF<sub>3</sub>) ppm. IR:  $\tilde{\nu}$  = 1759 (m), 1456 (m), 1422 (m), 1371 (m), 1250 (m), 1207 (s), 1140 (m), 1034 (m), 1020 (m), 941 (m), 922 (m), 885 (w), 851 (m), 768 (w), 737 (w), 702 (w), 617 (m), 590 (m), 490 (m) cm<sup>-1</sup>. HRMS (EI): Calcd. for C<sub>13</sub>H<sub>11</sub>F<sub>3</sub>FeO<sub>5</sub>S [M<sup>+</sup>] 391.9629, found 391.9628.

#### 6.2.2.29. (Cyclopentadienyl)(cyclopentadienone)cobalt(I) (**203**)<sup>[107]</sup>



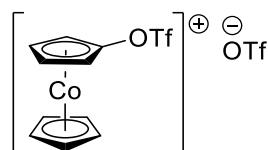
**203**

A suspension of cyclopentadienyl [2,5-bis(trimethylsilyl)cyclopentadienone](cyclopentadienyl)cobalt(I)<sup>[107]</sup> (**202**, 867 mg, 2.5 mmol) and caesium fluoride (1134 mg, 7.5 mmol) in DMF (40 mL) was vigorously stirred at  $110\text{ }^{\circ}\text{C}$  (oil bath) in a two-neck PTFE 100 mL flask for 16 h. The mixture was filtered into a Schlenk flask through a P3 frit. The solvent was removed under reduced pressure at  $70\text{ }^{\circ}\text{C}$  (oil bath). Ethyl acetate (3 x 20 mL) was added to the crude and the mixture was filtered into another Schlenk flask through a P3 frit. The solvent was removed under reduced pressure and the remaining red solid was recrystallized from slow diffusion of

hexane (50 mL) into ethyl acetate solution of **203** (10 mL). The remaining solution was transferred to another Schlenk flask, the solvent was removed under reduced pressure and the recrystallization repeated using half the amount used previously. After removal of the supernatant and remaining solvent removed under reduced pressure, (cyclopentadienyl)(cyclopentadienone)cobalt (I) (**203**, 428 mg, 2.1 mmol, 84%) was obtained as a crystalline red/orange solid (m. p. 46 °C). (The data diverges a little from the literature because **203** was obtained anhydrous as compared with the monohydrated from the literature).

$^1\text{H}$  NMR (400.1 MHz,  $\text{CDCl}_3$ ):  $\delta = 4.45 + 5.07$  (AA'BB',  $J = 2.1$  Hz, 2 x 2H,  $\text{C}_{\text{Cp}}\text{H}$ ), 5.11 (s, 5H, Cp') ppm.  $^{13}\text{C}$  NMR (100.6 MHz,  $\text{CDCl}_3$ , HSQC, HMBC):  $\delta = 64.4$  ( $\text{C}_{\text{Cp}}\text{H}$ ), 75.1 ( $\text{C}_{\text{Cp}}\text{H}$ ), 81.4 (Cp'), 161.6 (C=O) ppm. IR:  $\tilde{\nu} = 3098$  (m), 3049 (m), 1589 (m), 1545 (s), 1422 (m), 1410 (m), 1396 (m), 1348 (m), 1310 (m), 1260 (m), 1175 (m), 1109 (m), 1072 (m), 1045 (m), 1022 (m), 1003 (m), 901 (m), 853 (m), 827 (s), 685 (s), 667 (s), 588 (m), 484 (s), 457 (m), 426 (m)  $\text{cm}^{-1}$ . HRMS (EI): Calcd. for  $\text{C}_{10}\text{H}_9\text{CoO}$  [ $\text{M}^+$ ] 203.9985, found 203.9989.

6.2.2.30. [(trifluoromethylsulfonyl)oxy]cobaltocenium trifluoromethanesulfonate (**204**)

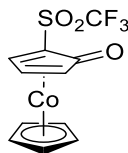


**204**

To a solution of (cyclopentadienyl)(cyclopentadienone)cobalt(I)<sup>[107]</sup> (**203**, 60 mg, 0.3 mmol) in dichloromethane (10 mL) at  $-78$  °C, triflic anhydride in dichloromethane (1.0 M, 0.88 mL, 0.9 mmol) was added dropwise. The red solution turned yellow immediately. The solution was stirred at  $-78$  °C for 15 min, slowly brought to 21 °C and further stirred for more 15 min. The solvent was evaporated and collected in a cold trap (to be later carefully quenched and neutralized), and a yellow oil was obtained. The oil was washed with diethyl ether (110 mL) and [(trifluoromethylsulfonyl)oxy]cobaltocenium trifluoromethanesulfonate (**204**, 116 mg, 81%) was obtained as a yellow solid (m. p. 176 °C, dec.).

$^1\text{H}$  NMR (400.1 MHz,  $\text{CD}_3\text{OD}$ ):  $\delta = 5.79 + 6.32$  (AA'BB',  $J = 2.3$  Hz, 2 x 2H,  $\text{C}_{5\text{H}_4\text{O}}\text{H}$ ), 6.01 (s, 5H, Cp') ppm.  $^{13}\text{C}$  NMR (100.6 MHz,  $\text{CD}_3\text{OD}$ , HSQC, HMBC):  $\delta = 78.1$  ( $\text{C}_{5\text{H}_4\text{O}}\text{H}$ ), 81.8 ( $\text{C}_{5\text{H}_4\text{O}}\text{H}$ ), 88.1 (Cp'), 119.8 (q,  $^1J_{\text{C,F}} = 320.5$  Hz,  $\text{CF}_3$ ), 121.8 (q,  $^1J_{\text{C,F}} = 321.5$  Hz,  $\text{CF}_3$ ), 125.9 ( $\text{C}_{5\text{H}_4\text{O}}\text{O}$ ) ppm.  $^{19}\text{F}$  NMR (376.5 MHz,  $\text{CD}_3\text{OD}$ ):  $\delta = -74.1$  ( $\text{OSO}_2\text{CF}_3$ ),  $-80.1$  ( $\text{OSO}_2\text{CF}_3$ ) ppm. IR:  $\tilde{\nu} = 3120$  (m), 1441 (m), 1420 (m), 1375 (w), 1279 (m), 1213 (s), 1165 (s), 1132 (s), 1022 (s), 932 (m), 870 (m), 839 (m), 814 (m), 768 (m), 712 (m), 635 (m), 617 (s), 598 (s), 573 (m), 517 (s), 463 (s), 424 (m)  $\text{cm}^{-1}$ . HRMS (ESI, MeOH): Calcd. for  $\text{C}_{11}\text{H}_9\text{CoF}_3\text{O}_3\text{S}$  [ $\text{M}^+$ ] 336.9556, found 336.9557. Calcd. for  $\text{CF}_3\text{O}_3\text{S}$  [ $\text{M}^-$ ] 148.9520, found 148.9516.

6.2.2.31. [2-(Trifluoromethylsulfonyl)cyclopentadienone]cyclopentadienylcobalt(I) (**205**)



**205**

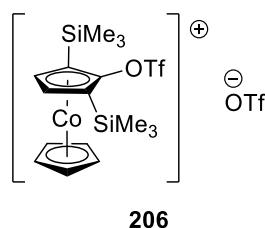
At  $-78$  °C lithium diisopropylamide [prepared from butyllithium in hexane (2.5 M, 0.78 mL, 1.9 mmol) and diisopropylamine (0.82 mL, 5.8 mmol) in THF (5 mL)] was added dropwise to [(trifluoromethylsulfonyl)oxy]cobaltocenium trifluoromethanesulfonate (**204**, 315 mg, 0.6 mmol) in THF (5 mL). The dark yellow solution turned red immediately and then brown. The solution was stirred at  $-78$  °C for 30 min, slowly brought to 25 °C and further stirred for more 15 min. The solvent was removed at reduced pressure and the remaining solid redissolved in DCM (20 mL). The solution was acidified by addition of oxygen free 37% aq. HCl under pH control until pH 6. After solvent and water removal at reduced pressure the crude product was purified by column chromatography {3 x 10 cm, alumina [(deactivated with water (15% w/v)], ethyl acetate followed by acetone/ methanol 7:3} affording [2-(trifluoromethylsulfonyl)cyclopentadienone]cyclopentadienylcobalt(I) (**205**, 67mg, 0.2 mmol, 31%) as a red/orange solid (m. p. 158 °C, dec.).

$^1\text{H}$  NMR (400.1 MHz,  $\text{CDCl}_3$ ):  $\delta = 4.76$  (dd,  $J = 3.1$  Hz,  $J = 1.7$  Hz, 1H,  $\text{C}_{5\text{H}_4\text{O}}\text{H}$ ), 5.41 (AMX,  $J = 3.2$  Hz, 1H,  $\text{C}_{5\text{H}_4\text{O}}\text{H}$ ), 5.42 (s, 5H, Cp'), 5.73 (dd,  $J = 3.3$  Hz,  $J = 1.7$  Hz, 1H,  $\text{C}_{5\text{H}_4\text{O}}\text{H}$ ) ppm.  $^{13}\text{C}$  NMR (100.6 MHz,  $\text{CDCl}_3$ , HSQC, HMBC):  $\delta = 65.5$  ( $\text{C}_{5\text{H}_4\text{O}}\text{H}$ ), 70.2 ( $\text{C}_{5\text{H}_4\text{O}}\text{S}$ ), 76.0

(C<sub>5</sub>H<sub>4</sub>O), 77.7 (C<sub>5</sub>H<sub>4</sub>O), 83.3 (Cp'), 119.2 (q, <sup>1</sup>J<sub>C,F</sub> = 325.6 Hz, CF<sub>3</sub>), 158.6 (C<sub>5</sub>H<sub>4</sub>O) ppm. <sup>19</sup>F NMR (376.5 MHz, CDCl<sub>3</sub>): δ = -78.0 (SO<sub>2</sub>CF<sub>3</sub>) ppm. IR:  $\tilde{\nu}$  = 3078 (w), 2922 (w), 2856 (w), 1734 (w), 1612 (s), 1584 (m), 1466 (w), 1458 (w), 1408 (w), 1364 (s), 1314 (w), 1198 (s), 1186 (s), 1175 (s), 1113 (s), 1080 (m), 1049 (w), 1032 (w), 997 (m), 837 (m), 793 (w), 764 (w), 708 (m), 692 (s), 631 (m), 610 (s), 569 (m), 517 (m), 503 (m), 469 (m), 432 (m), 413 (m) cm<sup>-1</sup>. HRMS (ESI, MeCN): Calcd. for C<sub>11</sub>H<sub>8</sub>CoF<sub>3</sub>O<sub>3</sub>Na [M<sup>+</sup>Na] 358.9376, found 358.9391.

Crystal Structure Analysis: Single crystals suitable for X-Ray analysis were obtained from slow evaporation of **205** in a solution of EtOAc. C<sub>22</sub>H<sub>18</sub>Co<sub>2</sub>F<sub>6</sub>O<sub>7</sub>S<sub>2</sub> (Two molecules of **205** and one water of crystallization), red block, M<sub>r</sub> = 690.34, crystal system monoclinic, space group C1c1, *a* = 9.750(6) Å, *b* = 9.775(5) Å, *c* = 26.071(15) Å, α = 90°, β = 98°, γ = 90°, V = 2463.0(3) Å<sup>3</sup>, Z = 4, *d*<sub>calc</sub> = 1.861 g.cm<sup>-3</sup>, μ = 1.605 mm<sup>-1</sup>, crystal size 0.25x0.21x0.10 mm<sup>3</sup>, F(000) = 1384, Bruker SMART X2S diffractometer, graphite crystal monochromator, T = 200 K, Mo-Kα radiation (*l* = 0.71073 Å), 2.96° ≤ θ ≤ 29.70°, index ranges -13 ≤ *h* ≤ 13, -13 ≤ *k* ≤ 13, -36 ≤ *l* ≤ 36, reflections collected/unique 6795/5358, numerical absorption correction, structure solution and refinement with SHELXL-2018/3,<sup>[150]</sup> parameter/restraints 360/2, R<sub>1</sub> = 0.0458 [*I* > 2σ(*I*)], wR<sub>2</sub> = 0.0981 (all data), S = 0.983, final maximum/minimum difference electron density 0.380/-0.478 eÅ<sup>-3</sup>.

#### 6.2.2.32. 1-[(trifluoromethylsulfonyl)oxy]-2,5-bis(trimethylsilyl)cobaltocenium trifluoromethanesulfonate (**206**)

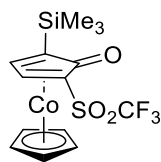


To a solution of [2,5-bis(trimethylsilyl)cyclopentadienone](cyclopentadienyl)cobalt(I)<sup>[107]</sup> (**202**, 40 mg, 0.1 mmol) in dichloromethane (8 mL) at -78 °C, triflic anhydride in dichloromethane (0.03 mL, 0.2 mmol) was added dropwise. The red solution turned yellow immediately. The solution was stirred at -78 °C for 15 min, slowly brought to 22 °C and further stirred for more 15 min. The solvent was evaporated and collected in a cold trap (to be later carefully quenched

and neutralized). The remaining yellow greenish solid was washed with diethyl ether (3 x 5 mL). The remaining solvent was removed under reduced pressure and redissolved in dichloromethane (1 mL). Diethyl ether (1 mL) was added and the mixture was left at  $-30\text{ }^{\circ}\text{C}$  for 48 h. The solvent was removed with a syringe and 1-[(trifluoromethylsulfonyl)oxy]-2,5-bis(trimethylsilyl)cobaltocenium trifluoromethanesulfonate (**206**, 63 mg, 0.1 mmol, 87% was obtained as a yellow crystalline solid (m. p.  $178\text{ }^{\circ}\text{C}$ , dec.).

$^1\text{H}$  NMR (600.3 MHz,  $\text{CD}_3\text{OD}$ ):  $\delta = 0.51$  (s, 18 H, 2 x  $\text{SiMe}_3$ ), 5.87 (s, 2H,  $\text{C}_{\text{CpH}}$ ), 6.00 (s, 5H,  $\text{Cp}'$ ) ppm.  $^{13}\text{C}$  NMR (150.9 MHz,  $\text{CD}_3\text{OD}$ , HSQC, HMBC):  $-0.7$  ( $\text{SiMe}_3$ ), 87.9 ( $\text{Cp}'$ ), 90.2 ( $\text{C}_{\text{CpH}}$ ), 92.0 ( $\text{C}_{\text{CpSi}}$ ), 119.4 (q,  $^1J_{\text{C,F}} = 319.6\text{ Hz}$ ,  $\text{CF}_3$ ), 121.8 (q,  $^1J_{\text{C,F}} = 318.4\text{ Hz}$ ,  $\text{CF}_3$ ), 130.5 ( $\text{C}_{\text{CpO}}$ ) ppm.  $^{19}\text{F}$  NMR (376.5 MHz,  $\text{CD}_2\text{Cl}_2$ ):  $\delta = -72.6$  ( $\text{SO}_2\text{CF}_3$ ),  $-78.9$  ( $\text{SO}_2\text{CF}_3$ ) ppm. IR:  $\tilde{\nu} = 3107$  (w), 3071 (w), 1412 (m), 1304 (m), 1263 (s), 1217 (s), 1148 (s), 1126 (s), 1088 (m), 1032 (s), 1015 (m), 891 (m), 835 (s), 822 (s), 764 (m), 723 (m), 708 (m), 637 (s), 611 (s), 573 (m), 536 (m), 517 (m), 503 (m), 474 (m), 424 (s)  $\text{cm}^{-1}$ . HRMS (ESI, MeOH): Calcd. for  $\text{C}_{17}\text{H}_{25}\text{CoF}_3\text{O}_3\text{SSi}_2$  [ $\text{M}^+$ ] 481.0347, found 481.0347. Calcd. for  $\text{CF}_3\text{O}_3\text{S}$  [ $\text{M}^-$ ] 148.9520, found 148.9524.

#### 6.2.2.33. (Cyclopentadienyl)[2-(trifluoromethylsulfonyl)-5-(trimethylsilyl)cyclopentadienone]cobalt(I) (**207**)



**207**

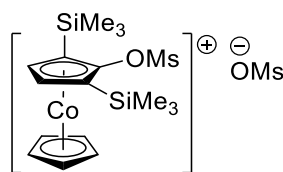
To a suspension of caesium fluoride (36 mg, 0.2 mmol) in DMF (1 mL) was added a solution of 1-[(trifluoromethylsulfonyl)oxy]-2,5-bis(trimethylsilyl)cobaltocenium trifluoromethanesulfonate (**206**, 148 mg, 0.2 mmol) in DMF (5 mL) at  $25\text{ }^{\circ}\text{C}$ . The yellow solution turned immediately red. The mixture was stirred for 1 h at  $28\text{ }^{\circ}\text{C}$  and the solvent was removed at  $70\text{ }^{\circ}\text{C}$  (oil bath) at reduced pressure. Dichloromethane (25 mL) was added, and the solution was filtered. After solvent removal at reduced pressure the crude product was purified by column chromatography [3 x 25 cm,  $\text{SiO}_2$ , (deactivated with  $\text{Et}_3\text{N}$ ), petroleum ether / ethyl acetate 6:4 gradient to 8:2



(v:v)] affording (cyclopentadienyl)[2-(trifluoromethylsulfonyl)-5(trimethylsilyl)cyclopentadienone]cobalt(I) (**207**, 57mg, 0.1 mmol, 59%) as an orange solid (m. p. 130 °C, dec.).

$^1\text{H}$  NMR (600.3 MHz,  $\text{C}_6\text{D}_6$ ):  $\delta$  = 0.14 (s, 9H, 3 x  $\text{CH}_3$ ), 4.40 (d,  $J$  = 3.1 Hz, 1H,  $\text{C}_{\text{C}_5\text{H}_4\text{O}\text{H}}$ ), 4.57 (s, 5H, Cp'), 5.28 (d,  $J$  = 3.1 Hz, 1H,  $\text{C}_{\text{C}_5\text{H}_4\text{O}\text{H}}$ ) ppm.  $^{13}\text{C}$  NMR (150.9 MHz,  $\text{C}_6\text{D}_6$ , HSQC, HMBC):  $\delta$  = -1.3 ( $\text{SiMe}_3$ ), 69.8 ( $\text{C}_{\text{C}_5\text{H}_4\text{O}\text{S}}$ ), 72.0 ( $\text{C}_{\text{C}_5\text{H}_4\text{O}\text{Si}}$ ), 77.4 ( $\text{C}_{\text{C}_5\text{H}_4\text{O}\text{H}}$ ), 82.2 (Cp'), 82.4 ( $\text{C}_{\text{C}_5\text{H}_4\text{O}\text{H}}$ ), 120.0 (q,  $^1J_{\text{C},\text{F}}$  = 326.2 Hz,  $\text{CF}_3$ ), 162.9 ( $\text{C}_{\text{C}_5\text{H}_4\text{O}\text{O}}$ ) ppm.  $^{19}\text{F}$  NMR (376.5 MHz,  $\text{C}_6\text{D}_6$ ):  $\delta$  = -78.2 ( $\text{SO}_2\text{CF}_3$ ) ppm. IR:  $\tilde{\nu}$  = 3115 (w), 2959 (w), 2926 (w), 1614 (s), 1408 (w), 1358 (s), 1252 (m), 1209 (s), 1186 (s), 1146 (m), 1125 (m), 1111 (m), 1094 (m), 1030 (w), 1011 (m), 866 (m), 824 (s), 762 (m), 727 (m), 706 (m), 692 (m), 669 (m), 619 (s), 569 (s), 523 (m), 509 (m), 474 (m), 455 (m), 412 (m)  $\text{cm}^{-1}$ . HRMS (ESI, MeCN): Calcd. for  $\text{C}_{14}\text{H}_{16}\text{CoF}_3\text{O}_3\text{SSiNa}$  [ $\text{M}^+\text{Na}$ ] 430.9771, found 430.9758.

#### 6.2.2.34. 1-[(methanesulfonyl)oxy]-2,5-bis(trimethylsilyl)cobaltocenium methanesulfonate (**224**)



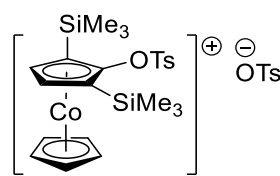
**224**

A solution of [2,5-bis(trimethylsilyl)cyclopentadienone](cyclopentadienyl)cobalt(I)<sup>[107]</sup> (**202**, 26 mg, 0.07 mmol) in dichloromethane (6 mL) was added to a solution of methanesulfonic anhydride (13 mg, 0.07 mmol) in dichloromethane (1 mL) at 25 °C. The red solution turned orange/yellow after approx. 2 h. The solution was stirred at 25 °C for 16 h. The solvent was evaporated and collected in a cold trap (to be later carefully quenched and neutralized). The remaining yellow solid was washed with cold diethyl ether (3 x 5 mL). The remaining solvent was removed under reduced pressure and redissolved in dichloromethane (1 mL). Diethyl ether (1 mL) was added and the mixture was left at -30 °C for 48 h. The solvent was removed with a syringe and 1-[(methanesulfonyl)oxy]-2,5-bis(trimethylsilyl)cobaltocenium methanesulfonate [**224**, 29 mg, 0.05 mmol (89% based on NMR integration), overall yield: 66%] was obtained as

a yellow crystalline solid. (In the NMR, it is possible to see a small amount of the starting material and some of the methanesulfonic anhydride).

$^1\text{H}$  NMR (400.1 MHz,  $\text{CDCl}_3$ ):  $\delta$  = 0.45 (s, 18 H, 2 x  $\text{SiMe}_3$ ), 2.95 (s, 3H,  $^-\text{OMs}$ ), 3.32 (s, 3H,  $\text{CpOSO}_2\text{CH}_3$ ), 5.81 (s, 5H,  $\text{Cp}'$ ), 5.92 (s, 2H,  $\text{C}_{\text{Cp}}\text{H}$ ) ppm.  $^{13}\text{C}$  NMR (100.6 MHz,  $\text{CDCl}_3$ , HSQC, HMBC): - 0.3 ( $\text{SiMe}_3$ ), 39.6 ( $\text{CpOSO}_2\text{CH}_3$ ), 39.6 ( $^-\text{OMs}$ ), 86.3 ( $\text{Cp}'$ ), 89.4 ( $\text{C}_{\text{Cp}}\text{H}$ ), 90.8 ( $\text{C}_{\text{Cp}}\text{Si}$ ), 129.2 ( $\text{C}_{\text{Cp}}\text{O}$ ) ppm. IR:  $\tilde{\nu}$  = 3422 (w), 3096 (w), 3015 (w), 2934 (w), 1418 (m), 1391 (w), 1356 (m), 1341 (m), 1323 (m), 1252 (m), 1180 (s), 1136 (m), 1096 (m), 1022 (m), 972 (m), 893 (m), 833 (s), 814 (s), 770 (s), 752 (s), 700 (m), 640 (m), 540 (s), 517 (s), 473 (m), 420 (s)  $\text{cm}^{-1}$ . HRMS (ESI, MeCN): Calcd. for  $\text{C}_{17}\text{H}_{28}\text{CoO}_3\text{SSi}_2$  [ $\text{M}^+$ ] 427.0624, found 427.0629. Calcd. for  $\text{CH}_3\text{O}_3\text{S}$  [ $\text{M}^-$ ] 97.9803, found 94.9803.

6.2.2.35. 1-[(*p*-toluenesulfonyl)oxy]-2,5-bis(trimethylsilyl)cobaltocenium *p*-toluenesulfonate (225)



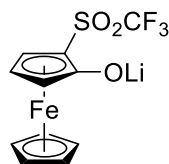
**225**

A solution of [2,5-bis(trimethylsilyl)cyclopentadienone](cyclopentadienyl)cobalt(I)<sup>[107]</sup> (**202**, 98 mg, 0.3 mmol) in dichloromethane (5 mL) was added to a solution of methanesulfonic anhydride (92 mg, 0.3 mmol) in dichloromethane (2 mL) at 25 °C. The red solution turned orange/yellow after approx. 2 h. The solution was stirred at 25 °C for 16 h. The solvent was evaporated and collected in a cold trap (to be later carefully quenched and neutralized). The remaining yellow solid was washed with cold diethyl ether (3 x 5 mL). The remaining solvent was removed under reduced pressure. Crystallization did not work. 1-[(*p*-toluenesulfonyl)oxy]-2,5-bis(trimethylsilyl)-cobaltocenium *p*-toluenesulfonate (**225**, 138 mg, 73%, based on NMR integration) was obtained as a mixture with starting material and *p*-toluenesulfonic anhydride as a yellow solid. Most of the  $^{13}\text{C}$  NMR peaks were assigned, but due to the mixture and an unclear HMBC, two quaternary carbons ( $\text{C}_{\text{Cp}}\text{O}$  and  $\text{C}_{\text{Cp}}\text{OSO}_2\text{C}_{\text{Ph}}$ ) were not referred.

$^1\text{H}$  NMR (400.1 MHz,  $\text{CDCl}_3$ ):  $\delta$  = 0.43 (s, 18 H, 2 x  $\text{SiMe}_3$ ), 2.37 (s, 3H,  $^-\text{OSO}_2\text{PhCH}_3$ ), 2.53 (s, 3H,  $\text{CpOSO}_2\text{PhCH}_3$ ), 5.82 (s, 5H,  $\text{Cp}'$ ), 6.13 (s, 2H,  $\text{C}_{\text{Cp}}\text{H}$ ), 7.17 + 7.81 (d,  $J$  = 7.8 Hz, 2 x 2H,  $^-\text{OSO}_2\text{PhCH}_3$ ), 7.47 + 7.86 (d,  $J$  = 8.2 Hz, 2 x 2H,  $\text{CpOSO}_2\text{PhCH}_3$ ) ppm.  $^{13}\text{C}$  NMR (100.6 MHz,  $\text{CDCl}_3$ , HSQC, HMBC):  $\delta$  = -0.17 ( $\text{SiMe}_3$ ), 21.5 ( $^-\text{OSO}_2\text{PhCH}_3$ ), 22.0 ( $\text{CpOSO}_2\text{PhCH}_3$ ), 86.3 ( $\text{Cp}'$ ), 90.2 ( $\text{C}_{\text{Cp}}\text{H}$ ), 90.3 ( $\text{C}_{\text{Cp}}\text{Si}$ ), 126.5 ( $\text{C}_{\text{Ph}}\text{H}$ , anion), 129.0 ( $\text{C}_{\text{Ph}}\text{H}$ , anion), 128.6 ( $\text{C}_{\text{Ph}}$ ), 130.6 ( $\text{C}_{\text{Ph}}\text{H}$ ), 140.8 ( $\text{C}_{\text{Ph}}\text{CH}_3$ , anion), 141.0 ( $^-\text{OSO}_2\text{C}_{\text{Ph}}$ ), 147.3 ( $\text{C}_{\text{Ph}}\text{CH}_3$ ) ppm.

IR:  $\tilde{\nu}$  = 2955 (m), 2920 (s), 2853 (m), 1715 (w), 1458 (m), 1418 (m), 1377 (m), 1364 (m), 1319 (m), 1258 (m), 1192 (m), 1177 (m), 1059 (m), 1024 (m), 1009 (m), 893 (m), 833 (m), 812 (s), 800 (s), 758 (m), 704 (m), 679 (m), 664 (m), 640 (m), 615 (m), 565 (m), 546 (m), 496 (m), 463 (m), 407 (m)  $\text{cm}^{-1}$ . HRMS (ESI, MeCN): Calcd. for  $\text{C}_{23}\text{H}_{32}\text{CoO}_3\text{SSi}_2$  [ $\text{M}^+$ ] 503.0937, found 503.0939.

#### 6.2.2.36. Lithium 2-(trifluoromethylsulfonyl)ferrocenolate (**237**)



**237**

At  $-78\text{ }^\circ\text{C}$ , LDA in THF [prepared from 2.5 M butyllithium (0.54 mL, 1.34 mmol) in hexane and diisopropylamine (0.57 mL, 4.0 mmol) in THF (3 mL)] was added dropwise to a solution of ferrocenyl triflate (**79**) in THF (4 mL). The colour changed from light yellow to red. The solution was stirred for 20 min at  $-78\text{ }^\circ\text{C}$ . The solvent was removed at reduced pressure, and the remaining red solid was washed with hexane (3x5 mL). The solid was dissolved in dichloromethane and filtered through a P4 frit into a Schlenk flask. The solvent was removed at reduced pressure affording **237** (437 mg, 1.29 mmol, 96%) as a red solid.

$^1\text{H}$ -NMR (600 MHz,  $\text{CD}_2\text{Cl}_2$ ): 4.49 (s, 5 H,  $\text{C}_{\text{Cp}}\text{H}$ ); 4.43–4.45 (m, 1 H,  $\text{C}_{\text{Cp}}\text{H}$ ); 4.43 (t, 1 H,  $\text{C}_{\text{Cp}}\text{H}$ ,  $J$  = 2.9), 4.38–4.40 (m, 1 H,  $\text{C}_{\text{Cp}}\text{H}$ ).  $^{13}\text{C}$ -NMR (151 MHz,  $\text{CD}_2\text{Cl}_2$ ): 60.68 ( $\text{C}_{\text{Cp}}\text{S}$ ); 61.59 ( $\text{C}_{\text{Cp}}\text{H}$ ); 62.95 ( $\text{C}_{\text{Cp}}\text{H}$ ); 67.16 ( $\text{C}_{\text{Cp}}\text{H}$ ); 71.63 (5  $\text{C}_{\text{Cp}}\text{H}$ ); 119.6 (q,  $\text{CF}_3$ ,  $J$ =325); 135.7 ( $\text{C}_{\text{Cp}}\text{O}$ ).  $^{19}\text{F}$ -NMR (376 MHz,  $\text{CD}_2\text{Cl}_2$ ):  $-80.5$  (s,  $\text{CF}_3$ ). IR: 3611 (w), 1647 (w), 1463 (s), 1379 (m), 1329 (m), 1203 (s), 1175 (s), 1123 (m), 1080 (m), 1003 (m), 849 (w), 738 (w), 712 (m), 604 (s), 563 (m), 507 (m)  $\text{cm}^{-1}$ .

Crystal Structure Analysis: CCDC-2046411. Single crystals suitable for X-ray crystallographic analysis were obtained from slow diffusion of hexane (5 mL) into dichloromethane solution of **236** (1 mL).  $C_{44}H_{32}F_{12}Fe_4Li_4O_{12}S_4$ , red block,  $M_r=1360.09$ , crystal system orthorhombic, space group  $P2_12_12_1$ ,  $a=14.9657(1)$  Å,  $b=15.2558(1)$  Å,  $c=22.9370(2)$  Å,  $\alpha=90^\circ$ ,  $\beta=90^\circ$ ,  $\gamma=90^\circ$ ,  $V=5236.83(7)$  Å<sup>3</sup>,  $Z=4$ ,  $d_{calc}=1.725$  g.cm<sup>-3</sup>,  $\mu=11.114$  mm<sup>-1</sup>, crystal size 0.14x0.13x0.09 mm<sup>3</sup>,  $F(000)=2720$ , Bruker KAPPA APEX II CCD diffractometer, graphite crystal monochromator,  $T=233$  K, Cu-K $\alpha$  radiation ( $\lambda=1.54187$  Å),  $3.48^\circ \leq \theta \leq 65.44^\circ$ , index ranges  $-17 \leq h \leq 15$ ,  $-17 \leq k \leq 18$ ,  $-26 \leq l \leq 21$ , reflections collected/unique 8785/5743, numerical absorption correction, structure solution and refinement with SHELX-97,<sup>[152]</sup> parameter/restraints 721/0,  $R_1=0.0470$  [ $I > 2\sigma(I)$ ],  $wR_2=0.0898$  (all data),  $S=0.962$ , final maximum/minimum difference electron density 0.449/−0.513 eÅ<sup>-3</sup>.

## References

- [1] K. Fries, G. Finck, *Ber. Dtsch. Chem. Ges.* **1908**, 41, 4271–4284.

- [2] C. B. Anderson, J.C., Reese, *Proc. Chem. Soc.* **1960**, 217.
- [3] J. W. Meyer, G. S. Hammond, *J. Am. Chem. Soc.* **1972**, *94*, 2219–2228.
- [4] M. Korb, H. Lang, *Chem. Soc. Rev.* **2019**, *48*, 2829–2882.
- [5] S. G. P. Plant, S. B. C. Williams, *J. Chem. Soc.* **1934**, 1142–1143.
- [6] E. Meitzner, *J. Am. Chem. Soc.* **1935**, *57*, 2327–2328.
- [7] Y. Ogata, H. Tabuchi, *Tetrahedron* **1964**, *20*, 1661–1666.
- [8] M. P. Sibi, V. Snieckus, *J. Org. Chem.* **1983**, *48*, 1935–1937.
- [9] J. L. Speier, *J. Am. Chem. Soc.* **1952**, *74*, 1003–1010.
- [10] J. P. H. Charmant, A. M. Dyke, G. C. Lloyd-Jones, *Chem. Commun.* **2003**, *3*, 380–381.
- [11] L. S. Melvin, *Tetrahedron Lett.* **1981**, *22*, 3375–3376.
- [12] J. M. Clough, *Synlett* **1990**, *1990*, 469–470.
- [13] A. Quattropiani, G. Bernardinelli, E. Peter Kündig, *Helv. Chim. Acta* **1999**, *82*, 90–104.
- [14] B. F. Bonini, C. Femoni, M. Fochi, M. Gulea, S. Masson, A. Ricci, *Tetrahedron: Asymmetry* **2005**, *16*, 3003–3010.
- [15] Z. Zhao, J. Messinger, U. Schön, R. Wartchow, H. Butenschön, *Chem. Commun.* **2006**, 3007–3009.
- [16] M. Korb, D. Schaarschmidt, H. Lang, *Organometallics* **2014**, *33*, 2099–2108.
- [17] G. Werner, C. W. Lehmann, H. Butenschön, *Adv. Synth. Catal.* **2010**, *352*, 1345–1355.
- [18] R. L. B. J. . Danheiser, *Comprehensive Organic Synthesis, Charge-Accelerated Rearrangements*, Press Oxford , Pergamon, **1991**.
- [19] D. A. Evans, A. M. Golob, *J. Am. Chem. Soc.* **1975**, *97*, 4765–4766.
- [20] W. Choy, H. Yang, *J. Org. Chem.* **1988**, *53*, 5796–5798.
- [21] M. Brands, R. Goddard, H. G. Wey, H. Butenschön, *Angew. Chem.* **1993**, *105*, 285-287; *Angew. Chem. Int. Ed. Engl.* **1993**, *32*, 267–269.

- [22] G. Wittig, G. Pieper, G. Fuhrmann, *Ber. Dtsch. Chem. Ges. (A B Ser.)* **1940**, 73, 1193–1197.
- [23] J. D. Roberts, H. E. Simmons, L. A. Carlsmith, C. W. Vaughan, *J. Am. Chem. Soc.* **1953**, 75, 3290–3291.
- [24] P. M. Tadross, B. M. Stoltz, *Chem. Rev.* **2012**, 112, 3550–3577.
- [25] T. R. Hoye, B. Baire, D. Niu, P. H. Willoughby, B. P. Woods, *Nature* **2012**, 490, 208–212.
- [26] A. M. Dyke, D. M. Gill, J. N. Harvey, A. J. Hester, G. C. Lloyd-Jones, M. P. Muñoz, I. R. Shepperson, *Angew. Chem.* **2008**, 120, 5145–5148; *Angew. Chem. Int. Ed. Engl.* **2008**, 47, 5067–5070.
- [27] J. de Paula, P. Atkins, *Physical Chemistry*, Oxford University Press, South Asia 10th Edition, **2014**.
- [28] S. Braverman, Y. Duar, *Phosphorus Sulfur Relat. Elem.* **1976**, 2, 213–215.
- [29] A. N. Nesmejanow, W. A. Ssasonowa, V. N. Drosd, *Chem. Ber.* **1960**, 93, 2717–2729.
- [30] A. N. Nesmeyanov, V. A. Sazonova, V. N. Drozd, *Tetrahedron Lett.* **1959**, 1, 13–15.
- [31] G. Werner, Towards Ferrocene and Benzene  $\pi$ -Complexes, Doctoral dissertation, Leibniz Universität Hannover, **2011**.
- [32] B. Breit, D. Breuninger, *Synthesis (Stuttg.)* **2005**, 2005, 2782–2786.
- [33] A. G. Martínez, L. R. Subramanian, M. Hanack, S. J. Williams, S. Régnier, in *Encycl. Reagents Org. Synth.*, John Wiley & Sons, Ltd, Chichester, UK, **2016**, pp. 1–17.
- [34] N. E. Heimer, R. E. Del Sesto, Z. Meng, J. S. Wilkes, W. R. Carper, *J. Mol. Liq.* **2006**, 124, 84–95.
- [35] M. J. Frisch, G. W. Trucks, H. B. Schlegel, G. E. Scuseria, M. a. Robb, J. R. Cheeseman, G. Scalmani, V. Barone, G. a. Petersson, H. Nakatsuji, X. Li, M. Caricato, a. V. Marenich, J. Bloino, B. G. Janesko, R. Gomperts, B. Mennucci, H. P. Hratchian, J. V. Ortiz, a. F. Izmaylov, J. L. Sonnenberg, Williams, F. Ding, F. Lipparini, F. Egidi, J. Goings, B. Peng, A. Petrone, T. Henderson, D. Ranasinghe, V. G. Zakrzewski, J.

- Gao, N. Rega, G. Zheng, W. Liang, M. Hada, M. Ehara, K. Toyota, R. Fukuda, J. Hasegawa, M. Ishida, T. Nakajima, Y. Honda, O. Kitao, H. Nakai, T. Vreven, K. Throssell, J. a. Montgomery Jr., J. E. Peralta, F. Ogliaro, M. J. Bearpark, J. J. Heyd, E. N. Brothers, K. N. Kudin, V. N. Staroverov, T. a. Keith, R. Kobayashi, J. Normand, K. Raghavachari, a. P. Rendell, J. C. Burant, S. S. Iyengar, J. Tomasi, M. Cossi, J. M. Millam, M. Klene, C. Adamo, R. Cammi, J. W. Ochterski, R. L. Martin, K. Morokuma, O. Farkas, J. B. Foresman, D. J. Fox, **2016**, Gaussian 16, Revision A.03, Gaussian, Inc., Wallingford.
- [36] J. P. Perdew, K. Burke, M. Ernzerhof, *Phys. Rev. Lett.* **1996**, *77*, 3865–3868.
- [37] C. Adamo, V. Barone, *J. Chem. Phys.* **1999**, *110*, 6158–6170.
- [38] J. P. Perdew, M. Ernzerhof, K. Burke, *J. Chem. Phys.* **1996**, *105*, 9982–9985.
- [39] W. R. Wadt, P. J. Hay, *J. Chem. Phys.* **1985**, *82*, 284–298.
- [40] P. J. Hay, W. R. Wadt, *J. Chem. Phys.* **1985**, *82*, 299–310.
- [41] P. J. Hay, W. R. Wadt, *J. Chem. Phys.* **1985**, *82*, 270–283.
- [42] T. H. Dunning, P. J. Hay, in *Methods Electron. Struct. Theory*, Springer US, Boston, MA, **1977**, pp. 1–27.
- [43] A. D. McLean, G. S. Chandler, *J. Chem. Phys.* **1980**, *72*, 5639–5648.
- [44] R. Krishnan, J. S. Binkley, R. Seeger, J. A. Pople, *J. Chem. Phys.* **1980**, *72*, 650–654.
- [45] M. J. Frisch, J. A. Pople, J. S. Binkley, *J. Chem. Phys.* **1984**, *80*, 3265–3269.
- [46] J. Clayden, *Organolithiums: Selectivity for Synthesis*, Pergamon, Amsterdam, **2002**.
- [47] F. Ujjainwalla, M. L. E. N. Da Mata, A. M. K. Pennell, C. Escolano, W. B. Motherwell, S. Vázquez, *Tetrahedron* **2015**, *71*, 6701–6719.
- [48] W. B. Motherwell, A. M. K. Pennell, *J. Chem. Soc. Chem. Commun.* **1991**, 877.
- [49] A. Talko, D. Antoniak, M. Barbasiewicz, *Synthesis (Stuttg)*. **2019**, *51*, 2278–2286.
- [50] G. Werner, H. Butenschön, *Organometallics* **2013**, *32*, 5798–5809.
- [51] J. Dong, L. Krasnova, M. G. Finn, K. Barry Sharpless, *Angew. Chem.* **2014**, *126*, 9584–

- 9603; *Angew. Chem. Int. Ed. Engl.* **2014**, *53*, 9430–9448.
- [52] C. Veryser, J. Demaerel, V. Bieliūnas, P. Gilles, W. M. De Borggraeve, *Org. Lett.* **2017**, *19*, 5244–5247.
- [53] N. Miyaura, A. Suzuki, *J. Chem. Soc. Chem. Commun.* **1979**, 866.
- [54] M. R. Yadav, M. Nagaoka, M. Kashihara, R.-L. Zhong, T. Miyazaki, S. Sakaki, Y. Nakao, *J. Am. Chem. Soc.* **2017**, *139*, 9423–9426.
- [55] P. Chatelain, A. Sau, C. N. Rowley, J. Moran, *Angew. Chem.* **2019**, *131*, 15101–15105; *Angew. Chem. Int. Ed. Engl.* **2019**, *58*, 14959–14963.
- [56] H. Chachignon, H. Guyon, D. Cahard, *Beilstein J. Org. Chem.* **2017**, *13*, 2800–2818.
- [57] C. Rhode, J. Lemke, M. Lieb, N. Metzler-Nolte, *Synthesis (Stuttg.)* **2009**, *2009*, 2015–2018.
- [58] Y. Wang, Z. Gao, B. Wang, W. Zhou, P. Yu, Y. Luo, *Ind. Eng. Chem. Res.* **2019**, *58*, 21913–21920.
- [59] M. S. Inkpen, S. Du, M. Hildebrand, A. J. P. White, N. M. Harrison, T. Albrecht, N. J. Long, *Organometallics* **2015**, *34*, 5461–5469.
- [60] A. N. Nesmeyanov, V. A. Sazonova, N. S. Sazonova, V. N. Plyukhina, *Dokl. Akad. Nauk SSSR* **1967**, *177*, 1352–1354.
- [61] V. Weinmayr, *J. Am. Chem. Soc.* **1955**, *77*, 3009–3011.
- [62] G. R. Knox, P. L. Pauson, *J. Chem. Soc.* **1958**, 692.
- [63] M. Herberhold, O. Nuyken, T. P. Öhlmann, *J. Organomet. Chem.* **1995**, *501*, 13–22.
- [64] M. Jonek, A. Makhoulfi, P. Rech, W. Frank, C. Ganter, *J. Organomet. Chem.* **2014**, *750*, 140–149.
- [65] O. A. Nesmeyanov, A. N.; Reutov, *Izv. Akad. Nauk SSSR, Seriya Khimicheskaya* **1959**, 926–929.
- [66] S. Prakash, N. Shao, F. Wang, C. Ni, *Org. Synth.* **2013**, *90*, 130.
- [67] C. J. Smedley, Q. Zheng, B. Gao, S. Li, A. Molino, H. M. Duivenvoorden, B. S. Parker,



- D. J. D. Wilson, K. B. Sharpless, J. E. Moses, *Angew. Chem.* **2019**, *131*, 4600–4604; *Angew. Chem. Int. Ed. Engl.* **2019**, *58*, 4552–4556.
- [68] A. A. Kolomeitsev, V. N. Movchun, N. V. Kondratenko, Y. L. Yagupolski, *Synthesis (Stuttg.)* **1990**, *1990*, 1151–1152.
- [69] C. F. R. A. C. Lima, A. M. Fernandes, A. Melo, L. M. Gonçalves, A. M. S. Silva, L. M. N. B. F. Santos, *Phys. Chem. Chem. Phys.* **2015**, *17*, 23917–23923.
- [70] M. Hesse, H. Meier, B. Zeeh, *Spektroskopische Methoden in Der Organischen Chemie*, Georg Thieme Verlag, Stuttgart, **2005**.
- [71] E. J. Rayment, N. Summerhill, E. A. Anderson, *J. Org. Chem.* **2012**, *77*, 7052–7060.
- [72] Y. Sumii, M. Taniguchi, X.-H. Xu, E. Tokunaga, N. Shibata, *Tetrahedron* **2018**, *74*, 5635–5641.
- [73] V. Gold, Ed. , *The IUPAC Compendium of Chemical Terminology*, International Union Of Pure And Applied Chemistry (IUPAC), Research Triangle Park, NC, **2019**.
- [74] K. Schlögl, in *Stereochemistry of Metallocenes, Top. Stereochem.* (Eds.: N.L. Allinger, E.L. Eliel), John Wiley & Sons, Ltd, **1967**, pp. 39–91.
- [75] E. L. Eliel, S. H. Wilen, *Stereochemistry of Organic Compounds*, Chichester : Wiley, New York, **1994**.
- [76] D. Marquarding, H. Klusacek, G. Gokel, P. Hoffmann, I. Ugi, *J. Am. Chem. Soc.* **1970**, *92*, 5389–5393.
- [77] D. A. Price, N. S. Simpkins, A. M. MacLeod, A. P. Watt, *J. Org. Chem.* **1994**, *59*, 1961–1962.
- [78] C. Metallinos, V. Snieckus, *Org. Lett.* **2002**, *4*, 1935–1938.
- [79] W. Maison, Pyrrolidines as Chiral Auxiliaries in *Heterocycles as Chiral Auxiliaries in Asymmetric Synthesis*. Topics in Heterocyclic Chemistry, vol. 55, **2019**, (Ed.: M. Braun) Springer, Cham, pp. 157–191.
- [80] W. von E. Doering, C. H. DePuy, *J. Am. Chem. Soc.* **1953**, *75*, 5955–5957.
- [81] F. Ramirez, S. Levy, *J. Org. Chem.* **1956**, *21*, 488–489.

- [82] D. Lloyd, J. S. Sneezum, *Chem. Ind.* **1955**, 1221.
- [83] C. K. Ingold, J. A. Jessop, *J. Chem. Soc.* **1929**, 28, 2357–2361.
- [84] C. K. Ingold, J. A. Jessop, *J. Chem. Soc.* **1930**, 713–718.
- [85] W. Schlenk, W. Schlenk, *Ber. Dtsch. Chem. Ges. (A B Ser.)* **1929**, 62, 920–924.
- [86] A. C. Cope, *J. Am. Chem. Soc.* **1935**, 57, 2238–2240.
- [87] Y. Ma, R. F. Algera, D. B. Collum, *J. Org. Chem.* **2016**, 81, 11312–11315.
- [88] T. J. Kealy, P. L. Pauson, *Nature* **1951**, 168, 1039–1040.
- [89] S. A. Miller, J. A. Tebboth, J. F. Tremaine, *J. Chem. Soc.* **1952**, 632.
- [90] E. O. Fischer, R. Jira, *Z. Naturforsch. B* **1953**, 8, 327–328.
- [91] G. Wilkinson, *J. Am. Chem. Soc.* **1952**, 74, 6148–6149.
- [92] J. E. Sheats, G. Hlatky, *J. Chem. Educ.* **1983**, 60, 1015.
- [93] N. G. Connelly, W. E. Geiger, *Chem. Rev.* **1996**, 96, 877–910.
- [94] R. B. Woodward, M. Rosenblum, M. C. Whiting, *J. Am. Chem. Soc.* **1952**, 74, 3458–3459.
- [95] M. Sato, H. Kono, M. Shiga, I. Motoyama, K. Hata, *Bull. Chem. Soc. Jpn.* **1968**, 41, 252–252.
- [96] C. R. Hauser, R. L. Pruett, T. A. Mashburn, *J. Org. Chem.* **1961**, 26, 1800–1801.
- [97] H. Butenschön, *CHEMKON* **2009**, 16, 77–82.
- [98] R. Sanders, U. T. Mueller-Westerhoff, *J. Organomet. Chem.* **1996**, 512, 219–224.
- [99] J. P. Tane, K. P. C. Vollhardt, *Angew. Chem.* **1982**, 94, 642–643; *Angew. Chem. Int. Ed. Engl.* **1982**, 21, 1360–1372.
- [100] S. Vanicek, H. Kopacka, K. Wurst, T. Müller, H. Schottenberger, B. Bildstein, *Organometallics* **2014**, 33, 1152–1156.
- [101] G. E. Herberich, E. Bauer, J. Schwarzer, *J. Organomet. Chem.* **1969**, 17, 445–452.

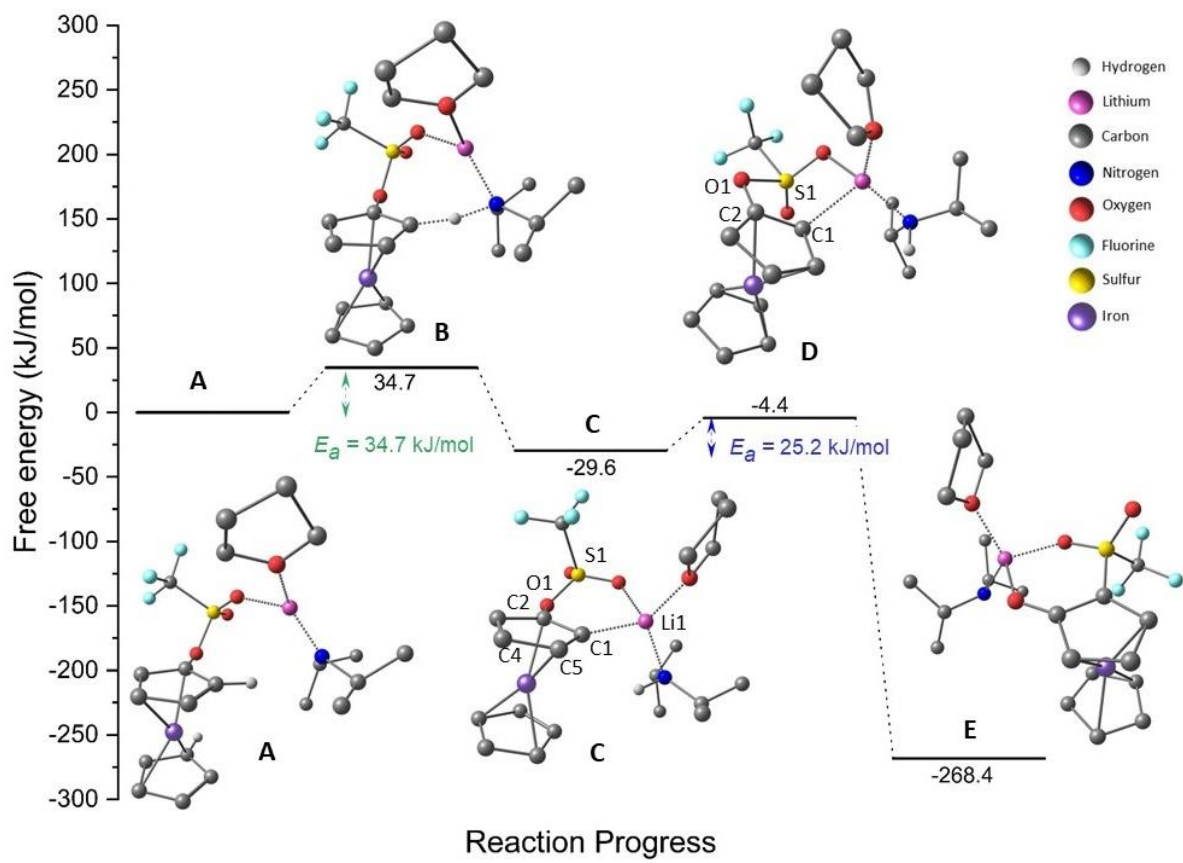
- [102] Y. Yan, P. Pageni, M. Kabir, C. Tang, *Synlett* **2016**, 27, 984–1005.
- [103] R. Jira, E. O. Fischer, *Z. Naturforsch.* **1954**, 9b, 618–619.
- [104] T. S. Piper, F. A. Cotton, G. Wilkinson, *J. Inorg. Nucl. Chem.* **1955**, 1, 165–174.
- [105] M. D. Rausch, R. A. Genetti, *J. Org. Chem.* **1970**, 35, 3888–3897.
- [106] C. Zhao, F. D. Toste, R. G. Bergman, *J. Am. Chem. Soc.* **2011**, 133, 10787–10789.
- [107] E. R. F. Gesing, J. P. Tane, K. P. C. Vollhardt, *Angew. Chem.* **1980**, 92, 1057–1058;  
*Angew. Chem. Int. Ed. Engl.* **1980**, 19, 1023–1024.
- [108] P. L. Pauson, I. U. Khand, *Ann. N. Y. Acad. Sci.* **1977**, 295, 2–14.
- [109] H.-J. Knölker, J. Heber, C. H. Mahler, *Synlett* **1992**, 1992, 1002–1004.
- [110] M. M. Heravi, M. Ghavidel, L. Mohammadkhani, *RSC Adv.* **2018**, 8, 27832–27862.
- [111] J. E. Sheats, G. Hlatky, R. S. Dickson, *J. Organomet. Chem.* **1979**, 173, 107–115.
- [112] M. von der Gruen, C. Schaefer, R. Gleiter, *Organometallics* **2003**, 22, 2370–2372.
- [113] I. Kaljurand, A. Kütt, L. Sooväli, T. Rodima, V. Mäemets, I. Leito, I. A. Koppel, *J. Org. Chem.* **2005**, 70, 1019–1028.
- [114] N. Ghosh, *Synlett* **2004**, 574–575.
- [115] Y. Himeshima, T. Sonoda, H. Kobayashi, *Chem. Lett.* **1983**, 12, 1211–1214.
- [116] R. Walsh, *Acc. Chem. Res.* **1981**, 14, 246–252.
- [117] T. Kiang, R. N. Zare, *J. Am. Chem. Soc.* **1980**, 102, 4024–4029.
- [118] S. J. Shafer, W. D. Closson, *J. Org. Chem.* **1975**, 40, 889–892.
- [119] D. Hellwinkel, M. Supp, *Chem. Ber.* **1976**, 109, 3749–3766.
- [120] Christopher J. Cramer, *Essentials of Computational Chemistry: Theories and Models*, Wiley, **2004**.
- [121] P. Hohenberg, W. Kohn, *Phys. Rev.* **1964**, 136, B864–B871.
- [122] R. Car, M. Parrinello, *Phys. Rev. Lett.* **1985**, 55, 2471–2474.

- [123] R. C. Büchel, D. A. Rudolph, I. Frank, *Int. J. Quantum Chem.* **2021**, *121*, 1–9.
- [124] M. Boero, A. Oshiyama, in *Encycl. Nanotechnol.*, Springer Netherlands, Dordrecht, **2015**, pp. 1–10.
- [125] E. M. Arnett, M. A. Nichols, A. T. McPhail, *J. Am. Chem. Soc.* **1990**, *112*, 7059–7060.
- [126] E. Weiss, *Angew. Chem.* **1993**, *105*, 1565; *Angew. Chem. Int. Ed. Engl.* **1993**, *32*, 1501–1523.
- [127] J. Niemeyer, G. Kehr, R. Fröhlich, G. Erker, *Dalt. Trans.* **2009**, *4*, 3731–3741.
- [128] C. Nottingham, R. Benson, H. Müller-Bunz, P. J. Guiry, *J. Org. Chem.* **2015**, *80*, 10163–10176.
- [129] CPMD, <http://www.cpmc.org/>, Copyright IBM Corp 1990-2019, Copyright MPI für Festkörperforschung Stuttgart 1997-2001.
- [130] A. D. Becke, *Phys. Rev. A* **1988**, *38*, 3098–3100.
- [131] C. Lee, W. Yang, R. G. Parr, *Phys. Rev. B* **1988**, *37*, 785–789.
- [132] S. Grimme, *J. Comput. Chem.* **2006**, *27*, 1787–1799.
- [133] S. Goedecker, M. Teter, J. Hutter, *Phys. Rev. B* **1996**, *54*, 1703–1710.
- [134] N. Troullier, J. L. Martins, *Phys. Rev. B* **1991**, *43*, 1993–2006.
- [135] P. Parois, R. I. Cooper, A. L. Thompson, *Chem. Cent. J.* **2015**, *9*, 30.
- [136] P. Muller, *Crystallogr. Rev.* **2009**, *15*, 57–83.
- [137] S. Grimme, J. Antony, S. Ehrlich, H. Krieg, *J. Chem. Phys.* **2010**, *132*, DOI 10.1063/1.3382344.
- [138] A. D. Becke, *J. Chem. Phys.* **1993**, *98*, 1372–1377.
- [139] J. Da Chai, M. Head-Gordon, *Phys. Chem. Chem. Phys.* **2008**, *10*, 6615–6620.
- [140] Y. Zhao, D. G. Truhlar, *Theor. Chem. Acc.* **2008**, *120*, 215–241.
- [141] E. Weiss, G. Hencken, *J. Organomet. Chem.* **1970**, *21*, 265–268.

- [142] J. C. Slater, *J. Chem. Phys.* **1964**, *41*, 3199–3204.
- [143] R. Resta, *Ferroelectrics* **1992**, *136*, 51–55.
- [144] R. D. King-Smith, D. Vanderbilt, *Phys. Rev. B* **1993**, *47*, 1651–1654.
- [145] R. Resta, *Rev. Mod. Phys.* **1994**, *66*, 899–915.
- [146] N. Marzari, D. Vanderbilt, *Phys. Rev. B* **1997**, *56*, 12847–12865.
- [147] P. L. Silvestrelli, *Phys. Rev. B* **1999**, *59*, 9703–9706.
- [148] G. Berghold, C. J. Mundy, A. H. Romero, J. Hutter, M. Parrinello, *Phys. Rev. B* **2000**, *61*, 10040–10048.
- [149] R. K. Harris, E. D. Becker, S. M. Cabral de Menezes, R. Goodfellow, P. Granger, *Solid State Nucl. Magn. Reson.* **2002**, *22*, 458–483.
- [150] G. M. Sheldrick, *Acta Crystallogr. Sect. C Struct. Chem.* **2015**, *71*, 3–8.
- [151] C. Imrie, D. C. Nonhebel, P. L. Pauson, *J. Chem. Soc. Perkin Trans. 1* **1991**, 2555.
- [152] G. M. Sheldrick, ‘*SHELX97, Programs for Crystal Structure Analysis*’, University of Göttingen, Germany, **1997**.

## Attachments

Cartesian coordinates obtained using Gaussian

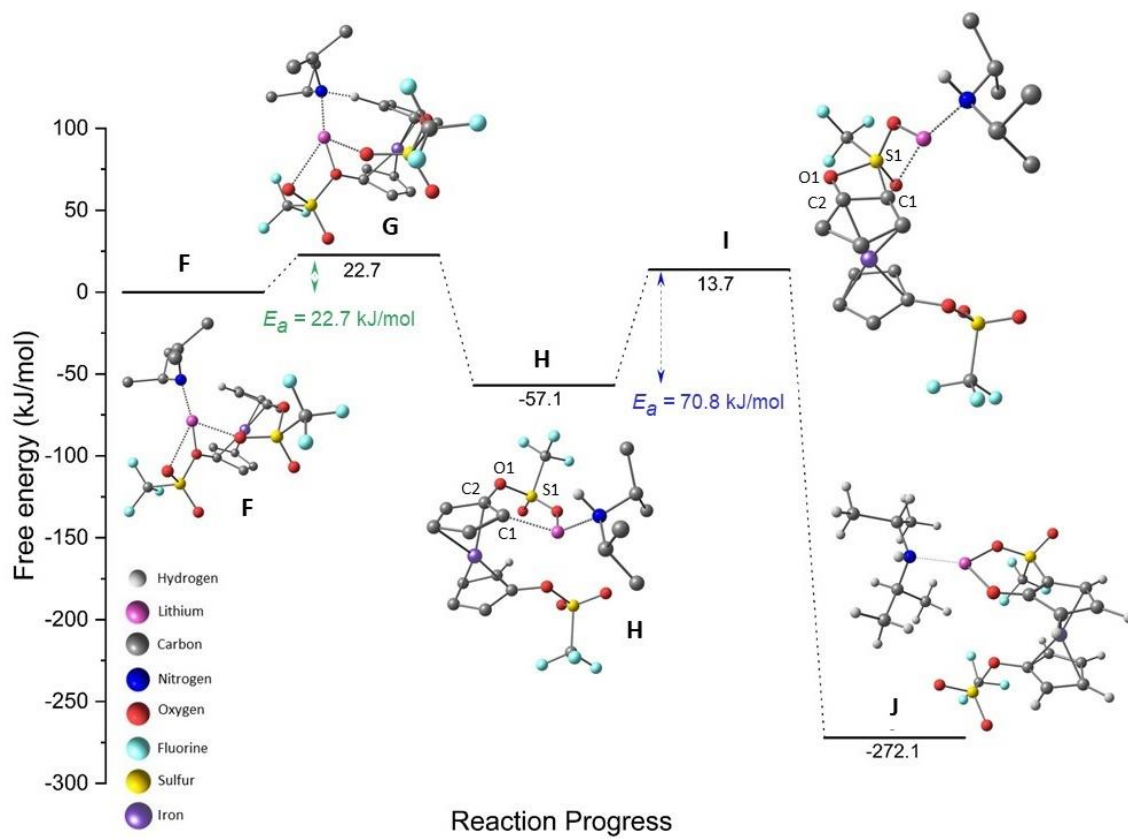


<b>A</b>					
C	-0.98118700	0.59317800	-2.12689100	H	3.30515400 -2.56560900 -3.79895100
C	-1.88059300	-0.47017500	-2.43365600	H	2.99362200 -0.83147000 -3.99092100
C	-2.09792800	-1.23222900	-1.25262100	H	5.23829700 -2.12011400 -2.35737400
C	-1.32415800	-0.60788200	-0.23672800	H	5.41195900 -0.85788400 -3.58946300
C	-0.62944900	0.51848800	-0.75052800		
H	-0.65240700	1.35925500	-2.81432800	<b>B</b>	
H	-2.34941100	-0.64878700	-3.39048500	C	0.74597600 -0.72706100 -1.92475200
H	-2.74138700	-2.09098500	-1.13252000	C	1.29168900 0.46222900 -2.50319800
Fe	-2.65560700	0.70752300	-0.95318400	C	1.40520600 1.43305800 -1.47082600
C	-3.80792000	1.37257300	0.59942500	C	0.92075500 0.78121700 -0.29977800
C	-3.18605100	2.47037700	-0.05968900	C	0.49768000 -0.55398500 -0.52474800
C	-3.60066700	2.45860300	-1.42159400	H	0.58665900 -1.64964200 -2.46887100
C	-4.48086600	1.35443300	-1.60388300	H	1.60689700 0.59509000 -3.52951000
C	-4.60891200	0.68286500	-0.35452000	H	1.80204800 2.43534300 -1.54681300
H	-3.66632600	1.09090400	1.63322700	Fe	2.50617500 -0.21441400 -1.01260800
H	-2.49044200	3.16641600	0.38633200	C	3.86847200 -0.53432600 0.48501900
H	-4.93972700	1.05524600	-2.53533600	C	3.60638600 -1.74838900 -0.20960800
H	-5.18403100	-0.21347200	-0.17144700	C	3.94401300 -1.55502300 -1.57899300
O	-1.29453000	-1.03361800	1.10067500	C	4.41861700 -0.22120400 -1.73023400
S	0.00013600	-1.77826900	1.68244900	C	4.37177400 0.41036800 -0.45408200
C	-0.30291100	-3.54752800	1.14947500	H	3.68392100 -0.35014700 1.53401800
O	-0.12245300	-1.73520600	3.11068200	H	3.18697000 -2.64772200 0.21735000
O	1.20278700	-1.35883200	0.99715000	H	4.72397900 0.24272100 -2.65736000
H	-3.27444300	3.14446200	-2.19024500	H	4.63950900 1.43577100 -0.24211400
F	-1.50037500	-3.92590900	1.55197700	O	0.91338100 1.42401400 0.96998600
F	-0.22231100	-3.63791900	-0.16544300	S	-0.45792500 1.92604900 1.59434500
F	0.62057800	-4.30837600	1.70728700	C	-0.65412600 3.62034200 0.82418600
H	0.04608600	1.16774900	-0.19028600	O	-0.22853600 2.13067600 2.99724500
Li	2.36412100	0.24565800	0.39776900	O	-1.58344100 1.14656700 1.11637500
C	3.86425300	3.45329200	0.50167000	H	3.82566000 -2.28088300 -2.37086100
C	2.34176700	3.21495000	0.47258800	F	0.44577400 4.32141800 1.02581800
C	1.42363200	2.05667900	2.40912900	F	-0.87891600 3.50475400 -0.47204000
N	1.94196200	1.95436600	1.05946900	F	-1.67994300 4.22119800 1.40141900
C	1.86300100	3.31648400	-0.98013900	H	-0.07754600 -1.45427500 0.33431300
C	2.38028700	2.66790200	3.45096500	Li	-2.04666300 -0.74224000 0.50232200
C	0.05992900	2.77015700	2.51127400	C	-2.57395200 -3.97909700 0.95219700
H	1.24141800	1.02356700	2.75060600	C	-1.10316700 -3.56155800 0.81133200
H	3.33574700	2.13344500	3.45484100	C	-0.34128200 -1.95858700 2.52762200
H	1.95561500	2.62150700	4.46182000	N	-0.86489500 -2.17451600 1.18515200
H	2.58642600	3.72161400	3.22958100	C	-0.64826600 -3.81368500 -0.62775600
H	0.13472900	3.81652700	2.19253400	C	-1.31466300 -2.30750700 3.65908500
H	-0.32682700	2.76755500	3.53837700	C	1.02061700 -2.61598900 2.79912100
H	-0.67394900	2.27550700	1.86822100	H	-0.16169500 -0.87382400 2.60055700
H	2.21514200	4.23217700	-1.47171400	H	-2.27929700 -1.81056700 3.51407800
H	0.76993700	3.29683100	-1.03191600	H	-0.91404000 -2.00056300 4.63230500
H	2.23917200	2.46111000	-1.55632300	H	-1.49472600 -3.38742700 3.70409000
H	4.24611800	3.40419600	1.52456400	H	0.95308000 -3.70903300 2.81160000
H	4.14267400	4.42799200	0.07644000	H	1.41508100 -2.30484600 3.77287800
H	4.37247100	2.67370300	-0.08023300	H	1.74179300 -2.32677000 2.03090100
H	1.88840800	4.07106200	1.00723900	H	-0.84426700 -4.84748800 -0.93160000
C	4.45845600	-0.20142800	-1.74235100	H	0.42077500 -3.61378100 -0.74327800
O	3.18841500	-0.57751800	-1.18126600	H	-1.18641300 -3.15367700 -1.31899800
C	2.55690100	-1.57231300	-2.00880600	H	-2.93814800 -3.81532700 1.96925600
C	3.35812200	-1.59689000	-3.29872900	H	-2.71885900 -5.03820300 0.70390200
C	4.75869500	-1.24407100	-2.80499400	H	-3.20102300 -3.38902700 0.27220600
H	4.36660900	0.80053900	-2.17731000		
H	5.19463800	-0.16915800	-0.93583500		
H	2.60120900	-2.53605100	-1.48909500		
H	1.50981900	-1.29220800	-2.14469300		

H	-0.51918500	-4.24328600	1.45104600	H	-1.55411000	3.91198700	2.19473700
C	-4.22238200	-1.10969900	-1.57947700	H	0.35722700	4.64092800	-2.11689400
O	-3.13197800	-0.33029800	-1.05496200	H	-0.72212200	3.29110900	-1.73545700
C	-2.81228700	0.74578300	-1.96009900	H	1.00668100	2.99700600	-1.99712300
C	-3.54311300	0.41837900	-3.24946900	H	2.13962100	4.78422800	1.14424200
C	-4.78775700	-0.29726600	-2.73153400	H	2.11571500	5.33868000	-0.52733100
H	-3.82943100	-2.07316400	-1.92390400	H	2.70652100	3.70955100	-0.14732000
H	-4.93881200	-1.28734400	-0.77390300	H	-0.15947900	4.68150200	0.26790600
H	-3.17025300	1.68425900	-1.52231300	C	4.04067500	0.64646300	-0.60761500
H	-1.72638400	0.79067900	-2.06491900	O	2.73884900	0.75185700	-1.20766900
H	-3.76842100	1.31212000	-3.83417800	C	2.76643700	0.22157100	-2.54543300
H	-2.94357600	-0.25636300	-3.86853800	C	4.23633000	0.03640600	-2.88198300
H	-5.52088700	0.42808700	-2.36533800	C	4.83519700	-0.27836400	-1.51367400
H	-5.27169800	-0.92640500	-3.48071100	H	4.48889200	1.64634500	-0.56340200
<b>C</b>				H	3.91945100	0.26721400	0.40960500
C	-1.27758000	-0.35859600	-2.17249300	H	2.22254400	-0.72923800	-2.55387400
C	-2.10108500	-1.53017200	-2.23345100	H	2.25082200	0.92442800	-3.20435700
C	-1.98728900	-2.19148300	-0.97941200	H	4.39454600	-0.75422400	-3.61770400
C	-1.09911700	-1.36858000	-0.22780400	H	4.65918300	0.96478800	-3.27864300
C	-0.60583600	-0.22650700	-0.90649100	H	4.65231400	-1.32416700	-1.24761700
H	-1.20221600	0.35590200	-2.98478100	H	5.90919300	-0.09197600	-1.45576700
H	-2.72826700	-1.84456700	-3.05764300	<b>D</b>			
H	-2.48178900	-3.09644100	-0.65604300	C	-0.54277200	0.46437300	-2.13356900
Fe	-2.73080900	-0.31892600	-0.73022500	C	-1.54102600	-0.26068800	-2.86797000
C	-3.78963100	0.15293600	0.95880500	C	-2.24191500	-1.11780400	-1.95640200
C	-3.34466600	1.34119600	0.31313400	C	-1.61165500	-0.89038100	-0.71159100
C	-3.87945100	1.35583900	-1.00669600	C	-0.58136100	0.05365900	-0.75510400
C	-4.66379700	0.17912500	-1.17459900	H	0.10960300	1.21027500	-2.56868800
C	-4.60728100	-0.56424000	0.03949500	H	-1.76522800	-0.15398500	-3.92128500
H	-3.53134400	-0.16145000	1.96025900	H	-3.07240200	-1.77102100	-2.17930000
H	-2.70810700	2.09705800	0.74942800	Fe	-2.39629800	0.84558500	-1.40433500
H	-5.18025300	-0.11662400	-2.07675000	C	-3.86389800	1.42948100	-0.10968600
H	-5.07480800	-1.52197100	0.21936000	C	-2.82108700	2.39768600	-0.14343500
O	-0.79653900	-1.72670100	1.13130400	C	-2.69986700	2.86900600	-1.48178100
S	0.68974700	-1.79928600	1.64668900	C	-3.66950200	2.19258600	-2.27700000
C	1.40135000	-3.24509600	0.68851600	C	-4.38856400	1.30299300	-1.42869300
O	0.62128000	-2.20565700	3.02511500	H	-4.17649900	0.86384600	0.75672300
O	1.47276400	-0.64075800	1.26557000	H	-2.19293400	2.67149800	0.69104200
H	-3.70038000	2.11260600	-1.75727100	H	-3.81102200	2.30766500	-3.34232300
F	0.58143800	-4.27742500	0.77483400	H	-5.17122300	0.62493400	-1.73854600
F	1.57757800	-2.92044500	-0.57894200	O	-1.81586500	-1.44597000	0.53886800
F	2.56857300	-3.55876800	1.22943700	S	-0.69241200	-0.68806000	1.52638900
H	-0.54677800	2.27132600	0.26355000	C	-1.29650900	-1.79215700	2.91342400
Li	1.06391300	0.83939800	-0.18218400	O	-1.02788600	0.62120300	2.07842600
C	1.96095700	4.46685100	0.11533400	O	0.69571100	-1.19031600	1.44416000
C	0.55379600	3.92232000	-0.08788700	H	-1.97825300	3.59004400	-1.83888400
C	0.22663500	2.65195600	2.09405100	F	-2.58354000	-1.58347200	3.17273900
N	0.33248900	2.64731200	0.61645000	F	-1.12142600	-3.07935400	2.63084000
C	0.28099900	3.69719800	-1.57029000	F	-0.59631100	-1.50439900	4.00938200
C	1.58022900	2.51697700	2.78622600	H	1.09479700	1.81370100	1.40941300
C	-0.57320100	3.81793600	2.67143900	Li	1.52129000	-0.06845400	-0.00226600
H	-0.32876100	1.73267300	2.31905600	C	3.08020800	2.59025300	-1.02674300
H	2.15475400	1.68889900	2.36472100	C	2.38064900	2.91857200	0.28758200
H	1.42878100	2.31378500	3.85085300	C	2.89610800	1.35152800	2.19027900
H	2.17884600	3.42741500	2.70936600	N	2.03324800	1.68727100	1.03498000
H	-0.04621300	4.77034400	2.55580900				
H	-0.73569000	3.66154700	3.74175600				



C	1.11828900	3.73244600	0.03864600	F	2.85205400	-1.92608300	2.02509300
C	4.33038700	1.08085900	1.76130200	F	1.60807800	-0.25046000	2.59397400
C	2.83210700	2.38001400	3.31831800	F	1.08776200	-2.24080800	3.23250300
H	2.48456300	0.41250500	2.57975100	H	-1.00373100	2.21701800	0.52567300
H	4.37208100	0.31941800	0.97747500	Li	-1.79061200	0.06562700	-0.20172400
H	4.91128600	0.72132100	2.61485600	C	-3.53373900	1.27696200	2.32656500
H	4.81983300	1.98647400	1.38892300	C	-2.50828100	2.31644900	1.88769400
H	3.25099800	3.34569600	3.01795200	C	-2.56315400	2.84741800	-0.57593200
H	3.40354500	2.02895000	4.18284700	N	-2.00328900	2.03111500	0.52550100
H	1.79917300	2.54033100	3.64221400	C	-1.33831800	2.35698000	2.86133900
H	1.34043000	4.62037200	-0.55926000	C	-4.06417800	2.64416800	-0.72264600
H	0.66803600	4.06159600	0.98049700	C	-2.20494000	4.32958000	-0.47740100
H	0.37834200	3.13244600	-0.50215400	H	-2.08332200	2.45243700	-1.47973800
H	3.97454100	1.98407300	-0.86612200	H	-4.30997300	1.58291000	-0.81646900
H	3.38273600	3.50875200	-1.53932900	H	-4.42034400	3.16030700	-1.61842200
H	2.40777200	2.03845200	-1.69360600	H	-4.61293200	3.05408700	0.13144100
H	3.06338700	3.53159700	0.89067000	H	-2.66318900	4.80525000	0.39559200
C	1.73620000	-2.54583900	-1.54078100	H	-2.55647800	4.86422300	-1.36501100
O	2.44351800	-1.35126800	-1.14859100	H	-1.12072500	4.46690100	-0.41187400
C	3.72398300	-1.30076600	-1.79817000	H	-1.68916300	2.52617100	3.88271600
C	3.66636600	-2.34989200	-2.89459700	H	-0.63736700	3.15892800	2.60754000
C	2.75691600	-3.40357000	-2.26830200	H	-0.79605800	1.40530600	2.84476800
H	1.32977300	-3.01005000	-0.64006700	H	-4.36389100	1.20528100	1.62096800
H	0.90691500	-2.25354900	-2.19395100	H	-3.94377600	1.53666400	3.30764700
H	3.88287200	-0.28577500	-2.16910300	H	-3.06650200	0.28962600	2.40510300
H	4.50230600	-1.53512200	-1.06184300	H	-2.99214400	3.30250500	1.90210100
H	3.20621000	-1.93450800	-3.79658100	C	-3.44630500	-1.37740800	-2.16636200
H	4.65598800	-2.72885600	-3.15650400	O	-3.33277400	-1.01741300	-0.77908300
H	2.29106300	-4.06507000	-3.00095500	C	-3.92400300	-2.03985800	0.04452300
H	3.31851700	-4.01857500	-1.55823400	C	-4.56721400	-3.03173100	-0.91477900
				C	-3.71128700	-2.87099600	-2.16892100
<b>E</b>				H	-4.28407000	-0.82373700	-2.60918000
C	2.61290300	-1.56113000	-1.15183400	H	-2.51887300	-1.08094900	-2.65974200
C	2.75715800	-0.96166200	-2.42289600	H	-3.12691500	-2.50227800	0.63595700
C	1.61047800	-0.15896400	-2.68888100	H	-4.63942300	-1.56941900	0.72421400
C	0.62997900	-0.30854100	-1.64855400	H	-4.56695600	-4.04760400	-0.51548700
C	1.33194400	-1.13172400	-0.64142500	H	-5.60299900	-2.74707900	-1.12442200
H	3.30174500	-2.23787300	-0.66888400	H	-2.77211700	-3.42392000	-2.06786800
H	3.62462200	-1.05700300	-3.06077800	H	-4.21188500	-3.20399300	-3.08021000
H	1.45509000	0.45461800	-3.56515800				
Fe	2.58094700	0.44455200	-0.97102600				
C	2.44863700	2.48263100	-0.72846900				
C	2.56171600	1.84861100	0.53563600				
C	3.78074900	1.10833100	0.56168200				
C	4.42205700	1.29005200	-0.69567400				
C	3.59948000	2.13201700	-1.49489300				
H	1.61915500	3.08798200	-1.06601300				
H	1.83463600	1.89457700	1.33269900				
H	5.35023300	0.83207800	-1.00730900				
H	3.79407800	2.42274600	-2.51740100				
O	-0.53387700	0.18661600	-1.58765000				
S	0.54605200	-1.82051900	0.71575400				
C	1.60564500	-1.52570200	2.24130200				
O	0.49815200	-3.27568800	0.63238300				
O	-0.69612700	-1.09558200	1.01332900				
H	4.14668700	0.50931600	1.38238900				



**F**

Fe	-0.10867100	-2.01448100	1.41200500
O	1.60355300	-0.29937900	-0.34008700
C	1.93303200	-2.04037700	1.38689400
C	1.39892100	-1.58798500	0.15314700
C	0.57913500	-2.59113100	-0.43065600
C	0.60553100	-3.69164600	0.46694900
H	0.06366300	-4.61644400	0.33555600
C	1.42742600	-3.35476000	1.57932500
H	1.60955600	-3.97647100	2.44342600
O	-2.76902000	-0.77492100	0.20898100
C	-1.04066800	-0.24030900	1.94737900
C	-1.92597900	-1.12002900	1.27707600
C	-2.04498400	-2.35505200	1.97006400
H	-2.65222300	-3.19685900	1.67328400
C	-1.20848500	-2.24227500	3.11289700
H	-1.04274600	-3.01542600	3.84904200
C	-0.59537400	-0.95524600	3.09200700
H	0.12118100	-0.58569800	3.81145200
S	2.26756600	-0.01759100	-1.78616400
C	4.06146500	0.21385800	-1.30701200
F	4.74897400	0.49217900	-2.39796000
F	4.50483000	-0.90924500	-0.76907300
F	4.16620800	1.19762300	-0.44105000
O	2.18560200	-1.15076400	-2.66026800
O	1.73373100	1.28537200	-2.11244500
S	-2.25217100	-0.58444900	-1.28851900
C	-3.77833200	0.33071500	-1.86204800
F	-3.59734600	0.61259700	-3.14032300
F	-3.92443800	1.44121900	-1.17343700
F	-4.83694700	-0.43987500	-1.71792600
O	-2.17708900	-1.83311600	-1.99677900
O	-1.13942100	0.34235500	-1.35242900
H	-0.75502800	0.78156400	1.63294100
H	2.56051200	-1.46970600	2.05463400
H	0.05649700	-2.53522800	-1.37230000
C	-2.11229300	3.53175600	1.79302300
C	-0.81464100	3.75740500	0.99754900
C	1.15452100	2.62472200	1.90603900
N	0.05466500	2.59744600	0.96225200
C	-1.18044300	4.17908500	-0.42934900
C	0.76660200	2.81774700	3.38347100
C	2.25554900	3.64003800	1.54605300
H	1.63133000	1.62957100	1.84822800
H	0.02136800	2.07960400	3.69639100
H	1.64053100	2.72363900	4.03940200
H	0.33881100	3.81174000	3.55406800
H	3.11039700	3.58365700	2.23235300
H	2.61513000	3.46202300	0.52798400
H	-1.87702900	5.02500400	-0.45504800
H	-0.28249300	4.45513500	-0.99201000
H	-1.67543400	3.34742400	-0.95293800
H	-1.89745500	3.24458000	2.82489500
H	-2.74490900	4.42896800	1.81414300
H	-2.69298200	2.72015300	1.33751300
H	-0.31072100	4.62858500	1.45528600
H	1.87115700	4.66545500	1.58584900

Li 0.18369400 1.67660200 -0.63727000

**G**

Fe	-0.03223600	-1.83927100	1.51478800
O	1.60919700	-0.24206300	-0.39386600
C	2.00614400	-1.83963800	1.46721100
C	1.44529100	-1.49636000	0.20946500
C	0.63795800	-2.55629200	-0.28462500
C	0.69616400	-3.58061100	0.69722700
H	0.16946800	-4.52198100	0.64737700
C	1.52721200	-3.14363200	1.76767700
H	1.73163100	-3.69258700	2.67493200
O	-2.74009400	-0.77084000	0.25116000
C	-0.98267600	0.00688700	1.88179500
C	-1.85542900	-0.97098400	1.34830400
C	-1.94651700	-2.15028600	2.14089000
H	-2.54220200	-3.02725400	1.93422200
C	-1.08959100	-1.91478100	3.24834500
H	-0.88997100	-2.61250700	4.04999300
C	-0.50851200	-0.61942800	3.07752300
H	0.22089200	-0.18670000	3.75029800
S	2.35631600	-0.04181900	-1.81875900
C	4.12169500	0.23968900	-1.26350500
F	4.85252800	0.50743500	-2.32874000
F	4.56637600	-0.85449000	-0.67394900
F	4.16342800	1.25142100	-0.42104800
O	2.33185900	-1.22350400	-2.62811900
O	1.81918700	1.23441300	-2.23580300
S	-2.25638500	-0.70572700	-1.25232100
C	-3.81940400	0.08361500	-1.90166400
F	-3.66039600	0.24726300	-3.20398300
F	-4.01192100	1.25289300	-1.32624700
F	-4.84676900	-0.70924400	-1.67283600
O	-2.12799600	-2.00328800	-1.85863500
O	-1.19018700	0.26659200	-1.43163400
H	-0.65121700	1.24726000	1.42958100
H	2.63136600	-1.20944000	2.08131200
H	0.10312100	-2.58424100	-1.22063100
C	-2.40027600	3.25404700	1.58346000
C	-1.07990000	3.54135700	0.86133900
C	1.02007700	2.66554600	1.80983200
N	-0.13822000	2.42545200	0.95417500
C	-1.34945600	3.90330900	-0.60123100
C	0.68124400	3.06094500	3.25396600
C	2.01390900	3.66678000	1.21236600
H	1.54099300	1.69514800	1.87100600
H	0.00188300	2.33477600	3.70879000
H	1.58704400	3.11550600	3.86801900
H	0.19980800	4.04361200	3.29920500
H	2.91015900	3.76732700	1.83553900
H	2.32592900	3.35584700	0.21033400
H	-2.05308700	4.73794400	-0.69675200
H	-0.41955000	4.18412300	-1.10714800
H	-1.78796800	3.05057900	-1.13550000
H	-2.22940200	3.03782000	2.64120500
H	-3.08769200	4.10457500	1.51350100
H	-2.90023900	2.38318000	1.14590500

H	-0.64775800	4.43986900	1.32762200
H	1.56367800	4.66187700	1.12454000
Li	0.17912000	1.40997200	-0.63787500

## H

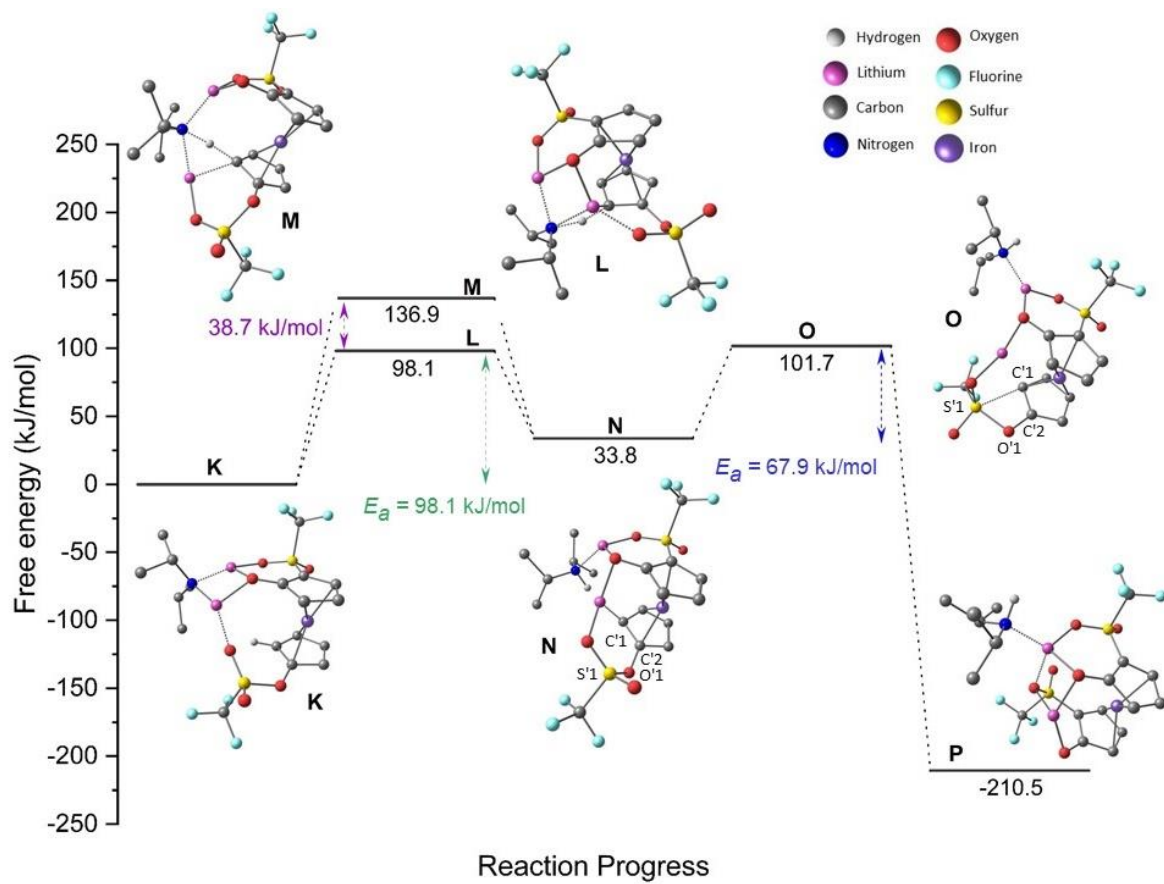
Fe	-0.01478100	-2.16499100	1.30703200
O	1.50823700	-0.24427400	-0.38234200
C	2.01161900	-2.14826300	1.14828500
C	1.37718200	-1.59063800	0.00442400
C	0.54411600	-2.55710200	-0.62230500
C	0.65638000	-3.73757400	0.16035500
H	0.12721800	-4.66063300	-0.02450000
C	1.54915200	-3.48915800	1.24183100
H	1.80735300	-4.18838300	2.02332400
O	-2.81445300	-1.18655000	0.28942200
C	-0.98759100	-0.36908800	1.84790300
C	-1.86285100	-1.36324900	1.34417200
C	-1.85695500	-2.59606000	2.05590100
H	-2.43643100	-3.48127600	1.83896900
C	-0.92479300	-2.39118800	3.10851700
H	-0.64049100	-3.12481600	3.85070500
C	-0.40798200	-1.06291200	2.96746300
H	0.36421300	-0.65640000	3.61034000
S	2.34314500	0.13120000	-1.73079600
C	4.10544900	-0.05091400	-1.11848200
F	4.90620900	0.49713600	-2.01567800
F	4.40876600	-1.32548700	-0.96933200
F	4.24171300	0.57657300	0.03908200
O	2.14363000	-0.85063800	-2.75761900
O	2.10603500	1.53712800	-1.91034500
S	-2.43674400	-0.61072400	-1.13030600
C	-4.08074200	0.21303500	-1.44219300
F	-4.02021300	0.78875100	-2.63195000
F	-4.30972700	1.13118300	-0.51993300
F	-5.04671000	-0.68416500	-1.43004900
O	-2.27571700	-1.64857600	-2.11267000
O	-1.45147300	0.45662800	-1.04975000
H	-0.85521200	2.53359600	1.89981500
H	2.67541700	-1.63326300	1.82609900
H	-0.04049900	-2.42159300	-1.51898000
C	-2.23049000	4.12090900	0.80029900
C	-0.73326000	4.04683800	0.53284000
C	1.07919200	3.08789500	1.99657600
N	-0.16624200	2.86852700	1.22837300
C	-0.44978600	3.98643400	-0.96333500
C	0.88200800	3.98389900	3.21845500
C	2.20922800	3.59295900	1.11163000
H	1.36055500	2.09165800	2.36452600
H	0.10635900	3.58349600	3.87879000
H	1.80863300	4.05385200	3.79610900
H	0.59630900	5.00145700	2.93315500
H	3.14317200	3.61508000	1.67985500
H	2.35310600	2.95394600	0.23786800
H	-0.81256100	4.89273900	-1.45860600
H	0.61706800	3.88905500	-1.17129200
H	-0.95673300	3.12732900	-1.41419800
H	-2.44005600	4.25054700	1.86696800

H	-2.67908200	4.96080600	0.26343700
H	-2.72782900	3.20546400	0.46241400
H	-0.27625200	4.96124000	0.93528900
H	2.01834200	4.61161300	0.75913000
Li	-0.23223100	0.96544600	0.44670800

## I

Fe	0.79342800	-1.07283600	1.28410800
O	2.77499700	0.68262500	-0.12013500
C	2.82042200	-1.18638800	1.51495400
C	2.46199600	-0.62396000	0.25920500
C	1.68556900	-1.54650100	-0.48900600
C	1.55597600	-2.70771900	0.31853800
H	0.98248800	-3.58565900	0.05946200
C	2.24593400	-2.48667100	1.54616200
H	2.29742200	-3.17614900	2.37607600
O	-1.96231900	-2.35770500	0.96608100
C	-1.01900200	-0.30650600	0.75547500
C	-1.21033400	-1.41462500	1.58713800
C	-0.55547200	-1.27093900	2.82828200
H	-0.49404400	-1.98382300	3.63621800
C	0.03449400	0.03921400	2.79038500
H	0.62437700	0.47923800	3.58309700
C	-0.23151700	0.63775400	1.51229500
H	0.15597600	1.59240300	1.18256200
S	3.80798400	0.95701700	-1.33376700
C	5.43885200	0.81882400	-0.43094400
F	6.40534300	1.18503600	-1.25540800
F	5.63878400	-0.42865100	-0.04071700
F	5.43608000	1.61358200	0.62712500
O	3.76975300	-0.10285000	-2.30283300
O	3.63495600	2.34186400	-1.66628900
S	-2.22102500	-1.54079200	-0.58320900
C	-3.28768300	-3.03423100	-0.99412000
F	-3.79840500	-2.86807500	-2.21138500
F	-4.29295500	-3.17504500	-0.13507200
F	-2.56557200	-4.15027700	-0.99108000
O	-1.23927500	-1.67749500	-1.65537800
O	-3.34514800	-0.54672700	-0.61783700
H	-4.03816800	2.65663600	1.22002100
H	3.38921300	-0.69965500	2.29276300
H	1.22613400	-1.37522500	-1.44972300
C	-5.64074300	2.85015100	-0.49722300
C	-4.19220500	3.26602500	-0.70954700
C	-2.38631400	3.78594200	0.98831800
N	-3.38270300	2.81772700	0.45832500
C	-3.64979400	2.68366000	-2.01012200
C	-3.02638200	5.03052600	1.59783100
C	-1.33791500	4.15006900	-0.05177200
H	-1.87785000	3.24631200	1.79748800
H	-3.75333700	4.76404200	2.37178500
H	-2.26225900	5.65858800	2.06420600
H	-3.53585800	5.64041800	0.84579700
H	-0.55870800	4.76233200	0.40895100
H	-0.85440800	3.26519100	-0.47624600
H	-4.20875500	3.07843300	-2.86331000
H	-2.59745800	2.93229400	-2.16507200

H	-3.75659100	1.59321400	-2.02620600	F	-0.02402400	-0.25101100	1.98697600
H	-6.06760000	3.32318800	0.39337100	F	1.00005700	-2.00503900	2.73658600
H	-6.25365200	3.13814700	-1.35458800	O	-0.99845600	-3.87882700	1.57076400
H	-5.71826300	1.76283600	-0.38627000	O	-2.18047900	-1.81496300	0.72700100
H	-4.15586500	4.36107500	-0.77313900	H	-4.21189700	0.61473500	-2.06953400
H	-1.76623700	4.73135700	-0.87356700	H	2.46657100	-0.45432600	1.50108500
Li	-2.60886200	0.97675600	0.11589700	H	2.62970300	0.38069000	-2.78149600
<b>J</b>				C	-2.98297300	2.62597400	-2.04796900
Fe	1.82053600	-1.62212600	-0.99847600	C	-3.53865800	2.02216400	-0.76608700
O	1.25803600	1.29488100	-0.42756500	C	-5.38469700	0.31724100	-0.45223700
C	2.74097600	-0.50729400	0.46090900	N	-4.08055700	0.66815000	-1.06261100
C	2.23105000	0.30920000	-0.59025800	C	-2.45645700	1.95039800	0.30600900
C	2.83798900	-0.05592500	-1.81685300	C	-6.54068500	1.17750200	-0.95878300
C	3.73182800	-1.12264400	-1.52745700	C	-5.31433300	0.31040800	1.06767700
H	4.32971100	-1.65401200	-2.25307100	H	-5.57646500	-0.71389100	-0.77642300
C	3.67231700	-1.39579400	-0.12949100	H	-6.60561700	1.15006600	-2.05127800
H	4.21477500	-2.17279800	0.38876300	H	-7.49040100	0.80911300	-0.56035100
O	-1.18206600	-0.95153600	-1.83911900	H	-6.43977700	2.22221000	-0.64961100
C	0.07053400	-2.51202000	-0.39467300	H	-6.25682700	-0.06091900	1.47849200
C	-0.28201700	-1.81761500	-1.64846600	H	-4.51152900	-0.33766200	1.42986900
C	0.69498900	-2.30586700	-2.58223100	H	-2.11814100	2.95480600	0.57335300
H	0.76554900	-1.95032600	-3.60001100	H	-2.81161600	1.45940900	1.21493700
C	1.47060100	-3.34849000	-1.99858700	H	-1.57437900	1.41536300	-0.06524100
H	2.24118700	-3.91847700	-2.49803700	H	-3.77253700	2.77714800	-2.79182400
C	1.12100100	-3.47366500	-0.63600700	H	-2.51210500	3.59110900	-1.84877000
H	1.50001600	-4.18849700	0.07855800	H	-2.21772900	1.97001200	-2.47723100
S	1.67322100	2.85709700	-0.48732600	H	-4.34919000	2.66694100	-0.40200800
C	2.08557300	3.16686900	1.30875300	H	-5.15728000	1.31673800	1.46795200
F	2.36148900	4.45186100	1.45763600	Li	-2.55679200	-0.63858600	-0.72138900
F	3.13471400	2.44543300	1.66741900				
F	1.05209900	2.84636700	2.06868900				
O	2.88097900	3.04741700	-1.24300400				
O	0.45604900	3.57174800	-0.75098500				
S	-0.93058400	-2.54776600	1.00184900				
C	-0.17656700	-1.51195000	2.37122700				
F	-0.99980100	-1.54688200	3.40855500				



**K**

C	-0.07243800	-2.11648700	1.99039100
C	-0.01274900	-3.44682300	1.49985400
C	1.03767600	-3.52434700	0.54187600
C	1.60790400	-2.22767100	0.46968000
C	0.94496600	-1.34206600	1.35757400
H	-0.79710400	-1.73728500	2.69630100
H	-0.67522800	-4.25318600	1.77652600
H	1.35105600	-4.38187600	-0.03348700
Fe	-0.33678800	-2.13272600	-0.04051300
C	-0.41734900	-1.53431100	-2.02089800
C	-1.06016500	-0.50193300	-1.26370100
C	-2.07507000	-1.21213700	-0.48794600
C	-2.10541300	-2.60408000	-0.85690000
C	-1.08476100	-2.77818700	-1.81982100
H	0.42243900	-1.36623400	-2.68076900
H	-2.78985000	-3.34743200	-0.47745300
H	-0.82930600	-3.71447700	-2.29465500
O	2.73948800	-2.02565100	-0.33367500
S	3.27440300	-0.62493300	-0.87019500
C	4.60948200	-0.29650900	0.39801200
O	3.90765400	-0.86493200	-2.13024400
O	2.29114500	0.42213300	-0.69910300
F	5.50605600	-1.25976100	0.34872300
F	4.06768300	-0.24666100	1.60108100
F	5.17111000	0.86141700	0.10870700
H	1.15482200	-0.29693000	1.51976200
Li	-1.37002800	1.99189200	0.10935700
C	1.92823500	3.13397500	1.62570800
C	0.66235200	3.86946600	1.18200800
C	-0.23514300	4.22994300	-1.07260400
N	0.10355800	3.26846200	-0.02270900
C	-0.33736400	3.89887100	2.34666700
C	0.98473600	4.92144800	-1.70487300
C	-1.27069400	5.29259200	-0.67260100
H	-0.70265200	3.64375600	-1.88427500
H	1.69571800	4.18124800	-2.08896200
H	0.69495200	5.57414800	-2.53625500
H	1.51635400	5.53902600	-0.97303400
H	-0.88172100	5.95007800	0.11236200
H	-1.54429100	5.92482300	-1.52471800
H	-2.18563800	4.82613900	-0.29116800
H	0.08395500	4.36726600	3.24480400
H	-1.24166400	4.44827300	2.07124100
H	-0.63584300	2.87741600	2.61845500
H	2.69438300	3.17562900	0.84488000
H	2.35073300	3.55358700	2.54582200
H	1.70126500	2.07782700	1.82443800
H	0.96150900	4.91413600	0.99661700
O	-0.77208100	0.74379600	-1.20410300
S	-3.09323300	-0.50148200	0.69886700
O	-3.49203900	-1.44630400	1.72156200
O	-2.56711600	0.81534400	1.08206300
C	-4.65863300	-0.09167200	-0.24690900
F	-4.37320700	0.73363500	-1.24617900
F	-5.19214600	-1.20129800	-0.73745400
F	-5.52004500	0.48956600	0.56996600

Li 0.81138900 1.69836400 -0.90988600

**L**

C	-0.45007600	0.02688600	2.14762000
C	-0.40744900	-1.27932800	2.71841100
C	0.78333200	-1.90224700	2.26202100
C	1.42484300	-0.93700600	1.44069800
C	0.70038100	0.28467400	1.32887300
H	-1.27031100	0.71925000	2.29033400
H	-1.15826900	-1.72437700	3.35519300
H	1.14532200	-2.89527600	2.48399700
Fe	-0.40885600	-1.37490500	0.67804700
C	-0.27399400	-1.96751900	-1.31565800
C	-1.11547200	-0.80925400	-1.23381200
C	-2.16031800	-1.19551800	-0.29118300
C	-1.95966200	-2.54965800	0.15299200
C	-0.79566500	-3.01318300	-0.50034700
H	0.61045500	-2.03290300	-1.93146200
H	-2.59489400	-3.08946600	0.83851600
H	-0.35817800	-3.99363800	-0.38188100
O	2.74025600	-1.18554800	0.97393200
S	3.09921800	-1.23174600	-0.57083100
C	4.89263200	-0.75785600	-0.35582700
O	3.04602500	-2.56132700	-1.11142600
O	2.45941000	-0.13238000	-1.27751400
F	5.50173300	-1.65063400	0.39774800
F	4.98021300	0.43605800	0.19572400
F	5.43997500	-0.73591000	-1.55856100
H	0.72210400	1.53204400	0.69075300
Li	-1.42525800	1.90890600	-0.79182800
C	0.58581900	3.50791200	2.31418500
C	0.03590300	3.72165900	0.90102600
C	1.41495400	3.06606100	-1.00764800
N	0.37955400	2.63742900	-0.04639700
C	-1.47054500	3.96779600	0.95811300
C	2.73615900	3.50921100	-0.37033700
C	0.90794200	4.11447200	-2.00245100
H	1.68407100	2.20000100	-1.63869600
H	3.12353300	2.73804500	0.30073600
H	3.49027200	3.70115000	-1.14033800
H	2.61569400	4.43092800	0.20682900
H	0.62792900	5.04570100	-1.50061600
H	1.67932600	4.35959600	-2.73972800
H	0.03238200	3.74468200	-2.54584200
H	-1.71145900	4.79789800	1.62986400
H	-1.86597100	4.23202700	-0.03133100
H	-2.01277100	3.08992100	1.32513100
H	1.66500700	3.33751300	2.29851800
H	0.38926600	4.38796200	2.93571700
H	0.12201900	2.64686400	2.80242700
H	0.48135900	4.65581800	0.53551900
O	-0.91791500	0.35827400	-1.76362500
S	-3.41190500	-0.16686300	0.27423700
O	-3.92974400	-0.58155700	1.56149000
O	-3.03667300	1.23872400	0.05415200
C	-4.80660100	-0.44268100	-0.94575500
F	-4.40316700	-0.14394700	-2.17121300

F -5.18563900 -1.71210500 -0.90712000  
F -5.82664200 0.33251100 -0.61597200  
Li 0.71101000 0.72101300 -0.91137600

**M**

C -0.01372200 -0.63199100 1.81931900  
C 0.30784700 -2.01790400 1.87403900  
C 1.29229900 -2.27460100 0.88068300  
C 1.52337900 -1.02052300 0.24942100  
C 0.74397600 0.04318100 0.79905900  
H -0.77370900 -0.16552400 2.43355800  
H -0.14527300 -2.75230900 2.52432800  
H 1.74843100 -3.22016400 0.62640400  
Fe -0.38270200 -1.51014000 0.00436400  
C -0.70551100 -1.61705800 -2.03885000  
C -1.58433600 -0.58316100 -1.56181000  
C -2.32387000 -1.25176000 -0.47531200  
C -1.97761800 -2.64824300 -0.40153300  
C -0.99102500 -2.85585800 -1.39453700  
H 0.04509000 -1.45363700 -2.79892000  
H -2.41323300 -3.37739200 0.26442300  
H -0.50511500 -3.79948400 -1.59833500  
O 2.43338200 -0.89377200 -0.83786500  
S 3.80354900 -0.12477200 -0.63371100  
C 4.82524600 -1.30418500 0.40608200  
O 4.43155200 -0.01275900 -1.91352000  
O 3.60671300 1.05373500 0.20551000  
F 4.77773000 -2.50745900 -0.13262400  
F 4.35859700 -1.34462600 1.63883200  
F 6.06983500 -0.86381000 0.41393100  
H 0.39448900 1.36490700 0.38773200  
Li -1.62825300 1.75284400 -0.44159100  
C 1.20526400 3.60517200 2.12916000  
C 0.05372500 3.65632400 1.10929900  
C 0.60272500 3.05840600 -1.26094900  
N 0.17065500 2.61767200 0.07620500  
C -1.28174800 3.57892200 1.84409800  
C 1.93070700 3.82658700 -1.29038500  
C -0.47349500 3.86905900 -1.98968800  
H 0.73949400 2.13142400 -1.83556400  
H 2.76363500 3.25073200 -0.86879900  
H 2.21292700 4.06454500 -2.32027300  
H 1.86244200 4.77506500 -0.74665200  
H -0.74113600 4.77215100 -1.42973100  
H -0.12558900 4.18646900 -2.97754600  
H -1.37779700 3.27440900 -2.15547000  
H -1.35222000 4.33921600 2.62880300  
H -2.11741100 3.73971000 1.15577700  
H -1.42249100 2.59835900 2.30953600  
H 2.18294800 3.77114200 1.65243000  
H 1.11304100 4.38184400 2.89322700  
H 1.20956400 2.64878700 2.67550900  
H 0.10329800 4.64277700 0.62844600  
O -1.63701000 0.63666100 -1.89651800  
S -3.35283300 -0.45157900 0.63242200  
O -3.54000300 -1.19902200 1.86105300  
O -2.99164700 0.97563400 0.69932900

C -5.03260400 -0.43636300 -0.19482000  
F -4.96754400 0.19080800 -1.35849900  
F -5.44009800 -1.68331300 -0.39358500  
F -5.89850600 0.18629100 0.59167000  
Li 1.96537400 1.82305300 0.81617600

**N**

C -0.20217100 -0.18205000 2.13290100  
C -0.02208900 -1.49514900 2.67542300  
C 1.22772700 -1.97292100 2.20135600  
C 1.73990700 -0.91090000 1.40623800  
C 0.89848000 0.23225200 1.30227500  
H -1.10367200 0.39640700 2.29661700  
H -0.71605600 -2.03457600 3.30459400  
H 1.69931000 -2.92474000 2.39655000  
Fe -0.02080600 -1.54656300 0.63889900  
C 0.19878600 -1.97423500 -1.38796600  
C -0.78221200 -0.94528600 -1.22132600  
C -1.77602800 -1.53905300 -0.32931700  
C -1.39421300 -2.88586300 0.01588900  
C -0.17927300 -3.13911500 -0.65795000  
H 1.08600900 -1.87483000 -1.99640400  
H -1.95566400 -3.55858900 0.64592600  
H 0.38405100 -4.05945700 -0.61112200  
O 3.07812500 -1.02470900 0.91056200  
S 3.48363700 -0.83390600 -0.60133800  
C 5.16862200 -0.10765400 -0.26528800  
O 3.66560100 -2.08784900 -1.27953000  
O 2.70931500 0.22006800 -1.24401300  
F 5.89668700 -0.96281400 0.42508400  
F 5.04848100 1.02399100 0.40145200  
F 5.74198400 0.12514900 -1.43492200  
H -0.15685800 2.46589500 0.74222400  
Li -1.71904000 1.60809700 -0.85218800  
C -1.69517300 3.47810600 2.26769700  
C -1.47848600 4.02800600 0.86515100  
C 0.43764700 3.70536000 -0.72899400  
N -0.63805500 3.08596100 0.08198300  
C -2.81682300 4.27304000 0.17502200  
C 1.53550500 4.34426100 0.11826200  
C -0.10624300 4.66780100 -1.77433900  
H 0.90369600 2.87865500 -1.28624400  
H 1.93974900 3.62206900 0.83352100  
H 2.35652800 4.68709500 -0.51813300  
H 1.16673700 5.21205400 0.67352700  
H -0.55691600 5.55160700 -1.31329500  
H 0.70769800 5.01312300 -2.41684500  
H -0.85626000 4.19054400 -2.41180800  
H -3.39565200 5.02560400 0.71897100  
H -2.69094500 4.62962600 -0.84988800  
H -3.41403800 3.35427100 0.15681300  
H -0.74603900 3.32543400 2.78982600  
H -2.30220500 4.16839100 2.85918700  
H -2.22573900 2.52147700 2.22623000  
H -0.95493300 4.98883600 0.95571500  
O -0.72663200 0.28386000 -1.65965700  
S -3.17724500 -0.76766700 0.28271900



O	-3.61245600	-1.30477500	1.55426000
O	-3.06923500	0.69351900	0.10995400
C	-4.51601600	-1.23252100	-0.94296300
F	-4.18038700	-0.81532500	-2.15686300
F	-4.67320500	-2.54749100	-0.96152100
F	-5.65275900	-0.65775800	-0.58222300
Li	0.89358700	0.67791300	-0.73028700

**O**

C	1.62470400	-1.33244600	1.67874900
C	1.97568800	-2.69956600	1.43870200
C	2.91223800	-2.73986000	0.35235700
C	3.12627500	-1.39389000	-0.01399000
C	2.32818900	-0.51239900	0.73834500
H	0.91140300	-1.00491400	2.42332900
H	1.58105400	-3.55883600	1.96336100
H	3.35957400	-3.61888300	-0.08700100
Fe	1.11832900	-1.90627400	-0.21203200
C	0.50536700	-1.46190600	-2.14681300
C	-0.41494900	-0.87383900	-1.22275600
C	-0.88139800	-1.98561700	-0.40007600
C	-0.27273200	-3.21328400	-0.84645700
C	0.56638300	-2.86832300	-1.93146200
H	1.07335100	-0.90176800	-2.87701000
H	-0.44999600	-4.19580100	-0.43663400
H	1.18710200	-3.55966200	-2.48246500
O	3.96779600	-0.80792500	-0.87992800
S	3.73012000	0.93259500	-0.64483800
C	3.49946500	2.12593400	0.83602900
O	5.07997400	1.32154000	-1.00446400
O	2.62339600	1.32908500	-1.54933400
F	4.08731100	1.65457500	1.91718400
F	2.19564200	2.29562700	1.07729300
F	4.01560000	3.30423800	0.53229400
H	-3.99344300	2.41430900	0.62898300
Li	1.09176200	0.76603400	-0.61696500
C	-0.99263000	3.55705500	0.85020800
C	-2.49872100	3.78591200	0.78940300
C	-3.64426700	2.93177800	-1.29498500
N	-3.16908300	2.65989700	0.08698200
C	-3.08421500	3.93965900	2.18533100
C	-2.48858300	3.26073800	-2.22863200
C	-4.74544400	3.98719400	-1.35507500
H	-4.07985100	1.98186500	-1.63148000
H	-1.73149600	2.47132000	-2.22479900
H	-2.86066500	3.36245200	-3.25127800
H	-2.01120700	4.20914200	-1.96240000
H	-4.38216100	4.97631600	-1.05982200
H	-5.13057200	4.07332200	-2.37493400
H	-5.58539400	3.72299100	-0.70447600
H	-2.57517100	4.73548600	2.73451500
H	-4.14960100	4.18749200	2.14520900
H	-2.96679100	3.01337100	2.75935600
H	-0.56811600	3.40288800	-0.14526200
H	-0.48387900	4.41632500	1.29563700
H	-0.75548500	2.68762200	1.47732900
H	-2.68267100	4.71581800	0.23763700

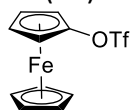
O	-0.69514800	0.39763400	-1.08460800
S	-1.97733800	-1.87497700	0.90971400
O	-1.73372600	-2.84399100	1.95498300
O	-2.19531800	-0.45882700	1.26003700
C	-3.62148800	-2.35856300	0.14960000
F	-3.91298700	-1.51784100	-0.84255400
F	-3.56548900	-3.59034000	-0.32929600
F	-4.57001900	-2.28361600	1.06934600
Li	-1.96944900	1.01254500	0.07542500

**P**

C	2.90768500	-1.34980400	-0.83009700
C	3.92021600	-1.39951500	0.15126800
C	3.35273500	-1.79315200	1.39868100
C	1.95277100	-2.09819100	1.24628500
C	1.69818500	-1.78022500	-0.16695000
H	3.00096100	-1.09550100	-1.87489200
H	4.95268300	-1.12306900	-0.00953800
H	3.87178100	-1.84978900	2.34470800
Fe	2.44003100	-0.08989000	0.68733400
C	1.97229400	0.97031900	2.40764400
C	0.89061000	1.11312400	1.49288700
C	1.51132200	1.66271300	0.27912700
C	2.91873300	1.86750100	0.49901500
C	3.18392500	1.44026300	1.81748000
H	1.87752700	0.51515100	3.38388600
H	3.61446300	2.28154300	-0.21517400
H	4.15623600	1.43564500	2.28845700
O	1.08845300	-2.41328000	2.12346200
S	0.17562100	-1.90425300	-0.92742100
C	-0.14460900	-3.74032900	-1.14096200
O	-0.89852900	-1.49602100	0.01991900
O	0.16726100	-1.35317800	-2.26572700
F	-0.18743600	-4.35226200	0.02737500
F	0.82014000	-4.26424900	-1.88097000
F	-1.30694500	-3.89129100	-1.76166200
H	-3.70826800	1.58702200	0.22724800
Li	-0.25858700	-1.16964000	1.93525300
C	-3.79110800	0.13862400	-1.92048000
C	-4.27310100	-0.21651600	-0.51880300
C	-3.71721000	0.42422700	1.90258300
N	-3.51658000	0.61051400	0.44367700
C	-5.79378400	-0.09635400	-0.43700900
C	-3.76431800	-1.05123100	2.27530800
C	-4.89521700	1.19873700	2.49122500
H	-2.81170300	0.84462200	2.35995000
H	-2.94593000	-1.61424100	1.81475700
H	-3.68940900	-1.15969300	3.36037100
H	-4.69919500	-1.52587400	1.96318500
H	-5.86210600	0.80886500	2.16657500
H	-4.86340800	1.14851100	3.58411400
H	-4.84332800	2.25661400	2.21352400
H	-6.25727100	-0.67909600	-1.23868500
H	-6.19307300	-0.46728400	0.50881000
H	-6.11101400	0.94568600	-0.55709900
H	-2.71471300	-0.00737500	-2.03865500
H	-4.29581100	-0.48258300	-2.66467300

H	-4.01620300	1.18536400	-2.15641300
H	-3.99424700	-1.25728800	-0.32140500
O	-0.33946700	0.72754200	1.66005100
S	0.70334400	2.14456400	-1.15372100
O	1.55821000	2.10918400	-2.31951700
O	-0.63833800	1.54676000	-1.18845500
C	0.34182200	3.96025400	-0.85873900
F	-0.37434900	4.10680400	0.25015600
F	1.47535500	4.63610100	-0.73438500
F	-0.34423700	4.43879000	-1.88528000
Li	-1.48318200	0.48149300	0.15710500

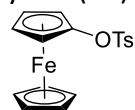
Ferrocenyl triflate (**79**)



**79**

C	-2.02180300	-2.04776500	0.44538300
C	-1.95357300	-1.86754400	-0.96619100
C	-0.82340900	-1.06041800	-1.26527100
C	-0.21431100	-0.74730800	-0.02150300
C	-0.93456800	-1.35455400	1.04275000
H	-2.78726500	-2.59391700	0.97667000
H	-2.65842400	-2.25423900	-1.68739200
H	-0.48776100	-0.72903300	-2.23584900
Fe	-2.09697800	-0.05637800	-0.02236900
C	-2.01098100	1.96798400	0.23755300
C	-2.75635700	1.36505100	1.28888700
C	-3.85854600	0.67648200	0.70860800
C	-3.79478500	0.85462800	-0.70183200
C	-2.65312500	1.65321300	-0.99262900
H	-1.09546400	2.53065900	0.35051000
H	-2.50916300	1.39608400	2.34009400
H	-4.47394100	0.43017600	-1.42686000
H	-2.31415500	1.94153900	-1.97704600
O	0.90970400	0.06079600	0.13403200
S	2.34462400	-0.70405600	0.17400800
C	3.32832700	0.85530700	-0.12055600
O	2.63299400	-1.16473200	1.50567100
O	2.49761800	-1.55565700	-0.97542400
H	-4.59479900	0.09319000	1.24225900
F	3.08251400	1.74041600	0.82740900
F	3.02663400	1.36777600	-1.29955900
F	4.60906400	0.52489600	-0.09713200
H	-0.69924600	-1.27524200	2.09319400

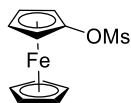
Ferrocenyl tosylate (**93**)



**93**

C	-1.66715500	-1.05846200	1.82843000
C	-1.23216100	-1.93118400	0.78898100
C	-0.52820500	-1.16074500	-0.17688200
C	-0.54741900	0.18738800	0.27748100
C	-1.24574400	0.26277100	1.51470700
H	-2.25049500	-1.34431500	2.69152200
H	-1.42925700	-2.99158800	0.72881900
H	-0.08631300	-1.50710500	-1.09901600
Fe	-2.43804600	-0.46836000	0.02913100
C	-3.30289500	0.74760800	-1.36309600
C	-4.01741700	0.81524400	-0.13456300
C	-4.47597700	-0.49476500	0.18195100
C	-4.04592500	-1.37268100	-0.85257400
C	-3.32153300	-0.60428000	-1.80714800
H	-2.79136200	1.56804600	-1.84554600
H	-4.15399500	1.69961300	0.47068700
H	-4.21134900	-2.43969300	-0.88953300
H	-2.83935000	-0.98602800	-2.69541200
O	-0.00307200	1.24744300	-0.41861800
S	1.36801600	1.94286300	0.18484800
O	1.64251500	2.99403600	-0.76097600
O	1.16087300	2.20854200	1.59080800
H	-5.02419000	-0.77848700	1.06860100
H	-1.41674700	1.16242100	2.08504600
C	2.57035900	0.65858800	0.01583200
C	3.27230800	0.54370100	-1.17858400
C	2.77963500	-0.22396500	1.06811700
C	4.19516100	-0.48177900	-1.31484800
H	3.09774700	1.25527500	-1.97787800
C	3.70736600	-1.24368600	0.91068800
H	2.22806100	-0.10330300	1.99347500
C	4.42797200	-1.38774700	-0.27635400
H	4.75124700	-0.57753600	-2.24262000
H	3.87705900	-1.93872300	1.72739800
C	5.45623700	-2.46984100	-0.42282500
H	5.53035700	-2.81281500	-1.45748600
H	6.44514200	-2.10160600	-0.12801400
H	5.22421000	-3.32978300	0.20940100

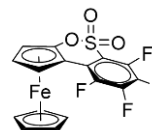
Ferrocenyl mesylate (**93**)



**94**

C	0.89766500	1.87637800	0.92880600
C	1.02765400	2.08231600	-0.47470000
C	0.14702600	1.18544200	-1.14162800
C	-0.51038500	0.42713100	-0.13214300
C	-0.05426100	0.84319200	1.14983500
H	1.45343800	2.39245700	1.69787400
H	1.69972400	2.77936700	-0.95341600
H	0.02078300	1.06093300	-2.20688400
Fe	1.48394300	0.15087700	0.00230400
C	1.82430200	-1.84306300	-0.27243000
C	2.29132600	-1.43203600	1.00701600
C	3.27065700	-0.41710100	0.81421900
C	3.41010200	-0.20148700	-0.58567200
C	2.51661300	-1.08335000	-1.25642000
H	1.04470100	-2.56721000	-0.46061500
H	1.93639200	-1.79976800	1.95876500
H	4.05643000	0.52603900	-1.05492700
H	2.36470500	-1.14158900	-2.32450300
O	-1.41631800	-0.58191600	-0.40225000
S	-2.96823600	-0.39692500	0.10910800
C	-3.52141700	0.95850600	-0.89910800
O	-3.61394300	-1.61418700	-0.30619800
O	-2.96512000	0.02158500	1.49230900
H	3.79125900	0.11904200	1.59438500
H	-4.55054300	1.16499900	-0.60419200
H	-2.88658600	1.82211300	-0.70140800
H	-3.47132200	0.65232500	-1.94308800
H	-0.38235400	0.43986400	2.09485000

Ferrocene annelated 6,7,8,9-tetrafluoro-benzo[c,e]- [1,2]oxathiine 5,5-dioxide (*rac*-**116**)



*rac*-**116**

C	2.53279500	-1.08374100	-1.84547900
C	2.38712500	0.33328700	-1.88254400
C	1.11483400	0.61927200	-1.34276200
C	0.46009800	-0.58944500	-0.96364100
C	1.36731100	-1.65579700	-1.27090200
H	3.40881500	-1.63082600	-2.16101700
H	3.09859000	1.05939100	-2.24438400
Fe	2.23603200	-0.36510100	0.04118500
C	1.86524300	-0.10947800	2.03732400
C	2.49569500	-1.36422400	1.80689700
C	3.75240400	-1.11346800	1.18730000
C	3.89500300	0.29441200	1.03735700
C	2.72881800	0.91537200	1.56376000
H	0.88295100	0.04894300	2.45757600
H	2.08220200	-2.33665200	2.03229600
H	4.72725000	0.80014000	0.56929900
H	2.50338100	1.97074400	1.56367100
H	4.45589200	-1.86209900	0.85241000
H	1.19684800	-2.70487400	-1.09167700
S	-0.61521900	2.17892500	-0.20777200
O	0.04873200	2.32975200	1.06332300
O	-1.39402900	3.24258900	-0.77129500
C	-1.53680300	0.65220300	-0.17849000
C	-2.85715200	0.69745200	0.24834600
C	-0.90409800	-0.57388000	-0.46967900
C	-3.59197600	-0.47116800	0.37654900
C	-1.67051100	-1.72735400	-0.33273400
C	-2.99231900	-1.68498400	0.08121000
F	-1.15101000	-2.92240200	-0.60770500
F	-3.68565900	-2.80379100	0.19816800
F	-4.84937800	-0.43287600	0.78583600
F	-3.44482800	1.83770100	0.56942600
O	0.50152500	1.84598600	-1.36093200

## *Curriculum Vitae*

### **Personal Information**

Name	Geanne Marize Romêro Boston
Date of Birth	12.02.1984
Place of Birth	Ipatinga, Minas Gerais, Brazil

### **Education**

07/2017 – current	PhD in organometallic chemistry in the group of Prof. Holger Butenschön, Institute of Organic Chemistry. The research project involves understanding the mechanism underlying thia-Fries rearrangement at ferrocene as well as developing further thia-Fries and ortho-lithiation methodologies at metallocene. The experimental part was complemented by computational studies in order to unravel the reaction mechanism using the software programs Gaussian and CPMD.
09/2009 – 05/2011	Master's studies in Chemistry at the University of Fribourg, Switzerland. Master's thesis: Trifluoromethyl benzocyclobutenedione chromium complexes
03/2002 – 12/2005	Bachelor's in chemistry at the State University of Campinas, Brazil. Bachelor's thesis: Synthesis of Chalcone derivatives with potential anti-malarial applications.

<b>Motherhood</b>	Between 2012 and 2017 I focused on bringing up my daughter and my son.
-------------------	--

### **Professional Experience**

01/2008 – 01/2009	Development chemist at The Dow Chemical Company, São Paulo, Brazil. Leadership of a project in the R&D department entitled "Dow sustainable solutions to enhance the performance of recycled plastics". Several highlights of the project included two potential patents, two internal scientific reports (both first author). Dow now has a portfolio of products to optimize the performance of recycled plastics which were first developed in my project. I worked mainly with copolymers of polyethylene and grafted polyethylene. Besides this, I also gained experience in many other areas
-------------------	--

of the company from supply chain to sales within the trainee program.

### Internships

- 07/2006 – 07/2007 Internship in analytical chemistry at the Swiss Environmental Analytics Laboratory, Schlieren. Analysis of soil and water samples using chromatographic methods, titration and spectroscopical techniques (UV-VIS).
- 01/2006 – 06/2006 Internship in utility engineering at the ALTANA Pharma Brazil. Mass and energy balance of utilities, such as steam, water, etc, with the aim of performing an analytical study of the company's consumption, production, production capacity, rate, and cost estimation for planning future utility improvements, allowing for expansion in infrastructure and medicine production, including participation in a project for water reuse.

### Publication list

1. "Trifluoromethyl-Substituted Benzocyclobutenone and Benzocyclobutenedione: The Structure Anomaly of (Benzocyclobutenedione)tricarbonylchromium Complexes." M. Böning, K. Dongol, G. Boston, S. Schmitz, R. Wartchow, J. Samaniego-Rojas, A. Köster, H. Buntenschön, *Organometallics*, **2019**, *38*, 3039-3052
2. "Anionic Thia- Fries Rearrangement at Ferrocene: A Computational and Experimental Study." G. Boston, I. Frank, H. Buntenschön, *Helv. Chim. Acta*, **2021**, *104*, e2100025.
3. Eur. J. Inorg. Chem. provisionally accepted: "Fluorosulfonylferrocene, (Trifluoromethylsulfonyl)ferrocene and New Ferrocenyl Sulfonates: Directed *ortho* Lithiation and New Anionic Thia-Fries Rearrangements at Ferrocene"